

Universality in Driven-Dissipative Quantum Many-Body Systems

DISSERTATION

zur Erlangung des akademischen Grades

“Doctor of Philosophy”

an der

Fakultät für Mathematik, Informatik und Physik

der

Leopold-Franzens-Universität Innsbruck

vorgelegt von

Mag. rer. nat. Lukas M. Sieberer

März 2015

Doktorvater/Thesis Advisor:

Prof. Dr. Sebastian Diehl, Dresden

ZUSAMMENFASSUNG

In jüngerer Zeit durchgeführte experimentelle Studien von Kondensationsphänomenen in getrieben-dissipativen Quantenvielteilchensystemen bringen die Frage auf, welche Art von neuem universellem Verhalten unter Nicht-Gleichgewichtsverhältnissen auftreten kann. Wir untersuchen verschiedene Aspekte von Universalität in diesem Kontext. Unsere Resultate haben Relevanz für zahlreiche offene Quantensysteme, von Exziton-Polariton-Kondensaten bis zu kalten atomaren Gasen.

In Teil I charakterisieren wir das dynamische kritische Verhalten am Bose-Einstein-Kondensations-Phasenübergang in getriebenen offenen Quantensystemen in drei räumlichen Dimensionen. Obwohl sich thermodynamische Gleichgewichtsverhältnisse bei niedrigen Frequenzen einstellen, wird die Annäherung an dieses thermalisierte Regime niedriger Frequenzen durch einen kritischen Exponenten beschrieben, der kennzeichnend für den Nicht-Gleichgewichts-Übergang ist und diesen außerhalb der Standardklassifikation von dynamischem kritischem Verhalten im Gleichgewicht einstuft. Unser theoretischer Ansatz beruht auf der funktionalen Renormierungsgruppe im Rahmen der Keldysh-Nicht-Gleichgewichts-Feldtheorie, welche äquivalent zu einer mikroskopischen Beschreibung der Dynamik des offenen Systems in Form einer Quantenvielteilchen-Mastergleichung ist.

Universelles Verhalten der Kohärenzeigenschaften von getrieben-dissipativen Kondensaten in reduzierten Dimensionen wird in Teil II untersucht. Wir zeigen, dass getriebene zweidimensionale Bose-Systeme keine algebraische Ordnung wie im thermodynamischen Gleichgewicht aufweisen können, sofern sie nicht hinreichend anisotrop sind. Dennoch finden wir Hinweise, dass sogar isotrope Systeme einen endlichen superfluiden Anteil haben können. In eindimensionalen Systemen sind Nicht-Gleichgewichtsbedingungen im Verhalten der Autokorrelationsfunktion nachweisbar. Wir erzielen diese Resultate durch eine Abbildung der Dynamik des Kondensats auf langen Wellenlängen auf die Kardar-Parisi-Zhang-Gleichung.

In Teil III zeigen wir, dass Systeme in thermodynamischem Gleichgewicht eine besondere Symmetrie haben, welche sie von allgemeinen getriebenen offenen Systemen unterscheidet. Das neuartige universelle Verhalten, welches in den Teilen II und III beschrieben wird, kann auf das Fehlen dieser Symmetrie außerhalb des Gleichgewichts zurückgeführt werden. Von einem praktischen Standpunkt aus bietet diese Symmetrie einen effizienten Test für das Vorliegen von thermodynamischen Gleichgewichtsbedingungen und macht die explizite Berechnung von Fluktuations-Dissipations-Relationen unnötig. Im klassischen Grenzfall finden wir die bekannte Gleichgewichtssymmetrie der stochastischen Dynamik klassischer, an thermische Bäder gekoppelter Systeme wieder.

ABSTRACT

Recent experimental investigations of condensation phenomena in driven-dissipative quantum many-body systems raise the question of what kind of novel universal behavior can emerge under non-equilibrium conditions. We explore various aspects of universality in this context. Our results are of relevance for a variety of open quantum systems on the interface of quantum optics and condensed matter physics, ranging from exciton-polariton condensates to cold atomic gases.

In Part I we characterize the dynamical critical behavior at the Bose-Einstein condensation phase transition in driven open quantum systems in three spatial dimensions. Although thermodynamic equilibrium conditions are emergent at low frequencies, the approach to this thermalized low-frequency regime is described by a critical exponent which is specific to the non-equilibrium transition, and places the latter beyond the standard classification of equilibrium dynamical critical behavior. Our theoretical approach is based on the functional renormalization group within the framework of Keldysh non-equilibrium field theory, which is equivalent to a microscopic description of the open system dynamics in terms of a many-body quantum master equation.

Universal behavior in the coherence properties of driven-dissipative condensates in reduced dimensions is investigated in Part II. We show that driven two-dimensional Bose systems cannot exhibit algebraic order as in thermodynamic equilibrium, unless they are sufficiently anisotropic. However, we find evidence that even isotropic systems may have a finite superfluid fraction. In one-dimensional systems, non-equilibrium conditions are traceable in the behavior of the autocorrelation function. We obtain these results by mapping the long-wavelength condensate dynamics onto the Kardar-Parisi-Zhang equation.

In Part III we show that systems in thermodynamic equilibrium have a specific symmetry, which makes them distinct from generic driven open systems. The novel universal behavior described in Parts I and II can be traced back to the absence of this symmetry out of equilibrium. From a practical viewpoint, this symmetry provides an efficient check for thermodynamic equilibrium conditions, making the explicit calculation of fluctuation-dissipation relations unnecessary. In the classical limit we recover the known equilibrium symmetry of the stochastic dynamics of classical systems coupled to thermal baths.

EIDESSTATTLICHE ERKLÄRUNG

Ich erkläre hiermit an Eides statt durch meine eigenhändige Unterschrift, dass ich die vorliegende Arbeit selbständig verfasst und keine anderen als die angegebenen Quellen und Hilfsmittel verwendet habe. Alle Stellen, die wörtlich oder inhaltlich den angegebenen Quellen entnommen wurden, sind als solche kenntlich gemacht. Die vorliegende Arbeit wurde bisher in gleicher oder ähnlicher Form noch nicht als Dissertation eingereicht.

CONTENTS

Zusammenfassung	v
Abstract	vii
Eidesstattliche Erklärung	ix
Contents	xi
Chapter 1. Introduction	1
1.1 Quantum Many-Body Systems out of Equilibrium	1
1.2 Universality in Non-Equilibrium Stationary States	6
1.3 Non-Equilibrium Field Theory and the Functional Renormalization Group	8
1.4 Outline of this Thesis	9
I Dynamical Critical Phenomena in Driven-Dissipative Systems	19
Chapter 2. Publication: Dynamical Critical Phenomena in Driven-Dissipative Systems	21
2.A Open system dynamics	27
2.B Functional Renormalization group equation	28
2.C The second variational derivative	29
2.D The regulator function	30
2.E Flow of the effective potential	30
2.F Flow of the inverse propagator	31
2.G Rescaled flow equations	32
2.H Critical properties	33
2.I Ginzburg Criterion	34

Chapter 3. Publication: Nonequilibrium functional renormalization for driven-dissipative Bose-Einstein condensation	39
3.1 Introduction	40
3.2 Key Results and physical picture	42
3.3 The Model	47
3.3.1 Quantum Master equation	47
3.3.2 Keldysh functional integral	49
3.3.3 Effective action	52
3.4 Preparatory Analysis	53
3.4.1 Mean-field theory	53
3.4.2 Infrared divergences near criticality	54
3.4.3 Canonical power counting	56
3.4.4 Equilibrium symmetry	57
3.5 Functional Renormalization Group	58
3.5.1 FRG approach for the Keldysh effective action	58
3.5.2 Truncation	59
3.6 Relation to equilibrium dynamical models	64
3.6.1 Model A with $N = 2$ and reversible mode couplings (MAR)	65
3.6.2 Truncation for MAR	66
3.6.3 Fluctuation-dissipation theorem	66
3.6.4 Geometric interpretation of the equilibrium symmetry	67
3.7 Non-Equilibrium FRG flow equations	68
3.8 Scaling solutions	72
3.8.1 Scaling form of the flow equations	72
3.8.2 Gaussian fixed point	73
3.8.3 Wilson-Fisher fixed point: critical behavior	73
3.9 Numerical integration of flow equations	78
3.10 Conclusions	83
3.A Markovian dissipative action	84
3.A.1 Translation table: Master equation vs. Keldysh functional integral	84
3.A.2 Derivation in the Keldysh setting	85
3.B Symmetry constraints on the action and truncation for MAR	89
3.C Non-Equilibrium FRG flow equations	89

3.C.1	Expansion in fluctuations	90
3.C.2	Flow equation for the effective potential	92
3.C.3	Flow equation for the inverse propagator	95
3.C.4	Computation of gradient coefficient anomalous dimensions	96

II Universality in Driven-Dissipative Systems in Reduced Dimensions 105

Chapter 4. Publication: Two-dimensional superfluidity of exciton-polaritons requires strong anisotropy 107

4.1	Introduction	107
4.2	Model	109
4.3	Mapping to a KPZ equation	110
4.4	Isotropic systems	112
4.5	Strong anisotropy	115
4.6	Outlook	117
4.7	Acknowledgements	117
4.A	Mapping to the Kardar-Parisi-Zhang equation	118
4.B	Polariton condensate model with reservoir	118

Chapter 5. Additional Material: Superfluidity in Driven-Dissipative Systems 125

5.1	Introduction	125
5.2	Superfluidity in systems without particle number conservation	127
5.3	Model	130
5.3.1	Quantum master equation and Keldysh action	130
5.3.2	Current in open systems	132
5.3.3	Density-phase representation of the Keldysh action	138
5.4	Superfluid density of a driven-dissipative condensate	141
5.5	The influence of topological defects	149
5.A	Equilibrium symmetry in the density-phase representation	151
5.B	Retarded response functions in the Keldysh formalism	154
5.C	Density-phase representation for a weakly interaction Bose gas	155

Chapter 6. Publication: Scaling properties of one-dimensional driven-dissipative condensates	161
6.1 Introduction	161
6.2 Model and Theoretical Approach	162
6.3 Scaling properties of the phase correlations	164
6.3.1 KPZ exponents	164
6.3.2 Crossover time scale	166
6.4 Scaling of the condensate field correlations	166
6.4.1 Spatial correlations	167
6.4.2 Temporal correlations	167
6.5 Predictions for experimental observation	168
6.6 Conclusions and Outlook	170
6.A Extraction of α, β , and t_c	171
6.A.1 Static roughness exponent α	171
6.A.2 Dynamical growth exponent β and cross over time scale t_c	171
III Thermodynamic Equilibrium as a Symmetry of the Keldysh Action	175
Chapter 7. Additional Material: Thermodynamic Equilibrium as a Symmetry of the Keldysh Action	177
7.1 Introduction	177
7.2 Symmetry transformation	179
7.3 Invariance of Keldysh action	182
7.3.1 Invariance of Hamiltonian dynamics	182
7.3.2 Dissipative contributions in equilibrium	185
7.3.3 Classical limit, detailed balance and microreversibility	188
7.4 Physical interpretation	191
7.4.1 Multi-time correlation functions in the Keldysh formalism	192
7.4.2 Time reversal	194
7.4.3 KMS condition	195
7.4.4 From KMS to a symmetry of the Keldysh action	199
7.5 Examples	200
7.5.1 Single-particle fluctuation-dissipation relation	200
7.5.2 Non-equilibrium nature of steady states of quantum master equations	201
7.6 Conclusions	204

Contents	xv
Acknowledgments	209
Curriculum Vitae	211

CHAPTER 1

INTRODUCTION

In this chapter we introduce the main topics of the thesis and put them into a broader context. We begin with a brief overview of the field of quantum many-body systems out of thermodynamic equilibrium in Sec. 1.1, which motivates the questions that are addressed in subsequent chapters. In particular, we shall be interested in *universal aspects* of condensation phenomena in driven-dissipative systems. The notion of universality is briefly discussed in Sec. 1.2. Studying this problem theoretically requires specific tools, and the development of an appropriate formalism has been a major part of the work that is documented in this thesis. This aspect is touched upon in Sec. 1.3. Finally, an outline of the following chapters is given in Sec. 1.4.

1.1 Quantum Many-Body Systems out of Equilibrium

In recent years, the field of quantum many-body systems out of thermodynamic equilibrium has gained strong and ever-growing interest. Various aspects have been studied, e.g., thermalization or the absence of thermalization in the unitary dynamics of *closed* systems following a quench [1, 2]. On the other hand, a crucial feature that has been explored in *open* systems is the interplay between coherent and driven-dissipative dynamics. In fact, while dissipation has often been perceived merely as a hindrance for investigating, in particular, *quantum* aspects of experimental setups, studies showed that it can actually be turned into a powerful resource for applications such as state preparation and quantum computation in various contexts, including cold atoms [3–5] and photons [6]. In these studies, the key idea is to *design* the time evolution of the system, using Hamiltonian and dissipative contributions as basic building blocks of the generator of the dynamics in such a way that in the long-time limit the system reaches a non-equilibrium stationary state with the desired qualities, e.g., specific forms of order [7–10] or topological properties [11, 12]. The topics studied in subsequent chapters are to a large extent situated in the field of quantum many-body systems out of equilibrium. Let us, therefore, in the following briefly review some of the recent theoretical and experimental highlights in this area of physics, and the questions that arise in this context.

The prime candidates for studying *dynamics in closed quantum systems* [1, 2] are experiments with cold atoms, which provide excellent control over all relevant parameters during all steps of an experimental sequence [13]. In particular, the time evolution of the system under study can be engineered, since on the one hand the Hamiltonian governing the dynamics is known precisely (which is often not the case, e.g., in solid state systems), and on the other hand the parameters in this Hamiltonian can be tuned on demand, e.g., using Feshbach resonances [14]. This puts cold atoms in an

ideal position to address questions such as whether the dynamics of a closed quantum system following a quench, i.e., a sudden or slow change in the parameters of the Hamiltonian of the system, leads to a thermal stationary state. Spectacular experiments have shown the absence of thermalization in integrable systems [15, 16], in which an extensive number of local integrals of motion strongly constrain the precise form of the stationary state. As a result, the latter is not a Gibbs thermal state, but rather described by what is known as generalized Gibbs ensemble [17–19]. Adding a small non-integrable contribution to the Hamiltonian causes the system to eventually thermalize, however, only after passing through a quasistationary *pre-thermal* regime [20], which was observed in a series of experiments performed by the group of Jörg Schmiedmayer [21–23]. While integrability is trivially guaranteed in non-interacting systems, generic interactions often break integrability. However, even interacting quantum many-body systems can under certain conditions be prevented from thermalizing by subjecting them to sufficiently strong disorder, which causes them to enter a many-body localized phase (for a review see Ref. [24]). This has been demonstrated in a recent experiment with cold atoms carried out by the group of Immanuel Bloch [25].

A crucial aspect for the experiments with cold atoms mentioned above is the almost perfect isolation of the sample from the enclosing environment. Indeed, the introduction of a coupling between the system and its surroundings in a controlled manner opens up the possibility to study a plethora of entirely new and intriguing phenomena. For example, by immersing a Bose-Einstein condensate into a high-finesse optical cavity, strong matter-light coupling has been achieved, which led to the realization of open Dicke models [26–28]. The leakage of photons out of the cavity requires continuous replenishment in the form of laser driving. As a result the system reaches a steady state that is not thermodynamic equilibrium but rather characterized by the dynamical balance between pumping and losses. Therefore, this system is an instance of a qualitatively new class of quantum matter far from thermodynamic equilibrium, which challenges traditional boundaries between different areas of physics such as quantum optics, statistical physics, and condensed matter physics.

Since its very beginning, the field of quantum optics (for an introduction see, e.g., [29]) was concerned with the study of inherently lossy systems. This is due to the omnipresent continuum of modes of the electromagnetic field, which is responsible for the finite linewidth of transitions between different atomic or ionic states, and also cavity modes. The dynamics of these systems is thus bound to be decay to the vacuum, unless an externally imposed field such as a laser beam provides for a continuous source of energy. In experimental and theoretical studies in this field, focus is often put on carving out just what is *quantum* about quantum optics and thus comes as a surprise to a mindset that is used to walk the beaten paths of classical electrodynamics. An example for distinctly quantum aspects of the light field are Fock states or number states, in particular those containing only a small number of excitations, which should be contrasted with coherent states, characterized by occupation numbers that are so high that the addition or removal of a single excitation is but a negligible disturbance—this can be regarded as the very definition of a classical state of the electromagnetic field, and is realized, e.g., in the output of a laser. The qualitative difference between classical and quantum states of light is revealed in their coherence properties: while the intensity correlations of a thermal light source exhibit photon bunching (this is known as the Hanbury Brown and Twiss effect) and those of a laser are completely flat, photon antibunching was observed for single-photon sources, which is considered a clear signature of the quantumness of such a source. In other words, the question whether a given state of the electromagnetic field is quantum or not is decided by considering the statistics of the photon number distribution.

A different notion of statistics is commonly employed in statistical physics, which is the study of

systems with a large number of degrees of freedom. However, concepts of this field can also be important for quantum optics, e.g., in the context of the Bose-Einstein condensation (BEC) of photons in an optical microcavity shown in a recent experiment performed by the group of Martin Weitz [30]. An example for such a concept is the idea that conserved quantities, due to a lack of knowledge of the microstate, are fixed in the description of the macrostate only on average by means of Lagrangian multipliers—in the case of the number of particles, this Lagrangian multiplier is just the chemical potential. Concerning photons, it is far from obvious how a finite and perhaps even externally tunable chemical potential can be realized in practice (a cleverly devised scheme was recently proposed in [31]). This, however, is a prerequisite for achieving a BEC: in the textbook problem of blackbody radiation, i.e., radiation in thermal equilibrium with the walls of the confining cavity, upon lowering the temperature photons simply disappear instead of piling up in the ground state as would be the signature of BEC. In the experiment [30], the solution to this problem was found by placing the photon gas inside a high-finesse optical microcavity, which acts as a “white-wall box,” and filling the cavity with a droplet of dye, thus providing the non-linear medium necessary for the photons to thermalize. At the point where non-linearities – or interactions – enter the game, a new source of correlations, qualitatively different from those due to the statistics of the constituent particles leading, e.g., to the effects of photon bunching and antibunching discussed above, is introduced, and the venue of condensed matter physics is entered.

These considerations highlight one of the main challenges in the study of quantum many-body systems out of equilibrium: it is a highly interdisciplinary field and calls for the merging of ideas, concepts, and both theoretical and experimental techniques from a wide range of areas of physics. In order to corroborate this point, let us consider some further examples.

In experiments with trapped ions [32], the number of particles involved has been scaled up over the years, and these systems are now at the verge of acquiring a true many-body character. In particular, trapped ions can be utilized as digital or analog quantum simulators [33], allowing for the realization, e.g., of spin models such as the two-dimensional Ising model [34]. While the dynamics of a single ion interacting with the electromagnetic field is clearly an atomic physics and quantum optics problem, as soon as the number of these elementary building blocks is increased to tens or even hundreds [34] and they are made to interact, considerations of condensed matter physics start to play a role. Another experimental platform that started out in the past with the study of small systems and is now being extended to include a larger number of constituents, are optomechanical setups [35–37], in which mechanical degrees of freedom are coupled to the light field, e.g., by allowing one of the mirrors that form a cavity to oscillate. A third example in which the elementary constituents of a system with many interacting degrees of freedom involve quantum optical building blocks are arrays of microcavities coupled to superconducting circuits [38–42]. Here a single site of the array, i.e., a basic circuit-quantum electrodynamical element, is described by the Jaynes-Cummings model—again an ubiquitous textbook problem in quantum optics [29]. The combination of many of these elements in a lattice, however, realizes a dissipative Bose-Hubbard model, the closed system version of which has become paradigmatic in condensed matter physics.

Let us reiterate that all of these examples are generically open systems, for the simple reason that excited states of ions and photons trapped in a cavity cannot be decoupled from the surrounding electromagnetic field and thus have only a finite lifetime. The latter is also true of quasiparticle excitations such as magnons, which nevertheless have been reported to exhibit BEC [43] in a non-equilibrium regime where losses are compensated by pumping. This gives confidence that BEC out of equilibrium might also be reached in other systems, e.g., excitons in semiconductors. Even cold atoms might be

made to condense in this intriguing non-equilibrium regime if three-body losses are counteracted by continuous loading [44]. However, at present the prime example exhibiting condensation phenomena in a non-equilibrium steady state are exciton-polaritons in semiconductor microcavities. Indeed, these systems seem to be the most promising when it comes to realizing the physics discussed in subsequent chapters of this thesis. Let us, therefore, review briefly some of their properties [45–47].

Microcavity polaritons are hybrid quasiparticles, composed of matter and light. The matter component is a Wannier-Mott exciton, and is coupled strongly to a photon confined in a semiconductor microcavity. An exciton is an excitation above the vacuum state of a semiconductor, which is created when an electron from the filled valence band absorbs enough energy to enter the empty conduction band and forms – under the influence of the attractive Coulomb force – a bound state with the hole that is left in the valence band upon removal of the electron, in close analogy to a hydrogen atom consisting of a bound electron-proton pair. However, the Bohr radius of an exciton is about $10 - 100 \text{ \AA}$, i.e., it is much larger than that of the hydrogen atom, and extends over tens of atomic sites in the crystal. Nevertheless, excitons can still be considered as elementary bosonic objects as long as their mean distance is larger than the exciton Bohr radius [46]. When excitons are confined in a quantum well (QW) to a thin layer with a thickness comparable to the exciton Bohr radius, their motion along the (transverse) confinement direction is quantized. Then, QW excitons behave as two-dimensional quasiparticles if the spacing between the lowest and the first excited state of the transverse motion is large enough to ensure that only the ground state is populated.

The positive and negative charges of the hole and electron, respectively, form a dipole that can interact with the electromagnetic field, and indeed the enhanced spatial overlap of the bound pair forming the exciton as compared to an unbound electron and hole results in an increase of the matter-light coupling. However, strong coupling (in a sense to be defined below) can be achieved only if in addition the photon is confined in the direction perpendicular to the QW by means of a microcavity. In typical experiments, the latter is formed by two distributed Bragg reflectors, i.e., alternating layers of high and low refractive index, which act as high-reflectance mirrors. Around the center of the cavity, where the electromagnetic field is concentrated, its amplitude is increased by a factor of up to 20 [46], and the QW is placed precisely in such an antinode of the light field. The regime of strong coupling is reached when the time scale associated with the coupling strength between photons and excitons becomes much faster than both the rate at which photons are lost from the cavity due to mirror imperfections and the non-radiative decay rate of excitons. Under these conditions, excitons and photons hybridize to form new bosonic quasiparticles called exciton-polaritons. In particular, excitons in the QW couple to photons with exactly the same in-plane momentum, creating two modes known as upper and lower polaritons. The fractions at which matter and light components contribute to the polaritons are referred to as the Hopfield coefficients, X and C , respectively. As a result of this specific mixture, polaritons inherit properties from both of their constituents, as we describe in the following.

The transverse (i.e., along the cavity axis) confinement leads for small momenta to a quadratic dispersion relation regarding the in-plane motion of the photons. In other words, the photons acquire an effective mass, which is typically of the order of $m_{\text{photon}} \approx 10^{-5} m_e$, where m_e is the mass of the electron, and thus much smaller than the mass of QW excitons, which is $m_{\text{exciton}} \approx 10^4 m_{\text{photon}}$. Since the sum of the inverse exciton and photon masses, weighted by the corresponding Hopfield coefficients, determines the mass of lower polaritons, the latter is approximately given by $m_{\text{LP}} \approx m_{\text{photon}} / |C|^2$, i.e., it is of the same order of magnitude as the photon mass. The decay rates of excitons and photons, on the other hand, add up linearly to yield the decay rate of the lower polariton. However,

since typically photons have a much shorter lifetime, which is of the order of 1 ps to several 10 ps in contrast to the excitonic lifetime of typically 1 ns, again the value corresponding to the photonic component essentially determines the lifetime of the lower polaritons, and the strong coupling regime is characterized by the exciton-photon coupling being much bigger than this value.

While single-particle properties of lower polaritons are mainly inherited from the photons, the interactions between polaritons stem primarily from the screened Coulomb interactions between electrons and holes forming the excitons [45]. In fact, the binary photon-photon interactions, which are due to third-order nonlinearities proportional to the $\chi^{(3)}$ nonlinear polarizability of the material from which the QW is made, are much weaker than the Coulomb interactions. The latter, in the low-energy scattering regime where relative wave vectors are much smaller than the exciton Bohr radius, can again be described accurately by a two-body contact interaction. Another effective quartic interaction channel originates from the Pauli exclusion principle for electrons and holes, which excludes that an additional exciton can be created at a distance shorter than the Bohr radius from an existing exciton with the same spin. However, typically this contribution is significantly smaller than the one from the electrostatic interaction [45]. An intriguing possibility is to exploit the fact that polaritons exist in distinct spin states in order to realize a polaritonic Feshbach resonance, as was demonstrated experimentally in Ref. [48].

From an experimental point of view, a very attractive feature of microcavity polaritons is their high optical accessibility [46]. In fact, when a polariton decays, a photon with the same in-plane momentum and total energy is emitted from the cavity, providing directly measurable information on the polariton field: from near and far field measurements, the real-space and momentum-space densities, respectively, can be extracted, while interferometric measurements yield the coherence properties of the polariton field. On the other hand, the finite decay rate of polaritons makes it necessary to continuously feed the system with energy in order to maintain a finite polariton population in steady state. In experiments, different pumping schemes have been realized. A first option is to inject energy coherently into the cavity, i.e., to resonantly drive a lower polariton state with a specific momentum and energy. In this way, high occupations of this particular state can be achieved, or in other words, a polariton condensate at a finite momentum can be created. Even more intriguingly, in the coherent pumping scheme the phase – and hence coherence – of the driving laser field is imprinted on the polariton field. This can be utilized to create on demand, e.g., finite angular momentum states of the polariton field by using Laguerre-Gauss beams as has been shown in experiments conducted by the group of Alberto Bramati [49]. The drawback of the coherent pumping scheme is that the phase rotation symmetry of the dynamics of the polariton field, which is crucial for many aspects in the study of condensation physics with polaritons, is broken explicitly. An alternative approach is to use a laser that is far blue-detuned from the bottom of the lower polariton band. During the relaxation of the thus created high-energy excitations, which is caused by phonon-polariton and stimulated polariton-polariton scattering, coherence is quickly lost. The effective dynamics of the low-momentum component of the lower polariton field can be described by a phenomenological model that is introduced in Ref. [50] and involves a dissipative Gross-Pitaevskii equation for the condensate dynamics that is coupled to a rate equation for the reservoir of high-energy excitations. A crucial aspect of this model is that the equations are invariant under phase rotations of the polariton field, which opens the possibility of spontaneous symmetry breaking in a condensation transition out of equilibrium [51–55]. An intriguing question that arises naturally in this context and to which major parts of this thesis are devoted is which kind of new universal behavior can emerge under such conditions. To make this question more precise, let us move on to discuss the notion of universality.

1.2 Universality in Non-Equilibrium Stationary States

In a broad sense, universality means that very distinct physical systems can – under specific conditions – show exactly the same behavior. To be more precise, the dependence of certain observables on the scale at which the system is viewed, is found to be given by power laws with exponents that take the same values for all systems belonging to the same *universality class*. However, this power-law dependence is found only on *large* scales, i.e., at scales on which the dynamics of the system is best described in a coarse-grained picture by, e.g., slowly fluctuating order parameter fields, rather than by keeping track of individual collisions of atoms or the like. Such microscopic processes are washed out if the system is viewed on larger scales, and the question arises which, if any, properties of the underlying microscopic dynamics survive the process of coarse graining and determine the observable behavior of the system on macroscopic scales. The remarkable answer to this question is that in systems with short-range interactions, the symmetries of the microscopic dynamics and the spatial dimensionality completely determine the universality class, which might thus comprise a large number of vastly different physical systems. This in turn indicates that the number of different universality classes is low. Therefore, each instance of novel universal behavior should definitely be considered as a remarkable discovery.

At present, various conditions are known under which universal scaling behavior can be observed. The most prominent example is certainly the tuning of system parameters close to a second order phase transition [56, 57], at which a mass scale vanishes, leading to diverging perturbative corrections. Critical scaling behavior at such a transition has been investigated extensively in thermodynamic equilibrium in classical and quantum systems, and a full classification of dynamical critical behavior in the classical case has been given already in the 1970s [58]. Associated with such *static* phase transitions in equilibrium are often *dynamical out-of-equilibrium* transitions, which become apparent in the dynamics of the system following a quench across a critical point, both at short [59, 60] and long times [61–63], and also in this case universal scaling behavior can be observed. An example for a non-equilibrium phase transition that does not have a counterpart in thermodynamic equilibrium is the roughening transition in the Kardar-Parisi-Zhang (KPZ) equation in $d \geq 3$ spatial dimensions [64] (for reviews see [65] and [66]). The KPZ universality class has become paradigmatic in non-equilibrium statistical mechanics, since it might be considered as the simplest model leading to non-trivial non-equilibrium scaling behavior. Unlike dynamical critical behavior at a second ordered phase transition, which is induced by the vanishing of a mass scale, in the case of the KPZ equation scaling behavior at long scales and long times is realized generically, i.e., even away from the critical point in the stable phases, since it is a massless model. This is to some extent similar to ordered phases that spontaneously break continuous symmetries: according to the Goldstone theorem, the symmetry breaking leads to the appearance of massless modes. The existence of a Goldstone mode in the low-temperature phase of the two-dimensional XY-model results in scaling behavior of spatial correlations in the whole phase, i.e., from zero temperature up to the critical one. Another example of universal scaling behavior in out-of-equilibrium dynamics is given by the non-thermal fixed points investigated in Refs. [67–75].

A major part of this thesis is dedicated to the study of non-equilibrium dynamical critical behavior at a driven-dissipative condensation transition in three spatial dimensions and the universal long-distance and long-time scaling behavior of correlations in the condensed phase in one and two-dimensional systems. Originally, non-equilibrium universal behavior has been found in several classical systems, examples including models with spatially anisotropic temperature distributions [76],

the driven-diffusive lattice gas [77], reaction-diffusion systems [78–81], the problems of directed percolation [82, 83] and self-organized criticality [84], and surface roughening phenomena, which are described by the KPZ equation.

As pointed out above, the universality class of a system with short-range interactions is determined solely by the spatial dimension and symmetries. Interestingly, also the difference between equilibrium and non-equilibrium stationary states can be traced back to a particular symmetry, which has been studied in the context of classical dynamical models in the past [85–88] and is extended to the quantum case in Chapter 7 below. As we show there, the absence of the symmetry in non-equilibrium stationary states is due to the different and completely independent physical origin of coherent and driven-dissipative dynamics: while the former is generated by the system Hamiltonian, the latter – in the case we consider in Parts I and II – encodes particle loss and pumping. In addition, these processes break the phase-rotation symmetry associated with particle number conservation, which is present in microscopic models of BEC in thermodynamic equilibrium, described by model F in the standard classification [58]. The combination of the breaking of equilibrium and phase-rotation symmetries lies at the heart of the universal non-equilibrium behavior studied in this thesis.

As anticipated in the previous section, exciton-polaritons in semiconductor microcavities are the prime experimental implementation of non-equilibrium BEC physics. Indeed, in these systems losses and pumping are naturally present due to the decay of cavity photons and laser driving. The specific driving scheme used in an experiment, however, has to ensure that the effective pumping of lower polaritons with small in-plane momentum is incoherent: only when the coherence of the laser is not forced onto the polariton field, is there still a specific kind of phase rotation symmetry intact, which is as we discuss in Chapter 5 different from the one associated with particle number conservation, and allows for a second order condensation transition that involves the spontaneous breaking this symmetry. The main challenge in exploring the physics discussed theoretically in this thesis experimentally in exciton-polariton systems lies in the fact that the large scales at which scaling behavior sets in are hard to reach in such experiments. This is partly due to difficulties associated with extending the effective system size, which is delimited by the laser pumping spot, while avoiding the overheating of the sample. In addition, disorder that hinders polariton condensation [45, 89, 90] cannot be eliminated completely. Strategies to circumvent these problems are discussed in Chapters 4 and 6. Apart from exciton-polaritons, there are various other experimental platforms in which the universal physics of driven-dissipative BEC could be studied. For the example of microcavity arrays, an incoherent pumping scheme has been proposed recently [91].

Thus, the experimental prospects for observing universality out of equilibrium seem promising. Making precise predictions, e.g., for the parameter regime an experiment should encompass and the observables that should be considered, requires sophisticated theoretical methods. The development of such tools has been an integral part of the work documented in this thesis, and we proceed to discuss this aspect in the following section.

1.3 Non-Equilibrium Field Theory and the Functional Renormalization Group

Since the pioneering work of Kenneth G. Wilson [92], the theoretical investigation of universal behavior in condensed matter physics has been the success story of renormalization group methods.

Modern variants of the latter are often based on the formalism of quantum field theory, and accordingly a substantial part of this thesis is concerned with developing a description of open Markovian quantum many-body systems in terms of the Keldysh functional integral technique (for an introduction see, e.g., Refs. [93] or [94]). Here we briefly summarize our advances in this area and point out relations to the existing literature.

We have already remarked in Sec. 1.1 that dynamics which results from the combination of coherent and driven-dissipative contributions is ubiquitous in quantum optics, and researchers in this field have come up with various ideas to tackle such problems theoretically. One paradigmatic approach is the use of quantum master equations, formulated in terms of second-quantized operators [29]. In this framework, we devise a simple model for a driven-dissipative condensate in Part I of this thesis. The crucial step that makes this model accessible to renormalization group techniques, and thus allows us to address universal critical phenomena, is to translate the resulting master equation into an equivalent Keldysh functional integral. This approach may be further generalized and applied to a large variety of other non-equilibrium situations [95–97].

In Parts I and II of this thesis we show that in order to describe the long-wavelength dynamics of a driven-dissipative condensate it is sufficient to consider the classical limit of the Keldysh action. In this limit the Keldysh formalism is reduced to the Martin-Siggia-Rose technique (for an introduction see, e.g., Ref. [98]), which was originally devised as an efficient description of the stochastic dynamics of classical systems in thermodynamic equilibrium. To deal with such problems the Martin-Siggia-Rose formalism allows to derive perturbation theory in the compact notation of Feynman diagrams, and it lends itself naturally to the application of renormalization group techniques such as the functional renormalization group (for reviews see Refs. [99–103]) based on the Wetterich equation [104]. We employ this method in the study of dynamical critical behavior at the driven-dissipative condensation transition in Chapters 2 and 3. The results we report in these chapters were fully confirmed and further developed in a recent complementary perturbative field theoretical study [105]. In the past, the functional renormalization group has already been used in combination with the Keldysh and Martin-Siggia-Rose formalisms to study dynamical critical behavior in classical systems in [106, 107] and out of thermodynamic equilibrium [81, 108–113], as well as to characterize stationary transport solutions corresponding to non-thermal fixed points [67, 68], to derive dynamical equations [114], and to calculate transport properties [115–117]. A short introduction to this technique in the context of dynamical critical behavior at the driven-dissipative condensation transition is provided in Chapter 3.

Apart from providing a suitable framework for applying renormalization group techniques, a description of open Markovian quantum many-body systems based on Keldysh non-equilibrium field theory has the additional advantage of allowing for an efficient discussion of symmetries and their consequences. In particular, the thermalization at low frequencies we find in the course of our analysis of dynamical critical behavior in the driven-dissipative BEC transition in three-dimensional systems in Part II is reflected in the emergence of the equilibrium symmetry that distinguishes thermodynamic equilibrium from non-equilibrium conditions mentioned in the previous section. To be precise, the long-wavelength effective action at the critical point turns out to be invariant under the form of the symmetry transformation suitable for *classical* statistical mechanical systems. In Part III of this thesis we derive – again relying on peculiarities of the Keldysh formalism at crucial points – the corresponding equilibrium symmetry transformation for *quantum* systems, and we show that it is equivalent to the Kubo-Martin-Schwinger condition for thermodynamic equilibrium [118–120]. By contrast, in the classical context [85–88] the symmetry transformation is commonly regarded as a manifestation of time-reversal invariance. Thus, we establish a surprising link between the Kubo-

Martin-Schwinger condition and time-reversal invariance in classical statistical systems. Moreover, we establish a connection between different forms of the symmetry and the problem of thermalization of closed quantum systems mentioned in Sec. 1.1.

1.4 Outline of this Thesis

In large part, this thesis is a collection of articles which have already been published in peer-reviewed journals or which are available as preprints on arXiv.org. The reprints differ slightly from the originally published articles for editorial reasons. At the beginning of each chapter, a footnote points out the contributions by the author of the present thesis. Chapters 5 and 7 contain additional unpublished material.

This thesis is divided into three parts. In Part I we explore the nature of the driven-dissipative BEC transition in three spatial dimensions using a functional renormalization group approach formulated in terms of the Keldysh non-equilibrium field theory. We find that at the point of the transition the equilibrium symmetry mentioned in Sec. 1.3 is emergent at low-frequencies, and as a result the dynamics in this regime follows a classical fluctuation-dissipation relation. Consequently, the common static exponents as well as the dynamical critical exponent are the same as in the corresponding equilibrium model without particle number conservation termed model A* [121, 122]. The non-equilibrium conditions are encoded in an additional independent critical exponent, which describes decoherence and the approach to effective equilibrium at low frequencies. These results are presented in Chapter 2, which is a reprint of the publication

- *Dynamical Critical Phenomena in Driven-Dissipative Systems*
L. M. Sieberer, S. D. Huber, E. Altman, and S. Diehl
Phys. Rev. Lett., **110**, 195301 (2013).

Details of the theoretical approach as well as numerical solutions to the renormalization group flow equations are reported in Chapter 3. The content of this chapter is also available as the journal article

- *Nonequilibrium functional renormalization for driven-dissipative Bose-Einstein condensation*
L. M. Sieberer, S. D. Huber, E. Altman, and S. Diehl
Phys. Rev. B, **89**, 134310 (2014).

In Part II of the thesis, we turn our attention to driven-dissipative systems in reduced dimensions, which is the scenario most relevant for experiments with exciton-polaritons. Then, the same non-equilibrium fluctuations that drive critical behavior at the condensation transition in three dimensions have much more profound implications: indeed, already in homogeneous two-dimensional Bose systems in equilibrium, long-range order in the low-temperature phase is destroyed by fluctuations of the Goldstone mode, and correlations decay algebraically instead of approaching a constant value at large distances as in three spatial dimensions. More drastically, under non-equilibrium conditions such fluctuations lead to stretched-exponential or potentially even faster decay of the static correlations, and a phase with algebraic order can only be observed in a strongly anisotropic driven-dissipative system. These results are derived by mapping the long-wavelength condensate dynamics to the anisotropic KPZ equation as discussed in Chapter 4, which is a reprint of the article

- *Two-Dimensional Superfluidity of Exciton-Polaritons Requires Strong Anisotropy*
E. Altman, L. M. Sieberer, L. Chen, S. Diehl, and J. Toner
Phys. Rev. X, **5**, 011017 (2015).

The contents of Chapters 2, 3, and 4 will be reviewed in a chapter of the book “Universal Themes of Bose-Einstein Condensation,” edited by David Snoke, Nikolaos Proukakis, and Peter Littlewood [123].

While the order parameter vanishes in the low-temperature phase of a two-dimensional homogeneous Bose system in thermodynamic equilibrium, such a system is nevertheless superfluid. Thus, a natural question is whether the same is true of a driven-dissipative condensate. In Chapter 5, we show that in spite of the absence of algebraic order a finite superfluid density, which we identify by means of the retarded current-current response, may still survive under non-equilibrium conditions. Our approach does not take into account topological defects in the phase of the condensate and is thus valid only when the density of the latter is sufficiently low. The intriguing question whether there is a vortex-unbinding transition out of equilibrium goes beyond the scope of this thesis. To answer this question, one would have to explicitly incorporate topological defects in a renormalization group approach, which has shown to be difficult since the KPZ equation for the phase of the order parameter is non-linear. Alternatively, one could numerically simulate the complex Ginzburg-Landau equation, which describes the long-wavelength condensate dynamics. Results of such simulations – as a first step only for one-dimensional systems though – are presented in Chapter 6, which is also available on arXiv.org as

- *Scaling properties of one-dimensional driven-dissipative condensates*
L. He, L. M. Sieberer, E. Altman, and S. Diehl
arXiv:1412.5579 (2014),

and at the time of writing being reviewed for publication. The numerical investigations of coherence properties of the condensate field and its phase presented in this chapter fully confirm the expectations based on the mapping of the long-wavelength dynamics of the condensate to the KPZ equation. In particular, they show that KPZ physics should be accessible to current experimental setups with exciton-polaritons.

We are leaving the field of driven-dissipative condensates and move on to consider a property present only in systems that reside in thermodynamic equilibrium in Part III. To be specific, we give an extensive discussion of the equilibrium symmetry already mentioned above regarding the Keldysh action describing a quantum many-body system in thermodynamic equilibrium. This includes a derivation of the symmetry transformation, which is shown to be equivalent to the Kubo-Martin-Schwinger condition [118–120]. Moreover, we demonstrate that the fluctuation-dissipation relations characterizing the linear response of a system to external perturbations at equilibrium can be derived as a consequence of this symmetry. This means that the symmetry provides an efficient check for thermodynamic equilibrium conditions, making the explicit calculation of fluctuation-dissipation relations unnecessary. The results presented in this chapter form the basis for a preprint that is currently being written.

Bibliography

- [1] A. Polkovnikov, K. Sengupta, A. Silva, and M. Vengalattore, “Colloquium: Nonequilibrium dynamics of closed interacting quantum systems,” Rev. Mod. Phys. **83**, 863 (2011).

- [2] T. Langen, R. Geiger, and J. Schmiedmayer, “Ultracold Atoms Out of Equilibrium,” *Annu. Rev. Condens. Matter Phys.* **6**, 150112144536003 (2014).
- [3] S. Diehl, A. Micheli, A. Kantian, B. Kraus, H. P. Büchler, and P. Zoller, “Quantum states and phases in driven open quantum systems with cold atoms,” *Nat. Phys.* **4**, 878 (2008).
- [4] F. Verstraete, M. M. Wolf, and J. Ignacio Cirac, “Quantum computation and quantum-state engineering driven by dissipation,” *Nat. Phys.* **5**, 633 (2009).
- [5] H. Weimer, M. Müller, I. Lesanovsky, P. Zoller, and H. P. Büchler, “A Rydberg quantum simulator,” *Nat. Phys.* **6**, 382 (2010).
- [6] M. Hafezi, P. Adhikari, and J. M. Taylor, “Engineering three-body interaction and Pfaffian states in circuit QED systems,” *Phys. Rev. B* **90**, 060503 (2014).
- [7] S. Diehl, A. Tomadin, A. Micheli, R. Fazio, and P. Zoller, “Dynamical Phase Transitions and Instabilities in Open Atomic Many-Body Systems,” *Phys. Rev. Lett.* **105**, 015702 (2010).
- [8] S. Diehl, W. Yi, A. J. Daley, and P. Zoller, “Dissipation-Induced d-Wave Pairing of Fermionic Atoms in an Optical Lattice,” *Phys. Rev. Lett.* **105**, 227001 (2010).
- [9] D. Marcos, A. Tomadin, S. Diehl, and P. Rabl, “Photon condensation in circuit quantum electrodynamics by engineered dissipation,” *New J. Phys.* **14**, 055005 (2012).
- [10] W. Yi, S. Diehl, A. J. Daley, and P. Zoller, “Driven-dissipative many-body pairing states for cold fermionic atoms in an optical lattice,” *New J. Phys.* **14**, 055002 (2012).
- [11] S. Diehl, E. Rico, M. A. Baranov, and P. Zoller, “Topology by dissipation in atomic quantum wires,” *Nat. Phys.* **7**, 971 (2011).
- [12] C.-E. Bardyn, M. A. Baranov, C. V. Kraus, E. Rico, A. Imamoglu, P. Zoller, and S. Diehl, “Topology by dissipation,” *New J. Phys.* **15**, 085001 (2013).
- [13] I. Bloch, J. Dalibard, and W. Zwerger, “Many-body physics with ultracold gases,” *Rev. Mod. Phys.* **80**, 885 (2008).
- [14] C. Chin, R. Grimm, P. Julienne, and E. Tiesinga, “Feshbach resonances in ultracold gases,” *Rev. Mod. Phys.* **82**, 1225 (2010).
- [15] T. Kinoshita, T. Wenger, and D. S. Weiss, “A quantum Newton’s cradle.” *Nature* **440**, 900 (2006).
- [16] T. Langen, S. Erne, R. Geiger, B. Rauer, T. Schweigler, M. Kuhnert, W. Rohringer, I. E. Mazets, T. Gasenzer, and J. Schmiedmayer, “Experimental Observation of a Generalized Gibbs Ensemble,” arXiv:1411.7185 (2014).
- [17] M. Rigol, V. Dunjko, V. Yurovsky, and M. Olshanii, “Relaxation in a Completely Integrable Many-Body Quantum System: An AbInitio Study of the Dynamics of the Highly Excited States of 1D Lattice Hard-Core Bosons,” *Phys. Rev. Lett.* **98**, 050405 (2007).
- [18] A. Iucci and M. A. Cazalilla, “Quantum quench dynamics of the Luttinger model,” *Phys. Rev. A* **80**, 063619 (2009).

- [19] T. Barthel and U. Schollwöck, “Dephasing and the Steady State in Quantum Many-Particle Systems,” *Phys. Rev. Lett.* **100**, 100601 (2008).
- [20] J. Berges, S. Borsányi, and C. Wetterich, “Prethermalization,” *Phys. Rev. Lett.* **93**, 142002 (2004).
- [21] T. Kitagawa, A. Imambekov, J. Schmiedmayer, and E. Demler, “The dynamics and prethermalization of one-dimensional quantum systems probed through the full distributions of quantum noise,” *New J. Phys.* **13**, 073018 (2011).
- [22] M. Gring, M. Kuhnert, T. Langen, T. Kitagawa, B. Rauer, M. Schreitl, I. Mazets, D. A. Smith, E. Demler, and J. Schmiedmayer, “Relaxation and prethermalization in an isolated quantum system.” *Science* **337**, 1318 (2012).
- [23] T. Langen, R. Geiger, M. Kuhnert, B. Rauer, and J. Schmiedmayer, “Local emergence of thermal correlations in an isolated quantum many-body system,” *Nat. Phys.* **9**, 640 (2013).
- [24] R. Nandkishore and D. A. Huse, “Many body localization and thermalization in quantum statistical mechanics,” arXiv:1404.0686 (2014).
- [25] M. Schreiber, S. S. Hodgman, P. Bordia, H. P. Lüschen, M. H. Fischer, R. Vosk, E. Altman, U. Schneider, and I. Bloch, “Observation of many-body localization of interacting fermions in a quasi-random optical lattice,” arXiv:1501.05661 (2015).
- [26] K. Baumann, C. Guerlin, F. Brennecke, and T. Esslinger, “Dicke quantum phase transition with a superfluid gas in an optical cavity.” *Nature* **464**, 1301 (2010).
- [27] F. Brennecke, R. Mottl, K. Baumann, R. Landig, T. Donner, and T. Esslinger, “Real-time observation of fluctuations at the driven-dissipative Dicke phase transition.” *Proc. Natl. Acad. Sci. U. S. A.* **110**, 11763 (2013).
- [28] H. Ritsch, P. Domokos, F. Brennecke, and T. Esslinger, “Cold atoms in cavity-generated dynamical optical potentials,” *Rev. Mod. Phys.* **85**, 553 (2013).
- [29] W. Vogel and D.-G. Welsch, *Quantum Optics*, 3rd ed. (Wiley-VCH, Weinheim, 2006).
- [30] J. Klaers, J. Schmitt, F. Vewinger, and M. Weitz, “Bose-Einstein condensation of photons in an optical microcavity.” *Nature* **468**, 545 (2010).
- [31] M. Hafezi, P. Adhikari, and J. M. Taylor, “A chemical potential for light,” arXiv:1405.5821 (2014).
- [32] R. Blatt and C. F. Roos, “Quantum simulations with trapped ions,” *Nat. Phys.* **8**, 277 (2012).
- [33] J. T. Barreiro, M. Müller, P. Schindler, D. Nigg, T. Monz, M. Chwalla, M. Hennrich, C. F. Roos, P. Zoller, and R. Blatt, “An open-system quantum simulator with trapped ions.” *Nature* **470**, 486 (2011).
- [34] J. W. Britton, B. C. Sawyer, A. C. Keith, C.-C. J. Wang, J. K. Freericks, H. Uys, M. J. Biercuk, and J. J. Bollinger, “Engineered two-dimensional Ising interactions in a trapped-ion quantum simulator with hundreds of spins.” *Nature* **484**, 489 (2012).

- [35] F. Marquardt and S. M. Girvin, “Optomechanics,” *Physics* (College Park, Md). **2**, 40 (2009).
- [36] D. E. Chang, A. H. Safavi-Naeini, M. Hafezi, and O. Painter, “Slowing and stopping light using an optomechanical crystal array,” *New J. Phys.* **13**, 023003 (2011).
- [37] M. Ludwig and F. Marquardt, “Quantum Many-Body Dynamics in Optomechanical Arrays,” *Phys. Rev. Lett.* **111**, 073603 (2013).
- [38] R. J. Schoelkopf and S. M. Girvin, “Wiring up quantum systems.” *Nature* **451**, 664 (2008).
- [39] J. Clarke and F. K. Wilhelm, “Superconducting quantum bits.” *Nature* **453**, 1031 (2008).
- [40] M. Hartmann, F. Brandão, and M. Plenio, “Quantum many-body phenomena in coupled cavity arrays,” *Laser Photonics Rev.* **2**, 527 (2008).
- [41] A. A. Houck, H. E. Türeci, and J. Koch, “On-chip quantum simulation with superconducting circuits,” *Nat. Phys.* **8**, 292 (2012).
- [42] S. Schmidt and J. Koch, “Circuit QED lattices: Towards quantum simulation with superconducting circuits,” *Ann. Phys.* **525**, 395 (2013).
- [43] S. O. Demokritov, V. E. Demidov, O. Dzyapko, G. A. Melkov, A. A. Serga, B. Hillebrands, and A. N. Slavin, “Bose-Einstein condensation of quasi-equilibrium magnons at room temperature under pumping.” *Nature* **443**, 430 (2006).
- [44] M. Falkenau, V. V. Volchkov, J. Rührig, A. Griesmaier, and T. Pfau, “Continuous Loading of a Conservative Potential Trap from an Atomic Beam,” *Phys. Rev. Lett.* **106**, 163002 (2011).
- [45] I. Carusotto and C. Ciuti, “Quantum fluids of light,” *Rev. Mod. Phys.* **85**, 299 (2013).
- [46] H. Deng, H. Haug, and Y. Yamamoto, “Exciton-polariton Bose-Einstein condensation,” *Rev. Mod. Phys.* **82**, 1489 (2010).
- [47] T. Byrnes, N. Y. Kim, and Y. Yamamoto, “Excitonpolariton condensates,” *Nat. Phys.* **10**, 803 (2014).
- [48] N. Takemura, S. Trebaol, M. Wouters, M. T. Portella-Oberli, and B. Deveaud, “Polaritonic Feshbach resonance,” *Nat. Phys.* **10**, 500 (2014).
- [49] T. Boulier, Q. Glorieux, E. Cancellieri, E. Giacobino, and A. Bramati, “Orbital angular momentum injection in a polariton superfluid.” in *SPIE OPTO*, edited by M. Razeghi, E. Tournié, and G. J. Brown (International Society for Optics and Photonics, 2015) p. 93702R.
- [50] M. Wouters and I. Carusotto, “Excitations in a Nonequilibrium Bose-Einstein Condensate of Exciton Polaritons,” *Phys. Rev. Lett.* **99**, 140402 (2007).
- [51] J. Kasprzak, M. Richard, S. Kundermann, A. Baas, P. Jeambrun, J. M. J. Keeling, F. M. Marchetti, M. H. Szymańska, R. André, J. L. Staehli, V. Savona, P. B. Littlewood, B. Deveaud, and L. S. Dang, “Bose-Einstein condensation of exciton polaritons.” *Nature* **443**, 409 (2006).

- [52] R. Balili, V. Hartwell, D. Snoke, L. Pfeiffer, and K. West, “Bose-Einstein condensation of microcavity polaritons in a trap.” *Science* **316**, 1007 (2007).
- [53] H. Deng, G. Solomon, R. Hey, K. Ploog, and Y. Yamamoto, “Spatial Coherence of a Polariton Condensate,” *Phys. Rev. Lett.* **99**, 126403 (2007).
- [54] G. Roumpos, M. Lohse, W. H. Nitsche, J. Keeling, M. H. Szymanska, P. B. Littlewood, A. Löffler, S. Höfling, L. Worschech, A. Forchel, and Y. Yamamoto, “Power-law decay of the spatial correlation function in exciton-polariton condensates.” *Proc. Natl. Acad. Sci. U. S. A.* **109**, 6467 (2012).
- [55] V. Belykh, N. Sibeldin, V. Kulakovskii, M. Glazov, M. Semina, C. Schneider, S. Höfling, M. Kamp, and A. Forchel, “Coherence Expansion and Polariton Condensate Formation in a Semiconductor Microcavity,” *Phys. Rev. Lett.* **110**, 137402 (2013).
- [56] J. Zinn-Justin, *Quantum Field Theory and Critical Phenomena*, 4th ed., International Series of Monographs on Physics No. 113 (Oxford University Press, Oxford, 2002).
- [57] H. Kleinert and V. Schulte-Frohlinde, *Critical Properties of $\{\phi^4\}$ -Theories*, 1st ed. (World Scientific, Singapore, 2001).
- [58] P. Hohenberg and B. Halperin, “Theory of dynamic critical phenomena,” *Rev. Mod. Phys.* **49**, 435 (1977).
- [59] H. K. Janssen, B. Schaub, and B. Schmittmann, “New universal short-time scaling behaviour of critical relaxation processes,” *Zeitschrift für Phys. B Condens. Matter* **73**, 539 (1989).
- [60] A. Chiocchetta, M. Tavora, A. Gambassi, and A. Mitra, “Short-time universal scaling in an isolated quantum system after a quench,” arXiv:1411.7939 (2014).
- [61] M. Eckstein, M. Kollar, and P. Werner, “Thermalization after an Interaction Quench in the Hubbard Model,” *Phys. Rev. Lett.* **103**, 056403 (2009).
- [62] B. Sciolla and G. Biroli, “Quantum Quenches and Off-Equilibrium Dynamical Transition in the Infinite-Dimensional Bose-Hubbard Model,” *Phys. Rev. Lett.* **105**, 220401 (2010).
- [63] A. Gambassi and P. Calabrese, “Quantum quenches as classical critical films,” *EPL (Europhysics Lett.)* **95**, 66007 (2011).
- [64] M. Kardar, G. Parisi, and Y.-C. Zhang, “Dynamic Scaling of Growing Interfaces,” *Phys. Rev. Lett.* **56**, 889 (1986).
- [65] T. Halpin-Healy and Y.-C. Zhang, “Kinetic roughening phenomena, stochastic growth, directed polymers and all that. Aspects of multidisciplinary statistical mechanics,” *Phys. Rep.* **254**, 215 (1995).
- [66] J. Krug, “Origins of scale invariance in growth processes,” *Adv. Phys.* (2006).
- [67] J. Berges, A. Rothkopf, and J. Schmidt, “Nonthermal Fixed Points: Effective Weak Coupling for Strongly Correlated Systems Far from Equilibrium,” *Phys. Rev. Lett.* **101**, 041603 (2008).

- [68] J. Berges and G. Hoffmeister, “Nonthermal fixed points and the functional renormalization group,” *Nucl. Phys. B* **813**, 383 (2009).
- [69] J. Berges and D. Mesterházy, “Introduction to the nonequilibrium functional renormalization group,” *Nucl. Phys. B - Proc. Suppl.* **228**, 37 (2012).
- [70] B. Nowak, D. Sexty, and T. Gasenzer, “Superfluid turbulence: Nonthermal fixed point in an ultracold Bose gas,” *Phys. Rev. B* **84**, 020506 (2011).
- [71] B. Nowak, J. Schole, D. Sexty, and T. Gasenzer, “Nonthermal fixed points, vortex statistics, and superfluid turbulence in an ultracold Bose gas,” *Phys. Rev. A* **85**, 043627 (2012).
- [72] J. Schole, B. Nowak, and T. Gasenzer, “Critical dynamics of a two-dimensional superfluid near a nonthermal fixed point,” *Phys. Rev. A* **86**, 013624 (2012).
- [73] M. Karl, B. Nowak, and T. Gasenzer, “Universal scaling at nonthermal fixed points of a two-component Bose gas,” *Phys. Rev. A* **88**, 063615 (2013).
- [74] S. Mathey, T. Gasenzer, and J. M. Pawłowski, “Anomalous scaling at non-thermal fixed points of Burgers’ and Gross-Pitaevskii turbulence,” arXiv:1405.7652 (2014).
- [75] J. Berges, K. Boguslavski, S. Schlichting, and R. Venugopalan, “Universality Far from Equilibrium: From Superfluid Bose Gases to Heavy-Ion Collisions,” *Phys. Rev. Lett.* **114**, 061601 (2015).
- [76] U. Täuber, V. Akkineni, and J. Santos, “Effects of Violating Detailed Balance on Critical Dynamics,” *Phys. Rev. Lett.* **88**, 045702 (2002).
- [77] B. Schmittmann and R. K. P. Zia, “Statistical mechanics of driven diffusive systems,” in *Stat. Mech. Driven Diffus. Syst., Phase Transitions and Critical Phenomena*, Vol. 17, edited by B. Schmittmann and R. K. P. Zia (Academic Press, 1995) pp. 3–214.
- [78] M. Doi, “Second quantization representation for classical many-particle system,” *J. Phys. A. Math. Gen.* **9**, 1465 (1976).
- [79] L. Peliti, “Path integral approach to birth-death processes on a lattice,” *J. Phys.* **46**, 1469 (1985).
- [80] J. Cardy and U. Täuber, “Theory of Branching and Annihilating Random Walks,” *Phys. Rev. Lett.* **77**, 4780 (1996).
- [81] L. Canet, “Reaction-diffusion processes and non-perturbative renormalization group,” *J. Phys. A. Math. Gen.* **39**, 7901 (2006).
- [82] S. Obukhov, “The problem of directed percolation,” *Phys. A Stat. Mech. its Appl.* **101**, 145 (1980).
- [83] H. Hinrichsen, “Non-equilibrium critical phenomena and phase transitions into absorbing states,” *Adv. Phys.* **49**, 815 (2000).
- [84] H. J. Jensen, *Self Organized Criticality* (Cambridge University Press, Cambridge, 1998).

- [85] H. K. Janssen, “Field-theoretic method applied to critical dynamics,” in *Dyn. Crit. Phenom. Relat. Top.*, Lecture Notes in Physics, Vol. 104, edited by C. Enz (Springer-Verlag, Berlin, 1979) pp. 25–47.
- [86] A. Andreanov, G. Biroli, and A. Lefèvre, “Dynamical field theory for glass-forming liquids, self-consistent resummations and time-reversal symmetry,” *J. Stat. Mech. Theory Exp.* **2006**, P07008 (2006).
- [87] C. Aron, G. Biroli, and L. F. Cugliandolo, “Symmetries of generating functionals of Langevin processes with colored multiplicative noise,” *J. Stat. Mech. Theory Exp.* **2010**, P11018 (2010).
- [88] C. Aron, D. G. Barci, L. F. Cugliandolo, Z. G. Arenas, and G. S. Lozano, “Dynamical symmetries of Markov processes with multiplicative white noise,” arXiv:1412.7564 (2014).
- [89] A. Janot, T. Hyart, P. Eastham, and B. Rosenow, “Superfluid Stiffness of a Driven Dissipative Condensate with Disorder,” *Phys. Rev. Lett.* **111**, 230403 (2013).
- [90] V. Savona, “Effect of interface disorder on quantum well excitons and microcavity polaritons.” *J. Phys. Condens. Matter* **19**, 295208 (2007).
- [91] J. Lebreuilly, I. Carusotto, and M. Wouters, “Strongly interacting photons in arrays of dissipative nonlinear cavities under a frequency-dependent incoherent pumping,” arXiv:1502.04016 (2015).
- [92] K. Wilson, “The renormalization group: Critical phenomena and the Kondo problem,” *Rev. Mod. Phys.* **47**, 773 (1975).
- [93] A. Kamenev, *Field Theory of Non-Equilibrium Systems* (Cambridge University Press, Cambridge, 2011).
- [94] A. Altland and B. Simons, *Condensed Matter Field Theory*, 2nd ed. (Cambridge University Press, Cambridge, 2010).
- [95] C. Ates, B. Olmos, J. P. Garrahan, and I. Lesanovsky, “Dynamical phases and intermittency of the dissipative quantum Ising model,” *Phys. Rev. A* **85**, 043620 (2012).
- [96] B. Olmos, D. Yu, and I. Lesanovsky, “Steady-state properties of a driven atomic ensemble with nonlocal dissipation,” *Phys. Rev. A* **89**, 023616 (2014).
- [97] T. E. Lee, S. Gopalakrishnan, and M. D. Lukin, “Unconventional Magnetism via Optical Pumping of Interacting Spin Systems,” *Phys. Rev. Lett.* **110**, 257204 (2013).
- [98] U. C. Täuber, *Critical Dynamics: A Field Theory Approach to Equilibrium and Non-Equilibrium Scaling Behavior* (Cambridge University Press, Cambridge, 2014).
- [99] J. Berges, N. Tetradis, and C. Wetterich, “Non-perturbative renormalization flow in quantum field theory and statistical physics,” *Phys. Rep.* **363**, 223 (2002).
- [100] B. Delamotte, “An Introduction to the Nonperturbative Renormalization Group,” in *Renorm. Gr. Eff. F. Theory Approaches to Many-Body Syst. SE - 2*, Lecture Notes in Physics, Vol. 852, edited by A. Schwenk and J. Polonyi (Springer Berlin Heidelberg, 2012) pp. 49–132.

- [101] J.-P. Blaizot, R. Méndez-Galain, and N. Wschebor, “A new method to solve the non-perturbative renormalization group equations,” *Phys. Lett. B* **632**, 571 (2006).
- [102] J. M. Pawłowski, “Aspects of the functional renormalisation group,” *Ann. Phys. (N. Y.)* **322**, 2831 (2007).
- [103] I. Boettcher, J. M. Pawłowski, and S. Diehl, “Ultracold atoms and the Functional Renormalization Group,” *Nucl. Phys. B - Proc. Suppl.* **228**, 63 (2012).
- [104] C. Wetterich, “Improvement of the average action,” *Zeitschrift für Phys. C Part. Fields* **60**, 461 (1993).
- [105] U. C. Täuber and S. Diehl, “Perturbative Field-Theoretical Renormalization Group Approach to Driven-Dissipative Bose-Einstein Criticality,” *Phys. Rev. X* **4**, 021010 (2014).
- [106] L. Canet and H. Chaté, “A non-perturbative approach to critical dynamics,” *J. Phys. A Math. Theor.* **40**, 1937 (2007).
- [107] D. Mesterházy, J. H. Stockemer, L. F. Palhares, and J. Berges, “Dynamic universality class of Model C from the functional renormalization group,” *Phys. Rev. B* **88**, 174301 (2013).
- [108] L. Canet, H. Chaté, and B. Delamotte, “Quantitative Phase Diagrams of Branching and Annihilating Random Walks,” *Phys. Rev. Lett.* **92**, 255703 (2004).
- [109] L. Canet, H. Chaté, B. Delamotte, I. Dornic, and M. Muñoz, “Nonperturbative Fixed Point in a Nonequilibrium Phase Transition,” *Phys. Rev. Lett.* **95**, 100601 (2005).
- [110] L. Canet, H. Chaté, B. Delamotte, and N. Wschebor, “Nonperturbative Renormalization Group for the Kardar-Parisi-Zhang Equation,” *Phys. Rev. Lett.* **104**, 150601 (2010).
- [111] L. Canet, H. Chaté, and B. Delamotte, “General framework of the non-perturbative renormalization group for non-equilibrium steady states,” *J. Phys. A Math. Theor.* **44**, 495001 (2011).
- [112] L. Canet, H. Chaté, B. Delamotte, and N. Wschebor, “Nonperturbative renormalization group for the Kardar-Parisi-Zhang equation: General framework and first applications,” *Phys. Rev. E* **84**, 061128 (2011).
- [113] L. Canet, “Erratum: Nonperturbative renormalization group for the Kardar-Parisi-Zhang equation: General framework and first applications [Phys. Rev. E 84, 061128 (2011)],” *Phys. Rev. E* **86** (2012), 10.1103/PhysRevE.86.019904.
- [114] T. Gasenzer and J. M. Pawłowski, “Towards far-from-equilibrium quantum field dynamics: A functional renormalisation-group approach,” *Phys. Lett. B* **670**, 135 (2008).
- [115] R. Gezzi, T. Pruschke, and V. Meden, “Functional renormalization group for nonequilibrium quantum many-body problems,” *Phys. Rev. B* **75**, 045324 (2007).
- [116] S. Jakobs, V. Meden, and H. Schoeller, “Nonequilibrium Functional Renormalization Group for Interacting Quantum Systems,” *Phys. Rev. Lett.* **99**, 150603 (2007).

-
- [117] C. Karrasch, S. Andergassen, M. Pletyukhov, D. Schuricht, L. Borda, V. Meden, and H. Schoeller, “Non-equilibrium current and relaxation dynamics of a charge-fluctuating quantum dot,” *EPL (Europhysics Lett.)* **90**, 30003 (2010).
- [118] R. Kubo, “Statistical-Mechanical Theory of Irreversible Processes. I. General Theory and Simple Applications to Magnetic and Conduction Problems,” *J. Phys. Soc. Japan* **12**, 570 (1957).
- [119] P. Martin and J. Schwinger, “Theory of Many-Particle Systems. I,” *Phys. Rev.* **115**, 1342 (1959).
- [120] S. G. Jakobs, M. Pletyukhov, and H. Schoeller, “Properties of multi-particle Green’s and vertex functions within Keldysh formalism,” *J. Phys. A Math. Theor.* **43**, 103001 (2010).
- [121] R. Folk and G. Moser, “Critical dynamics: a field-theoretical approach,” *J. Phys. A Math. Gen.* **39**, R207 (2006).
- [122] C. De Dominicis, E. Brézin, and J. Zinn-Justin, “Field-theoretic techniques and critical dynamics. I. Ginzburg-Landau stochastic models without energy conservation,” *Phys. Rev. B* **12**, 4945 (1975).
- [123] J. Keeling, L. M. Sieberer, E. Altman, L. Chen, S. Diehl, and J. Toner, “Superfluidity and Phase Correlations of Driven Dissipative Condensates,” in *Universal Themes in Bose-Einstein Condensation*, edited by D. W. Snoke, N. P. Proukakis, and P. B. Littlewood (Cambridge University Press, Cambridge, 2015).

Part I

Dynamical Critical Phenomena in Driven-Dissipative Systems

CHAPTER 2

PUBLICATION

Dynamical Critical Phenomena in Driven-Dissipative Systems[†]

Phys. Rev. Lett., **110**, 195301 (2013)

L. M. Sieberer,^{1,2} S. D. Huber,^{3,4} E. Altman,^{4,5} and S. Diehl^{1,2}

¹*Institute for Theoretical Physics, University of Innsbruck, A-6020 Innsbruck, Austria*

²*Institute for Quantum Optics and Quantum Information of the Austrian Academy of Sciences, A-6020 Innsbruck, Austria*

³*Theoretische Physik, Wolfgang-Pauli-Strasse 27, ETH Zurich, CH-8093 Zurich, Switzerland*

⁴*Department of Condensed Matter Physics, Weizmann Institute of Science, Rehovot 76100, Israel*

⁵*Department of Physics, University of California, Berkeley, CA 94720, USA*

We explore the nature of the Bose condensation transition in driven open quantum systems, such as exciton-polariton condensates. Using a functional renormalization group approach formulated in the Keldysh framework, we characterize the dynamical critical behavior that governs decoherence and an effective thermalization of the low frequency dynamics. We identify a critical exponent special to the driven system, showing that it defines a new dynamical universality class. Hence critical points in driven systems lie beyond the standard classification of equilibrium dynamical phase transitions. We show how the new critical exponent can be probed in experiments with driven cold atomic systems and exciton-polariton condensates.

Recent years have seen major advances in the exploration of many-body systems in which matter is strongly coupled to light [1]. Such systems include for example polariton condensates [2], superconducting circuits coupled to microwave resonators [3, 4], cavity quantum electrodynamics [5] as well as ultracold atoms coupled to high finesse optical cavities [6]. As in traditional quantum optics settings, these experiments are subject to losses, which may be compensated by continuous drive, yet they retain the many-body character of condensed matter. This combination of ingredients from atomic physics and quantum optics in a many-body context defines a qualitatively new class of quantum matter far from thermal equilibrium. An intriguing question from the theoretical perspective is what new universal behavior can emerge under such conditions.

[†]The author of the thesis carried out the majority of the calculations presented in this publication and was strongly involved in preparing the manuscript together with the other authors.

A case in point are exciton-polariton condensates. Polaritons are short lived optical excitations in semiconductor quantum wells. Continuous pumping is required to maintain their population in steady state. But in spite of the non-equilibrium conditions, experiments have demonstrated Bose condensation [2] and, more recently, have even observed the establishment of a critical phase with power-law correlations in a two dimensional system below a presumed Kosterlitz-Thouless phase transition [7]. At a fundamental level however there is no understanding of the condensation transition in the presence of loss and external drive, and more generally of continuous phase transitions under such conditions.

In this letter we develop a theory of dynamical critical phenomena in driven-dissipative systems in three dimensions. Motivated by the experiments described above we focus on the case of Bose condensation with the following key results. (i) *Low-frequency thermalization* – The microscopic dynamics of a driven system is incompatible with an equilibrium-like Gibbs distribution at steady state. Nevertheless a scale independent effective temperature emerges at low frequencies in the universal regime near the critical point, and all correlations in this regime obey a classical fluctuation-dissipation relation (FDR). Such a phenomenon of low frequency effective equilibrium has been identified previously in different contexts [8–14]. (ii) *Universal low-frequency decoherence* – In spite of the effective thermalization, the critical dynamics is significantly affected by the non-equilibrium conditions set by the microscopic theory. Specifically we show that all coherent dynamics, as measured by standard response functions, fades out at long wavelengths as a power-law with a new universal critical exponent. The decoherence exponent cannot be mimicked by any equilibrium model and places the critical dynamics of a driven system in a new dynamical universality class beyond the Halperin-Hohenberg classification of equilibrium dynamical critical behavior [15].

Open system dynamics– A microscopic description of driven open systems typically starts from a Markovian quantum master equation or an equivalent Keldysh action (see Supplementary Information (SI)). However, the novel aspects in the critical dynamics of driven dissipative systems discussed below can be most simply illustrated by considering an effective mesoscopic description of the order parameter dynamics using a stochastic Gross-Pitaevskii equation [16]

$$i\partial_t\psi = \left[-(A - iD)\nabla^2 - \mu + i\chi + (\lambda - i\kappa)|\psi|^2 \right] \psi + \zeta. \quad (2.1)$$

As we show below, this equation can be rigorously derived from a fully quantum microscopic description of the condensate when including only the relevant terms near the critical point. The different terms in (2.1) have a clear physical origin. $\chi = (\gamma_p - \gamma_l)/2$ is the effective gain, which combines the incoherent pump field minus the local single-particle loss terms. $\kappa, \lambda > 0$ are respectively two-body loss and interaction parameters. The diffusion term D is not contained in the original microscopic model, and is not crucial to describe most non-universal aspects of, e.g., exciton-polariton condensates [17–20] (but see [21, 22]). In a systematic treatment of long-wavelength universal critical behavior, however, such term is generated upon integrating out high frequency modes during the renormalization group (RG) flow, irrespective of its microscopic value. We therefore include it at the mesoscopic level with a phenomenological coefficient. Finally ζ is a Gaussian white noise with correlations $\langle \zeta^*(t, \mathbf{x})\zeta(t', \mathbf{x}') \rangle = \gamma\delta(t-t')\delta(\mathbf{x}-\mathbf{x}')$ where $\gamma = \gamma_p + \gamma_l$. Such noise is necessarily induced by the losses and sudden appearances of particles due to pumping.

The dGP describes a mean field transition from a stationary condensate solution with density $|\psi|^2 = \chi/\kappa$ for $\chi > 0$ to the vacuum state when χ crosses zero. Dynamical stability [23] determines the chemical potential as $\mu = \lambda|\psi|^2$. Similar to a temperature, the noise term in Eq. (2.1) can drive a transition at finite particle density, thereby inducing critical fluctuations.

As the equation of motion is cast in Langevin form, one might suspect that it can be categorized into one of the well-known models of dynamical critical phenomena classified by Hohenberg and Halperin [15]. However, this is not true in general. Crucially coherent (real parts of the couplings in Eq. (2.1)) and dissipative (imaginary parts) dynamics have different physical origins in driven-dissipative systems. In particular, the dissipative dynamics is determined by the intensity of the pump and loss terms, independently of the intrinsic Hamiltonian dynamics of the system. Equilibrium models [15], on the other hand, are constrained to have a specific relation between the reversible and dissipative terms to ensure a thermal Gibbs ensemble in steady state [24, 25] (see below). The unconstrained dynamics in driven systems is the key feature that can lead to novel dynamic critical behavior.

Microscopic Model – Having illustrated the nature of the problem with the effective classical equation (2.1) we turn to a fully quantum description within the Keldysh framework. Our starting point is a non-unitary quantum evolution described by a many-body master equation in Lindblad form, or equivalently by the following dissipative Keldysh action (see SI for details of the correspondence)

$$\mathcal{S} = \int_{t,x} \left\{ \begin{pmatrix} \phi_c^* & \phi_q^* \\ P^R & P^K \end{pmatrix} \begin{pmatrix} 0 & P^A \\ P^R & P^K \end{pmatrix} \begin{pmatrix} \phi_c \\ \phi_q \end{pmatrix} + i4\kappa\phi_c^*\phi_c\phi_q^*\phi_q - [(\lambda + i\kappa)(\phi_c^{*2}\phi_c\phi_q + \phi_q^{*2}\phi_c\phi_q) + \text{c.c.}] \right\}. \quad (2.2)$$

Here ϕ_c, ϕ_q are the "classical" and "quantum" fields, defined by the symmetric and anti-symmetric combinations of the fields on the forward and backward parts of the Keldysh contour [26, 27]. The microscopic inverse Green's functions are given by $P^R = i\partial_t + A\nabla^2 + \mu - i\chi$, $P^A = P^{R\dagger}$, $P^K = i\gamma$.

The importance of the various terms in the microscopic action (2.2) in the vicinity of the critical point can be inferred from canonical power counting, which serves as a valuable guideline for the explicit evaluation of the problem. Vanishing of the mass scale χ defines a Gaussian fixed point with dynamical critical exponent $z = 2$ ($\omega \sim k^z$, k a momentum scale). Canonical power counting determines the scaling dimensions of the fields and interaction constants with respect to this fixed point: At criticality, the spectral components of the Gaussian action scale as $P^{R/A} \sim k^2$, while the Keldysh component generically takes a constant value, i.e., $P^K \sim k^0$. Hence, to maintain scale invariance of the quadratic action, the scaling dimensions of the fields must be $[\phi_c] = \frac{d-2}{2}$ and $[\phi_q] = \frac{d+2}{2}$. From this result we read off the canonical scaling dimensions of the interaction constants. This analysis shows that in the case of interest $d = 3$, local vertices containing more than two quantum fields or more than five classical fields are irrelevant. For the critical problem, the last terms in both lines of Eq. (2.2) can thus be skipped, massively simplifying the complexity of the problem. The only marginal term with two quantum fields is the Keldysh component of the single-particle inverse Green's function, i.e., the noise vertex. In this sense, the critical theory is equivalent to a stochastic *classical* problem [28, 29], as previously observed in [8, 30]. But as noted above it cannot be *a priori* categorized in one of the dynamical universality classes [15] subject to an intrinsic equilibrium constraint.

Functional RG – In order to focus quantitatively on the critical behavior we use a functional RG approach formulated originally by Wetterich [31] and adapted to the Keldysh real time framework in Refs. [32, 33] (see SI for details). At the formal level this technique provides an exact functional flow equation for an effective action functional $\Gamma_\Lambda[\phi_c, \phi_q]$, which includes information on increasingly long wavelength fluctuations (at the microscopic cutoff scale $\Gamma_{\Lambda_0} \approx \mathcal{S}$). In practice one works with an ansatz for the effective action and thereby projects the functional flow onto scaling equations for a finite set of coupling constants. For the description of general equilibrium [34–39] and Ising

dynamical [40] critical behavior the functional RG gave results that are competitive with high-order epsilon expansion and with Monte Carlo simulations already in rather simple approximation schemes.

Our ansatz for the effective action is motivated by the power counting arguments introduced above. We include in Γ_Λ all couplings that are relevant or marginal in this scheme:

$$\Gamma_\Lambda = \int_{t,x} \left\{ \left(\phi_c^*, \phi_q^* \right) \begin{pmatrix} 0 & iZ\partial_t + \bar{K}\nabla^2 \\ iZ^*\partial_t + \bar{K}^*\nabla^2 & i\bar{\gamma} \end{pmatrix} \begin{pmatrix} \phi_c \\ \phi_q \end{pmatrix} - \left(\frac{\partial \bar{U}}{\partial \phi_c} \phi_q + \frac{\partial \bar{U}^*}{\partial \phi_c^*} \phi_q^* \right) \right\}. \quad (2.3)$$

The dynamical couplings Z and \bar{K} have to be taken complex valued in order to be consistent with power counting, even if the respective imaginary parts vanish (or are very small) at the microscopic scale: Successive momentum mode elimination implemented by the RG flow generates these terms due to the simultaneous presence of local coherent and dissipative couplings in the microscopic model. The fact that the spectral components of the effective action depend only linearly on ϕ_q allowed us to introduce an effective potential \bar{U} determined by the complex static couplings. $\bar{U}(\rho_c) = \frac{1}{2}\bar{u}(\rho_c - \rho_0)^2 + \frac{1}{6}\bar{u}'(\rho_c - \rho_0)^3$ is a function of the $U(1)$ invariant combination of classical fields $\rho_c = \phi_c^*\phi_c$ alone. It has a mexican hat structure ensuring dynamical stability. With this choice we approach the transition from the ordered side, taking the limit of the stationary state condensate $\rho_0 = \phi_c^*\phi_c|_{ss} = \phi_0^*\phi_0 \rightarrow 0$.

All the parameters appearing in (2.3) including the stationary condensate density ρ_0 are functions of the running cutoff Λ . Hence, the functional flow of Γ_Λ is reduced by means of the approximate ansatz to the flow of a finite number of couplings $\mathbf{g} = (Z, \bar{K}, \rho_0, \bar{u}, \bar{u}', \bar{\gamma})^T$ determined by the β -functions $\Lambda\partial_\Lambda \mathbf{g} = \beta_{\mathbf{g}}(\mathbf{g})$ (see SI). The critical system is described by a scaling solution to these flow equations. It is obtained as a fixed point of the flow of dimensionless renormalized couplings, which we derive in the following. First we rescale couplings with Z ,

$$K = \bar{K}/Z, \quad u = \bar{u}/Z, \quad u' = \bar{u}'/Z, \quad \gamma = \bar{\gamma}/|Z|^2. \quad (2.4)$$

Coherent and dissipative processes are encoded, respectively, in the real and imaginary parts of the renormalized coefficients $K = A + iD$, $u = \lambda + ik$, and $u' = \lambda' + ik'$.

We define the first three dimensionless scaling variables to be the ratios of coherent to dissipative coefficients: $r_K = A/D$, $r_u = \lambda/\kappa$, and $r_{u'} = \lambda'/\kappa'$. Another three dimensionless variables are defined by rescaling the loss coefficients κ and κ' and the condensate density ρ_0 :

$$w = \frac{2\kappa\rho_0}{\Lambda^2 D}, \quad \tilde{\kappa} = \frac{\gamma\kappa}{2\Lambda D^2}, \quad \tilde{\kappa}' = \frac{\gamma^2\kappa'}{4D^3}. \quad (2.5)$$

The flow equations for the couplings $\mathbf{r} = (r_K, r_u, r_{u'})^T$ and $\mathbf{s} = (w, \tilde{\kappa}, \tilde{\kappa}')^T$ form a closed set,

$$\Lambda\partial_\Lambda \mathbf{r} = \beta_{\mathbf{r}}(\mathbf{r}, \mathbf{s}), \quad \Lambda\partial_\Lambda \mathbf{s} = \beta_{\mathbf{s}}(\mathbf{r}, \mathbf{s}) \quad (2.6)$$

(see SI for the explicit form). As a consequence of the transformations (2.4) and (2.5), these β -functions acquire a contribution from the running anomalous dimensions $\eta_a(\mathbf{r}, \mathbf{s}) = -\Lambda\partial_\Lambda \ln a$ associated with $a = Z, D, \gamma$.

Critical properties – The universal behavior near the critical point is controlled by the infrared flow to a Wilson-Fisher like fixed point. The values of the coupling constants at the fixed point, determined by solving $\beta_{\mathbf{s}}(\mathbf{r}_*, \mathbf{s}_*) = 0$ and $\beta_{\mathbf{r}}(\mathbf{r}_*, \mathbf{s}_*) = 0$, are given by:

$$\begin{aligned} \mathbf{r}_* &= (r_{K*}, r_{u*}, r_{u'*}) = \mathbf{0}, \\ \mathbf{s}_* &= (w_*, \tilde{\kappa}_*, \tilde{\kappa}'_*) \approx (0.475, 5.308, 51.383). \end{aligned} \quad (2.7)$$

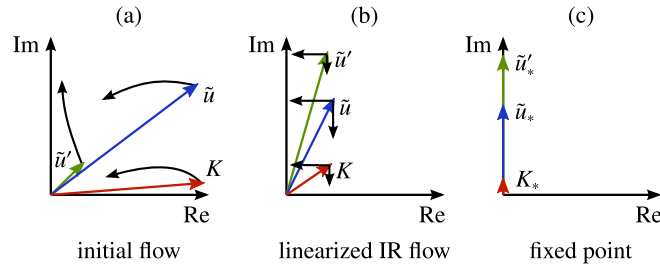


Figure 2.1. *Flow in the complex plane of dimensionless renormalized couplings. (a) The microscopic action determines the initial values of the flow. Typically, the coherent propagation will dominate over the diffusion, $A \gg D$, while two-body collisions and two-body loss are on the same order of magnitude, $\tilde{\lambda} \approx \tilde{\kappa}$, with a similar relation for the marginal complex coupling \tilde{u} . The initial flow is non-universal. (b) At criticality, the infrared (IR) flow approaches a universal linear domain encoding the critical exponents and anomalous dimensions. In particular, this regime is independent of the precise microscopic initial conditions. (c) The Wilson-Fisher fixed point describing the interacting critical system is purely imaginary.*

The fact that $\mathbf{r}_* = 0$ implies that the fixed point action is purely imaginary (or dissipative), as in Model A of Hohenberg and Halperin [15], cf. Fig. 2.1 (c). We interpret the fact that the ratios of coherent vs. dissipative couplings are zero at the fixed point as a manifestation of decoherence at low frequencies in an RG framework. The coupling values \mathbf{s}_* are identical to those obtained in an equilibrium classical $O(2)$ model from functional RG calculations at the same level of truncation [34].

Let us turn to the linearized flow, which determines the universal behavior in the vicinity of the fixed point. We find that the two sectors corresponding to \mathbf{s} and \mathbf{r} decouple in this regime, giving rise to a block diagonal stability matrix

$$\frac{\partial}{\partial \ln \Lambda} \begin{pmatrix} \delta \mathbf{r} \\ \delta \mathbf{s} \end{pmatrix} = \begin{pmatrix} N & 0 \\ 0 & S \end{pmatrix} \begin{pmatrix} \delta \mathbf{r} \\ \delta \mathbf{s} \end{pmatrix}, \quad (2.8)$$

where $\delta \mathbf{r} \equiv \mathbf{r}$, $\delta \mathbf{s} \equiv \mathbf{s} - \mathbf{s}_*$, and N, S are 3×3 matrices (see SI).

The anomalous dimensions entering this flow are found by plugging the fixed point values $\mathbf{r}_*, \mathbf{s}_*$ into the expressions for $\eta_a(\mathbf{r}, \mathbf{s})$. We obtain the scaling relation between the anomalous dimensions $\eta_Z = \eta_{\tilde{\gamma}}$, valid in the universal infrared regime. This leads to cancellation of η_Z with $\eta_{\tilde{\gamma}}$ in the static sector S (see SI). The critical properties in this sector, encoded in the eigenvalues of S , become identical to those of the standard $O(2)$ transition. This includes the correlation length exponent $\nu \approx 0.716$ and the anomalous dimension $\eta \approx 0.039$ associated with the bare kinetic coefficient \bar{K} . These values are in good agreement with more sophisticated approximations [41].

The equilibrium-like behavior in the S sector can be seen as a result of an emergent symmetry. Locking of the noise to the dynamical term implied by $\eta_Z = \eta_{\tilde{\gamma}}$ leads to invariance of the long wavelength effective action (times i) under the transformation $\Phi_c(t, \mathbf{x}) \rightarrow \Phi_c(-t, \mathbf{x})$, $\Phi_q(t, \mathbf{x}) \rightarrow \Phi_q(-t, \mathbf{x}) + \frac{2}{\gamma} \sigma^z \partial_t \Phi_c(-t, \mathbf{x})$, $i \rightarrow -i$ with $\Phi_\nu = (\phi_\nu, \phi_\nu^*)^T$, $\nu = (c, q)$, σ^z the Pauli matrix. It generalizes the symmetry noted in Refs. [42, 43] to models that include also reversible couplings. The presence of this symmetry implies a classical FDR with a distribution function $F = 2T_{\text{eff}}/\omega$, governed by an effective temperature $T_{\text{eff}} = \tilde{\gamma}/(4|Z|)$. This quantity becomes scale independent in the universal

critical regime where $\bar{\gamma} \sim k^{-\eta_{\bar{\gamma}}}$ and $Z \sim k^{-\eta_Z}$ cancel. We interpret this finding as an asymptotic low-frequency thermalization mechanism of the driven system at criticality. The thermalized regime sets in below the Ginzburg scale where fluctuations start to dominate, for which we estimate perturbatively $\chi_G = (\gamma\kappa)^2 / (16\pi^2 D^3)$ (see SI). The values entering here are determined on the mesoscopic scale, and we specify them for exciton-polariton systems in the SI based on Ref. [21, 22]. Above the scale χ_G , no global (scale independent) temperature can be defined in general. We note that, unlike Hohenberg-Halperin type models, here the symmetry implied by $\eta_Z = \eta_{\bar{\gamma}}$ is not imposed at the microscopic level of the theory, but rather is emergent at the critical point.

The key new element in the driven-dissipative dynamics is encoded in the decoupled ‘‘drive’’ sector (the 3×3 matrix N in our case). It describes the flow towards the emergent purely dissipative Model A fixed point (see Fig. 2.1 (b)) and thus reflects a mechanism of low frequency decoherence. This sector has no counterpart in the standard framework of dynamical critical phenomena and is special to driven-dissipative systems. In the deep infrared regime, only the lowest eigenvalue of this matrix governs the flow of the ratios. This means that only one new critical exponent $\eta_r \approx -0.101$ is encoded in this sector. Just as the dynamical critical exponent z is independent of the static ones, the block diagonal structure of the stability matrix ensures that the drive exponent is independent of the exponents of the other sectors.

The fact that the inverse Green’s function in Eq. (2.3) is specified by three real parameters, $\text{Re } \bar{K}$, $\text{Im } \bar{K}$, and $|Z|$ (the phase of Z can be absorbed by a $U(1)$ transformation) allows for only three independent anomalous dimensions: η_D , η_Z and the new exponent η_r . Hence the extension of critical dynamics described here is *maximal*, i.e., no further independent exponent will be found. Moreover this extension of the purely relaxational (Model A) dynamics leads to different universality than an extension that adds reversible couplings compatible with relaxation towards a Gibbs ensemble. The latter is obtained by adding real couplings to the imaginary ones with the same ratio of real to imaginary parts for all couplings [44–47]; in this case the above symmetry is present, while absent in the general non-equilibrium case. The compatible extension adds only an independent 1×1 sector N to the purely relaxational problem, for which we find $\eta_R = -0.143 \neq \eta_r$. This proves that the independence of dissipative and coherent dynamics defines indeed a new non-equilibrium universality class with no equilibrium counterpart. It is rooted in different symmetry properties of equilibrium vs. non-equilibrium situation.

Experimental detection – The novel anomalous dimension identified here leaves a clear fingerprint in single-particle observables accessible with current experimental technologies on different platforms. For ultracold atomic systems this can be achieved via RF-spectroscopy [48] close to the driven-dissipative BEC transition. In exciton-polariton condensates, the dispersion relation can be obtained from the energy- and momentum resolved luminescence spectrum as demonstrated in [49]. Using the RG scaling behavior of the diffusion and propagation coefficients $D \sim D_0 \Lambda^{-\eta_D}$, $A = Dr_K \sim A_0 \Lambda^{-\eta_r - \eta_D}$, we obtain the anomalous scaling of the frequency and momentum resolved, renormalized retarded Green’s function $G^R(\omega, \mathbf{q}) = (\omega - A_0 |\mathbf{q}|^{2-\eta_r - \eta_D} + iD_0 |\mathbf{q}|^{2-\eta_D})^{-1}$, with A_0 and D_0 non-universal constants. Peak position and width are implied by the complex dispersion $\omega \approx A_0 |\mathbf{q}|^{2.22} - iD_0 |\mathbf{q}|^{2.12}$. The energy resolution necessary to probe the critical behavior is again set by the Ginzburg scale χ_G (see above).

Conclusions – We have developed a Keldysh field theoretical approach to characterize the critical behavior of driven-dissipative three dimensional Bose systems at the condensation transition. The main result presents a hierarchical extension of classical critical phenomena. First, all static aspects

are identical to the classical $O(2)$ critical point. In the next shell of the hierarchy a sub-class of the dynamical phenomena is identical to the purely dissipative Model A dynamics of the equilibrium critical point. Finally we identify manifestly non-equilibrium features of the critical dynamics, encoded in a new independent critical exponent that betrays the driven nature of the system.

Acknowledgements – We thank J. Berges, M. Buchhold, I. Carusotto, T. Esslinger, T. Gasenzer, A. Imamoglu, J. M. Pawłowski, P. Strack, S. Takei, U. C. Täuber, C. Wetterich and P. Zoller for useful discussions. This research was supported by the Austrian Science Fund (FWF) through the START grant Y 581-N16 and the SFB FoQuS (FWF Project No. F4006-N16). Institut für Quanteninformaton GmbH.

2.A Open system dynamics

Open system dynamics with local particle loss and gain can be modeled microscopically by a many-body quantum master equation ($\hbar = 1$)

$$\partial_t \hat{\rho} = -i [\hat{H}, \hat{\rho}] + \mathcal{L}[\hat{\rho}]. \quad (2.9)$$

The dynamics of the system density matrix $\hat{\rho}$ has both a coherent contribution due to the standard Hamiltonian for bosons of mass m ($\int_{\mathbf{x}} = \int d^3\mathbf{x}$)

$$\hat{H} = \int_{\mathbf{x}} \hat{\psi}^\dagger(\mathbf{x}) \left(-\frac{\Delta}{2m} - \mu \right) \hat{\psi}(\mathbf{x}) + \lambda \int_{\mathbf{x}} \hat{\psi}^\dagger(\mathbf{x})^2 \hat{\psi}(\mathbf{x})^2, \quad (2.10)$$

and a dissipative one that is incorporated by the Liouville operator

$$\begin{aligned} \mathcal{L}[\hat{\rho}] = & \gamma_p \int_{\mathbf{x}} \left(\hat{\psi}^\dagger(\mathbf{x}) \hat{\rho} \hat{\psi}(\mathbf{x}) - \frac{1}{2} \{ \hat{\psi}(\mathbf{x}) \hat{\psi}^\dagger(\mathbf{x}), \hat{\rho} \} \right) + \gamma_l \int_{\mathbf{x}} \left(\hat{\psi}(\mathbf{x}) \hat{\rho} \hat{\psi}^\dagger(\mathbf{x}) - \frac{1}{2} \{ \hat{\psi}^\dagger(\mathbf{x}) \hat{\psi}(\mathbf{x}), \hat{\rho} \} \right) \\ & + 2\kappa \int_{\mathbf{x}} \left(\hat{\psi}(\mathbf{x})^2 \hat{\rho} \hat{\psi}^\dagger(\mathbf{x})^2 - \frac{1}{2} \{ \hat{\psi}^\dagger(\mathbf{x})^2 \hat{\psi}(\mathbf{x})^2, \hat{\rho} \} \right). \end{aligned} \quad (2.11)$$

Local Lindblad operators $\hat{\psi}^\dagger(\mathbf{x})$ and $\hat{\psi}(\mathbf{x})$, respectively, correspond to the processes of incoherent pumping and loss of single particles; $\hat{\psi}(\mathbf{x})^2$ describes the simultaneous loss of two particles. Associated rates are γ_p , γ_l , and 2κ .

The investigation of critical phenomena at the stationary state phase transition exhibited by this model is facilitated by a formulation in terms of a Keldysh partition function [26, 27] $\mathcal{Z} = \int \mathcal{D}\psi_+ \mathcal{D}\psi_- e^{i\mathcal{S}}$, which can be subject to renormalization group methods. This partition function is fully equivalent to the master equation (2.9) and defined in terms of a Keldysh action $\mathcal{S} = \mathcal{S}_H + \mathcal{S}_D$ with two contributions corresponding to the commutator with the Hamiltonian (from now on we will be using units such that $2m = 1$; $\int_{t,\mathbf{x}} = \int dt \int d\mathbf{x}$),

$$\mathcal{S}_H = \sum_{\sigma=\pm} \sigma \int_{t,\mathbf{x}} \left[\psi_\sigma^* (i\partial_t + \Delta + \mu) \psi_\sigma - \lambda (\psi_\sigma^* \psi_\sigma)^2 \right], \quad (2.12)$$

and the dissipative Liouvillian,

$$\begin{aligned} \mathcal{S}_D = & -i\gamma_p \int_{t,\mathbf{x}} \left[\psi_+^* \psi_- - \frac{1}{2} (\psi_+ \psi_+^* + \psi_- \psi_-^*) \right] - i\gamma_l \int_{t,\mathbf{x}} \left[\psi_+ \psi_-^* - \frac{1}{2} (\psi_+^* \psi_+ + \psi_-^* \psi_-) \right] \\ & - i2\kappa \int_{t,\mathbf{x}} \left\{ (\psi_+ \psi_-^*)^2 - \frac{1}{2} [(\psi_+^* \psi_+)^2 + (\psi_-^* \psi_-)^2] \right\}. \end{aligned} \quad (2.13)$$

Expressing the Keldysh action in terms of classical and quantum fields, which are defined as

$$\phi_c = \frac{1}{\sqrt{2}}(\psi_+ + \psi_-), \quad \phi_q = \frac{1}{\sqrt{2}}(\psi_+ - \psi_-), \quad (2.14)$$

we recover Eq. (2) of the main text.

2.B Functional Renormalization group equation

Our approach to studying critical dynamics is based on the Wetterich functional renormalization group [31] adapted to the Keldysh framework (see [34–39] for reviews on the equilibrium formulation). Central to this method is the functional $\Gamma_\Lambda[\phi_c, \phi_q]$ defined by ¹

$$e^{i\Gamma_\Lambda[\phi_c, \phi_q]} = \int \mathcal{D}\delta\phi_c \mathcal{D}\delta\phi_q e^{i\mathcal{S}[\phi_c + \delta\phi_c, \phi_q + \delta\phi_q] + i\Delta\mathcal{S}_\Lambda[\delta\phi_c, \delta\phi_q]}. \quad (2.15)$$

Here $\Delta\mathcal{S}_\Lambda$ is a regulator function which suppresses contributions to the above path integral from modes with spatial wave-vector below the running cutoff Λ . Thus Γ_Λ interpolates between the classical action \mathcal{S} , when Λ equals the UV cutoff Λ_0 , and the effective action functional $\Gamma[\phi_c, \phi_q]$ [50] when $\Lambda \rightarrow 0$. The latter includes the effects of fluctuations on all scales. The equation

$$\partial_\Lambda \Gamma_\Lambda = \frac{i}{2} \text{Tr} \left[\left(\Gamma_\Lambda^{(2)} + R_\Lambda \right)^{-1} \partial_\Lambda R_\Lambda \right] \quad (2.16)$$

describes the flow of the interpolating functional as a function of the running cutoff Λ . In the following sections we first discuss the objects appearing in (2.16), namely the second functional derivative $\Gamma_\Lambda^{(2)}$ and the cutoff function R_Λ . Then we explain how a closed set of flow equations for a finite number of coupling constants can be obtained from the functional flow equation. Finally we detail the linearized equations for the infrared flow to the Wilson-Fisher fixed point from which the critical properties are inferred.

In suitable truncation schemes, results from high order epsilon expansion can be reproduced from the exact flow equation (2.16). In our practical calculation, we approach the critical point from the ordered phase. This allows us to calculate the anomalous dimensions at one-loop order, due to the presence of a finite condensate during the flow. Results obtained in this way have proven to be competitive with high-order epsilon expansion or Monte Carlo simulations, as referenced in the main text.

2.C The second variational derivative

The second variation $\Gamma_\Lambda^{(2)}$ with respect to the fields is the full inverse Green's function at the scale Λ , which in the case of an interacting theory is field dependent. Practically we work in a basis of real fields, related to the complex fields by

$$\begin{pmatrix} \chi_{v,1}(Q) \\ \chi_{v,2}(Q) \end{pmatrix} = \frac{1}{\sqrt{2}} \begin{pmatrix} 1 & 1 \\ -i & i \end{pmatrix} \begin{pmatrix} \phi_v(Q) \\ \phi_v^*(-Q) \end{pmatrix}, \quad (2.17)$$

¹This representation holds for the stationary states that obey $\frac{\delta\Gamma_\Lambda}{\delta\phi_c} = \frac{\delta\Gamma_\Lambda}{\delta\phi_q} = 0$.

where $\nu = c, q$ is the Keldysh index. We gather the resulting four independent field components in a field vector,

$$\chi(Q) = \left(\chi_{c,1}(Q), \chi_{c,2}(Q), \chi_{q,1}(Q), \chi_{q,2}(Q) \right)^T. \quad (2.18)$$

In this basis, $\Gamma_\Lambda^{(2)}$ is defined as

$$\left(\Gamma_\Lambda^{(2)} \right)_{ij}(Q, Q') = \frac{\delta^2 \Gamma_\Lambda}{\delta \chi_i(-Q) \delta \chi_j(Q')}, \quad (2.19)$$

which is a matrix in the discrete field index $i = 1, 2, 3, 4$ and in the continuous momentum variable $Q = (\omega, \mathbf{q})$ collecting frequency and spatial momentum. Accordingly, the trace in (2.16) involves both an integration over momenta and a sum over internal indices.

$\Gamma_\Lambda^{(2)}(Q, Q')$ is conveniently decomposed into a constant part and a fluctuation part. The latter is a polynomial in momentum-dependent fields and, therefore, a non-diagonal matrix in momentum space. In contrast, the constant part is obtained by (i) inserting spatially constant field configurations, i.e., $\chi(Q) = \chi \delta(Q)$ in momentum space, and (ii) evaluating them at their stationary state values in the ordered phase. These read

$$\chi(Q)|_{\text{ss}} = \left(\sqrt{2\rho_0}, 0, 0, 0 \right)^T \delta(Q). \quad (2.20)$$

(Without loss of generality we choose the condensate amplitude to be real.) As a result, the constant part is diagonal in momentum space,

$$P_\Lambda(Q) \delta(Q - Q') \equiv \Gamma_\Lambda^{(2)}(Q, Q')|_{\text{ss}}, \quad (2.21)$$

and is structured into retarded, advanced, and Keldysh blocks,

$$P_\Lambda(Q) = \begin{pmatrix} 0 & P^A(Q) \\ P^R(Q) & P^K \end{pmatrix}. \quad (2.22)$$

(For notational simplicity, we suppress the scale index Λ for the different blocks and their respective entries.) The retarded and advanced blocks are mutually hermitian conjugate (we decompose Z and \bar{K} into real and imaginary parts, $Z = Z_R + iZ_I$, $\bar{K} = \bar{A} + i\bar{D}$),

$$\begin{aligned} P^R(Q) &= \begin{pmatrix} -iZ_I\omega - \bar{A}\mathbf{q}^2 - 2\text{Re}(\bar{u})\rho_0 & iZ_R\omega - \bar{D}\mathbf{q}^2 \\ -iZ_R\omega + \bar{D}\mathbf{q}^2 + 2\text{Im}(\bar{u})\rho_0 & -iZ_I\omega - \bar{A}\mathbf{q}^2 \end{pmatrix}, \\ P^A(Q) &= \left(P^R(Q) \right)^\dagger. \end{aligned} \quad (2.23)$$

Note that $\det P^R(Q=0) = \det P^A(Q=0) = 0$; the existence of a gapless mode associated to the broken $U(1)$ symmetry is thus ensured in our truncation at all scales Λ . For the Keldysh block we have

$$P^K = i\bar{y}\mathbb{1}. \quad (2.24)$$

2.D The regulator function

The cutoff contribution ΔS_Λ is used in Eq. (2.15) to generate the effective action Γ_Λ from the microscopic action S by suppressing contributions from momenta below Λ . Its second functional derivative

$R_\Lambda = \Delta \mathcal{S}_\Lambda^{(2)}$ enters the exact flow equation (2.16). We choose an optimized cutoff function [51] of the form

$$R_\Lambda(Q) = (\mathbf{q}^2 - \Lambda^2) \theta(\Lambda^2 - \mathbf{q}^2) \begin{pmatrix} 0 & R^R \\ R^A & 0 \end{pmatrix}, \quad (2.25)$$

where

$$R^R = \begin{pmatrix} -\bar{A} & -\bar{D} \\ \bar{D} & -\bar{A} \end{pmatrix}, \quad R^A = (R^R)^T. \quad (2.26)$$

Due to the θ -function in (2.25), in the regularized inverse Green's function

$$G_\Lambda^{-1} = P_\Lambda + R_\Lambda, \quad (2.27)$$

momenta \mathbf{q}^2 smaller than the running scale Λ^2 acquire an effective mass $\propto \Lambda^2$ and we have $\det G_\Lambda^{-1}(Q = 0) \neq 0$, which ensures that momentum integrals over Green's functions are infrared convergent. Note that it is sufficient for R_Λ to modify only the retarded and advanced blocks (i.e., the spectrum) of the inverse Green's function. The choice of a frequency-independent cutoff allows us to perform frequency integrals analytically.

The interpolation property of Γ_Λ between the classical action \mathcal{S} and the effective action Γ is guaranteed by the limiting behavior [33]

$$\lim_{\Lambda^2 \rightarrow \Lambda_0^2} R_\Lambda \sim \Lambda_0^2, \quad \lim_{\Lambda^2 \rightarrow 0} R_\Lambda = 0. \quad (2.28)$$

2.E Flow of the effective potential

In equilibrium problems, an important object for practical calculations is the effective potential. It describes the homogeneous part of the effective action and is obtained by evaluating the full effective action at spatially homogeneous field configurations, $\bar{U} = \Gamma/\Omega \big|_{\chi(Q)=\chi\delta(Q)}$ (Ω is the quantization volume). In the framework of a derivative expansion, a closed flow equation can be derived for this object, which serves as a compact generating functional for the flow of all local couplings to arbitrarily high order. Here we provide the Keldysh analog of this construction, where the key difference roots in the occurrence of two field variables ϕ_c, ϕ_q , in contrast to a single field in equilibrium. However, for a theory which obeys the power counting discussed in the main text, we can parameterize the homogeneous part of the effective action as

$$\bar{V} = \frac{\partial \bar{U}}{\partial \phi_c} \phi_q + \frac{\partial \bar{U}^*}{\partial \phi_c^*} \phi_q^* + i\bar{\gamma} \phi_q^* \phi_q, \quad (2.29)$$

with $\bar{U} = \bar{U}(\phi_c^* \phi_c)$ dependent on the $U(1)$ invariant combination of classical fields only, this function thus being the direct counterpart of the effective potential. A flow equation can be derived for the auxiliary object \bar{V} , which reads (we introduce a dimensionless scale derivative $\partial_\ell \equiv \Lambda \partial_\Lambda$)

$$\partial_\ell \bar{V} = -\frac{i}{2} \int_Q \text{tr} [\mathcal{G}_\Lambda(Q) \partial_\ell R_\Lambda(Q)]. \quad (2.30)$$

Here, the inverse of \mathcal{G}_Λ is obtained from the full second functional variation by evaluating it at homogeneous field configurations (step (i) above Eq. (2.20)), however without inserting the stationary state values (step (ii)): $\mathcal{G}_\Lambda^{-1} = \Gamma_\Lambda^{(2)} \big|_{\chi(Q)=\chi\delta(Q)} + R_\Lambda$. \mathcal{G}_Λ is then diagonal in momentum space, and so

the trace in Eq. (2.16) reduces to a single momentum integration, giving rise to the above compact form. In contrast to G_Λ^{-1} , \mathcal{G}_Λ^{-1} has a non-vanishing upper left block P^H . However, it vanishes when the background fields are set to their stationary state values, $P^H|_{\text{ss}} = 0$, which is a manifestation of causality in the Keldysh formalism [26, 27].

From this equation we obtain the β -functions for the momentum-independent couplings by evaluating appropriate derivatives with respect to the $U(1)$ invariants

$$\rho_c = \phi_c^* \phi_c, \quad \rho_{cq} = \phi_c^* \phi_q = \rho_{qc}^*, \quad \rho_q = \phi_q^* \phi_q. \quad (2.31)$$

at their stationary state values $\rho_c|_{\text{ss}} = \rho_0$, $\rho_{cq}|_{\text{ss}} = \rho_{qc}|_{\text{ss}} = \rho_q|_{\text{ss}} = 0$. Specifically, we use the projection prescriptions

$$\begin{aligned} \partial_\ell \rho_0 &= \beta_{\rho_0} = -\frac{1}{u} \left[\partial_{\rho_{cq}} \partial_\ell \bar{V} \right]_{\text{ss}}, \\ \partial_\ell \bar{u} &= \beta_{\bar{u}} = \bar{u}' \partial_\ell \rho_0 + \left[\partial_{\rho_c \rho_{cq}}^2 \partial_\ell \bar{V} \right]_{\text{ss}}, \\ \partial_\ell \bar{u}' &= \beta_{\bar{u}'} = \left[\partial_{\rho_c}^2 \partial_{\rho_{cq}} \partial_\ell \bar{V} \right]_{\text{ss}}, \\ \partial_\ell \bar{\gamma} &= \beta_{\bar{\gamma}} = i \rho_0 \left[\partial_{\rho_{cq} \rho_{qc}}^2 \partial_\ell \bar{V} \right]_{\text{ss}}. \end{aligned} \quad (2.32)$$

Calculation of the explicit expressions here and below is largely automatized using MATHEMATICA.

2.F Flow of the inverse propagator

While the flow equation for the effective potential (2.30) generates β -functions for all momentum-independent couplings, the flow of the complex dynamic Z and kinetic \bar{K} couplings, which constitute the momentum-dependent part of the effective action (3), is determined by the flow equation for the inverse propagator. We obtain the latter by taking the second variational derivative of the exact flow equation (2.16) and setting the background fields to their stationary state values Eq. (2.20),

$$\partial_\ell P_{\Lambda,ij}(Q) = \frac{i}{2} \int_{Q'} \text{tr} \left[G_\Lambda^2(Q' - Q) \partial_\ell R_\Lambda(Q' - Q) \gamma_i G_\Lambda(Q') \gamma_j + G_\Lambda(Q' - Q) \gamma_i G_\Lambda^2(Q') \partial_\ell R_\Lambda(Q') \gamma_j \right], \quad (2.33)$$

where

$$\gamma_{i,jl} \delta(P - P' + Q) = \frac{\delta \Gamma_{\Lambda,jl}^{(2)}(P, P')}{\delta \chi_i(Q)} \Big|_{\text{ss}}. \quad (2.34)$$

In Eq. (2.33) we omit tadpole contributions $\propto \Gamma_\Lambda^{(4)}$, which do not depend on the external momentum Q and hence do not contribute to the flow of Z or \bar{K} . For these we use the projection prescriptions

$$\begin{aligned} \partial_\ell Z &= \beta_Z = -\frac{1}{2} \partial_\omega \text{tr} \left[(\mathbb{1} + \sigma_y) \partial_\ell P^R(Q) \right] \Big|_{Q=0}, \\ \partial_\ell \bar{K} &= \beta_{\bar{K}} = \partial_{q^2} \left[\partial_\ell P_{22}^R(Q) + i \partial_\ell P_{12}^R(Q) \right] \Big|_{Q=0}. \end{aligned} \quad (2.35)$$

The β -functions (2.32) and (2.35) constitute the components of $\beta_{\mathbf{g}} = (\beta_Z, \beta_{\bar{K}}, \beta_{\rho_0}, \beta_{\bar{u}}, \beta_{\bar{u}'}, \beta_{\bar{\gamma}})^T$.

2.G Rescaled flow equations

We write the flow equation for the complex dynamic coupling Z in the form

$$\partial_\ell Z = -\eta_Z Z. \quad (2.36)$$

The anomalous dimension η_Z is an algebraic function of the rescaled couplings (6) and ρ_0 . The same applies to the β -functions of the latter,

$$\begin{aligned} \partial_\ell K &= \beta_K = \eta_Z K + \frac{1}{Z} \beta_{\bar{K}}, \\ \partial_\ell u &= \beta_u = \eta_Z u + \frac{1}{Z} \beta_{\bar{u}}, \\ \partial_\ell u' &= \beta_{u'} = \eta_Z u' + \frac{1}{Z} \beta_{\bar{u}'}, \\ \partial_\ell \gamma &= \beta_\gamma = (\eta_Z + \eta_Z^*) \gamma + \frac{1}{|Z|^2} \beta_{\bar{\gamma}}. \end{aligned} \quad (2.37)$$

In particular, the very right expressions in these equations ($\beta_{\bar{K}}/Z$ etc.) are functions of the rescaled couplings alone. In terms of these variables, therefore, all explicit reference to the running coupling Z is gone, and we have effectively traded the differential flow equation for Z for the algebraic expression for its anomalous dimension η_Z .

All couplings except for γ are complex valued. Taking real and imaginary parts of the β -functions for K , u , and u' yields the flow equations for A , D , λ , κ , λ' , and κ' respectively,

$$\begin{aligned} \partial_\ell A &= \beta_A = \text{Re } \beta_K, & \partial_\ell D &= \beta_D = \text{Im } \beta_K, \\ \partial_\ell \lambda &= \beta_\lambda = \text{Re } \beta_u, & \partial_\ell \kappa &= \beta_\kappa = \text{Im } \beta_u, \\ \partial_\ell \lambda' &= \beta_{\lambda'} = \text{Re } \beta_{u'}, & \partial_\ell \kappa' &= \beta_{\kappa'} = \text{Im } \beta_{u'}. \end{aligned} \quad (2.38)$$

The β -functions for the ratios $\mathbf{r} = (r_K, r_u, r_{u'})^T$ are then

$$\begin{aligned} \partial_\ell r_K &= \beta_{r_K} = \frac{1}{D} \beta_A - \frac{r_K}{D} \beta_D, \\ \partial_\ell r_u &= \beta_{r_u} = \frac{1}{\kappa} \beta_\lambda - \frac{r_u}{\kappa} \beta_\kappa, \\ \partial_\ell r_{u'} &= \beta_{r_{u'}} = \frac{1}{\kappa'} \beta_{\lambda'} - \frac{r_{u'}}{\kappa'} \beta_{\kappa'}. \end{aligned} \quad (2.39)$$

The number of flow equations can be further reduced by introducing anomalous dimensions for D and γ ,

$$\begin{aligned} \partial_\ell D &= -\eta_D D, \\ \partial_\ell \gamma &= -\eta_\gamma \gamma. \end{aligned} \quad (2.40)$$

As for the dynamic coupling Z in terms of the rescaled variables K , u , u' , γ and ρ_0 , all explicit reference to D and γ drops out, and we obtain for the couplings $\mathbf{s} = (w, \tilde{\kappa}, \tilde{\kappa}')^T$ defined in Eq. (5)

$$\begin{aligned} \partial_\ell w &= \beta_w = -(2 - \eta_D) w + \frac{w}{\kappa} \beta_\kappa + \frac{2\kappa}{\Lambda^2 D} \beta_{\rho_0}, \\ \partial_\ell \tilde{\kappa} &= \beta_{\tilde{\kappa}} = -(1 - 2\eta_D + \eta_\gamma) \tilde{\kappa} + \frac{\gamma}{2\Lambda D^2} \beta_\kappa, \\ \partial_\ell \tilde{\kappa}' &= \beta_{\tilde{\kappa}'} = -(-3\eta_D + 2\eta_\gamma) \tilde{\kappa}' + \frac{\gamma^2}{4D^3} \beta_{\kappa'}. \end{aligned} \quad (2.41)$$

In summary, the transformations (4) and (5) result in the closed system (6) for \mathbf{r} and \mathbf{s} with $\beta_{\mathbf{r}} = (\beta_{r_K}, \beta_{r_u}, \beta_{r_{u'}})^T$ given by Eq. (2.39) and $\beta_{\mathbf{s}} = (\beta_w, \beta_{\tilde{k}}, \beta_{\tilde{k}'})^T$ given by Eq. (2.41). The flows of Z , D , and γ are decoupled and determined by the anomalous dimensions (2.36) and (2.40), which are themselves functions of \mathbf{r} and \mathbf{s} .

2.H Critical properties

For the analysis of critical behavior, we need to find a scaling solution to the flow equations for the bare couplings or, equivalently, a fixed point \mathbf{r}_* , \mathbf{s}_* of the flow of dimensionless rescaled couplings,

$$\beta_{\mathbf{r}}(\mathbf{r}_*, \mathbf{s}_*) = \beta_{\mathbf{s}}(\mathbf{r}_*, \mathbf{s}_*) = \mathbf{0}. \quad (2.42)$$

This non-linear algebraic set of equations has a non-trivial solution given by Eq. (7). In order to characterize the infrared flow in the vicinity of the fixed point (encoding the critical exponents we are interested in here), we study the flow of the couplings linearized around the fixed point, cf. Eq. (8). The stability matrices N and S in this equation read explicitly

$$N = \nabla_{\mathbf{r}}^T \beta_{\mathbf{r}} \Big|_{\mathbf{r}=\mathbf{r}_*, \mathbf{s}=\mathbf{s}_*} = \begin{pmatrix} 0.0525 & 0.0586 & 0.0317 \\ -0.0002 & -0.0526 & 0.1956 \\ 0.4976 & -2.3273 & 1.9725 \end{pmatrix}, \quad (2.43)$$

$$S = \nabla_{\mathbf{s}}^T \beta_{\mathbf{s}} \Big|_{\mathbf{r}=\mathbf{r}_*, \mathbf{s}=\mathbf{s}_*} = \begin{pmatrix} -1.6204 & 0.0881 & 0.0046 \\ -3.1828 & 0.2899 & 0.0363 \\ -15.3743 & -42.2487 & 2.1828 \end{pmatrix}, \quad (2.44)$$

without coupling between \mathbf{r} and \mathbf{s} sectors. At present we cannot rule out that an extended truncation would couple them. However, since we already include all relevant and marginal couplings, we expect the decoupling to be robust or at least approximately valid to a good accuracy.

The infrared flow of Z , D , and γ is determined by the values of the respective anomalous dimensions at the fixed point. Equations (2.36) and (2.40) imply the scaling behavior

$$Z \sim \Lambda^{-\eta_Z}, \quad D \sim \Lambda^{-\eta_D}, \quad \gamma \sim \Lambda^{-\eta_\gamma} \quad (2.45)$$

for $\Lambda \rightarrow 0$. While η_D and η_γ describe the flow of real quantities and are, therefore, themselves real by definition, η_Z is in general a complex valued function of \mathbf{r} and \mathbf{s} . At the fixed point, however, the imaginary part vanishes,

$$\text{Im } \eta_Z = 0, \quad (2.46)$$

which ensures scale invariance of the full effective action at the critical point.

As is indicated in the main text, the emergence of $O(2)$ model critical properties in the sector \mathbf{s} is due to the scaling relation $\eta_Z = \eta_{\tilde{\gamma}}$, which ensures that these anomalous dimensions compensate each other in the β -functions for the couplings \mathbf{s} . (The anomalous dimensions $\eta_{\tilde{\gamma}}$ and η_γ associated with the bare and renormalized noise vertices, respectively, are related via $\eta_\gamma = \eta_{\tilde{\gamma}} - 2 \text{Re } \eta_Z$, as follows from Eq. (4) in the main text.) This can be seen most simply by expressing, e.g., \tilde{k} in terms of bare quantities,

$$\tilde{k} = \frac{\gamma \text{Im}(u)}{2\Lambda \text{Im}(K)^2} = \frac{\gamma \text{Im}(\tilde{u}/Z)}{2\Lambda \text{Im}(\tilde{K}/Z)^2}. \quad (2.47)$$

In this form it is apparent that the scaling $\sim \Lambda^{-\eta_Z}$ which applies to both Z and $1/\gamma$ drops out. Similar arguments hold for w and $\tilde{\kappa}'$. Alternatively, the cancellation of η_Z and η_γ in the β -functions can be seen explicitly by inserting Eqs. (2.37) and (2.38) in (2.41). What remains is a dependence on $\eta \equiv \eta_D + \eta_Z$ which is just the anomalous dimension associated with the bare kinetic coefficient \bar{K} .

2.1 Ginzburg Criterion

We estimate the extent of the universal critical domain governed by the linearized regime of the Wilson-Fisher fixed point, which provides us with an estimate of both the extent of the thermalized regime as well as the energy resolution necessary to probe the critical behavior. This is done by calculating the Ginzburg scale, i.e., the distance from the phase transition where fluctuations on top of the quadratic Bogoliubov-type theory become dominant [50]: We equate the bare distance from the phase transition χ to the corresponding one-loop correction, yielding

$$\chi_G = \frac{1}{D^3} \left(\frac{\gamma\kappa}{4\pi} \right)^2. \quad (2.48)$$

Here, the parameters γ , κ , and D are those appearing in the mesoscopic description of the system. In the case of exciton-polariton condensates, γ and κ can thus be read off from the dGPE and the noise correlator [16, 17, 20]. The parameter D typically does not appear explicitly in this description. However, it is included effectively in a complex prefactor of the time derivative in the dGPE (m_{LP} is the mass of the lower polariton)

$$i(1 + i\Delta Z) \partial_t \psi = \left(-\frac{1}{2m_{LP}} \nabla^2 + \dots \right) \psi. \quad (2.49)$$

Such a term results from two physical mechanisms. First, it describes the leading frequency dependence of the pumping process [21]. To account for this effect, a convenient parameterization is $\Delta Z = P/(2\Omega_K)$ which is proportional to the pumping strength P , and where Ω_K is the gain cutoff frequency. Second, it results from energy relaxation due to scattering of the lower polaritons with high frequency photons and excitons [22]. These processes are captured by the form $\Delta Z = \kappa\bar{n}/2$ scaling linearly with the time averaged density \bar{n} , and a phenomenological relaxation constant κ .

Dividing the dGPE (2.49) by $1 + i\Delta Z$ leads to an effective kinetic term $-\frac{1-i\Delta Z}{1+\Delta Z^2} \frac{\nabla^2}{2m_{LP}} \psi$, resulting in a mesoscopic coherent propagation coefficient $A = \frac{1}{1+\Delta Z^2} \frac{1}{2m_{LP}}$ and an effective mesoscopic diffusion constant $D = \frac{\Delta Z}{1+\Delta Z^2} \frac{1}{2m_{LP}}$ entering Eq. (1) in the main text, and the above Ginzburg criterion.

Finally, we would like to contrast the Ginzburg scale to a scale identified in [16, 17, 20, 21]. This scale indicates a crossover between a sonic and a purely diffusive excitation spectrum within the symmetry broken phase, and takes the value $\omega_c = \kappa\rho_0$.

The Ginzburg scale identifies the frequency scale below which critical fluctuations become more dominant than the “bare” terms, which occur in Bogoliubov theory. It is therefore only meaningful – and makes a statement about – the physics close to the phase transition, where the order parameter goes to zero.

Instead, the crossover scale in [16, 17, 20, 21] is determined within the symmetry broken phase and is obtained within Bogoliubov theory, without the need of a calculation of fluctuation corrections.

This is justified, because within the symmetry broken phase there are no critical fluctuations and mean field plus Bogoliubov theory are valid.

As implied by this comparison, these two scales are not directly related to each other and address different physical questions. In particular, the crossover scale in [16, 17, 20, 21] tends to zero when approaching the phase transition by construction, $\rho_0 \rightarrow 0$. Therefore, in the vicinity of the critical point, the discussion of diffusive vs. coherent dynamics is a more subtle issue. How it works quantitatively is addressed by the calculation of the critical exponents, with the key finding of universal decoherence: The coherent dynamics fades out faster than the dissipative one, measured by the critical exponent η_r .

Bibliography

- [1] I. Carusotto and C. Ciuti, *Rev. Mod. Phys.* **85**, 299 (2013).
- [2] J. Kasprzak, M. Richard, S. Kundermann, A. Baas, P. Jeambrun, J. M. J. Keeling, F. M. Marchetti, M. H. Szymańska, R. Andre, J. L. Staehli, V. Savona, P. B. Littlewood, B. Deveaud, and L. S. Dang, *Nature* **443**, 409 (2006).
- [3] R. J. Schoelkopf and S. M. Girvin, *Nature* **451**, 664 (2008).
- [4] J. Clarke and F. K. Wilhelm, *Nature* **453**, 1031 (2008).
- [5] M. Hartmann, F. Brandao, and M. Plenio, *Laser & Photonics Reviews* **2**, 527 (2008).
- [6] H. Ritsch, P. Domokos, F. Brennecke, and T. Esslinger, *Rev. Mod. Phys.* **85**, 553 (2013).
- [7] G. Roumpos, M. Lohse, W. H. Nitsche, J. Keeling, M. H. Szymańska, P. B. Littlewood, A. Löffler, S. Höfling, L. Worschech, A. Forchel, and Y. Yamamoto, *PNAS* **109**, 6467 (2012).
- [8] A. Mitra, S. Takei, Y. B. Kim, and A. J. Millis, *Phys. Rev. Lett.* **97**, 236808 (2006).
- [9] S. Diehl, A. Micheli, A. Kantian, B. Kraus, H. P. Buchler, and P. Zoller, *Nat. Phys.* **4**, 878 (2008).
- [10] S. Diehl, A. Tomadin, A. Micheli, R. Fazio, and P. Zoller, *Phys. Rev. Lett.* **105**, 015702 (2010).
- [11] E. G. Dalla Torre, E. Demler, T. Giamarchi, and E. Altman, *Nat. Phys.* **6**, 806 (2010).
- [12] E. G. D. Torre, S. Diehl, M. D. Lukin, S. Sachdev, and P. Strack, *Phys. Rev. A* **87**, 023831 (2013).
- [13] B. Öztop, M. Bordyuh, Özgür E Müstecaplıoğlu, and H. E. Türeci, *New J. Phys.* **14**, 085011 (2012).
- [14] M. Wouters and I. Carusotto, *Phys. Rev. B* **74**, 245316 (2006).
- [15] P. C. Hohenberg and B. I. Halperin, *Rev. Mod. Phys.* **49**, 435 (1977).
- [16] I. Carusotto and C. Ciuti, *Phys. Rev. B* **72**, 125335 (2005).

- [17] M. Wouters and I. Carusotto, *Phys. Rev. Lett.* **99**, 140402 (2007).
- [18] J. Keeling, P. R. Eastham, M. H. Szymańska, and P. B. Littlewood, *Phys. Rev. Lett.* **93**, 226403 (2004).
- [19] M. H. Szymańska, J. Keeling, and P. B. Littlewood, *Phys. Rev. Lett.* **96**, 230602 (2006).
- [20] J. Keeling and N. G. Berloff, *Phys. Rev. Lett.* **100**, 250401 (2008).
- [21] M. Wouters and I. Carusotto, *Phys. Rev. Lett.* **105**, 020602 (2010).
- [22] M. Wouters, T. C. H. Liew, and V. Savona, *Phys. Rev. B* **82**, 245315 (2010).
- [23] J. Keeling, M. Szymańska, and P. Littlewood, in *Optical Generation and Control of Quantum Coherence in Semiconductor Nanostructures*, NanoScience and Technology, edited by G. Slavcheva and P. Roussignol (Springer Berlin Heidelberg, 2010) pp. 293–329.
- [24] P. M. Chaikin and T. C. Lubensky, *Principles of Condensed Matter Physics* (Cambridge University Press, Cambridge, 1995).
- [25] U. C. Täuber, in *Ageing and the Glass Transition*, Lecture Notes in Phys., Vol. 716, edited by M. Henkel, M. Pleimling, and R. Sanctuary (Springer-Verlag, Berlin, 2007) pp. 295–348.
- [26] A. Kamenev and A. Levchenko, *Adv. Phys.* **58**, 197 (2009).
- [27] A. Altland and B. Simons, *Condensed Matter Field Theory*, 2nd ed. (Cambridge University Press, Cambridge, 2010).
- [28] P. C. Martin, E. D. Siggia, and H. A. Rose, *Phys. Rev. A* **8**, 423 (1973).
- [29] C. De Dominicis, *Le Journal de Physique Colloques* **37**, C1 (1976).
- [30] A. Mitra and A. Rosch, *Phys. Rev. Lett.* **106**, 106402 (2011).
- [31] C. Wetterich, *Phys. Lett. B* **301**, 90 (1993).
- [32] T. Gasenzer and J. M. Pawłowski, *Phys. Lett. B* **670**, 135 (2008).
- [33] J. Berges and G. Hoffmeister, *Nucl. Phys. B* **813**, 383 (2009).
- [34] J. Berges, N. Tetradis, and C. Wetterich, *Phys. Rept.* **363**, 223 (2002).
- [35] M. Salmhofer and C. Honerkamp, *Progress of Theoretical Physics* **105**, 1 (2001).
- [36] J. M. Pawłowski, *Annals of Physics* **322**, 2831 (2007).
- [37] B. Delamotte, in *Renormalization Group and Effective Field Theory Approaches to Many-Body Systems SE - 2*, Lecture Notes in Physics, Vol. 852, edited by A. Schwenk and J. Polonyi (Springer Berlin Heidelberg, 2012) pp. 49–132.
- [38] O. J. Rosten, *Physics Reports* **511**, 177 (2012).
- [39] I. Boettcher, J. M. Pawłowski, and S. Diehl, *Nuclear Physics B - Proceedings Supplements* **228**, 63 (2012).

-
- [40] L. Canet and H. Chaté, *Journal of Physics A: Mathematical and Theoretical* **40**, 1937 (2007).
- [41] R. Guida and J. Zinn-Justin, *Journal of Physics A: Mathematical and General* **31**, 8103 (1998).
- [42] C. Aron, G. Biroli, and L. F. Cugliandolo, *J. Stat. Mech.* **2010**, P11018 (2010).
- [43] L. Canet, H. Chaté, and B. Delamotte, *J. Phys. A: Math. Theor.* **44**, 495001 (2011).
- [44] R. Graham, in *Quantum Statistics in Optics and Solid-State Physics*, Springer Tracts in Modern Physics, Vol. 66 (Springer-Verlag, Berlin, 1973) pp. 1–97.
- [45] U. Decker and F. Haake, *Phys. Rev. A* **11**, 2043 (1975).
- [46] U. C. Täuber, V. K. Akkineni, and J. E. Santos, *Phys. Rev. Lett.* **88**, 045702 (2002).
- [47] L. M. Sieberer, S. D. Huber, E. Altman, and S. Diehl, *Physical Review B* **89**, 134310 (2014).
- [48] J. T. Stewart, J. P. Gaebler, and D. S. Jin, *Nature* **454**, 744 (2008).
- [49] S. Utsunomiya, L. Tian, G. Roumpos, C. W. Lai, N. Kumada, T. Fujisawa, M. Kuwata-Gonokami, A. Löffler, S. Höfling, A. Forchel, and Y. Yamamoto, *Nat. Phys.* **4**, 700 (2008).
- [50] D. J. Amit and V. Martin-Mayor, *Field Theory, the Renormalization Group, and Critical Phenomena*, 3rd ed. (World Scientific, Singapore, 2005).
- [51] D. F. Litim, *Phys. Lett. B* **486**, 92 (2000).

CHAPTER 3

PUBLICATION

Nonequilibrium functional renormalization for driven-dissipative Bose-Einstein condensation[†]

Phys. Rev. B, **89**, 134310 (2014)

L. M. Sieberer,^{1,2} S. D. Huber,^{3,4} E. Altman,^{4,5} and S. Diehl^{1,2}

¹*Institute for Theoretical Physics, University of Innsbruck, A-6020 Innsbruck, Austria*

²*Institute for Quantum Optics and Quantum Information of the Austrian Academy of Sciences, A-6020 Innsbruck, Austria*

³*Theoretische Physik, Wolfgang-Pauli-Straße 27, ETH Zurich, CH-8093 Zurich, Switzerland*

⁴*Department of Condensed Matter Physics, Weizmann Institute of Science, Rehovot 76100, Israel*

⁵*Department of Physics, University of California, Berkeley, CA 94720, USA*

We present a comprehensive analysis of critical behavior in the driven-dissipative Bose condensation transition in three spatial dimensions. Starting point is a microscopic description of the system in terms of a many-body quantum master equation, where coherent and driven-dissipative dynamics occur on an equal footing. An equivalent Keldysh real time functional integral reformulation opens up the problem to a practical evaluation using the tools of quantum field theory. In particular, we develop a functional renormalization group approach to quantitatively explore the universality class of this stationary non-equilibrium system. Key results comprise the emergence of an asymptotic thermalization of the distribution function, while manifest non-equilibrium properties are witnessed in the response properties in terms of a new, independent critical exponent. Thus the driven-dissipative microscopic nature is seen to bear observable consequences on the largest length scales. The absence of two symmetries present in closed equilibrium systems – underlying particle number conservation and detailed balance, respectively – is identified as the root of this new non-equilibrium critical behavior. Our results are relevant for broad ranges of open quantum systems on the interface of quantum optics and many-body physics, from exciton-polariton condensates to cold atomic gases.

[†]The author of the thesis performed most of the analytical and all of the numerical calculations. He wrote substantial parts of the manuscript.

3.1 Introduction

In recent years, there has been tremendous progress in realizing systems with many degrees of freedom, in which matter is strongly coupled to light [1]. This concerns vastly different experimental platforms: In ensembles of ultracold atoms, the immersion of a Bose-Einstein condensate (BEC) into an optical cavity has allowed to achieve strong matter-light coupling, and lead to the realization of open Dicke models [2–4]; In the context of semiconductor quantum wells in optical cavities, non-equilibrium Bose condensation has been achieved [5–7] – here the effective degrees of freedom, the exciton-polaritons, result from a strong hybridization of cavity light and excitonic matter degrees of freedom [1, 8, 9]. Further promising platforms, which are at the verge of the transition to true many-body systems, are arrays of microcavities [10–13] or trapped ions [14, 15], as well as optomechanical setups [16–18].

Those systems have three key properties in common. First, they are strongly driven by external fields, such as lasers, placing them far away from thermodynamic equilibrium even under stationary conditions. Equilibrium detailed balance relations therefore are not generically present. Second, they exhibit the characteristics of quantum optical setups, in that coherent and dissipative dynamics occur on an equal footing, but at the same time are also genuine many-body systems. Finally, a third characteristic is the absence of the conservation of particle number. In particular, the admixture of light opens up strong loss channels for the effective hybrid light-matter degrees of freedom, and it becomes necessary to counterpoise these losses by continuous pumping mechanisms in order to achieve stable stationary flux equilibrium states. The pumping mechanisms can be either coherent or incoherent. In the latter case, e.g., single particle pumping directly counteracts the incoherent single particle loss; once it starts to dominate over the losses, a second order phase transition results on the mean-field level, in close analogy to a laser threshold.

At this point a clear difference between the quantum optical single mode problem of a laser and a driven-dissipative many-body problem becomes apparent: While the inclusion of fluctuations in the treatment of a laser smears out the mean-field transition, in a system with a continuum of spatial degrees of freedom a genuine out-of-equilibrium second order phase transition with true universal critical behavior can be expected. The theoretical challenge is then to understand the universal phenomena that can emerge due to the many-body complexity in a driven non-equilibrium setting.

In this work we address this challenge, focusing on a key representative that shows all the above characteristics: The driven-dissipative Bose condensation transition, relevant to experiments with exciton-polariton condensates, or more generally to any driven-dissipative system equipped with a $U(1)$ symmetry of global phase rotations tuned to its critical point. We provide a comprehensive characterization of the resulting non-equilibrium critical behavior in three dimensions, extending and corroborating results presented recently [19]. A key finding concerns the existence of an additional, independent critical exponent associated with the non-equilibrium drive. It describes universal decoherence at long distances, and is observable, e.g., in the single particle response, as probed in homodyne detection of exciton-polariton systems [20]. This entails evidence that the microscopic non-equilibrium character bears observable consequences up to the largest distances in driven Bose condensation. Furthermore an asymptotic thermalization mechanism for the low frequency distribution function is found. Such a phenomenon has been observed previously in other contexts [21–29]. Here it is reflected in a symmetry that is emergent in the critical system on the longest scales.

By contrast, in systems at true thermal equilibrium, this symmetry is present at all scales as a

microscopic symmetry. It then places severe restrictions on the relations between the noise and the coherent and dissipative dynamics in the system [30, 31], leading to fluctuation dissipation relations valid at all frequencies and wavelengths. This is the case, e.g., in the models for dynamical universality classes established by Hohenberg and Halperin (HH) [32]. Non-equilibrium perturbations to these models that have been discussed in the literature concern, e.g., modifications of the noise term by spatial anisotropies, violating fluctuation-dissipation relations on a microscopic scale. For models without conserved order parameter, such as model A (MA) of HH, it has been shown that this does not lead to the existence of new universal critical behavior, but rather to a modification of non-universal amplitude ratios [33, 34]. Genuinely non-equilibrium universal critical behavior has been found in several classical, driven systems with different microscopic origins. Examples include models with conserved order parameter with spatially anisotropic temperature [33], the driven-diffusive lattice gas, [35] reaction-diffusion systems [36–39], the problems of directed percolation [40, 41] and self-organized criticality [42], or kinetic roughening phenomena such as described by the Kardar-Parisi-Zhang equation [43–46].

At the technical level, the purpose of this paper is to lay out a general framework for addressing universal critical phenomena in open markovian many-body quantum systems. This framework may be further generalized and applied to a large variety of non-equilibrium situations, such as driven or driven-dissipative systems with different symmetries [47–50], driven-dissipative systems with disorder [51], and even superfluid turbulence [52–55]. We start from a microscopic, second quantized description of the system in terms of quantum master equations, and show how to translate the master equation into a Keldysh real-time functional integral, which opens up the toolbox of well-established techniques of quantum field theory. Next, we develop a functional renormalization group (FRG) approach based on the Wetterich equation [56], which allows us to compute both the dynamical critical behavior as well as certain non-universal aspects of the problem. For example, in addition to determining critical exponents we can also extract a Ginzburg scale which marks the extent of the critical fluctuation regime.

The paper is organized as follows. In the next section we present our key results and sketch the resulting physical picture. Section 3.3 introduces to our model and provides the mapping of the master equation to an equivalent Keldysh functional integral. Using this framework, in Sec. 3.4 we reproduce the results from mean-field and Bogoliubov theory, and show how the physics of a semi-classical driven-dissipative Gross-Pitaevskii equation emerges naturally as a low frequency limit of the full quantum master equation. We highlight the additional challenges which arise from the need to treat a continuum of spatial degrees of freedom in order to capture critical behavior, and show in Sec. 3.5 how they are properly addressed by means of the FRG approach. The precise manifestation of the non-equilibrium character of the problem is worked out in Sec. 3.6. A detailed comparison of our non-equilibrium versus more conventional equilibrium models highlights a symmetry which is only present in thermal equilibrium and expresses detailed balance. We summarize the computation of the flow equations in Sec. 3.7 and explain the hierarchical structure of the universal critical behavior implied by the flow. In Sec. 3.9 we discuss the numerical analysis of the flow equations. We conclude in Sec. 3.10.

At this point, we remark that the physical picture described in this work, and summarized in the following section, has been fully confirmed and further developed in a recent complementary perturbative field theoretical study presented in Ref. [57]. There, in particular, analytical estimates for the critical exponents are provided.

3.2 Key Results and physical picture

Driven-dissipative Bose condensation transition – Driven open quantum systems are commonly modeled microscopically by means of quantum master equations or in terms of Keldysh functional integrals as shown below. Starting from such a microscopic model of a driven Bose condensate we derive in Sec. 3.4.3 an effective long-wavelength description of the critical dynamics. The result, after dropping all irrelevant terms in the sense of renormalization group (RG), is a stochastic equation of motion for the order parameter, which may be cast in Langevin form,

$$i\partial_t\psi = \left[-(A - iD)\Delta - \mu - i\kappa_1 + 2(\lambda - i\kappa)|\psi|^2 \right] \psi + \xi. \quad (3.1)$$

Such a dissipative stochastic Gross-Pitaevskii equation has been used as a model for exciton-polariton condensates [58–63]. This equation includes terms describing coherent dynamics, as well as ones capturing the dissipative processes and the drive. The coherent terms are the inverse mass $A = 1/(2m)$, the chemical potential μ and the elastic two-body interaction λ , whereas dissipative contributions include a kinetic coefficient D , the effective single-particle loss rate κ_1 as the difference between single-particle loss and pump rates, as well as two-body loss κ . The loss and gain processes induce noise, which is taken into account by the Gaussian white noise source ξ of strength γ with zero mean, $\langle \xi(t, \mathbf{x}) \rangle = 0$, and correlations

$$\langle \xi(t, \mathbf{x}) \xi^*(t', \mathbf{x}') \rangle = \frac{\gamma}{2} \delta(t - t') \delta(\mathbf{x} - \mathbf{x}'). \quad (3.2)$$

Unlike the models of critical dynamics classified in Ref. [32], the coherent and dissipative terms in a driven condensate stem from completely independent physical processes. In particular, this implies that the steady state of the Langevin equation (3.1) is not characterized by a thermal (Gibbs) distribution of the fields, and this leads to the distinct critical behavior analyzed in this paper.

Equation (3.1) admits a time-independent homogeneous mean-field solution $|\psi_0|^2 = -\kappa_1/(2\kappa)$ if the single-particle pump rate exceeds the corresponding loss rate, i.e., the effective single-particle loss rate κ_1 becomes negative, and the chemical potential is set to be $\mu = 2\lambda|\psi_0|^2$. Thus at the mean-field level a continuous transition is tuned by varying the single particle pump rate: ψ_0 vanishes as κ_1 goes from negative values to zero. Mean-field theory, however, breaks down in the vicinity of the phase transition as the inclusion of fluctuations may induce non-trivial scaling behavior or even render the transition first order [64, 65]. In this paper we verify that the system described by (3.1) in three spatial dimensions indeed has a critical point characterized by universal dynamics. We argue that this dynamics is governed by a “Wilson-Fisher” like fixed point, but with another layer of dynamical critical behavior that is not found in non-driven systems.

Universality and extent of the critical domain – Our main technical tool for the analysis is a functional RG carried out for the dynamical problem. Emergence of a universal critical point is evident from the flow of the coupling constants to a fixed point independent of the initial conditions, as long as the system is tuned to the phase transition (cf. also Sec. 3.9). This is demonstrated in Fig. 3.1 (a), showing the flow of the real and imaginary parts of the complex interaction parameter $\tilde{u}_2 = \tilde{\lambda} + i\tilde{\kappa}$ (see Sec. 3.8.1). At the fixed point the real parts of all couplings vanish, which implies that the effective long-wavelength dynamics is purely dissipative. Integrating out fast fluctuations in the course of the RG flow, therefore, leads to a loss of coherence.

An important aspect of the phase transition which we analyze in detail here concerns the extent of the critical domain, which is delimited by the Ginzburg momentum scale k_G . Knowledge of this non-universal scale is important for assessing the requirements from experiments aimed at measuring the critical phenomena. We find it to be given by (cf. Sec. 3.9)

$$k_G = \gamma_\Lambda \kappa_\Lambda / (2CD_\Lambda^2), \quad (3.3)$$

where $C \approx 14.8$ and γ_Λ , κ_Λ , and D_Λ are, respectively, the noise-strength, two-body loss rate and dissipative kinetic coefficient appearing in the description of the system at a mesoscopic scale Λ (see Sec. 3.5.2). Here we confirm this behavior quantitatively by a full numerical solution of the flow equations outside the critical domain, highlighting the capability of the FRG approach to compute universal and non-universal physics in a single framework.

Asymptotic thermalization of the distribution function – An interesting result of the RG analysis is that the distribution function of the order parameter field at the critical point effectively thermalizes at long wavelengths and low frequencies. The effective thermalization is manifest as an emergent symmetry of the equations of motion at the fixed point that is not present at the mesoscopic level, cf. Sec. 3.6. For this reason the dynamical critical exponent z is the same as that of MA of the equilibrium classification. The presence of this symmetry implies a fluctuation-dissipation theorem (FDT), or, more physically speaking, a detailed balance condition valid at asymptotically long wavelengths.

In order to better understand this aspect, consider an equilibrium problem with detailed balance. This means that all subparts of the system are in equilibrium with each other. In other words, temperature is invariant under the system's partition in such a state. This statement is easily translated into a RG language: Natural system partitions are the momentum shells. Partition invariance of the temperature thus becomes a scale invariance of temperature under renormalization, which successively integrates out high momentum shells. The “equilibrium symmetry” expresses precisely this physical intuition.

In a non-equilibrium problem such as the driven condensate we discuss, this symmetry is in general absent at arbitrary momentum scales. In order to demonstrate how it emerges at long scales, we compute the scale dependence of an effective temperature, entering the (non-equilibrium) FDT, cf. Sec. 3.6. Indeed, we find scale dependent behavior at high momenta, which becomes universal and scale independent within the critical region delimited by the Ginzburg scale, cf. Fig. 3.2.

We note that, in principle, it is conceivable that the system might allow for different stationary scaling solutions far from equilibrium with different universal scaling behavior, not captured in the present approach. Indeed, in two dimensions, such a scenario is realized [66]. In three dimensions, however, such a behavior could be present only beyond a threshold value for the microscopic strength of violation of detailed balance.

Hierarchical shell structure of non-equilibrium criticality – A key result of the RG analysis is the hierarchical organization of the non-equilibrium criticality. This structure consists of three shells of critical exponents. The innermost shell in this hierarchy contains the two independent exponents ν, η describing the static (spatial) critical behavior of the classical $O(2)$ model.¹ We find that the

¹The continuous planar rotations of $O(2)$ reflect the continuous phase rotation symmetry $U(1) \cong SO(2)$ of the driven open Bose system.

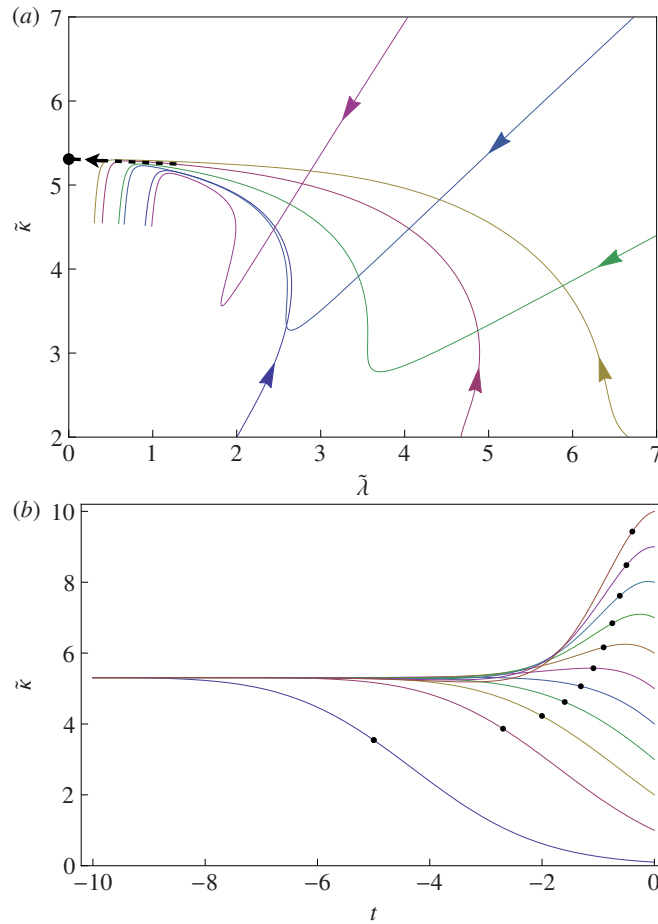


Figure 3.1. (Color online) Emergence of universality: (a) We show the flow of the complex renormalized two-body coupling $\tilde{u}_2 = \tilde{\lambda} + i\tilde{\kappa}$ (see Sec. 3.8.1) for various initial values $\tilde{u}_{2\Lambda}$. As a result of fine-tuning the initial values w_Λ of the dimensionless mass parameter close to criticality, all flow trajectories approach the Wilson-Fisher fixed point $\tilde{u}_{2*} = i5.308$ (indicated by the black dot) before eventually bending away. Shown are numerical solutions to the flow equations for $r_{K\Lambda} = 10$, $r_{u_3\Lambda} = 1$, $\tilde{\kappa}_{3\Lambda} = 0.01$, and values of $\tilde{u}_{2\Lambda}$ lying on a rectangle with sides $\tilde{\lambda} \in [0, 10]$, $\tilde{\kappa} = 2, 10$ and $\tilde{\lambda} = 10$, $\tilde{\kappa} \in [2, 10]$. (See Sec. 3.8.1 for definitions of the parameters.) (b) Flow of $\tilde{\kappa}$ as a function of the dimensionless infrared cutoff $t = \ln(k/\Lambda)$ for various starting values $\tilde{\kappa}_\Lambda$. Dots on the lines indicate the extent of the critical domain, which is set by the Ginzburg scale Eq. (3.3). Initial values are the same as in (a), apart from $\tilde{\kappa}_\Lambda = 0.1, 1, 2, \dots, 10$ and $r_{u_2\Lambda} = 10$.

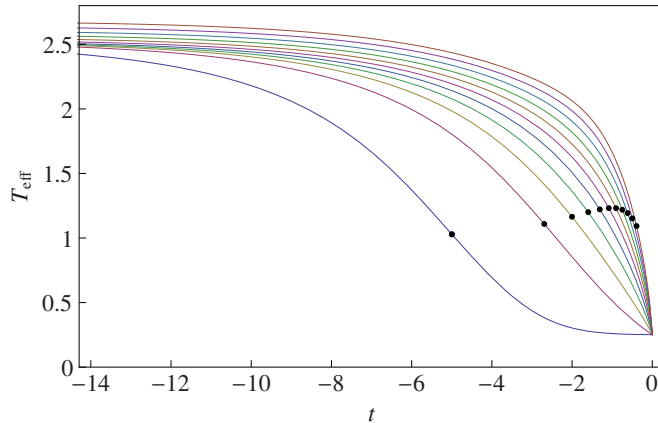


Figure 3.2. (Color online) Scale dependence at criticality of the effective temperature $T_{\text{eff}} = \bar{\gamma}/(4|Z|)$, where $\bar{\gamma}$ denotes the Keldysh mass and Z is the wave-function renormalization (see Secs. 3.5.2 and 3.8.1). For $t \rightarrow -\infty$ the effective temperature saturates to a constant value. Initial values are the same as in Fig. 3.1 (b).

static exponents coincide with those of an *ab initio* computation of the classical $O(2)$ exponents at the same level of approximation. Thus the non-equilibrium conditions do not modify the static critical behavior.

The intermediate shell contains the so-called dynamical exponent z which describes the dynamical (temporal) critical behavior. This intermediate shell is already present in models for equilibrium dynamical criticality. Crucially, it extends the static critical behavior but does not modify it. In fact there is a certain dynamical fine structure: The same static universality class splits up into various dynamical universality classes, classified in models A to J by HH [32]. Again, we find the dynamic exponents to coincide with the one of an *ab initio* computation for one of HH’s models (MA) – the non-equilibrium conditions do not modify the dynamical critical behavior either. A stronger physical consequence of this finding is discussed in the next subsection.

The unique element found only in the driven system is the outer shell of the aforementioned hierarchy. The related exponent η_r identified in Ref. [19], which we refer to as the “drive exponent”, physically describes universal decoherence of the long-wavelength dynamics as explained above. Crucially, η_r relates to the dynamical MA in the same way as MA relates to the classical $O(2)$ model: It adds a new shell, but does not “feed back” or modify the inner shells of the hierarchy. In Sec. 3.6 we argue that this exponent manifestly witnesses non-equilibrium conditions.

Independence of the drive exponent and maximality of the extension – It is important to demonstrate the independence of the drive exponent: At a second order phase transition, many critical exponents can be defined, each characterizing a different observable. However, only few of them are independent, i.e., cannot be expressed in terms of a smaller set by means of scaling relations.

The independence of the four critical exponents identified with our FRG approach is manifest in the block diagonal structure of the linearized RG flow in the vicinity of the Wilson-Fisher fixed point, cf. Sec. 3.8: There are two blocks, and the lowest eigenvalue of each of them determines an independent critical exponent. In addition we have the independent anomalous dimension η and the

dynamical exponent z .

A general way to determine the number of independent exponents and thereby see the need for one and only one additional exponent in this system (as compared to equilibrium MA dynamics) comes from the UV limit of the problem. Any independent critical exponent must be related to a short-distance mass scale in the problem [67]. For example, this can be seen in the case of the anomalous dimension associated with the spatial two-point correlation function. An anomalous dimension η implies decay of the correlation function as $\langle \phi^*(\mathbf{x})\phi(\mathbf{0}) \rangle \sim |\mathbf{x}|^{2-d+\eta}$. Since the physical units of this correlation are $[L]^{2-d}$ we require a microscopic scale a , to fix the units so that $\langle \phi^*(\mathbf{x})\phi(\mathbf{0}) \rangle \sim a^{-\eta} |\mathbf{x}|^{2-d+\eta} \sim [L]^{2-d}$. In the same way any non-trivial independent exponent requires such a microscopic scale.

To determine the number of independent critical exponents in our problem we therefore need to count the microscopic mass scales in the bare action. The corresponding quadratic part of the action reads

$$\sigma_m = \int dt d^d \mathbf{x} \left[(\phi_c^*, \phi_q^*) \begin{pmatrix} 0 & \mu - i\kappa_1 \\ \mu + i\kappa_1 & i\gamma \end{pmatrix} \begin{pmatrix} \phi_c \\ \phi_q \end{pmatrix} + f (j_c^* \phi_q + j_q^* \phi_c + \text{c.c.}) \right], \quad (3.4)$$

with real parameters μ, κ_1, γ, f . κ_1 and f , which describe the tuning parameter of the phase transition and an external ordering field respectively, have direct counterparts in the equilibrium $O(2)$ model. They give rise to the two critical exponents ν , which characterizes the divergence of the correlation length, and η , the anomalous dimension of the static two-point function. γ is introduced in the theory of dynamical critical phenomena and is associated to the dynamical exponent in the purely relaxational MA of HH [32]. In the full non-equilibrium problem however, there is yet another mass scale μ . This scale is at the origin of the additional independent exponent identified in Ref. [19].

From this discussion we conclude that the extension of the critical behavior at the condensation transition is maximal, i.e., no more independent exponents can exist. This is due to general requirements on the mass matrix above: the off-diagonal elements must be hermitian conjugates; the lower diagonal must be anti-hermitian; and the upper diagonal must be zero due to the conservation of probability.

It is worth noting how this analysis would change if the critical point in question involved breaking of a Z_2 symmetry rather than a continuous $O(N)$ symmetry as we discuss here. Such an Ising transition in a driven system is relevant for the formation of a super-solid due to interaction of a BEC with the modes of an optical cavity [2, 3]. In this case the reality of the Ising fields rules out an imaginary mass term ($\kappa_1 = 0$). Hence the maximal number of independent critical exponents is 3, which implies that there can be no modification of MA dynamics.

Interpretation and observability of the drive exponent – The drive critical exponent describes the universal flow behavior of all possible ratios of coherent vs. dissipative couplings (real vs. imaginary parts, see Sec. 3.8.1) to zero upon moving to larger and larger distances. In the competition of coherent and dissipative dynamics, loosely speaking dissipation always wins. Physically, this should be interpreted as a universal mechanism of decoherence. The drive exponent therefore is subleading and not observable in the correlation functions of the system. However, it is directly observable in the single particle dynamical response (single particle retarded Green's function).

The dynamical response can be measured with any probe that couples directly to the field operator $\hat{\psi}(\mathbf{x})$, i.e., any probe that out-couples single particles from the system. This is the case, e.g., in the

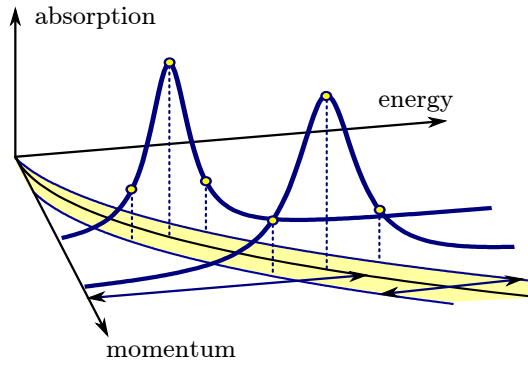


Figure 3.3. (Color online) Illustration of the observability of the drive exponent: The absorption peak for a measurement that observes the single particle dynamical response. The drive exponent η_r reveals itself in a different scaling of the peak location and peak-width as a function of the momentum.

angle-resolved detection of leakage photons in exciton-polariton systems [20], or in angle-resolved radio-frequency spectroscopy in ultra-cold atoms [68] As we argue in Sec. 3.8.3., the excitation spectrum close to the critical point is given by ($q = |\mathbf{q}|$)

$$\omega(q) \sim A_0 q^{z-\eta_r} - iD_0 q^z \sim A_0 q^{2.223} - iD_0 q^{2.121}, \quad (3.5)$$

where A_0 and D_0 are non-universal constants. This excitation spectrum leads to a broadened signal in the experiment, cf. Fig. 3.3. The drive exponent η_r can be observed due to the different scaling with momentum of the location ($\sim q^{z-\eta_r}$) and the width ($\sim q^z$) of the measured peak. We note here, however, that technical noise and other uncertainties in the measurement setup will unavoidably also lead to a broadening of the spectrum. The small value of $\eta_r = -0.101$ thus challenges experiments to verify this prediction.

3.3 The Model

In this section we introduce a generic microscopic description of driven-dissipative Bose systems, written in terms of a second quantized master equation. We then show how to translate this model into the Keldysh functional integral framework, which provides a convenient starting point for obtaining the long wavelength universal properties of the system. Moreover we introduce the concept of the effective action, which generalizes the action principle to include all quantum and statistical fluctuations and is the key object for the formulation of the FRG.

3.3.1 Quantum Master equation

Our model with particle loss and pumping is described microscopically by a many-body master equation that determines the time evolution of the system density operator (units are chosen such that $\hbar = 1$),

$$\partial_t \hat{\rho} = -i [\hat{H}, \hat{\rho}] + \mathcal{L}[\hat{\rho}]. \quad (3.6)$$

This equation incorporates both coherent dynamics generated by the Hamiltonian \hat{H} and dissipation that is subsumed in the action of the Liouville operator \mathcal{L} . The Hamiltonian \hat{H} describes interacting bosonic degrees of freedom of mass m and is given by (we use the shorthand $\int_{\mathbf{x}} = \int d^d \mathbf{x}$)

$$\hat{H} = \int_{\mathbf{x}} \hat{\psi}^\dagger(\mathbf{x}) \left(-\frac{\Delta}{2m} \right) \hat{\psi}(\mathbf{x}) + \frac{g}{2} \int_{\mathbf{x}} \hat{\psi}^\dagger(\mathbf{x})^2 \hat{\psi}(\mathbf{x})^2, \quad (3.7)$$

where $\hat{\psi}(\mathbf{x})$ are bosonic field operators. Note that we do not explicitly introduce any system chemical potential, as the density of the system will be fixed by the balance of pumping and losses. Two-body interactions are described by a density-density interaction with coupling constant g . In the following we shall be interested in dynamically stable systems which are characterized by a positive coupling constant $g > 0$. This modeling of interactions is valid on length scales which are not sufficient to resolve details of the microscopic interaction potential.

In our model, dissipative dynamics comes in the form of one-body pumping (p) and losses (l) as well as two-body losses (t). Accordingly, the Liouville operator can be decomposed into the sum of three terms $\mathcal{L} = \sum_{\alpha} \mathcal{L}_{\alpha}$ with $\alpha = p, l, t$ which have the common Lindblad structure

$$\mathcal{L}_{\alpha}[\hat{\rho}] = \gamma_{\alpha} \int_{\mathbf{x}} \left(\hat{L}_{\alpha}(\mathbf{x}) \hat{\rho} \hat{L}_{\alpha}^{\dagger}(\mathbf{x}) - \frac{1}{2} \{ \hat{L}_{\alpha}^{\dagger}(\mathbf{x}) \hat{L}_{\alpha}(\mathbf{x}), \hat{\rho} \} \right), \quad (3.8)$$

with local Lindblad or quantum jump operators $\hat{L}_{\alpha}(\mathbf{x})$ that create (p) and destroy (l) single particles; for $\alpha = t$ two particles are destroyed at the same instant in time, i.e., the quantum jump operators are given by

$$\hat{L}_p(\mathbf{x}) = \hat{\psi}^{\dagger}(\mathbf{x}), \quad \hat{L}_l(\mathbf{x}) = \hat{\psi}(\mathbf{x}), \quad \hat{L}_t(\mathbf{x}) = \hat{\psi}(\mathbf{x})^2. \quad (3.9)$$

These processes occur at rates γ_p, γ_l , and γ_t , respectively.

The net effect of single-particle pumping and losses is determined by the relative size of the respective rates: For $\gamma_p > \gamma_l$, there is an effective gain of single particles. Nevertheless, Eq. (3.6) leads (in a suitably chosen rotating frame, as we will show below) to a stationary state $\hat{\rho}_{ss}$ in which the gain of single particles is balanced by two-body losses. In this situation, a finite condensate amplitude builds up,

$$\langle \hat{\psi}(\mathbf{x}) \rangle_{ss} = \text{tr} \left(\hat{\psi}(\mathbf{x}) \hat{\rho}_{ss} \right) = \psi_0 \neq 0, \quad \gamma_p > \gamma_l. \quad (3.10)$$

That is, in stationary state the system is in a condensed phase in which the symmetry of the dynamics described by Eq. (3.6) under global $U(1)$ transformations of the field operators $\hat{\psi}(\mathbf{x}) \mapsto \hat{\psi}(\mathbf{x}) e^{i\phi}$ is broken. When the loss rate γ_l exceeds the pumping rate γ_p , on the other hand, no condensate emerges in stationary state, and the expectation value of the bosonic field operator is zero,

$$\langle \hat{\psi}(\mathbf{x}) \rangle_{ss} = 0, \quad \gamma_p \leq \gamma_l. \quad (3.11)$$

Equations (3.10) and (3.11) can be derived from the master equation (3.6) in mean-field approximation by making the ansatz of a coherent stationary state $\hat{\rho}_{\psi} = |\psi\rangle\langle\psi|$, where we assume that the amplitude in $|\psi\rangle = \frac{1}{\mathcal{N}} \exp\left(\psi \int_{\mathbf{x}} \hat{\psi}^{\dagger}(\mathbf{x})\right) |0\rangle$ is spatially homogeneous but possibly time-dependent. Proper normalization of the coherent state is ensured by the choice $\mathcal{N} = e^{V|\psi|^2}$ with the system volume V . The time-dependence of the condensate amplitude is determined by taking the time derivative on both sides of the equality $\psi = \text{tr} \left(\hat{\psi}(\mathbf{x}) \hat{\rho}_{\psi} \right)$ and using the master equation (3.6), which results in

$$i\partial_t \psi = \left[g |\psi|^2 + \frac{i}{2} (\gamma_p - \gamma_l - 2\gamma_t |\psi|^2) \right] \psi. \quad (3.12)$$

For $\gamma_p > \gamma_l$ this equation allows for a solution of the form $\psi = \psi_0 e^{-i\mu t}$, where the condensate density is determined by the imaginary part of the term in brackets on the right-hand side (RHS) as

$$|\psi_0|^2 = \frac{\gamma_p - \gamma_l}{2\gamma_t}. \quad (3.13)$$

The parameter μ is then given by $\mu = g |\psi_0|^2$. We obtain the steady state density matrix of Eq. (3.10) by means of a transformation to a rotating frame with the unitary operator $\hat{U} = \exp(i\mu \hat{N} t)$, where the particle number operator is $\hat{N} = \int_{\mathbf{x}} \hat{\psi}^\dagger(\mathbf{x}) \hat{\psi}(\mathbf{x})$: We have $\hat{\rho}_{\text{ss}} = \hat{U} \hat{\rho}_\psi \hat{U}^\dagger$, which is indeed time-independent, and recover Eqs. (3.10) and (3.11). Under the transformation to this rotating frame, the Hamiltonian acquires a contribution $-\mu \hat{N}$, whereas the Liouvillian \mathcal{L} remains invariant. In the following we will always be working in the rotating frame.

In summary, the steady state phase diagram of our model exhibits two phases: A symmetric one characterized by Eq. (3.11) and an ordered one where the global $U(1)$ symmetry is broken by a finite condensate amplitude Eq. (3.10) with definite phase. These two phases are separated by a continuous phase transition with order parameter ψ_0 . The transition is crossed by tuning the single-particle pumping rate from $\gamma_p < \gamma_l$ in the ‘‘symmetric’’ to $\gamma_p > \gamma_l$ in the ‘‘symmetry-broken’’ or ‘‘ordered’’ phase.

In the following we shall be interested in the critical behavior that is induced by tuning $\gamma_p - \gamma_l$ to zero. Powerful tools for investigating critical phenomena at a second order phase transition are provided by a multitude of variants of the RG. The particular flavor we employ here is the FRG in the formulation of Wetterich [56] (for reviews see Refs. [69–74]), which builds upon the use of functional integrals. Therefore, as a first step towards implementing a FRG investigation of our model, we will reformulate the physics that is encoded in the quantum master equation (3.6) in terms of Keldysh functional integrals [75, 76].

3.3.2 Keldysh functional integral

The Keldysh approach provides a means to tackle general non-equilibrium problems in the language of functional integrals. For the model at hand, the dynamics described by the master equation (3.6) can be represented equivalently as a Keldysh partition function (see App. 3.A): By $\Psi_\sigma = (\psi_\sigma, \psi_\sigma^*)^T$ for $\sigma = +, -$ we denote Nambu spinors of fields on the forward- and backward-branch of the closed time contour, respectively. Then, collecting time and space in a single variable $X = (t, \mathbf{x})$ and using the abbreviation $\int_X = \int dt \int d^d \mathbf{x}$, the Keldysh partition function reads

$$\mathcal{Z}[J_+, J_-] = \int \mathcal{D}[\Psi_+, \Psi_-] e^{i\sigma[\Psi_+, \Psi_-] + i \int_X (J_+^\dagger \Psi_+ - J_-^\dagger \Psi_-)}. \quad (3.14)$$

The fields $J_\sigma = (j_\sigma, j_\sigma^*)^T$ are external sources inserted here for the purpose of calculating correlation functions of the bosonic fields in the usual manner by means of functional differentiation. When they are set to zero, $J_+ = J_- = 0$, the partition function reduces to unity [75, 76], i.e., we have the normalization $\mathcal{Z}[0, 0] = 1$. While the Keldysh approach can in principle be utilized to study time evolution, here we are assuming translational invariance in time, as appropriate for the investigation of steady state properties.

In complete analogy to the separation of coherent and dissipative contributions to the time evolution of the density operator in Eq. (3.6), the action σ in the functional integral Eq. (3.14) can be

decomposed as $\sigma = \sigma_H + \sigma_D$ into a Hamiltonian part σ_H and a part σ_D corresponding to the dissipative Liouvillian \mathcal{L} in the master equation. The former is given by (from now on we will use units such that $2m = 1$)

$$\sigma_H = \sum_{\sigma=\pm} \sigma \int_X \left[\psi_{\sigma}^* (i\partial_t + \Delta + \mu) \psi_{\sigma} - \frac{g}{2} (\psi_{\sigma}^* \psi_{\sigma})^2 \right]. \quad (3.15)$$

As a general rule (see App. 3.A), normally ordered operators in Eq. (3.6) acting on the density matrix $\hat{\rho}$ from the left (right) result in corresponding fields on the $\sigma = +$ ($\sigma = -$) contour. Consequently, the commutator with the Hamiltonian in Eq. (3.6) is transferred into the two contributions to Eq. (3.15) with a relative minus sign.

The same rule applies to the dissipative part in the master equation (3.6). Passing from the Liouvillian \mathcal{L} on to a dissipative action σ_D , quantum jump operators \hat{L}_{α} are replaced by corresponding jump fields $L_{\alpha,\sigma}$ on the $\sigma = +$ ($\sigma = -$) contour. (In App. 3.A we will discuss regularization issues related to normal ordering of Lindblad operators.) As above we have the three contributions $\sigma_D = \sum_{\alpha} \sigma_{\alpha}$ that are due to single-particle pumping (p) and losses (l) as well as two-body losses (t). The form of the jump fields can directly be inferred from Eq. (3.9) as

$$L_{p,\sigma} = \psi_{\sigma}^*, \quad L_{l,\sigma} = \psi_{\sigma}, \quad L_{t,\sigma} = \psi_{\sigma}^2. \quad (3.16)$$

Then, for the dissipative parts of the action we find the expression

$$\sigma_{\alpha} = -i\gamma_{\alpha} \int_X \left[L_{\alpha,+} L_{\alpha,-}^* - \frac{1}{2} (L_{\alpha,+}^* L_{\alpha,+} + L_{\alpha,-}^* L_{\alpha,-}) \right]. \quad (3.17)$$

As we can see, the transition from a description of a specific problem in terms of a master equation to one in terms of Keldysh functional integrals reduces to the application of simple rules. For our model, Eqs. (3.14), (3.15) and (3.17) provide us with a convenient starting point for the investigation of the steady state phase transition described in the previous section.

While the translation rules from the master equation to the Keldysh functional integral are most simply applied in a basis of fields ψ_{\pm} that can be ascribed to the forward and backward branches of the Keldysh contour, subsequently we will find it advantageous to introduce so-called classical and quantum fields, given by the symmetric and anti-symmetric combinations

$$\begin{pmatrix} \phi_c \\ \phi_q \end{pmatrix} = M \begin{pmatrix} \psi_+ \\ \psi_- \end{pmatrix}, \quad M = \frac{1}{\sqrt{2}} \begin{pmatrix} 1 & 1 \\ 1 & -1 \end{pmatrix}. \quad (3.18)$$

Condensation is described by a time-independent, homogeneous expectation value of the fields on the $\sigma = \pm$ contours, $\langle \psi_+(X) \rangle = \langle \psi_-(X) \rangle = \psi_0$, cf. Eq. (3.10). In the basis of classical and quantum fields, this is expressed as $\langle \phi_c(X) \rangle = \phi_0 = \sqrt{2}\psi_0$, $\langle \phi_q(X) \rangle = 0$, i.e., only ϕ_c can condense (and, therefore, become a ‘‘classical’’ variable), whereas ϕ_q is a purely fluctuating field with zero expectation value by construction.

By means of the transformation Eq. (3.18), the inverse propagator, determined by the quadratic part of the action, is cast in the characteristic causality structure [75, 76] with retarded, advanced, and Keldysh components P^R , P^A , and P^K , respectively (in the following we will denote the two-body coupling constant and loss rate by, respectively, $\lambda = g/2$ and $\kappa = \gamma_t/2$),

$$\sigma = \int_X \left\{ \begin{pmatrix} \phi_c^* & \phi_q^* \end{pmatrix} \begin{pmatrix} 0 & P^A \\ P^R & P^K \end{pmatrix} \begin{pmatrix} \phi_c \\ \phi_q \end{pmatrix} + i4\kappa \phi_c^* \phi_c \phi_q^* \phi_q - [(\lambda + i\kappa) (\phi_c^{*2} \phi_c \phi_q + \phi_q^{*2} \phi_c \phi_q) + \text{c.c.}] \right\}. \quad (3.19)$$

The inverse retarded and advanced single-particle Green's functions are given by $P^R = P^{A\dagger} = i\partial_t + \Delta + \mu + i\kappa_1$ where $\kappa_1 = (\gamma_l - \gamma_p)/2$. For the Keldysh component of the inverse propagator we have $P^K = i\gamma$, where $\gamma = \gamma_l + \gamma_p$ is the sum of single-particle pumping and loss rates – both of them increase the noise level in the system.

The spectrum of single-particle excitations is encoded in the poles of the retarded propagator in frequency-momentum space or, equivalently, in the zeros of the inverse propagator. Solving $P^R(Q) = 0$ for ω , where $Q = (\omega, \mathbf{q})$ collects the frequency and spatial momentum, we obtain the dispersion relation

$$\omega = q^2 - \mu - i\kappa_1. \quad (3.20)$$

For $\kappa_1 > 0$ (i.e., $\gamma_p < \gamma_l$) the pole is located in the lower complex half-plane, and the effective loss rate κ_1 takes the role of an inverse lifetime. One has single-particle excitations that decay exponentially in time, a situation that is well-known from the general theory of the analytic structure of correlation functions [77]. As κ_1 is tuned to negative values (i.e., as we cross the phase transition), however, the pole Eq. (3.20) is shifted into the upper complex half-plane, signaling an instability. After crossing this threshold, the system develops a condensate, and the proper analytical structure of the retarded propagator is restored only by taking the tree-level shifts due to the condensate into account. We will discuss the corresponding modifications of the dispersion relation Eq. (3.20) below in Sec. 3.4.1.

Inversion of the 2×2 matrix in Eq. (3.19) yields the propagator with retarded, advanced, and Keldysh components,

$$G = \begin{pmatrix} G^K & G^R \\ G^A & 0 \end{pmatrix}. \quad (3.21)$$

The components along with their respective usual diagrammatic representation [75, 76] are given by

$$\begin{aligned} G^R(Q) &= 1/P^R(Q) = \text{---}\longrightarrow, \\ G^A(Q) &= 1/P^A(Q) = \text{---}\longleftarrow, \\ G^K(Q) &= -P^K/(P^R(Q)P^A(Q)) = \text{---}\longrightarrow, \end{aligned} \quad (3.22)$$

which shows that the poles of $G(Q)$ are determined solely by the zeros of $P^R(Q)$ and $P^A(Q)$. The Keldysh component P^K of the inverse propagator enters the expression for $G^K(Q)$ multiplicatively. Therefore, even in a situation where P^K is a polynomial in frequency and/or momentum, it can not give rise to further poles in the propagator $G(Q)$.

In the Keldysh formalism elastic two-body collisions and two-body losses are treated on an equal footing: Both appear in the action Eq. (3.19) as quartic vertices, however, with a real coupling constant λ in the case of elastic collisions and a purely imaginary coupling constant $i\kappa$ for two-body losses. The vertices in Eq. (3.19) can further be distinguished by the number of quantum fields they contain: We have the so-called classical vertex $-\int_X [(\lambda + i\kappa) \phi_c^{*2} \phi_c \phi_q + \text{c.c.}]$ which contains only one quantum field and three classical fields, and two quantum vertices: The first one $i4\kappa \int_X \phi_c^* \phi_c \phi_q^* \phi_q$ containing two and the second one $-\int_X [(\lambda + i\kappa) \phi_q^{*2} \phi_c \phi_q + \text{c.c.}]$ containing three quantum fields. Diagrammatically, these vertices are depicted as

$$\begin{aligned} & \begin{array}{c} \phi_q \quad \phi_c^* \\ \diagdown \quad \diagup \\ \lambda + i\kappa \\ \diagup \quad \diagdown \\ \phi_c^* \quad \phi_c \end{array}, & \begin{array}{c} \phi_q \quad \phi_c^* \\ \diagdown \quad \diagup \\ i\kappa \\ \diagup \quad \diagdown \\ \phi_q^* \quad \phi_c \end{array}, & \begin{array}{c} \phi_q \quad \phi_q^* \\ \diagdown \quad \diagup \\ \lambda + i\kappa \\ \diagup \quad \diagdown \\ \phi_q^* \quad \phi_c \end{array}. \end{aligned} \quad (3.23)$$

The fact that there are no vertices consisting only of classical fields is a manifestation of causality or conservation of probability in the Keldysh framework [75, 76]. Below we will find that only the classical vertex is relevant (in the sense of the RG) once the system is tuned close to the phase transition.

3.3.3 Effective action

Having established a description of our model in terms of a Keldysh functional integral, we proceed by introducing the concept of the effective action [78–80], which is central to the FRG. It is also a convenient starting point for a discussion of the phase transition on the mean-field level (see Sec. 3.4.1).

In equilibrium statistical physics the effective action Γ is related to the free energy as a functional of a space-dependent order parameter, and the equilibrium state is determined as the order parameter configuration that minimizes Γ . However, in the present context of non-equilibrium statistical physics we do not have a sensible notion of a free energy. In fact, already the Keldysh partition function Eq. (3.14) reduces for vanishing external sources to a representation of unity $\mathcal{Z}[0, 0] = 1$, independently of the parameters that characterize the action [75, 76]. Still, the Keldysh effective action, defined analogously to its equilibrium counterpart as the Legendre transform of the generating functional for connected correlation functions, is a very useful object. From Γ we can derive, e.g., field equations that determine the stationary configurations of classical and quantum fields $\Phi_\nu = (\phi_\nu, \phi_\nu^*)^T$, $\nu = c, q$. On a more formal level, Γ is the generating functional of one-particle irreducible vertices [78–80]. Most importantly for our model, however, the FRG provides us with a means of calculating critical exponents for the phase transition by studying the RG flow of Γ as a function of an infrared cutoff k .

Our starting point for introducing the effective action is the generating functional Eq. (3.14) for correlation functions, expressed in the basis of classical and quantum fields Φ_ν , i.e., the action is given by Eq. (3.19), and we introduce classical and quantum sources $J_\nu = (j_\nu, j_\nu^*)^T$ with $\nu = c, q$ according to the Keldysh rotation

$$\begin{pmatrix} j_c \\ j_q \end{pmatrix} = M \begin{pmatrix} j_+ \\ j_- \end{pmatrix}, \quad (3.24)$$

where the matrix M is defined in Eq. (3.18). For the generating functional \mathcal{W} for connected correlation functions and \mathcal{Z} we have the relation

$$\mathcal{W}[J_c, J_q] = -i \ln \mathcal{Z}[J_c, J_q]. \quad (3.25)$$

The idea is now to express \mathcal{W} , which is a functional of the external sources J_ν , in terms of the corresponding field expectation values $\bar{\Phi}_\nu = \langle \Phi_\nu \rangle_{J_c, J_q} = \delta \mathcal{W} / \delta J_{\nu'}$ where $\nu' = q$ for $\nu = c$ and *vice versa*. Introducing these as new variables is accomplished by means of a Legendre transform:

$$\Gamma[\bar{\Phi}_c, \bar{\Phi}_q] = \mathcal{W}[J_c, J_q] + \int_X (J_c^\dagger \bar{\Phi}_q + J_q^\dagger \bar{\Phi}_c). \quad (3.26)$$

The difference between the in this way defined effective action Γ and the action σ consists in the inclusion of both statistical and quantum fluctuations in the former. This becomes apparent in the representation of Γ as a functional integral [69],

$$e^{i\Gamma[\bar{\Phi}_c, \bar{\Phi}_q]} = \int \mathcal{D}[\delta\bar{\Phi}_c, \delta\bar{\Phi}_q] e^{i\sigma[\bar{\Phi}_c + \delta\bar{\Phi}_c, \bar{\Phi}_q + \delta\bar{\Phi}_q]}, \quad (3.27)$$

which holds for the equilibrium states that obey $\delta\Gamma/\delta\bar{\Phi}_c = \delta\Gamma/\delta\bar{\Phi}_q = 0$ at vanishing external sources $J_c = J_q = 0$. The most straightforward way of evaluating the functional integral Eq. (3.27) approximately is by performing a perturbative expansion around the configuration that minimizes the action σ . To zeroth order this corresponds to mean-field theory, an approach we will discuss in the following section. In the FRG, the fluctuations $\delta\bar{\Phi}_\nu$ are included stepwise by introducing an infrared regulator which suppresses fluctuations with momenta less than an infrared cutoff scale k . A short review of this method, adapted to the Keldysh framework, is provided in Sec. 3.5.1. We will apply it to our model in Sec. 3.7.

3.4 Preparatory Analysis

Here we carry out a basic analysis of the model in preparation for setting up a full functional RG calculation used to obtain the critical properties at the phase transition. We summarize the mean-field theory for the effective action and discuss the generic emergence of infrared divergences near a critical point. Furthermore, using dimensional analysis we identify the important terms in the action which are potentially relevant at the critical point. These terms are then included in the ansatz of the effective action used to carry out the FRG calculation. Finally we contrast this ansatz with the equilibrium dynamical models of HH [32].

3.4.1 Mean-field theory

In Sec. 3.3.1 we identified the precise balance between single-particle losses and pumping as the transition point, cf. Eqs. (3.10) and (3.11). Here we will derive this result from the Keldysh functional integral Eq. (3.27), again employing a mean-field approximation. We will then proceed by calculating the excitation spectrum above the stationary mean-field by treating quadratic fluctuations in a Bogoliubov (tree-level) expansion. While this issue, as well as going beyond the mean-field approximation by perturbative methods, can equally well be addressed in the master equation formalism of Sec. 3.3.1 [81], in performing a perturbative expansion at and below the critical point we encounter infrared divergences. Proper treatment of these requires RG methods, which are well-established and elegantly formulated in terms of functional integrals.

Mean-field theory corresponds to a saddle-point approximation of the functional integral in Eq. (3.27) in which fluctuations around the classical fields are completely neglected. In the present context, by classical fields we mean spatially homogeneous solutions to the classical field equations

$$\frac{\delta\sigma}{\delta\phi_c^*} = 0, \quad \frac{\delta\sigma}{\delta\phi_q^*} = 0. \quad (3.28)$$

As already mentioned above, there are no terms in the action Eq. (3.19) that have zero power of both ϕ_q^* and ϕ_q , and the same is obviously true for $\delta\sigma/\delta\phi_c^*$. Therefore, the first equation (3.28) is solved by $\phi_q = 0$. Inserting this condition in the second equation (3.28), we have

$$\left[\mu + i\kappa_1 - (\lambda - i\kappa) |\phi_0|^2 \right] \phi_0 = 0. \quad (3.29)$$

The solution $\phi_c = \phi_0$ is determined by the imaginary part of Eq. (3.29): For $\kappa_1 \geq 0$, in the symmetric phase, the classical field is zero, $\rho_0 = |\phi_0|^2 = 0$, whereas for $\kappa_1 < 0$ we have a finite condensate

density $\rho_0 = -\kappa_1/\kappa$. In a second step, the parameter μ is determined by the real part of Eq. (3.29) as $\mu = -\lambda\kappa_1/\kappa$.

Quadratic fluctuations around the mean-field order parameter can be investigated in a Bogoliubov or tree-level expansion: We set $\phi_c = \phi_0 + \delta\phi_c, \phi_q = \delta\phi_q$ in the action Eq. (3.19) and expand the resulting expression to second order in the fluctuations $\delta\phi_\nu$. The poles of the retarded propagator (which is now a 2×2 matrix in the space of Nambu spinors $\delta\Phi_\nu = (\delta\phi_\nu, \delta\phi_\nu^*)^T$) are then [58]

$$\omega_{1,2}^R = -i\kappa\rho_0 \pm \sqrt{q^2(q^2 + 2\lambda\rho_0) - (\kappa\rho_0)^2}. \quad (3.30)$$

Real and imaginary parts of both branches are shown in Fig. 3.4 in panels (a) and (b), respectively. Due to the tree-level shifts $\propto \rho_0$ the instability of Eq. (3.20) for $\kappa_1 < 0$ is lifted: Both poles are located in the lower complex half-plane, indicating a physically stable situation with decaying single-particle excitations. For $\kappa = 0$, Eq. (3.30) reduces to the usual Bogoliubov result [82], where for $q \rightarrow 0$ the dispersion is phononic, $\omega_{1,2}^R = \pm cq$, with speed of sound $c = \sqrt{2\lambda\rho_0}$ whereas particle-like behavior $\omega_{1,2}^R \sim q^2$ is recovered at high momenta. Here, due to the presence of two-body loss $\kappa \neq 0$, the dispersion is strongly modified: While at high momenta the dominant behavior is still given by $\omega_{1,2}^R \sim q^2$, at low momenta we obtain purely dissipative non-propagating modes $\omega_1^R \sim -i\frac{\lambda}{\kappa}q^2$ and $\omega_2^R \sim -i2\kappa\rho_0$. In particular, for $q = 0$ we have $\omega_1^R = 0$: This is a dissipative Goldstone mode [27, 58, 60], associated with the spontaneous breaking of the global $U(1)$ symmetry in the ordered phase. The existence of such a mode is not bound to the mean-field approximation but rather an exact property of the theory guaranteed by the $U(1)$ invariance of the effective action, even in the present case of a driven-dissipative condensate.

3.4.2 Infrared divergences near criticality

The discussion of our model on the mean-field level has illustrated some of the benefits of the Keldysh approach: Not only have we gained a simple physical picture of the phase transition as a condensation instability in the retarded and advanced propagators, but we were able to investigate excitations in both the symmetric and ordered phases quite straightforwardly. Mean-field theory, however, while providing us with a good qualitative understanding of the stationary state physics of our model far away from the phase transition, has major shortcomings when it comes to the discussion of critical phenomena. In particular, the critical exponents that can be extracted from an analysis of quadratic fluctuations around the mean-field configuration are not indicative of the universality class of the phase transition, as they correspond to the RG flow in the vicinity of a non-interacting (or Gaussian) fixed point. Critical behavior at the phase transition, however, is encoded in the RG flow in the vicinity of an interacting (or Wilson-Fisher) fixed point.

In a many-body system, excitations and their interactions get dressed due to scattering from other particles. The mean-field results of this section can be taken as the starting point for a calculation of the effective dressed parameters in a perturbative expansion. In the functional integral Eq. (3.27), diagrammatically this amounts to an expansion in the number of loops around the mean-field configuration. To lowest (one-loop) order, the correction $\Delta\lambda$ to the real part of the bare classical vertex (the

first diagram in Eq. (3.23)) reads ($v_d = (2^{d+1}\pi^{d/2}\Gamma(d/2))^{-1}$)

$$\begin{aligned} \Delta\lambda &= \text{diagram} + \dots \\ &= -\frac{v_d\gamma(\lambda^2 + \kappa^2)^2}{\lambda\kappa} \int_{q_{\text{IR}}}^{\infty} \frac{dq}{q^{5-d}}, \end{aligned} \quad (3.31)$$

where the elements appearing in the diagram are defined in Eqs. (3.31) and (3.22) (here, however, lines correspond to propagators of fluctuations $\delta\Phi_v$ and acquire an additional 2×2 matrix structure in Nambu space), and the ellipsis indicates that all diagrams with four external legs and one closed loop corresponding to a single internal momentum integration have to be included. In the integrand we have only kept the dominant contribution for $q \rightarrow 0$, and we have introduced an infrared cutoff q_{IR} in order to regularize the divergence at low momenta. Such infrared divergences, however, appear not only in our specific example of the loop correction to λ , but rather are characteristic of perturbative expansions in symmetry broken phases. They are due to the presence of a massless Goldstone mode, which results in a pole of the retarded and advanced propagators at $\omega = q = 0$. This problem is even enhanced as we approach the phase transition: Then both modes become degenerate, with also the second mode $\omega_2^R \sim -i2\kappa\rho_0$ for $q \rightarrow 0$ becoming massless. A method that allows us to go beyond mean-field theory, therefore, has to provide for a proper treatment of infrared divergences. In the FRG, this is achieved by effectively introducing a mass term $\propto k^2$ in the inverse propagators by hand. In consequence, the integrand in Eq. (3.31) is replaced by $\int_{q_{\text{IR}}}^{\infty} dq q^{d-1} / (q^2 + k^2)^2$ and we may safely set q_{IR} to zero since the effective mass k^2 acts as an infrared cutoff. The resulting loop-corrected coupling is a function of this cutoff, $\lambda = \lambda(k)$, and we obtain the fully dressed or renormalized coupling by following the RG flow of the running coupling $\lambda(k)$ for $k \rightarrow 0$. This procedure can be implemented efficiently by introducing the cutoff in the functional integral Eq. (3.27). We will discuss how this is done in practice for the present non-equilibrium problem [83–90] in the following section. Critical exponents can then be extracted from the flow of the critical system, i.e., when κ_1 is fine-tuned to zero.

So far we have discussed only corrections to the bare interaction vertices due to the inclusion of loop diagrams. However, also the propagators appearing in these diagrams are themselves renormalized. In particular, the inverse propagator can be written as $P(Q) - \Sigma(Q)$, i.e., as the sum of the bare inverse propagator $P(Q)$ and a self-energy correction $\Sigma(Q)$ [78–80]. The self-energy contribution at one-loop order to the retarded propagator is represented diagrammatically as

$$\Sigma^R(Q) = \text{diagram 1} + \text{diagram 2}. \quad (3.32)$$

where effective cubic couplings, which are obtained upon expanding the interaction vertex around the field expectation value, appear in the second diagram. Lines beginning and terminating in crosses indicate that particles are scattered out of and into the condensate, respectively. Due to momentum conservation, the first diagram does not depend on the external momentum $Q = (\omega, \mathbf{q})$ and gives a correction to the constant part of the inverse propagator, i.e., the so-called mass terms. Since the coupling $\lambda + i\kappa$ associated with the vertex appearing in this diagram is complex, both the real and imaginary masses, μ and κ_1 , are affected by the loop correction. The second diagram in Eq. (3.32) gives a frequency- and momentum-dependent contribution to the self-energy. Symmetry under spatial

rotations implies that it depends only on the modulus of the momentum and we may write $\Sigma^R(Q) = \Sigma^R(\omega, q^2)$. For small ω and q^2 we can expand $\Sigma^R(\omega, q^2) \approx \Sigma^R(0, 0) + \omega \partial_\omega \Sigma^R(0, 0) + q^2 \partial_{q^2} \Sigma^R(0, 0)$. Transforming back to the time domain and real space, the derivatives of the self-energy with respect to frequency and momentum give corrections to the coefficients of ∂_t and Δ in the inverse propagators, which are again complex valued. An imaginary part of the coefficient of the Laplacian corresponds to an effective dissipative kinetic coefficient due to the interaction with other particles; A complex prefactor of the time derivative, on the other hand, has significant consequences for the physical interpretation of all other couplings, as we will discuss in detail in later sections.

3.4.3 Canonical power counting

While the proper theoretical approach to critical phenomena has to cope efficiently with the infrared divergences discussed above, such systems also exhibit an important ordering principle, which is provided by the classification of couplings according to their canonical scaling dimension. In the following we will briefly review this procedure, often referred to as canonical power counting or dimensional analysis. It lays the basis for a suitable choice of ansatz for the effective action that will contain only couplings which are relevant or marginal according to this counting scheme [78–80].

At second order phase transitions, physical quantities exhibit scaling behavior, which means that they depend on the distance from the phase transition (in our case this distance is measured by κ_1) in a power-law fashion $\sim \kappa_1^\tau$, with a generally non-integer exponent τ . In order to study critical behavior in the RG, we investigate the RG flow starting from the action fine-tuned to criticality, i.e., with $\kappa_1 = 0$, and approach the critical point by lowering k . Then, scaling behavior of a physical quantity g shows up as power-law dependence $g \sim k^\theta$ on k for $k \rightarrow 0$ with a critical exponent θ . In other words, phase transitions are associated to scaling solutions of the RG flow (not all scaling solutions correspond to phase transitions [91]), or – equivalently – fixed points of the flow of rescaled couplings $\tilde{g} = k^{-\theta} g$. The dominant contribution to the exponent θ associated to a coupling g is determined by its physical dimension measured in units of momentum k , i.e., the canonical scaling dimension or engineering dimension $[g]$ (we have $[k] = 1$). Anticipating that deviations from canonical scaling will be small (see Sec. 3.8), let us study the flow of the dimensionless two-body elastic collision coupling $\tilde{\lambda} = \lambda/k$ (we will see below that $\tilde{\lambda}$ is indeed dimensionless). In Sec. 3.4.1 we saw that the flow of λ is generated by the loop diagrams Eq. (3.31). Then, to the flow of the dimensionless variable $\tilde{\lambda}$ we have an additional contribution due to the engineering dimension,

$$\partial_t \tilde{\lambda} = -\tilde{\lambda} + \text{loop diagrams}, \quad (3.33)$$

where we are taking the derivative with respect to the dimensionless logarithmic scale $t = \ln(k/\Lambda)$ which is zero for $k = \Lambda$ and goes to $-\infty$ for $k \rightarrow 0$. The loop contribution to the flow of $\tilde{\lambda}$ is of order $\tilde{\lambda}^2, \tilde{\lambda}\tilde{\kappa}, \tilde{\kappa}^2$ and higher in the dimensionless two-body couplings $\tilde{\lambda}, \tilde{\kappa}$. We find, therefore, a trivial fixed point $\partial_t \tilde{\lambda} = 0$ for $\tilde{\lambda}_* = \tilde{\kappa}_* = 0$. The flow for small $\tilde{\lambda}$ in the vicinity of this Gaussian fixed point is determined by the canonical scaling contribution on the RHS of Eq. (3.33) and is directed towards higher values of $\tilde{\lambda}$, i.e., the coupling $\tilde{\lambda}$ is relevant at the Gaussian fixed point. For increasing $\tilde{\lambda}$, the loop contributions become important and balance canonical scaling at a second fixed point. This non-trivial Wilson-Fisher fixed point at finite $\tilde{\lambda}_*, \tilde{\kappa}_*$ corresponds to the phase transition in the interacting system, and for small deviations $\tilde{\lambda} - \tilde{\lambda}_*$ the flow is attracted to $\tilde{\lambda}_*$.

The described scenario changes drastically for a coupling with negative canonical scaling dimension, i.e., when instead of the prefactor -1 for the first term on the RHS in Eq. (3.33) we had a positive

integer. Such a coupling is irrelevant at the Gaussian fixed point, which means that its flow is attracted to that fixed point. We can, therefore, as a starting point for a systematic expansion in the relevance of couplings, set all irrelevant couplings to zero. Unlike perturbative expansions, the inclusion of irrelevant couplings in higher orders in the expansion in canonical scaling dimensions results not only in enhanced quantitative accuracy, but rather refines our picture of the phase transition, as it involves higher order vertices and a refined treatment of the momentum dependence of propagators [92].

We proceed by determining the canonical dimensions of the couplings appearing in the action Eq. (3.19). They are not uniquely fixed by the requirement that the action is dimensionless, $[\sigma] = 0$: Still we have the freedom of assigning different scaling dimensions to the classical ϕ_c and quantum fields ϕ_q . We exploit this freedom in order to impose a scaling dimension upon the Keldysh component of the inverse propagator in Eq. (3.19) that is the same as in finite-temperature thermodynamic equilibrium [75, 76], i.e., we require $[\gamma] = 0$. While this choice yields a consistent picture of the driven-dissipative Bose condensation transition as detailed below, it is inappropriate for the investigation of stationary transport solutions that define genuine nonequilibrium states with nonvanishing flux which might be contained in our model. As already pointed out in Sec. 3.2, in two dimensions, such a scenario indeed has been recently identified in Ref. [66], showing that the Kardar-Parisi-Zhang non-equilibrium fixed point [43] governs the long wavelength behavior. In three dimensions, a similar scenario is conceivable in principle, however only beyond a certain threshold value for the strength of violation of detailed balance.

Denoting the dynamical exponent by $[\partial_t] = z$ we find, from the quadratic part of the action and in d dimensions,

$$z = [\mu] = [\kappa_1] = 2, \quad [\phi_c] = \frac{d-2}{2}, \quad [\phi_q] = \frac{d+2}{2}. \quad (3.34)$$

The different scaling dimensions of classical and quantum fields result in different behavior of the complex couplings associated with the classical and quantum vertices Eq. (3.23) under renormalization, even though their values at $k = \Lambda$ are the same. In particular, for a local vertex that contains n_c classical and n_q quantum fields, the canonical scaling dimension of the corresponding coupling is

$$[\lambda_{n_c, n_q}] = d + 2 - n_c[\phi_c] - n_q[\phi_q]. \quad (3.35)$$

We observe that all couplings λ_{n_c, n_q} with $n_q > 2$ ($n_q \geq 1$ is required by causality [75–77]) or $n_c > 5$ are irrelevant. The coupling $\lambda_{3,1}$ associated with the classical quartic vertex has canonical dimension $4 - d$, i.e., its upper critical dimension is $d = 4$ and, in the case of interest $d = 3$, it is relevant with canonical scaling dimension equal to unity. All other quartic couplings are irrelevant, as are sextic couplings with $n_q > 1$. The classical three-body coupling $\lambda_{5,1}$ is marginal and we will include it (with both real and imaginary parts) in our ansatz for the running effective action below, even though it is not present in the action σ . Higher order couplings λ_{n_c, n_q} with $n_c + n_q > 6$ are irrelevant and we will discard them.

3.4.4 Equilibrium symmetry

According to the canonical power counting scheme outlined in the previous section, in order to describe critical properties at the driven-dissipative Bose condensation transition we may disregard quantum vertices in the action Eq. (3.19) – this corresponds to a semiclassical approximation [75–77, 93], and the resulting simplified “mesoscopic” action has the same structure as the classical dynamical models considered in Ref. [32] inasmuch as it is linear in the quantum fields apart from the

noise term which is quadratic. Therefore, like in the classical dynamical models, the functional integral with the mesoscopic action is equivalent to a Langevin equation for the classical field. This is just the stochastic dissipative Gross-Pitaevskii equation Eq. (3.1) for a single non-conserved complex field ψ and bears close resemblance to the equation of motion of MA of HH with $N = 2$ real components. There are, however, two key differences: First the dynamics in MA is purely relaxational whereas Eq. (3.1) contains both coherent and dissipative contributions. Second, and more importantly, dropping all coherent contributions on the RHS of Eq. (3.1) we find that it is invariant under the transformation of the fields [90, 94, 95]:

$$\begin{aligned}\psi(t, \mathbf{x}) &\mapsto \psi^*(-t, \mathbf{x}), \\ \xi(t, \mathbf{x}) &\mapsto -\xi^*(-t, \mathbf{x}) - i2\partial_t\psi^*(t, \mathbf{x}).\end{aligned}\tag{3.36}$$

This symmetry of the dynamics implies a FDT for the retarded response and correlation functions. Its absence in the driven-dissipative model (DDM), therefore, may be seen as indicating non-equilibrium conditions. In Sec. 3.6 below we discuss a generalized version of the symmetry transformation Eq. (3.36) and we are led to consider an extension of MA by coherent dynamics that then differs from the DDM precisely in the obedience to this generalized symmetry. With regard to critical phenomena, the difference in symmetries between equilibrium and non-equilibrium situations renders it possible that novel universal behavior may be found in the latter case. We proceed to perform an FRG analysis of the critical properties of both models in the following sections.

3.5 Functional Renormalization Group

3.5.1 FRG approach for the Keldysh effective action

The transition from the action σ to the effective action Γ consists in the inclusion of both statistical and quantum fluctuations in the latter (see Eq. (3.27)). In the FRG, the functional integral over fluctuations is carried out stepwise by introducing an infrared regulator which suppresses fluctuations with momenta less than an infrared cutoff scale k [69]. This is achieved by adding to the action in Eq. (3.14) a term

$$\Delta\sigma_k = \int_X (\phi_c^*, \phi_q^*) \begin{pmatrix} 0 & R_{k,\bar{K}}(-\Delta) \\ R_{k,\bar{K}}^*(-\Delta) & 0 \end{pmatrix} \begin{pmatrix} \phi_c \\ \phi_q \end{pmatrix}\tag{3.37}$$

with a cutoff function $R_{k,\bar{K}}$ which will be specified below in Sec. 3.5.2. We denote the resulting cutoff-dependent Keldysh partition function and generating functional for connected correlation functions by, respectively, \mathcal{Z}_k and \mathcal{W}_k . The effective running action Γ_k is then defined as the modified Legendre transform

$$\Gamma_k[\bar{\Phi}_c, \bar{\Phi}_q] = \mathcal{W}_k[J_c, J_q] + \int_X (J_c^\dagger \bar{\Phi}_c + J_q^\dagger \bar{\Phi}_q) - \Delta\sigma_k[\bar{\Phi}_c, \bar{\Phi}_q].\tag{3.38}$$

Here the subtraction of $\Delta\sigma_k$ on the RHS guarantees that the only difference between the functional integral representations for Γ and Γ_k is the inclusion of the cutoff term in the latter,

$$e^{i\Gamma_k[\bar{\Phi}_c, \bar{\Phi}_q]} = \int \mathcal{D}[\delta\bar{\Phi}_c, \delta\bar{\Phi}_q] e^{i\sigma[\bar{\Phi}_c + \delta\bar{\Phi}_c, \bar{\Phi}_q + \delta\bar{\Phi}_q] + i\Delta\sigma_k[\delta\bar{\Phi}_c, \delta\bar{\Phi}_q]}.\tag{3.39}$$

Physically, Γ_k can be viewed as the effective action for averages of fields over a coarse-graining volume with size $\sim k^{-d}$.

We choose the form of the cutoff term $\Delta\sigma_k$ such that it modifies the inverse retarded and advanced propagators: Comparing Eqs. (3.19) and (3.37), we see that associated with the action $\sigma + \Delta\sigma_k$ are the regularized retarded and advanced inverse propagators $P^R(Q) + R_{k,\bar{K}}^*(q^2)$ and $P^A(Q) + R_{k,\bar{K}}(q^2)$ respectively, whereas the Keldysh part P^K of the inverse propagator remains unchanged. In other words, by introducing the cutoff $\Delta\sigma_k$ we manipulate the spectrum of single-particle excitations, which is encoded in the zeros of the inverse propagators $P^{R/A}(Q)$ or, equivalently, in the poles of the propagators Eq. (3.22). At the transition, these poles are determined by Eq. (3.20) with $\kappa_1 = 0$, i.e., we have a pole at $\omega = q = 0$, and as we have pointed out in the paragraph following Eq. (3.31), this leads to infrared divergences that drive critical behavior. For the regularized propagators, on the other hand, we have $G^R(\omega = 0, q^2 = 0) = 1/R_{k,\bar{K}}^*(0)$ and $G^A(\omega = 0, q^2 = 0) = 1/R_{k,\bar{K}}(0)$ which are finite for

$$R_{k,\bar{K}}(q^2) \sim k^2, \quad q \rightarrow 0. \quad (3.40)$$

To regulate infrared divergences, it is sufficient to introduce the cutoff function in the retarded and advanced inverse propagators, as becomes clear from the discussion following Eq. (3.22).

We have seen that the effective action Γ_k defined by Eq. (3.39) has an infrared-finite loop expansion. Its main usefulness, however, lies in the fact that it interpolates between the action σ for $k \rightarrow \Lambda$ where Λ is an ultraviolet cutoff scale, and the full effective action Γ for $k \rightarrow 0$. This is ensured by the requirements on the cutoff function [84]

$$\begin{aligned} R_{k,\bar{K}}(q^2) &\sim \Lambda^2, & k \rightarrow \Lambda, \\ R_{k,\bar{K}}(q^2) &\rightarrow 0, & k \rightarrow 0, \end{aligned} \quad (3.41)$$

where under the condition that Λ exceeds all energy scales in the action by far, for $k \rightarrow \Lambda$ we may evaluate the functional integral Eq. (3.39) in a stationary phase approximation. Then, to leading order we find $\Gamma_\Lambda \sim \sigma$. The evolution of Γ_k from this starting point in the ultraviolet to the full effective action in the infrared for $k \rightarrow 0$ is described by the exact Wetterich flow equation [56, 69]

$$\partial_k \Gamma_k = \frac{i}{2} \text{Tr} \left[\left(\Gamma_k^{(\bar{2})} + \bar{R}_k \right)^{-1} \partial_k \bar{R}_k \right], \quad (3.42)$$

where $\Gamma_k^{(\bar{2})}$ and \bar{R}_k denote, respectively the second variations of the effective action and the cutoff $\Delta\sigma_k$ and will be specified in Sec. 3.5.2; Tr denotes summation over internal field degrees of freedom as well as integration over frequencies and momenta. The flow equation provides us with an alternative but fully equivalent formulation of the functional integral Eq. (3.39) as a functional differential equation. Like the functional integral, the flow equation can not be solved exactly. It is, however, amenable to various systematic approximation strategies. Here we perform an expansion of the effective action Γ_k in canonical scaling dimensions as outlined above in Sec. 3.4.3, keeping only those couplings which are – in the sense of the RG – relevant or marginal at the phase transition.

3.5.2 Truncation

In three dimensional classical $O(N)$ -symmetric models, already the inclusion of non-irrelevant couplings gives a satisfactory description of critical phenomena [69]. As we will show below, static critical properties of our non-equilibrium phase transition are described by such a model with $N = 2$.

Therefore, in the following, we will as well restrict ourselves to the inclusion of relevant and marginal couplings in the ansatz for the effective action, i.e., we choose a truncation of the form

$$\Gamma_k = \int_X \left[(\bar{\phi}_c^*, \bar{\phi}_q^*) \begin{pmatrix} 0 & \bar{D}^A \\ \bar{D}^R & i\bar{\gamma} \end{pmatrix} \begin{pmatrix} \bar{\phi}_c \\ \bar{\phi}_q \end{pmatrix} - \left(\frac{\partial \bar{U}}{\partial \bar{\phi}_c} \bar{\phi}_q + \frac{\partial \bar{U}^*}{\partial \bar{\phi}_c^*} \bar{\phi}_q^* \right) \right]. \quad (3.43)$$

(Here all couplings depend on the infrared cutoff scale k . However, for the sake of keeping the notation simple, we will not state this dependence explicitly.) All terms involving derivatives are contained in $\bar{D}^R = iZ^* \partial_t + \bar{K}^* \Delta$ and $\bar{D}^A = \bar{D}^{R\dagger}$. In contrast to the action Eq. (3.19), however, we allow for complex coefficients $Z = Z_R + iZ_I$ and $\bar{K} = \bar{A} + i\bar{D}$: Due to the presence of complex couplings $\lambda + i\kappa$ in the classical action, imaginary parts of Z and \bar{K} will be generated in the RG flow as indicated at the end of Sec. 3.4.1, even though they are zero initially at $k \rightarrow \Lambda$.

A complex prefactor Z of the time derivative – often referred to as wave-function renormalization – obscures the physical interpretation of the other complex couplings: The field equation $\delta\Gamma_k/\delta\bar{\phi}_q^* = 0$ contains $iZ^* \partial_t \bar{\phi}_c = -\bar{K}^* \Delta \bar{\phi}_c + \dots$. The physical meaning of the gradient coefficient \bar{K} becomes clear only after division by Z^* , i.e., in the form $i\partial_t \bar{\phi}_c = -(A - iD) \Delta \bar{\phi}_c + \dots$ where we introduced the decomposition $K = \bar{K}/Z = A + iD$ into real and imaginary parts. In this form, the interpretation of A and D as encoding coherent propagation and diffusive behavior of particles is apparent. Similar considerations hold for the other couplings in Eq. (3.43), and we will elaborate on this point in Sec. 3.6.4.

In our truncation containing only non-irrelevant contributions, the only momentum-independent couplings we keep are the Keldysh and spectral masses, $\bar{\gamma}$ and $\bar{u}_1 = -\bar{\mu} + i\bar{\kappa}_1$, as well as the classical quartic and sextic couplings (i.e., those vertices containing only one quantum field but three and five classical field variables respectively). These are included in the part in Eq. (3.43) that involves the potential \bar{U} , which is a function of the $U(1)$ invariant $\bar{\rho}_c = |\bar{\phi}_c|^2$ and given by

$$\bar{U}(\bar{\rho}_c) = \bar{u}_1 (\bar{\rho}_c - \bar{\rho}_0) + \frac{1}{2} \bar{u}_2 (\bar{\rho}_c - \bar{\rho}_0)^2 + \frac{1}{6} \bar{u}_3 (\bar{\rho}_c - \bar{\rho}_0)^3, \quad (3.44)$$

where both $\bar{u}_2 = \bar{\lambda} + i\bar{\kappa}$ and $\bar{u}_3 = \bar{\lambda}_3 + i\bar{\kappa}_3$ are complex. In the symmetric phase, we keep $\bar{u}_1 \neq 0$ as a running coupling and set $\bar{\rho}_0 = 0$, whereas in the ordered phase we set the masses to zero, $\bar{u}_1 = 0$, and regard the condensate amplitude as a running coupling, $\bar{\rho}_0 \neq 0$. Then, the parameterization Eq. (3.44) corresponds to an expansion of the potential around its minimum in both the symmetric and ordered phases. It ensures that the field equations $\delta\Gamma_k/\delta\bar{\phi}_c^* = 0$, $\delta\Gamma_k/\delta\bar{\phi}_q^* = 0$ are solved by $\bar{\rho}_c = 0$ and $\bar{\rho}_c = \bar{\rho}_0$ in the symmetric and ordered phases respectively (in both cases we require $\bar{\phi}_q = \bar{\phi}_q^* = 0$) for all values of k .

In what follows we will find it advantageous to introduce renormalized fields $\phi_c = \bar{\phi}_c$, $\phi_q = Z\bar{\phi}_q$ (the various symbols for bare/renormalized fields etc. are summarized in Tab. 3.1). With this choice the complex wave-function renormalization Z that multiplies the time derivative in Eq. (3.43) is absorbed in the field variables and we can write the effective action in the form (σ_z denotes the Pauli matrix)

$$\Gamma_k = \int_X \Phi_q^\dagger \left[i\sigma_z \left(\partial_t \Phi_c + \frac{\delta \mathcal{U}_D}{\delta \Phi_c^*} \right) - \frac{\delta \mathcal{U}_H}{\delta \Phi_c^*} + i\frac{\gamma}{2} \Phi_q \right]. \quad (3.45)$$

The renormalized Keldysh mass is $\gamma = \bar{\gamma}/|Z|^2$. For the variational derivatives with respect to the classical fields we are using the notation $\delta/\delta\Phi_c^* = (\delta/\delta\phi_c^*, \delta/\delta\phi_c)^T$, and the renormalized potential

$\hat{\psi}$	field operator	3.3.1
$\psi_\sigma, \sigma = \pm$	fields on Keldysh contour	3.3.2
$\Psi_\sigma = (\psi_\sigma, \psi_\sigma^*)^T$	spinor of \pm -fields	3.3.2
$\phi_\nu, \nu = c, q$	classical and quantum fields	3.3.2
$\Phi_\nu = (\phi_\nu, \phi_\nu^*)^T$	spinor of c and q fields	3.3.3
$\bar{\Phi}_\nu$	field expectation values/bare fields	3.3.3
$\Gamma_k^{(\bar{2})}, \bar{R}_k$	derivatives WRT bare fields	3.5.1
$\phi_c = \bar{\phi}_c, \phi_q = Z\bar{\phi}_q$	renormalized fields	3.5.2
$\chi_{\nu,n}, n = 1, 2$	real fields	3.5.2
$\Gamma_k^{(2)}, R_k$	derivatives WRT renormalized fields	3.5.2
$Z, \bar{K}, \bar{u}_1, \bar{u}_2, \dots$	bare couplings	3.5.2
K, u_1, u_2, \dots	renormalized couplings	3.5.2
$\tilde{\Phi}_\nu, \hat{\Phi}_\nu$	transformed bare fields	3.6
$\tilde{u}_1, \tilde{u}_3, \dots$	dimensionless couplings	3.8.1

Table 3.1. Summary of notation. The columns are symbols, their meaning, and the section in which they are introduced.

functionals that encode unitary and dissipative terms respectively, read

$$\begin{aligned} \frac{\delta \mathcal{U}_H}{\delta \Phi_c^*} &= (-A\Delta + U'_H) \Phi_c, \\ \frac{\delta \mathcal{U}_D}{\delta \Phi_c^*} &= (-D\Delta + U'_D) \Phi_c, \end{aligned} \quad (3.46)$$

where A and D are the real and imaginary parts of the renormalized gradient coefficient $K = \bar{K}/Z = A + iD$. Primes denote derivatives with respect to $\rho_c = |\phi_c|^2$ of the real and imaginary parts of the renormalized potential $U = \bar{U}/Z = U_H + iU_D$, which is given by

$$U(\rho_c) = u_1(\rho_c - \rho_0) + \frac{1}{2}u_2(\rho_c - \rho_0)^2 + \frac{1}{6}u_3(\rho_c - \rho_0)^3 \quad (3.47)$$

with renormalized couplings $u_1 = \bar{u}_1/Z = -\mu + i\kappa_1$, $u_2 = \bar{u}_2/Z = \lambda + i\kappa$, and $u_3 = \bar{u}_3/Z = \lambda_3 + i\kappa_3$. The inclusion of the classical three-body coupling u_3 adds the vertex

$$(3.48)$$

to the building blocks Eqs. (3.22) and (3.31).

As we have already indicated, the first variational derivative of the effective action yields field equations that determine the stationary state values of the classical and quantum fields. In the ordered phase, these are constant in space and time and read $\phi_c|_{\text{ss}} = \phi_c^*|_{\text{ss}} = \sqrt{\rho_0}$ (our choice of a real condensate amplitude does not cause a loss of generality) and $\phi_q|_{\text{ss}} = \phi_q^*|_{\text{ss}} = 0$. Then, the scale-dependent inverse connected propagator is given by the second variational derivative of the effective

action [78–80], evaluated in stationary state. We will carry out this variational derivative in a basis of real fields, which we introduce by decomposing the classical and quantum fields into real and imaginary parts according to $\phi_\nu = \frac{1}{\sqrt{2}}(\chi_{\nu,1} + i\chi_{\nu,2})$ for $\nu = c, q$. The inverse propagator at the scale k is then given by

$$P_{ij}(Q)\delta(Q - Q') = \frac{\delta^2\Gamma_k}{\delta\chi_i(-Q)\delta\chi_j(Q')} \Big|_{\text{ss}}. \quad (3.49)$$

Here the indices i, j enumerate the four components of the field vector

$$\chi(Q) = (\chi_{c,1}(Q), \chi_{c,2}(Q), \chi_{q,1}(Q), \chi_{q,2}(Q))^T. \quad (3.50)$$

Analogous to the inverse propagator in the action Eq. (3.19), the inverse propagator at the scale k is structured into retarded, advanced, and Keldysh blocks,

$$P(Q) = \begin{pmatrix} 0 & P^A(Q) \\ P^R(Q) & P^K \end{pmatrix}. \quad (3.51)$$

However, here these blocks are themselves 2×2 matrices. (This additional Nambu structure emerges in the ordered phase.) We have explicitly

$$\begin{aligned} P^R(Q) &= \begin{pmatrix} -Aq^2 - 2\lambda\rho_0 & i\omega - Dq^2 \\ -i\omega + Dq^2 + 2\kappa\rho_0 & -Aq^2 \end{pmatrix} = P^A(Q)^\dagger, \\ P^K &= i\gamma\mathbb{1}. \end{aligned} \quad (3.52)$$

These expressions can be used to deduce the dispersion relation for single-particle excitations. It is determined by solving

$$\det P(Q) = \det(P^R(Q)) \det(P^A(Q)) = 0 \quad (3.53)$$

for ω . Due to the second relation Eq. (3.52), two of the four solutions to Eq. (3.53) are complex conjugate. The zeros of the determinant of the retarded inverse propagator encode the two branches

$$\omega_{1,2}^R = -iDq^2 - i\kappa\rho_0 \pm \sqrt{Aq^2(Aq^2 + 2\lambda\rho_0) - (\kappa\rho_0)^2}, \quad (3.54)$$

which differ from the mean-field expression Eq. (3.30) by the contribution $-iDq^2$ due to the explicit inclusion of a dissipative kinetic term in our truncation, and by the appearance of the scale dependent gradient coefficient A . The dissipative Goldstone mode is now characterized by the low-momentum behavior $\omega_1^R \sim -i(D + A\frac{1}{k})q^2$, whereas for the “massive” (the mass is purely imaginary) mode we reproduce the form of the mean-field expression $\omega_2^R \sim -i2\kappa\rho_0$ – however, in a scale-dependent version with all couplings running in the course of the RG. In this way, structural properties such as Goldstone’s theorem are preserved during the flow. The dispersion relation Eq. (3.54) is depicted in Fig. 3.4.

We proceed by specifying the cutoff function $R_{k,\bar{K}}$ which appears in Eq. (3.37). We will work with an optimized cutoff [96]

$$R_{k,\bar{K}}(q^2) = -\bar{K}(k^2 - q^2)\theta(k^2 - q^2), \quad (3.55)$$

which obviously meets the requirements Eqs. (3.40) and (3.41). The regularized propagator, which appears in the loop diagrams that generate the RG flow, reads

$$G_k(Q) = (P(Q) + R_k(Q))^{-1}, \quad (3.56)$$

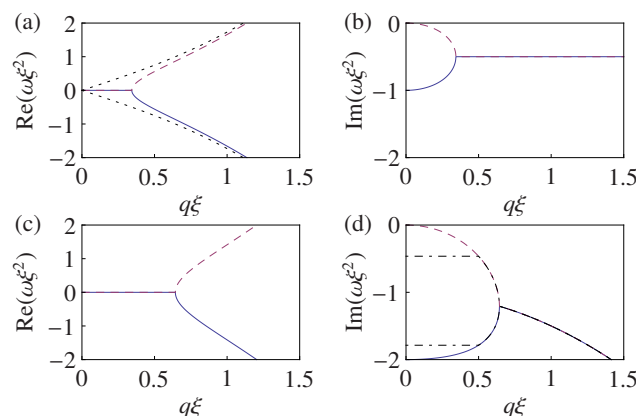


Figure 3.4. (Color online) Dispersion relation of single-particle excitations in the ordered phase. Frequencies and momenta are measured in units of the healing length $\xi = 1/\sqrt{\lambda\rho_0}$. (a) and (b): The Goldstone and massive modes Eq. (3.30), obtained in mean-field approximation, are shown as, respectively, dashed and solid lines for $\kappa = \lambda/2$. For small momenta both modes are purely diffusive and non-propagating. The dotted lines in (a) correspond to the usual Bogoliubov dispersion relations for $\kappa = 0$. (c) and (d): Dispersion relations Eq. (3.54) with gradient coefficients A, D that are generated upon renormalization. (d) For finite D , the damping rate grows $\propto q^2$ for large q . The regularized dispersion relations, where aq^2 is replaced by $p_a(q^2)$ for $a = A, D$ (cf. Eq. (3.58)), are shown as a dash-dotted lines. Here we chose parameters $A = 1, D = 1/2, \kappa = \lambda, k = 1/(2\xi)$.

where the 4×4 matrix $R_k(Q)$ is defined in analogy to the inverse propagator Eq. (3.49) as the second variational derivative of the cutoff Eq. (3.37) with respect to the real fields Eq. (3.50),

$$R_{k,ij}(q^2)\delta(Q - Q') = \frac{\delta^2 \Delta\sigma_k}{\delta\chi_i(-Q)\delta\chi_j(Q')}. \quad (3.57)$$

Due to the cutoff $R_k(Q)$ in the denominator in Eq. (3.56), the poles of $G_k(Q)$ are given by Eq. (3.54), however, with Aq^2 and Dq^2 replaced by $p_A(q^2)$ and $p_D(q^2)$ respectively, where the function $p_a(q^2)$ for $a = A, D$ reads

$$p_a(q^2) = aq^2 - R_{k,a}(q^2) = \begin{cases} ak^2 & \text{for } q^2 < k^2, \\ aq^2 & \text{for } q^2 \geq k^2. \end{cases} \quad (3.58)$$

The thus modified dispersion relations are finite for $q \rightarrow 0$, i.e., infrared divergences of loop diagrams are regularized. In panel (d) in Fig. 3.4 the regularized dispersion relations are shown as dashed-dotted lines.

In Sec. 3.5 we introduced most of the ingredients for a FRG investigation of the steady state driven-dissipative Bose condensation transition. Before we present the explicit flow equations in Sec. 3.7, we will now provide a detailed discussion of the relation between our non-equilibrium model and the classical equilibrium dynamical MA of HH [32].

3.6 Relation to equilibrium dynamical models

Here we extend the discussion of Sec. 3.4.4 and work out the precise relation of the DDM to MA with $N = 2$ components. We reemphasize that these considerations rely on the power counting introduced in Sec. 3.4.3, which implies that we may omit quantum vertices from an effective long-wavelength description close to criticality; The resulting action Eq. (3.45) is equivalent to a Langevin equation of the form of Eq. (3.1) [75, 76, 93, 97].

Originally, MA was formulated in terms of such a Langevin equation for a non-conserved, coarse-grained order parameter. It provides for a phenomenological description of the relaxational dynamics of the order parameter subject to stochastic fluctuations, which are introduced necessarily as a consequence of the coarse-graining over a volume of extent k_{cg}^{-d} : The effects of fluctuations with momenta q greater than the coarse-graining scale k_{cg} are included by introducing random noise sources in the evolution equation.

For our model, coarse-graining amounts to integrating out fluctuations with momenta q greater than k_{cg} in the functional integral Eq. (3.39) [69], which results in an effective action Γ_{cg} that can be regarded as the starting point of a phenomenological description in the spirit of HH, i.e., we may interpret it as the action $\sigma_{\text{cg}} = \Gamma_{\text{cg}}$ for slow modes with momenta $q < k_{\text{cg}}$.

The equation of motion of MA is constructed such that its stationary state is thermodynamic equilibrium, which manifests itself in a FDT [32] relating the order parameter retarded response and correlation functions. The FDT can be derived as a consequence of a specific equilibrium symmetry of the dynamics which is related to time reversal and expresses detailed balance [90, 94, 95]. This symmetry, however, does not restrict the dynamics to be purely relaxational as is the case in MA. In fact, one can conceive an extension of MA by reversible mode couplings (MAR) which differs from the DDM *only* in the obedience of the symmetry. (Note that the DDM generically features both coherent and dissipative contributions). As universality classes are fully characterized by the spatial dimensionality and symmetries of a system, however, this opens up the possibility of novel critical behavior in the DDM.

In the remainder of this section we illuminate the consequences of the equilibrium symmetry through a detailed comparison between MAR in which it is present at the outset and the DDM model, where it is only emergent at long scales. We give a simple geometric interpretation of the restriction that the symmetry imposes on the couplings that parameterize the effective action and specify the submanifolds in the coupling space for the DDM that correspond to MA and MAR.

While these considerations demonstrate formally the non-equilibrium character of the DDM, the equilibrium MAR constructed in the above way may seem a bit academic. In fact, as we will see in Sec. 3.6.4 it amounts to an unrealistic fine-tuning of the ratios of all coherent vs. dissipative couplings. The physically relevant model which the DDM should be compared to is model E, which describes the equilibrium Bose condensation transition. An important difference between the DDM and model E is the presence of an exact particle number conservation in the latter case which can be seen to rule out a finite κ_1 mass term.² Therefore, according to the arguments given in Sec. 3.2, the standard equilibrium Bose condensation transition exhibits only three independent exponents (as opposed to four in the DDM) and, in particular, no counterpart to η_r . Moreover, as a consequence of the exact

²It may – and does – occur as a regularization, meaning however that it has to be sent to zero in such a way that it does not affect any physical result.

particle number conservation an additional slow mode occurs at criticality and modifies the *dynamical* exponent.

3.6.1 Model A with $N = 2$ and reversible mode couplings (MAR)

We specify the equilibrium symmetry in terms of fields $\tilde{\Phi}_\nu$, which are related to the bare fields $\bar{\Phi}_\nu$ of Eq. (3.43) via

$$\tilde{\Phi}_c = \bar{\Phi}_c, \quad \tilde{\Phi}_q = \frac{Z_{R,\text{cg}} - \bar{r}Z_{I,\text{cg}}}{1 + \bar{r}^2} (\bar{r}\mathbb{1} + i\sigma_z) \bar{\Phi}_q, \quad (3.59)$$

where $Z_{R,\text{cg}}$ and $Z_{I,\text{cg}}$ denote the real and imaginary parts of the wave-function renormalization at the coarse-graining scale k_{cg} and \bar{r} is a real parameter, the physical meaning of which will become clear in the following. The symmetry transformation is denoted by \mathcal{T} and reads [90, 94, 95]

$$\begin{aligned} \mathcal{T}\tilde{\Phi}_c(t, \mathbf{x}) &= \sigma_x \tilde{\Phi}_c(-t, \mathbf{x}), \\ \mathcal{T}\tilde{\Phi}_q(t, \mathbf{x}) &= \sigma_x \left(\tilde{\Phi}_q(-t, \mathbf{x}) + \frac{i}{2T} \partial_t \tilde{\Phi}_c(-t, \mathbf{x}) \right), \end{aligned} \quad (3.60)$$

cf. the implementation in the Langevin formulation Eq. (3.36). It includes complex conjugation (in the form of multiplication with the Pauli matrix σ_x) and time reversal; T is the temperature. As outlined above, we now construct the action for MAR as follows: We identify the effective action Eq. (3.43) at the coarse-graining scale k_{cg} with the action for low-momentum modes, $\sigma_{\text{cg}} = \Gamma_{\text{cg}}$, and enforce thermodynamic equilibrium by requiring invariance of σ_{cg} under the transformation \mathcal{T} , which results in

$$\mathcal{S}_{\text{cg}}^{\text{MAR}} = \int_X \tilde{\Phi}_q^\dagger \left[(Z_{R,\text{cg}}\sigma_z - iZ_{I,\text{cg}}\mathbb{1}) i\partial_t \tilde{\Phi}_c + (i\sigma_z - \bar{r}\mathbb{1}) \frac{\delta \bar{\mathcal{U}}_{D,\text{cg}}}{\delta \bar{\Phi}_c^*} + i\frac{\bar{\gamma}_{\text{cg}}}{2} \bar{\Phi}_q \right]. \quad (3.61)$$

(See App. 3.B for details of the derivation.) The action $\mathcal{S}_{\text{cg}}^{\text{MAR}}$ contains coherent dynamics in the form of $\bar{\mathcal{U}}_{H,\text{cg}} = \bar{r}\bar{\mathcal{U}}_{D,\text{cg}}$, i.e., the parameter \bar{r} plays the role of the common fixed ratio between coherent and dissipative couplings. This relation ensures compatibility of coherent dynamics with the equilibrium symmetry. We note that here, crucially, both the irreversible and the reversible dynamics have the same physical origin, being generated by the same functional $\bar{\mathcal{U}}_{D,\text{cg}}$. This is motivated in the frame of a phenomenological, effective model for relaxation dynamics in the absence of explicit drive.

However, not only the values of the couplings encoding coherent dynamics are restricted by the symmetry, but also the Keldysh mass $\bar{\gamma}_{\text{cg}}$ is determined by the temperature that appears in the symmetry transformation as

$$\bar{\gamma}_{\text{cg}} = \frac{4}{1 + \bar{r}^2} (Z_{R,\text{cg}} - \bar{r}Z_{I,\text{cg}})^2 T. \quad (3.62)$$

Finally we note that Eq. (3.61) includes MA with effectively purely dissipative dynamics as a special case: Indeed we can derive the action for MA in the same way as we derived the action for MAR from the truncation for the DDM, i.e., by enforcing an additional symmetry. Requiring invariance of $\mathcal{S}_{\text{cg}}^{\text{MAR}}$ under complex conjugation of the fields,

$$C\tilde{\Phi}_\nu = \sigma_x \tilde{\Phi}_\nu, \quad (3.63)$$

we find the additional constraint $\bar{r} = -Z_{I,\text{cg}}/Z_{R,\text{cg}}$ (see App. 3.B), reducing the number of independent parameters further. Then, after rescaling the quantum fields with Z_{cg} it becomes apparent that this model describes purely dissipative dynamics as we will show in Sec. 3.6.4.

3.6.2 Truncation for MAR

We proceed by specifying the truncation for a FRG analysis of MAR. Here it is crucial to note that the transformation \mathcal{T} Eq. (3.60) not only leaves the action Eq. (3.61) invariant, but is actually a symmetry of the full theory [95], i.e., of the effective action. Then, if the cutoff $\Delta\sigma_k$ in Eq. (3.39) is \mathcal{T} -invariant as well (this is indeed the case for the choice Eq. (3.37)), also the scale-dependent effective action Γ_k^{MAR} must obey the symmetry. This requirement implies restrictions on the RG flow: Invariance of the effective action on all scales is guaranteed by the ansatz

$$\Gamma_k^{\text{MAR}} = \int_X \bar{\Phi}_q^\dagger \left[(Z_R \sigma_z - iZ_I \mathbb{1}) i\partial_t \bar{\Phi}_c + (i\sigma_z - \bar{r} \mathbb{1}) \frac{\delta \bar{\mathcal{U}}_D}{\delta \bar{\Phi}_c^*} + i\frac{\bar{\gamma}}{2} \bar{\Phi}_q \right], \quad (3.64)$$

which follows by enforcing the symmetry on the truncation Eq. (3.43) (see App. 3.B for details). We note in particular that compatibility of coherent and dissipative dynamics is conserved in the RG flow. In contrast to the DDM, here the Keldysh mass is not an independent running coupling, as it is linked to the wave-function renormalization $Z = Z_R + iZ_I$ by the Ward identity of the symmetry Eq. (3.60),

$$\bar{\gamma} = \frac{Z_R - \bar{r}Z_I}{Z_{R,\text{cg}} - \bar{r}Z_{I,\text{cg}}} \bar{\gamma}_{\text{cg}}. \quad (3.65)$$

In comparison to the DDM, therefore, MAR is described by a reduced number of couplings: Our truncation Eq. (3.43) for the DDM is parameterized by a vector of couplings

$$\bar{\mathbf{g}} = \left(Z, \bar{K}, \bar{\rho}_0, \bar{u}_1, \bar{u}_2, \bar{u}_3, \bar{\gamma} \right)^T, \quad (3.66)$$

where $Z, \bar{K}, \bar{u}, \bar{u}_3$ are complex whereas $\bar{\rho}_0, \bar{\gamma}$ are positive real numbers. In MAR, the real parts of the complex couplings in the functional $\bar{\mathcal{U}}$ are determined by imaginary ones and the ratio \bar{r} which appears as a fixed parameter in the action at the coarse-graining scale k_{cg} . Additionally the Keldysh mass is related to the wave-function renormalization via Eq. (3.65), so that a reduced set of running couplings,

$$\bar{\mathbf{g}}_{\text{MAR}} = \left(Z, \bar{D}, \bar{\rho}_0, \bar{\kappa}_1, \bar{\kappa}, \bar{\kappa}_3 \right)^T, \quad (3.67)$$

is sufficient to fully specify the truncation Eq. (3.64). In the purely dissipative MA, finally, the symmetry Eq. (3.63) determines the ratio of imaginary to real parts of the wave-function renormalization Z as $\bar{r} = -Z_I/Z_R$ (see App. 3.B), so that Z can be parametrized in terms of a single real running coupling. The truncation for MA, therefore, is described by the couplings:

$$\bar{\mathbf{g}}_{\text{MA}} = \left(Z_R, \bar{D}, \bar{\rho}_0, \bar{\kappa}_1, \bar{\kappa}, \bar{\kappa}_3 \right)^T. \quad (3.68)$$

3.6.3 Fluctuation-dissipation theorem

In the following we will show that the symmetry Eq. (3.60) implies a classical FDT for MAR [90, 94, 95]. If we regard the full propagators of the theory as the $k \rightarrow 0$ limits of the RG flow of scale-dependent propagators, we may say that the FDT holds for MAR (and, *a fortiori*, for MA) for all $0 < k < k_{\text{cg}}$. In addition we will see that this is not the case for the driven-dissipative system we consider. There the equilibrium symmetry is not present at mesoscopic scales but rather emergent for the system at criticality in the infrared for $k \rightarrow 0$. As a result, thermalization sets in only at low frequencies and long wavelengths.

As indicated at the beginning of the preceding section, the transformation \mathcal{T} Eq. (3.60) is a symmetry of the full theory. In particular, for two-point correlation functions we have

$$\langle \tilde{\phi}_\nu(t, \mathbf{x}) \tilde{\phi}_{\nu'}^*(t', \mathbf{x}') \rangle = \langle \mathcal{T} \tilde{\phi}_\nu(t, \mathbf{x}) \mathcal{T} \tilde{\phi}_{\nu'}^*(t', \mathbf{x}') \rangle, \quad (3.69)$$

and corresponding relations hold for higher correlation functions. Here expectation values are defined as

$$\langle \dots \rangle = \int \mathcal{D}[\Phi_c, \Phi_q] \dots e^{i\mathcal{S}_{\text{eg}}^{\text{MAR}}[\Phi_c, \Phi_q]}. \quad (3.70)$$

The relation Eq. (3.69) implies a FDT: For the particular choice of correlations between quantum fields $\nu = \nu' = q$ which vanish by construction of the Keldysh functional integral [75–77], we find

$$0 = \langle \tilde{\phi}_q(t, \mathbf{x}) \tilde{\phi}_q^*(t', \mathbf{x}') \rangle = \langle \mathcal{T} \tilde{\phi}_q(t, \mathbf{x}) \mathcal{T} \tilde{\phi}_q^*(t', \mathbf{x}') \rangle. \quad (3.71)$$

Inserting here explicit expressions for the \mathcal{T} -transformed fields and performing a Fourier transformation, we obtain the classical FDT

$$\tilde{G}^K(\omega, \mathbf{q}) = \frac{2T}{\omega} \left(\tilde{G}^R(\omega, \mathbf{q}) - \tilde{G}^A(\omega, \mathbf{q}) \right). \quad (3.72)$$

Such a relation is in general not valid in the DDM. It is, however, emergent for the critical system in the long-wavelength limit: In the basis $\hat{\phi}_c = \bar{\phi}_c$, $\hat{\phi}_q = i(Z/|Z|)\bar{\phi}_q$ we have for the inverse propagators at the scale k (for convenience we are working here in the symmetric phase; the scale-dependent inverse propagators are determined by the quadratic part of the effective action Eq. (3.43)) $\hat{P}^R(\omega, \mathbf{q}) = i|Z|(\omega - \xi^*(q)) = \hat{P}^A(\omega, \mathbf{q})^\dagger$ where $\xi(q) = Kq^2 + u_1$ (note that here the renormalized quantities appear) and $\hat{P}^K = \bar{P}^K$. With these inverse propagators we form the ratio

$$\frac{\omega}{2} \frac{\hat{P}^K}{\hat{P}^R(Q) - \hat{P}^A(Q)} = \frac{\tilde{\gamma}}{4|Z|} \frac{\omega}{\omega - \text{Re} \xi(q)}, \quad (3.73)$$

which would equal the temperature if a FDT were valid.³ As we will see in Sec. 3.8.3, the effective action for the critical system becomes purely dissipative for $k \rightarrow 0$. In particular we have $\text{Re} \xi(q) \rightarrow 0$ so that Eq. (3.73) indeed reduces to an FDT with an effective temperature

$$T_{\text{eff}} = \frac{\tilde{\gamma}}{4|Z|}. \quad (3.74)$$

Note that for purely dissipative dynamics Eq. (3.65) implies that the ratio $\tilde{\gamma}/|Z|$ is a constant of the RG flow. For the DDM the emergence of an FDT with T_{eff} manifests itself in the relation Eq. (3.114) between the anomalous dimensions of $\tilde{\gamma}$ and Z valid at the fixed point. The flow of $\tilde{\gamma}/(4|Z|)$ is shown in Fig. 3.2.

3.6.4 Geometric interpretation of the equilibrium symmetry

For our truncation of the effective action Γ_k^{MAR} , the relation $\bar{\mathcal{U}}_H = \bar{r}\bar{\mathcal{U}}_D$ between the real and imaginary parts of the functional $\bar{\mathcal{U}} = \bar{\mathcal{U}}_H + i\bar{\mathcal{U}}_D$ implies that the couplings parameterizing $\bar{\mathcal{U}}_H$ and $\bar{\mathcal{U}}_D$ share a common ratio \bar{r} of real to imaginary parts

$$\bar{r} = \frac{\bar{A}}{\bar{D}} = \frac{\bar{\lambda}_1}{\bar{\kappa}_1} = \frac{\bar{\lambda}}{\bar{\kappa}} = \frac{\bar{\lambda}_3}{\bar{\kappa}_3}. \quad (3.75)$$

³Due to the relation $\hat{G}^K(\omega, \mathbf{q}) = -\hat{G}^R(\omega, \mathbf{q})\hat{P}^K\hat{G}^A(\omega, \mathbf{q})$, in Eq. (3.72) the propagators can be replaced by the inverse propagators.

The same applies to the renormalized couplings, however, with a different value r : With $z = -Z_I/Z_R$ we have

$$r = \frac{A}{D} = \frac{\lambda_1}{\kappa_1} = \frac{\lambda}{\kappa} = \frac{\lambda_3}{\kappa_3} = \frac{\bar{r} - z}{1 + \bar{r}z}. \quad (3.76)$$

This can be visualized conveniently in the complex plane, where the ratio of real to imaginary parts contains the same information as the argument of a complex number (the argument is $\tan(1/r)$): The renormalization of a complex coupling \bar{g} with Z corresponds to a rescaling $|g| = |\bar{g}|/|Z|$ of the modulus and a rotation of the phase by the argument of Z , $\arg g = \arg \bar{g} - \arg Z$. The condition Eq. (3.75) corresponding to MAR is depicted in Fig. 3.5 (b): All bare⁴ couplings lie on a single ray. In the purely dissipative case with $r = 0$ and $\bar{r} = z$, which is shown in Fig. 3.5 (a), this ray is perpendicular to Z . As a result, in this case the renormalized couplings are purely imaginary. Generally, only the renormalized quantities allow for an immediate physical interpretation: A and D describe propagation and diffusive behavior of particles, respectively, while λ (λ_3) and κ (κ_3) are two-body (three-body) elastic collisions and loss. In the generic driven-dissipative case, we have no *a priori* relations between these couplings because they are due to different physical mechanisms: Dissipative couplings describe local incoherent single particle pump and loss, as well as local two-body loss. On the other hand, unitary dynamics is given by coherent propagation and elastic collisions. Geometrically, the physical couplings point in different directions in the first quadrant of the complex plane (see Fig. 3.5 (c)), the latter restriction being due to the physical stability of the system (see Sec. 3.3.1).

This concludes our discussion of the relation of the DDM to dynamical equilibrium models. In the following section we will proceed to derive explicit flow equations for the couplings Eq. (3.66).

3.7 Non-Equilibrium FRG flow equations

In the following we discuss how the functional differential equation Eq. (3.42) for the effective action is reduced to a set of ordinary differential equations by virtue of the ansatz Eq. (3.43) for Γ_k . First we derive the flow equation for the effective potential, i.e., the part of the effective action that involves all momentum-independent couplings. Then we proceed to specify the flow of the inverse propagator which determines flow equations for the wave-function renormalization Z and the gradient coefficient \bar{K} . In the FRG, we approach the critical point from the ordered (symmetry-broken) side of the transition. This allows us to capture the leading divergences of two-loop effects in a calculation that is formally one-loop [69] by means of diagrams like the second one in Eq. (3.32) in the spirit of the background field method in gauge theories [98].

We denote the truncation Eq. (3.43), evaluated for homogeneous, i.e., space- and time-independent “background fields” by

$$\Gamma_{k,cq} = -\Omega \left(\bar{U}' \bar{\rho}_{cq} + \bar{U}'^* \bar{\rho}_{qc} - i\bar{\gamma} \bar{\rho}_q \right), \quad (3.77)$$

(the subscript cq indicates that we have classical and quantum background fields) where Ω is the quantization volume and the $U(1)$ invariant combinations of fields are $\bar{\rho}_{cq} = \bar{\phi}_c^* \bar{\phi}_q = \bar{\rho}_{qc}^*$ and $\bar{\rho}_q = |\bar{\phi}_q|^2$. This representation of $\Gamma_{k,cq}$ implies that the flow equation for the potential \bar{U}' can be obtained

⁴Here we denote the couplings that are not divided by Z as bare.

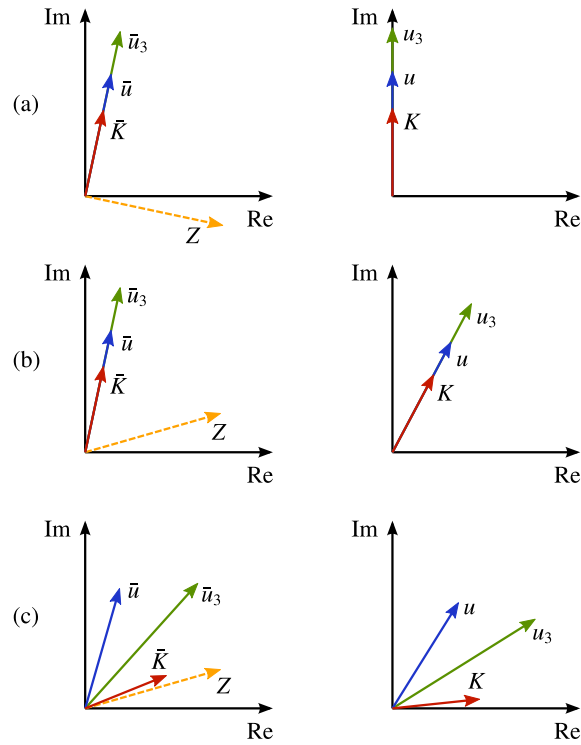


Figure 3.5. (Color online) Visualization of the renormalization with Z . Left column: Bare couplings. Right column: Renormalized couplings. The renormalization of a complex coupling \bar{g} corresponds to a rescaling $|g| = |\bar{g}| / |Z|$ of the modulus and a rotation of the phase by the argument of Z , $\arg g = \arg \bar{g} - \arg Z$. (a) When all bare couplings lie on a single ray that is perpendicular to Z , the renormalized couplings are purely imaginary as in MA. (b) Deviations from the right angle incorporate MA with compatible reversible mode couplings. (c) In a generic non-equilibrium situation there is no fixed relation between the arguments of the various couplings.

from Eq. (3.42) by taking the derivative with respect to $\bar{\rho}_{cq}$ and setting the quantum background fields to their stationary value (which is zero) afterwards,

$$\partial_t \bar{U}' = -\frac{1}{\Omega} \left[\partial_{\bar{\rho}_{cq}} \partial_t \Gamma_{k,cq} \right]_{\bar{\phi}_q = \bar{\phi}_q^* = 0}, \quad (3.78)$$

where the dimensionless RG flow parameter t is related to the cutoff scale k via $t = \ln(k/\Lambda)$. The flow equation for the renormalized potential follows straightforwardly by taking the scale derivative of the relation $\bar{U} = ZU$, which results in

$$\partial_t \bar{U}' = Z(-\eta_Z U' + \partial_t U'), \quad (3.79)$$

where we introduced the anomalous dimension of the wave-function renormalization,

$$\eta_Z = -\partial_t Z/Z. \quad (3.80)$$

Then, using $\partial_{\bar{\rho}_{cq}} = Z \partial_{\rho_{cq}}$, the flow equation for the renormalized potential can be written as

$$\partial_t U' = \eta_Z U' + \zeta', \quad \zeta' = -\frac{1}{\Omega} \left[\partial_{\rho_{cq}} \partial_t \Gamma_{k,cq} \right]_{\phi_q = \phi_q^* = 0}. \quad (3.81)$$

We proceed by specifying the projection prescriptions that allow us to derive the flow of the couplings u_n in the ordered phase from the flow equation (3.81). Taking the scale derivatives of the relation $u_n = U^{(n)}(\rho_0)$ we find

$$\partial_t u_n = \left(\partial_t U^{(n)} \right) (\rho_0) + U^{(n+1)}(\rho_0) \partial_t \rho_0. \quad (3.82)$$

Based on the power-counting arguments of Sec. 3.4.3, our truncation includes terms up to cubic order in the $U(1)$ invariants, i.e., for derivatives of the effective potential of the order of $n \geq 4$ we have $U^{(n)} = 0$. The flow equations for the quartic and sextic couplings are then given by (the RHS of these equations determine the so-called β -functions)

$$\partial_t u_2 = \beta_{u_2} = \eta_Z u_2 + u_3 \partial_t \rho_0 + \partial_{\rho_c} \zeta' \Big|_{\text{ss}}, \quad (3.83)$$

$$\partial_t u_3 = \beta_{u_3} = \eta_Z u_3 + \partial_{\rho_c^2} \zeta' \Big|_{\text{ss}}, \quad (3.84)$$

where according to Eq. (3.82) in ζ' we specify the classical background field ρ_c it to its stationary value $\rho_{c|\text{ss}} = \rho_0$. As we have seen above (cf. Secs. 3.3.1 and 3.4.1, the latter is determined by the dissipative part of the field equation, i.e., by the condition $\text{Im } U'(\rho_0) = 0$). Taking here the derivative with respect to the RG parameter t , we find

$$\partial_t \rho_0 = -(\text{Im } \partial_t U')(\rho_0) / \text{Im } U''(\rho_0) = -\text{Im } \zeta' \Big|_{\text{ss}} / \kappa. \quad (3.85)$$

Having thus specified the flow equations for the couplings that parameterize the potential U , we proceed to the Keldysh mass $\bar{\gamma}$, which is the coefficient of the term that is proportional to the quantum $U(1)$ invariant $\bar{\rho}_q$ in Eq. (3.77). We obtain the flow equation for $\bar{\gamma}$ as

$$\partial_t \bar{\gamma} = -\frac{i}{\Omega} \left[\partial_{\bar{\rho}_q} \partial_t \Gamma_{k,cq} \right]_{\text{ss}}. \quad (3.86)$$

For the renormalized Keldysh mass, which is related to the bare one via $\gamma = \bar{\gamma}/|Z|^2$, we have (the transformation from bare to renormalized fields implies $\partial_{\bar{\rho}_q} = |Z|^2 \partial_{\rho_q}$)

$$\partial_t \gamma = \beta_\gamma = 2\eta_{ZR}\gamma + \zeta_\gamma, \quad \zeta_\gamma = -\frac{i}{\Omega} \left[\partial_{\rho_q} \partial_t \Gamma_{k,cq} \right]_{\text{ss}}. \quad (3.87)$$

While the flow of $\Gamma_{k,cq}$ (i.e., the flow equation evaluated at homogeneous background fields) yields flow equations for all momentum-independent couplings, we have to consider the flow of the inverse propagator

$$\partial_t \bar{P}_{ij}(Q) \delta(Q - Q') = \left[\frac{\delta^2 \partial_t \Gamma_k}{\delta \bar{\chi}_i(-Q) \delta \bar{\chi}_j(Q')} \right]_{\text{ss}}, \quad (3.88)$$

in order to derive flow equations for the wave-function renormalization Z and the gradient coefficient \bar{K} . The retarded component of the inverse propagator in the presence of real stationary background fields $\bar{\phi}_c = \bar{\phi}_c^* = \bar{\phi}_0$ reads

$$\bar{P}^R(Q) = \begin{pmatrix} -iZ_I\omega - \bar{K}_R q^2 - 2\bar{\lambda}\bar{\rho}_0 & iZ_R\omega - \bar{K}_I q^2 \\ -iZ_R\omega + \bar{K}_I q^2 + 2\bar{\kappa}\bar{\rho}_0 & -iZ_I\omega - \bar{K}_R q^2 \end{pmatrix}, \quad (3.89)$$

Then, for the kinetic coefficient \bar{K} we choose from the flow equation (3.88) the elements of the inverse propagator that do not have mass-like contributions [69] $2\bar{\lambda}\bar{\rho}_0$ and $2\bar{\kappa}\bar{\rho}_0$,

$$\partial_t \bar{K} = -\partial_{q^2} \left(\partial_t \bar{P}_{22}^R(Q) + i\partial_t \bar{P}_{12}^R(Q) \right) \Big|_{Q=0}. \quad (3.90)$$

The flow equation for the wave-function renormalization Z as specified below, on the other hand, mixes massive and massless components symmetrically

$$\partial_t Z = -\frac{1}{2} \partial_\omega \text{tr} \left[\left(\mathbb{1} + \sigma_y \right) \partial_t \bar{P}^R(Q) \right] \Big|_{Q=0}. \quad (3.91)$$

This choice allows for the locking of the flows of the Keldysh mass and Z as implied by the emergence of the symmetry Eq. (3.60) in the purely dissipative IR regime (see Sec. 3.8). Finally, the flow equation for the renormalized coefficient K follows by straightforward differentiation of its definition $K = \bar{K}/Z$ in terms of bare quantities. We find

$$\partial_t K = \beta_K = \eta_Z K + \partial_t \bar{K}/Z. \quad (3.92)$$

The truncation Eq. (3.43) is parameterized in terms of the couplings Eq. (3.66). Renormalization of the fields with Z leads to a description in terms of $\mathbf{g} = (K, \rho_0, u_2, u_3, \gamma)^T$ (where we omit the mass u_1 : as indicated above we approach the critical point from the ordered phase, i.e., we parameterize the effective action in terms of the stationary condensate density ρ_0 instead of the mass u_1). In this section we derived the β -functions for these renormalized couplings, i.e., we have specified a closed set of flow equations $\partial_t \mathbf{g} = \beta_{\mathbf{g}}(\mathbf{g})$ from which Z can be completely eliminated (the anomalous dimension η_Z entering the β -functions can again be expressed in terms of the couplings \mathbf{g} alone). More explicit expressions for the β -functions are provided in App. 3.C.3).

3.8 Scaling solutions

As one considers an effective description of a system at a continuous phase transition at longer and longer scales (which is equivalent to following the RG flow to smaller values of k), physical observables and the couplings that describe the system exhibit scaling behavior. The search for such scaling solutions to the flow equations is facilitated by introducing rescaled dimensionless (in the sense of the canonical power counting introduced in Sec. 3.4.3) couplings which remain constant, i.e., by searching for a fixed point of the flow equations of these rescaled couplings instead. In the following section we introduce such rescaled couplings and derive the corresponding flow equations.

3.8.1 Scaling form of the flow equations

As a first step we trade the real parts of K , u_2 , and u_3 for the ratios of real to imaginary parts

$$r_K = A/D, \quad r_{u_2} = \lambda/\kappa, \quad r_{u_3} = \lambda_3/\kappa_3, \quad (3.93)$$

which measure the relative strength of coherent and dissipative dynamics. As we will show below, at criticality all these ratios flow to zero signaling decoherence. Their flow is given by

$$\partial_t r_K = \beta_{r_K} = \frac{1}{D} (\beta_A - r_K \beta_D), \quad (3.94)$$

$$\partial_t r_{u_2} = \beta_{r_{u_2}} = \frac{1}{\kappa} (\beta_\lambda - r_{u_2} \beta_\kappa), \quad (3.95)$$

$$\partial_t r_{u_3} = \beta_{r_{u_3}} = \frac{1}{\kappa_3} (\beta_{\lambda_3} - r_{u_3} \beta_{\kappa_3}). \quad (3.96)$$

(The β -functions for the real and imaginary parts of K , u_2 , and u_3 are specified in App. 3.C.2, see Eq. (3.194).) We proceed by introducing a dimensionless mass term

$$w = \frac{2\kappa\rho_0}{k^2 D}, \quad (3.97)$$

the flow equation of which mixes contributions from the β -functions of ρ_0 , κ , and D , and reads

$$\partial_t w = \beta_w = -(2 - \eta_D) w + \frac{w}{\kappa} \beta_\kappa + \frac{2\kappa}{k^2 D} \beta_{\rho_0}, \quad (3.98)$$

where the anomalous dimension of D is defined as

$$\eta_D = -\partial_t D/D. \quad (3.99)$$

Finally we replace the quartic and sextic couplings by dimensionless ones. For a momentum-independent n -body coupling u_n we can construct a corresponding dimensionless coupling by means of the relation

$$\tilde{u}_n = \frac{k^{(d-2)n-d}}{D^n} \left(\frac{\gamma}{2}\right)^{n-1} u_n. \quad (3.100)$$

The flow equations for the imaginary parts $\tilde{\kappa}$ and $\tilde{\kappa}_3$ of the dimensionless quartic and sextic couplings, therefore, are given by

$$\partial_t \tilde{\kappa} = \beta_{\tilde{\kappa}} = -(4 - d - 2\eta_D + \eta_\gamma) \tilde{\kappa} + \frac{k^{-4+d} \gamma}{2D^2} \beta_\kappa, \quad (3.101)$$

$$\partial_t \tilde{\kappa}_3 = \beta_{\tilde{\kappa}_3} = -(6 - 2d - 3\eta_D + 2\eta_\gamma) \tilde{\kappa}_3 + \frac{k^{-6+2d} \gamma^2}{4D^3} \beta_{\kappa_3}, \quad (3.102)$$

and include contributions from the anomalous dimension

$$\eta_\gamma = -\partial_t \gamma / \gamma. \quad (3.103)$$

Thus we are left with six dimensionless running couplings, which we collect in vectors $\mathbf{r} = (r_K, r_{u_2}, r_{u_3})^T$ and $\mathbf{s} = (w, \tilde{\kappa}, \tilde{\kappa}_3)^T$. Their flow equations form a closed set,

$$\partial_t \mathbf{r} = \beta_{\mathbf{r}}(\mathbf{r}, \mathbf{s}), \quad \partial_t \mathbf{s} = \beta_{\mathbf{s}}(\mathbf{r}, \mathbf{s}). \quad (3.104)$$

The β -functions on the RHS of these equations contain the anomalous dimensions η_Z, η_D , and η_γ , which in turn can be expressed as functions of the running couplings \mathbf{r} and \mathbf{s} alone. We note in passing that according to the discussion of Sec. 3.6.4, the equilibrium model MAR is described by $r_K = r_{u_2} = r_{u_3} = r$, i.e.,

$$\mathbf{r}_{\text{MAR}} = r(1, 1, 1)^T \quad (3.105)$$

(MA is realized for the special case $r = 0$). Inserting the same value r for all three ratios in the respective β -functions we find $\beta_{r_K} = \beta_{r_{u_2}} = \beta_{r_{u_3}}$, which shows that for MAR the common ratio is preserved by the flow as it should be.

Our analysis of the flow equations (3.104) will proceed in two steps: First we will search for fixed points \mathbf{r}_* and \mathbf{s}_* , which are solutions to the algebraic equations

$$\beta_{\mathbf{r}}(\mathbf{r}_*, \mathbf{s}_*) = \beta_{\mathbf{s}}(\mathbf{r}_*, \mathbf{s}_*) = \mathbf{0}. \quad (3.106)$$

In Sec. 3.8.2 we briefly discuss the trivial Gaussian fixed point and then turn to the Wilson-Fisher fixed point that describes the critical system in 3.8.3). Second we will solve the full flow equations numerically and provide our results in Sec. 3.9. While already the linearized flow equations in the vicinity of the Wilson-Fisher fixed point encode universal physics at the phase transition and determine the asymptotic flow of the system for $k \rightarrow 0$ (or $t \rightarrow -\infty$), the numerical integration of the full flow equations provides us with information on non-universal aspects such as the extent of the scaling regime.

3.8.2 Gaussian fixed point

All β -functions vanish on the manifold of Gaussian fixed points which is parameterized by $\mathbf{s}_* = \mathbf{0}$ and $\mathbf{r}_* \in \mathbb{R}^3$. We note that the combination of vanishing imaginary parts $\tilde{\kappa}_*$ and $\tilde{\kappa}_{3*}$ of the quartic and sextic couplings and arbitrary finite ratios of real to imaginary parts implies that also the real parts of \tilde{u}_{2*} and \tilde{u}_{3*} are zero on this fixed point manifold. In a linearization of the flow equations around $\mathbf{s}_* = \mathbf{0}$, the fluctuation contributions vanish and the scaling behavior is determined solely by the canonical scaling dimensions, implying in particular that the Gaussian fixed point is unstable (for small values $\mathbf{s} \neq \mathbf{s}_*$ the flow is directed away from the fixed point) and, therefore, physically not relevant. Non-trivial scaling behavior at criticality is governed by the Wilson-Fisher fixed point which we will discuss in the next section.

3.8.3 Wilson-Fisher fixed point: critical behavior

As discussed in Sec. 3.6, our driven-dissipative model reduces to MA when we set the real parts of all renormalized couplings to zero, cf. Fig. 3.5, i.e., for $\mathbf{r} = \mathbf{0}$. It is well-known that MA exhibits a

non-trivial Wilson-Fisher fixed point [32], and indeed we find this fixed point at

$$\begin{aligned}\mathbf{r}_* &= (r_{K*}, r_{u*}, r_{u'*}) = \mathbf{0}, \\ \mathbf{s}_* &= (w_*, \tilde{\kappa}_*, \bar{\kappa}'_*) = (0.475, 5.308, 51.383).\end{aligned}\quad (3.107)$$

The values of the coupling \mathbf{s}_* are identical to those obtained in an equilibrium classical $O(2)$ model from functional RG calculations at the same level of truncation [69]. We note that this fixed point is also contained in the subspace of couplings corresponding to MAR, which is characterized by Eq. (3.105), i.e., the phase transitions in both the equilibrium and non-equilibrium models are described by the same fixed point. Critical behavior, however, is determined by the RG flow in the vicinity of the fixed point. Here the non-equilibrium setting adds two more independent directions, thereby opening up the possibility for deviations from equilibrium criticality as we will now show.

The asymptotic flow for $k \rightarrow 0$ of the critical system is determined by a linearization of the flow equations in the deviations $\delta\mathbf{s} = \mathbf{s} - \mathbf{s}_*$, $\delta\mathbf{r} = \mathbf{r}$ from the fixed point. In the linear regime the two sectors corresponding to \mathbf{s} and \mathbf{r} decouple as described by the block diagonal stability matrix

$$\partial_t \begin{pmatrix} \delta\mathbf{r} \\ \delta\mathbf{s} \end{pmatrix} = \begin{pmatrix} N & 0 \\ 0 & S \end{pmatrix} \begin{pmatrix} \delta\mathbf{r} \\ \delta\mathbf{s} \end{pmatrix}, \quad (3.108)$$

where the 3×3 submatrices S and N are given by

$$S = \nabla_{\mathbf{s}}^T \beta_{\mathbf{s}} \Big|_{\mathbf{r}=\mathbf{r}_*, \mathbf{s}=\mathbf{s}_*} = \begin{pmatrix} -1.620 & 0.088 & 0.005 \\ -3.183 & 0.290 & 0.036 \\ -15.374 & -42.249 & 2.183 \end{pmatrix}, \quad (3.109)$$

$$N = \nabla_{\mathbf{r}}^T \beta_{\mathbf{r}} \Big|_{\mathbf{r}=\mathbf{r}_*, \mathbf{s}=\mathbf{s}_*} = \begin{pmatrix} 0.053 & 0.059 & 0.032 \\ 0 & -0.053 & 0.196 \\ 0.498 & -2.327 & 1.973 \end{pmatrix}. \quad (3.110)$$

The matrix N would be identically zero in the absence of anomalous additions to the canonical scaling dimensions (note that the ratios \mathbf{r} have canonical scaling dimension zero), or even if coherent and dissipative couplings would exhibit identical anomalous scaling. The non-vanishing of this block thus indicates a different universal behavior of these two types of couplings. Due to the decoupling of the flows of \mathbf{r} and \mathbf{s} we may discuss the linearized flow of each set of couplings separately.

In the matrix S we find one negative eigenvalue s_1 corresponding to the correlation length exponent $\nu = -1/s_1 = 0.716$ (our findings for critical exponents are summarized in Tab. 3.2). Considering that we are restricting ourselves to relevant and marginal terms in our truncation, the agreement of the numerical value of ν with results from more sophisticated calculations [99] is reasonable. Furthermore there are two complex conjugate eigenvalues $s_{2,3} = 1.124 \pm i0.622$ with positive real parts (indicating that these directions are stable). The imaginary parts are known artifacts of this level of truncation for the $O(2)$ model and vanish upon inclusion of higher order terms in the effective potential [100].

The scaling behavior of the couplings Z, D , and γ is determined by the values of the respective anomalous dimensions at the fixed point. In addition we define the anomalous dimension for the bare kinetic coefficient \bar{K} as

$$\eta = -\partial_t \bar{K} / \bar{K} = \frac{1}{1 + r_K^2} \left[r_K^2 \bar{\eta}_A + \bar{\eta}_D - i r_K (\bar{\eta}_A - \bar{\eta}_D) \right], \quad (3.111)$$

	ν	η	z	η_r
$O(2)$	0.716	0.039		
MA	0.716	0.039	2.121	
MAR	0.716	0.039	2.121	- 0.143
DDM	0.716	0.039	2.121	- 0.101

Table 3.2. Results for the correlation length exponent ν , the anomalous dimension η , the dynamical critical exponent z , and the decoherence exponent η_r in our truncation.

where the representation in terms of $\bar{\eta}_A$ and $\bar{\eta}_D$ follows from the definition of these quantities in Eq. (3.192). At the fixed point η takes the value

$$\eta = 0.039, \quad (3.112)$$

which is again the result for the anomalous dimension of the classical $O(2)$ model in $d = 3$ dimensions at the same level of truncation [69] and agrees well with results from more accurate calculations [99]. In summary, the static critical behavior coincides precisely with the one of the classical $O(2)$ model, implying that the dynamical anomalous dimension η_Z effectively does not enter the corresponding equations. This can be seen as follows: Inserting $\mathbf{r} = \mathbf{0}$ in the expressions for the anomalous dimensions, we find

$$\eta_{ZR} = -\eta_\gamma, \quad \eta_{ZI} = 0. \quad (3.113)$$

(We note that this holds for all values of the static couplings \mathbf{s} , i.e., it is always realized in MA.) These relations ensure that η_{ZR} and η_γ compensate each other in all flow equations.⁵ Moreover they imply that the ratio $\bar{\gamma}/|Z|$ appearing on the RHS of the fluctuation-dissipation relation Eq. (3.73) approaches a constant value at the fixed point: According to the definition of the anomalous dimensions Eqs. (3.80) and (3.103), close to the fixed point the flow of Z and γ is described by $Z \sim k^{-\eta_Z}$ (note that η_Z is real so that this behavior indeed describes algebraic scaling and does not contain oscillatory parts) and $\gamma \sim k^{-\eta_\gamma}$ with η_Z and η_γ evaluated at \mathbf{r}_* and \mathbf{s}_* . Thus we find $\bar{\gamma}/|Z| = |Z|\gamma \sim k^{-\eta_Z - \eta_\gamma} = \text{const.}$, i.e., the symmetry Eq. (3.60), which manifests itself in this quantity approaching a constant value (cf. Eq. (3.74)), emerges in the IR without imposing it in the microscopic model. In other words, the driven-dissipative system obeys a classical FDT in the long-wavelength limit (see Fig. 3.2). At the fixed point we find the value

$$\eta_Z = -\eta_\gamma = 0.161. \quad (3.114)$$

Let us now consider the upper left block N of the stability matrix. It has three positive eigenvalues,

$$n_1 = 0.101, \quad n_2 = 0.143, \quad n_3 = 1.728, \quad (3.115)$$

which indicates that the ratios \mathbf{r} are attracted to their fixed point value zero. The corresponding eigenvectors are

$$\mathbf{u}_1 = \begin{pmatrix} 0.022 \\ 0.109 \\ 0.994 \end{pmatrix}, \quad \mathbf{u}_2 = \frac{1}{\sqrt{3}} \begin{pmatrix} 1 \\ 1 \\ 1 \end{pmatrix}, \quad \mathbf{u}_3 = \begin{pmatrix} 0.802 \\ 0.469 \\ 0.370 \end{pmatrix}. \quad (3.116)$$

⁵The cancellation of η_{ZR} and η_γ can be made explicit by inserting the β -functions for κ and κ_3 , Eqs. (3.215) and (3.216) respectively, as well as the expression for η_D that follows from Eq. (3.211), in the flow equations for $\bar{\kappa}$ and $\bar{\kappa}_3$. In the resulting expressions the anomalous dimensions η_{ZR} and η_γ appear only as the sum $\eta_{ZR} + \eta_\gamma$.

The smallest of the eigenvalues determines the scaling behavior of \mathbf{r} in the deep IR. In order to see this let us expand \mathbf{r} in the basis of eigenvectors of the matrix N ,

$$\mathbf{r} = \sum_{i=1}^3 \mathbf{u}_i c_i. \quad (3.117)$$

The coefficients in this expansion are given by $c_i = \mathbf{v}_i \cdot \mathbf{r}$, where \mathbf{v}_i are the left eigenvectors of N (the latter is not symmetric and its left and right eigenvectors, therefore, are not equal), normalized such that $\mathbf{u}_i \cdot \mathbf{v}_j = \delta_{ij}$. The asymptotic behavior of the flow of the so-called scaling fields [77] c_i is given by $c_i \sim e^{n_i t} = k^{n_i}$, which implies that for \mathbf{r} we indeed find

$$\mathbf{r} \sim \mathbf{u}_1 k^{n_1} = \mathbf{u}_1 k^{-\eta_r}, \quad (3.118)$$

with only subdominant contributions in the directions of \mathbf{u}_2 and \mathbf{u}_3 . This leads us to identify the decoherence exponent

$$\eta_r = -n_1 = -0.101. \quad (3.119)$$

From the scaling behavior of the ratios \mathbf{r} we may infer the one of the coherent couplings. For the coefficient of coherent propagation A , in particular, we have

$$A = r_K D \sim k^{n_1 - \eta_D} = k^{-\eta_A}. \quad (3.120)$$

Then, with the anomalous dimension of the dissipative kinetic coefficient D at the fixed point,

$$\eta_D = -0.121, \quad (3.121)$$

we obtain the value

$$\eta_A = -0.223. \quad (3.122)$$

Let us discuss the consequences of this result for the effective dispersion relation of long-wavelength excitations, which is encoded in the running inverse propagator Eq. (3.49). Once the cutoff scale k becomes smaller than the external momentum q , the effective infrared cutoff is given by q instead of k [101] Then, in the dispersion relation Eq. (3.54)., which we rewrite here in terms of the scaling variables introduced in Sec. 3.8.1 as

$$\omega_{1,2}^R = Dq^2 \left[-i(1 + w/2) \pm \sqrt{r_K^2 + r_K r_{u_2} w - (w/2)^2} \right], \quad (3.123)$$

we may insert the scaling forms $w \sim w_*$, $r_K \sim r_{K0} q^{-\eta_r}$, $r_{u_2} \sim r_{u_20} q^{-\eta_r}$, and $D \sim D_0 q^{-\eta_D}$. For $q \rightarrow 0$ both modes are purely diffusive with $\omega_1^R \sim -iD_0 q^{2-\eta_D}$ and $\omega_2^R \sim -iD_0 q^{2-\eta_D} (1 + w_*)$, and for the dynamical critical exponent z which is defined via the relation $\omega^R \sim -iq^z$ we find the value

$$z = 2 - \eta_D = 2.121. \quad (3.124)$$

Above the purely diffusive IR regime, when $w \ll r_K, r_{u_2}$, the dispersion relation simplifies to

$$\omega_{1,2}^R \sim (-iD \pm Dr_K) q^2 \sim -iD_0 q^{2-\eta_D} \pm A_0 q^{2-\eta_A}, \quad (3.125)$$

i.e., coherent propagation and diffusive contributions scale differently with the momentum q . In the symmetric phase the branch ω_2^R is absent and the bare retarded response function is dominated by

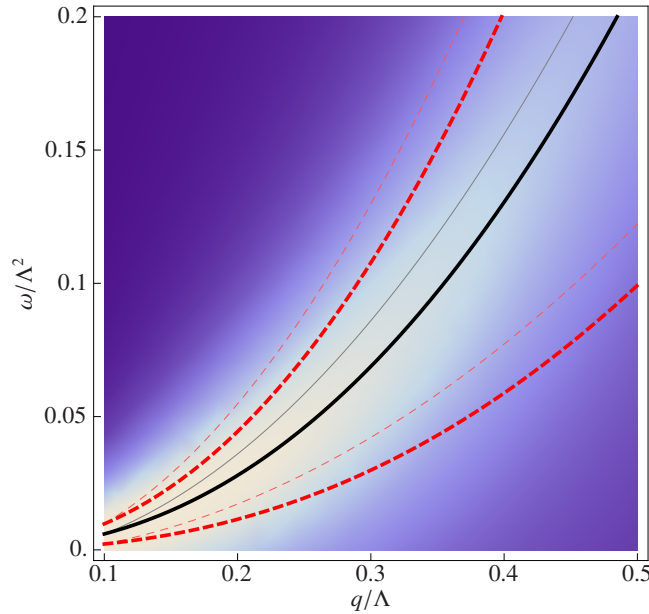


Figure 3.6. (Color online) Spectral density Eq. (3.128) in the scaling regime. The solid line corresponds to the position $\sim A_0 q^{2-\eta_A}$ of the peak of the Lorentzian curve while its width $\sim D_0 q^{2-\eta_D}$ is indicated by dashed lines. For comparison we also show peak position and width for canonical scaling $\sim q^2$ as thin solid and dashed lines, respectively. (Canonical and anomalous scaling forms are chosen to coincide at $q\Lambda = 0.1$.) Parameters are $A_0\Lambda^{\eta_A} = Z_0\Lambda^{\eta_Z} = 1$ and $D_0\Lambda^{\eta_D} = 1/2$.

a single pole at $\omega = \omega_1^R$, i.e., we have (the bare scale-dependent propagators are determined by the quadratic part of the effective action Eq. (3.43))

$$\bar{G}^R(Q) = \frac{1}{Z^*(\omega - \omega_1^R)}. \quad (3.126)$$

As explained at the end of Sec. 3.2 this quantity and, in particular, the spectral density which is related to its imaginary part [77],

$$A(Q) = -2 \text{Im} \bar{G}^R(Q), \quad (3.127)$$

are direct experimental observables. For $\omega \approx \omega_1^R$ the spectral density has the shape of a Lorentzian centered at $\text{Re} \omega_1^R$ and with width determined by $\text{Im} \omega_1^R$,

$$A(Q) = \frac{2}{|Z|^2} \frac{Z_R \text{Im} \omega_1^R}{(\omega - \text{Re} \omega_1^R)^2 + (\text{Im} \omega_1^R)^2}. \quad (3.128)$$

Inserting here the scaling forms $Z \sim Z_0 k^{-\eta_Z}$ and Eq. (3.125) for ω_1^R with different scaling behavior of real and imaginary parts, the structure sketched in Fig. 3.3 emerges. For the specific values of the anomalous dimensions obtained in this section the spectral density is shown in Fig. 3.6, where a pronounced feature is clearly visible.

Before moving on to a numerical integration of the flow equations in the next section, we briefly contrast our findings for the DDM with the equilibrium case of MAR. There, analyzing the stability

of the fixed point Eq. (3.107) we have to take into account only one direction $r = r_K = r_{u_2} = r_{u_3}$, and we find (as $r_* = 0$ we have $\delta r = r$)

$$\partial_t \begin{pmatrix} \delta r \\ \delta \mathbf{s} \end{pmatrix} = \begin{pmatrix} R & 0 \\ 0 & S \end{pmatrix} \begin{pmatrix} \delta r \\ \delta \mathbf{s} \end{pmatrix} \quad (3.129)$$

where the matrix S is the same as above and the element R is given by the “middle” eigenvalue Eq. (3.115) of the stability matrix N in the non-equilibrium problem,

$$R = \partial_r \beta_r \Big|_{r=r_*, s=s_*} = n_2, \quad (3.130)$$

i.e., also in the equilibrium setting we find decoherence at the longest scales, however, with a value of the decoherence exponent that is different from the one in non-equilibrium. Let us finally remark that in the linearized regime, the fact that MAR is contained as a special case in the non-equilibrium problem, becomes visible in the form of the second eigenvector Eq. (3.116) which realizes the constraint Eq. (3.105).

We finally comment on the relation of the critical exponents obtained here with other approaches. The static critical exponent η shows very good agreement with sophisticated high order perturbative calculations. For the dynamical critical exponent z , to the best of our knowledge, currently there are no high-precision results for MA with $N = 2$ components available. (The situation is different for the Ising-symmetric case with $N = 1$, where the dynamical critical exponent has been calculated with high accuracy, see Ref. [102] and references therein.) Thus the value $z = 2.121$ obtained here has to be compared to $z = 2.026$ which corresponds to the third order in ϵ -expansion [80, 103]. The decoherence exponent ($\eta_r = -0.101$ here) has been computed in a recent complementary perturbative field theoretical study to second order in ϵ -expansion, where it takes the value $\eta_r = -0.003$, see Ref. [57]. The discrepancy between these values can only be resolved by extending the truncation advocated here, by including higher order corrections in perturbative field theoretical approaches, or by means of large-scale computer simulations.

3.9 Numerical integration of flow equations

In the previous section we have seen that the flow equations Eq. (3.104) entail non-trivial critical behavior governed by the Wilson-Fisher fixed point Eq. (3.107). While these results were based on an analysis of the linearized flow equations in the vicinity of the fixed point, we will now turn to a numerical integration of the full non-linear equations. On the one hand, this serves to illustrate the concept of universality: Independently from the initial values $\mathbf{r}_\Lambda, \tilde{\kappa}_\Lambda$, and $\tilde{\kappa}_{3\Lambda}$ at the mesoscopic starting point of the RG flow, critical behavior can be induced by a proper fine-tuning of w_Λ and becomes apparent in the approach of the RG flow to the scaling solution. Apart from that, the availability of the full flow in the framework of the FRG allows us to extract non-universal aspects. In particular, we will give an estimate of the Ginzburg scale, i.e., the scale that separates the region of non-universal flow from the universal scaling regime and thus is important for determining experimental requirements on the necessary frequency resolution.

Our approach for finding numerical solutions to the flow equations that exhibit critical behavior is as follows: We choose initial values $\mathbf{r}_\Lambda, \tilde{\kappa}_\Lambda$, and $\tilde{\kappa}_{3\Lambda}$ at the mesoscopic scale $k = \Lambda$ ($t = 0$), which are appropriate for the description of the model introduced in Sec. 3.3. This model contains two-body elastic interactions and loss, while three-body terms are contained only in an effective low-momentum

description, implying $\tilde{\kappa}_\Lambda \approx 1$ and $\tilde{\kappa}_{3\Lambda} \ll 1$. The dissipative kinetic coefficient D is very small in the microscopic description, so that $r_{K\Lambda} \gg 1$ initially, while for the two-body terms we have $r_{u_2\Lambda} \approx 1$. The latter generate the three-body couplings and we assume that $r_{u_3\Lambda} \approx 1$ as well. For such a choice of initial values, there is a critical value $w_\Lambda = w_c$ so that the resulting RG trajectories $\mathbf{r}(t)$ and $\mathbf{s}(t)$ approach the scaling solution, i.e., the fixed point, for $k \rightarrow 0$ ($t \rightarrow -\infty$). Any solution obtained by *numerically* integrating the flow equations with w_Λ fine-tuned to w_c , however, eventually always flows away from the fixed point, as due to limited accuracy the solution develops a non-zero component in the unstable direction of the fixed point at some stage. For all solutions shown in the figures we choose w_Λ slightly below w_c , so that the trajectory at large RG “times” t flows to the symmetric phase with $w = 0$.

When such a near-critical trajectory approaches the scaling solution, the couplings \mathbf{s} flow towards their fixed point values \mathbf{s}_* on a scale $1/\text{Re } s_{2,3} \approx 1$ determined by the eigenvalues $s_{2,3}$ of the stability matrix S , cf. Fig. 3.7, and stay there for a long “time” t_s . Depending on how close w_Λ is to w_c , this duration is typically $t_s = 10$ to 20 which corresponds to several orders of magnitude in k/Λ . During t_s the ratios \mathbf{r} decay according to Eq. (3.117), i.e., as the sum of three exponentials, with decay rates given by the eigenvalues Eq. (3.115) of the stability matrix N . In order to extract these eigenvalues from the numerical solution, we consider the flow of the coefficients $c_i \sim e^{n_i t}$ in the expansion of \mathbf{r} in the basis of eigenvectors of N Eq. (3.117). Figure 3.7 shows $c_{1,2}$ along with exponential fits, which reproduce the eigenvalues $n_{1,2}$ to satisfactory accuracy.

An important result of the previous section is the scaling relation Eq. (3.114) between the anomalous dimensions η_Z and η_γ of the wave-function renormalization and the Keldysh mass respectively, which implies that when evaluated along a critical trajectory, the value of $-\eta_\gamma$ approaches the one of the real part η_{ZR} of η_Z , while the imaginary part η_{ZI} flows to zero. This prediction – physically implying asymptotic thermalization – is verified numerically in Fig. 3.8.

As the anomalous dimensions η_a of $a = Z, D$, and γ are functions of the renormalized dimensionless couplings \mathbf{r} and \mathbf{s} alone and not the quantities a themselves, we get the solutions to the flow equations $\partial_t a = -\eta_a a$ simply by exponentiating the integrals of the anomalous dimensions along RG trajectories $\mathbf{r}(t)$ and $\mathbf{s}(t)$, i.e.,

$$a(t) = a_\Lambda e^{-\int_0^t dt' \eta_a}. \quad (3.131)$$

In this way we obtain the trajectories of K shown in Fig. 3.9 and the flow of the effective temperature $T_{\text{eff}} = \bar{\gamma}/(4|Z|) = \gamma|Z|/4$ which according to the discussion in Sec. 3.6.3 at low frequencies saturates to a constant value as illustrated in Fig. 3.2. While this asymptotic value depends on the initial values of $\bar{\gamma}$ and Z at the scale Λ and is, therefore, non-universal, the manner in which it is approached is universal as it is determined by the exponent η_γ : According to Eq. (3.131) the flow of T_{eff} is given by

$$T_{\text{eff}}(t) = T_{\text{eff}\Lambda} e^{-\int_0^t dt' (\eta_{ZR} + \eta_\gamma)}. \quad (3.132)$$

Close to the fixed point we may expand the anomalous dimensions in the exponential in powers of $\delta\mathbf{r} = \mathbf{r}$ and $\delta\mathbf{s}$. As both η_{ZR} and η_γ are even functions of \mathbf{r} there is no linear term in the expansion and we may write for $a = ZR$ and γ (here we are indicating the anomalous dimension evaluated at the fixed point explicitly as η_{a*}):

$$\eta_a = \eta_{a*} + \frac{1}{2} \mathbf{r} \cdot \left[\nabla_{\mathbf{r}}^T \nabla_{\mathbf{r}} \eta_a \right]_{\mathbf{r}=\delta\mathbf{s}=0} \mathbf{r}, \quad (3.133)$$

where we are neglecting corrections that are quartic in $|\mathbf{r}|$ or contain mixed powers of $|\mathbf{r}|$ and $|\delta\mathbf{s}|$. Both types of corrections are small as compared to the leading contribution that is quadratic in $|\mathbf{r}|$: In the

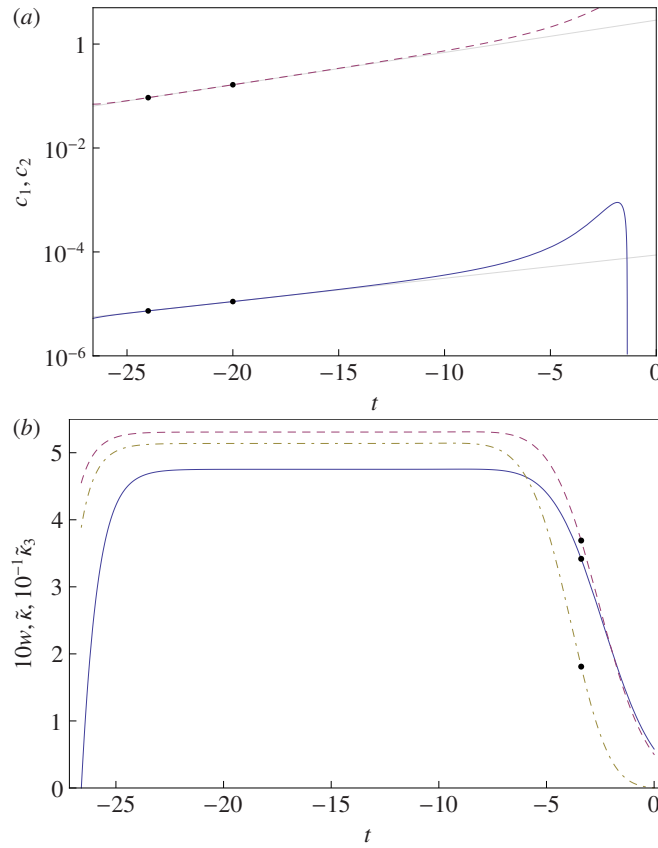


Figure 3.7. (Color online) (a) The flow of c_1 (solid line) describes the vanishing of coherent dynamics. A fit with $\ln c_1 = a_1 t + b_1$ in the region $t \in [-24, -20]$ (the points $t = -24$ and $t = -20$ are highlighted by dots on the trajectory) yields the slope $a_1 = 0.10$ in agreement with smallest eigenvalue $n_1 = -\eta_r$ of the stability matrix Eq. (3.110). We also show the evolution of the coefficient c_2 (dashed line). For the evolution of c_2 , the slope of a linear fit is $a_2 = 0.14$ and reproduces the eigenvalue n_2 . In the scaling region, the coefficient c_3 drops to very small values $\lesssim 10^{-11}$ on a scale $1/n_3 \approx 0.6$. The exponential decay of the components of \mathbf{r} is in this range still dominated by the contribution stemming from c_2 . (b) The couplings $10w$ (solid), $\tilde{\kappa}$ (dashed), and $10^{-1}\tilde{\kappa}_3$ (dot-dashed) are close to their fixed point values in the range from $t \approx -5$ to $t \approx -25$. A measure for the extent of the universal domain is given by the Ginzburg scale Eq. (3.136) which here takes the value $t_G \approx -3.4$. Initial conditions for both (a) and (b) are $r_{K\Lambda} = r_{u\Lambda} = 10$, $r_{u_3\Lambda} = 1$, $w_\Lambda \approx 0.05810$, $\tilde{\kappa} = 0.5$, and $\tilde{\kappa}_3 = 0.01$.

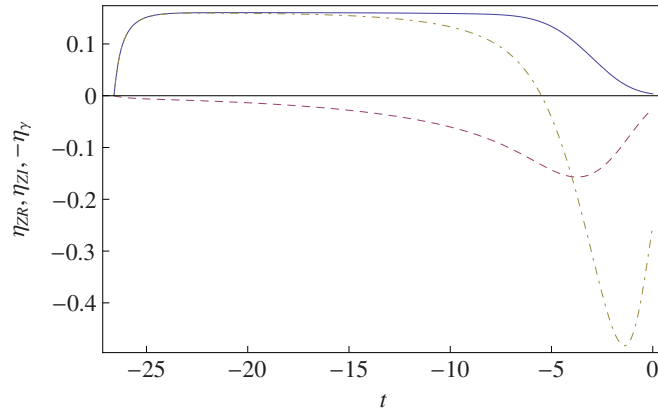


Figure 3.8. (Color online) Anomalous dimensions η_{ZR} (solid), η_{ZI} (dashed), and $-\eta_\gamma$ (dot-dashed) for the solution of Fig. 3.7. From $t \approx -5$ to $t \approx -25$, where the values of \mathbf{s} are close to the scaling solution, η_{ZR} takes the constant value Eq. (3.114), while η_{ZI} decays to zero. The value of $-\eta_\gamma$ approaches the one of η_{ZR} so that Eq. (3.114) is satisfied at late “times” t . Eventually, as the trajectory is driven away from the fixed point and enters the symmetric phase with $w = 0$, the anomalous dimensions drop to zero.

scaling regime we have $|\mathbf{r}| \sim e^{-\eta_{rs}t} \gg |\delta\mathbf{s}| \sim e^{\text{Re } s_{2,3}t}$, where $s_{2,3}$ are eigenvalues with positive real parts $\text{Re } s_2 = \text{Re } s_3$ of the stability matrix S Eq. (3.109) and determine the leading corrections to scaling in the static sector. Therefore, neglecting exponentially small corrections, we have

$$\eta_a = \eta_{a*} + \eta_a'' e^{-2\eta_{rs}t}. \quad (3.134)$$

Note that the quantities η_a'' depend on the precise prefactor in the scaling form Eq. (3.118) of \mathbf{r} , i.e., they depend on microscopic parameters and are thus non-universal. Then, using Eq. (3.134) and keeping in mind that $\eta_{\gamma*} = -\eta_{ZR*}$, we find the asymptotic behavior

$$T_{\text{eff}}(t) = T_{\text{eff}0} \left(1 + \frac{\eta_{ZR}'' + \eta_\gamma''}{2\eta_{r*}} e^{-2\eta_{rs}t} \right), \quad (3.135)$$

where in the last line we are again dropping exponentially small corrections. This form confirms the physical intuition that long-wavelength thermalization of the DDM is governed by the exponent that is unique to this model and manifestly witnesses the microscopic non-equilibrium nature of this model. We finally note that the effective temperature defined in Eq. (3.74) is not the one that enters the FDT Eq. (3.72) for MAR. The latter can be established by means of the basis transformation Eq. (3.59) which involves the parameter \bar{r} . This parameter, however, is characteristic of MAR and has no counterpart in the DDM.

The near-critical trajectories we consider in this section illustrate the concept of universality in that they show how details of the microscopic model, which determine the initial conditions of the RG flow, are lost as we lower $k \rightarrow 0$, where all of these trajectories converge towards the scaling solution, cf. Fig. 3.1. However, a distinctly non-universal feature of these trajectories is the point where the crossover to the universal regime takes place, which is known as the Ginzburg scale [78–80]. Physically, the Ginzburg scale marks the breakdown of mean-field theory as we approach the

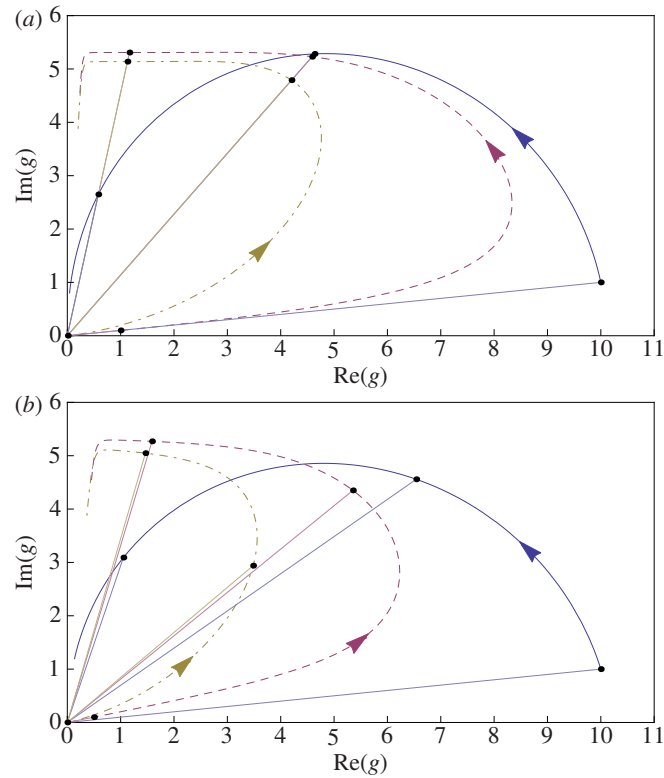


Figure 3.9. (Color online) *Equilibrium vs. non-equilibrium flow: (a) As discussed in Sec. 3.6.4, in thermodynamic equilibrium all couplings lie on a single ray in the complex plane. (b) This geometric constraint is absent out-of-equilibrium. We show $g = 10K, \tilde{u}$, and $10^{-1}\tilde{u}_3$ as solid, dashed, and dot-dashed lines respectively. Stages of the flow at $t = 0, -8$, and -16 are indicated with points on the trajectories. Initial values are (a) $r_\Lambda = 10, w_\Lambda = 0.01281$ and (b) $r_{K\Lambda} = 10, r_{u\Lambda} = 5, r_{u_3\Lambda} = 1, w_\Lambda = 0.01264$. In both cases we have $\tilde{\kappa}_\Lambda = 0.1, \tilde{\kappa}_{3\Lambda} = 0.01$, and $K_\Lambda = 1 + i0.1$.*

fluctuation-dominated critical region. In a perturbative estimate in the symmetric phase, we compare the bare distance from the phase transition κ_1 to the corresponding one-loop correction. Demanding these quantities to be of the same order of magnitude yields [19]

$$\kappa_{1G} = \frac{1}{D_\Lambda^3} \left(\frac{\gamma_\Lambda \kappa_\Lambda}{2C} \right)^2, \quad (3.136)$$

where C is a numerical constant (we find $C = 2\pi$ if we set the bare value κ_{1G} exactly equal to its one-loop correction). Expressing κ_{1G} through a momentum scale as $\kappa_{1G} = D_\Lambda k_G^2$ we find Eq. (3.3), and for the dimensionless RG “time” $t_G = \ln(k_G/\Lambda)$, in terms of the dimensionless two-body loss rate $\tilde{\kappa}$ introduced in Sec. 3.8.1, we have

$$t_G = \ln(\tilde{\kappa}_\Lambda/C). \quad (3.137)$$

Fitting this logarithmic dependence to numerically obtained trajectories in Fig. 3.1, we find $C \approx 14.8$. The Ginzburg scale delimits also the region where the driven-dissipative system obeys a FDT and the ratio $T_{\text{eff}} = \tilde{\gamma}/(4|Z|)$ saturates to a constant value as shown in Fig. 3.2.

3.10 Conclusions

We have studied the nature of Bose criticality in driven open systems. To this end, starting from a description of the microscopic physics in terms of a many-body quantum master equation, we have developed and put into practice a FRG approach based on a Keldysh functional integral reformulation of the quantum master equation for the quantitative determination of the universality class. The absence of both an exact particle number conservation and the detailed balance condition were seen to underly the existence of a new and independent critical exponent governing universal decoherence, while the distribution function shows asymptotic thermalization despite the microscopic driven nature of the system.

This work is just a first step in the exploration of non-equilibrium critical behavior. Key questions for future studies concern the status of critical points in lower dimensionality as, e.g., relevant for current exciton-polariton systems. In particular, in Ref. [66] it has been shown that the thermal fixed point is unstable in two dimensions, and instead is replaced by the non-equilibrium Kardar-Parisi-Zhang [43] fixed point. It is also a key issue to investigate different symmetries beyond the $O(2)$ case. For example, Heisenberg models realized with ensembles of trapped ions may exhibit $O(3)$ symmetry [104]. Furthermore, given the fact that many light-matter systems are pumped coherently as opposed to the incoherent pump considered here, it will be important to understand the impact of the coherent drive on potential criticality in these classes of systems. Finally, it is an intriguing question whether driven open systems which realize non-equilibrium counterparts of quantum criticality can be identified. In the long run, it remains to be seen whether a classification of non-equilibrium criticality with similarly clear structure as familiar from equilibrium dynamical criticality [32] can be reached.

Acknowledgments

We thank J. Berges, I. Boettcher, M. Buchhold, I. Carusotto, T. Gasenzer, S. G. Hofer, A. Imamoglu, J.M. Pawłowski, A. Rosch, U.C. Täuber, A. Tomadin, C. Wetterich, and P. Zoller for stimulating

discussions. This work was supported by the Austrian Science Fund (FWF) through the START Grant No. Y 581-N16, the SFB FoQuS (FWF Project No. F4006- N16) (LMS, SD), and the ISF under Grant No. 1594/11 (EA).

3.A Markovian dissipative action

3.A.1 Translation table: Master equation vs. Keldysh functional integral

Here we specify the relation between second quantized master equation and the equivalent Keldysh functional integral, defined with a markovian dissipative action. In particular, we review how the presence of external driving underlies the validity of the master equation and markovian dissipative action. We start from a master equation governing the time evolution of a system density matrix,

$$\partial_t \hat{\rho} = -i [\hat{H}_s, \hat{\rho}] + \kappa \left(\hat{L} \hat{\rho} \hat{L}^\dagger - \frac{1}{2} \{ \hat{L}^\dagger \hat{L}, \hat{\rho} \} \right). \quad (3.138)$$

Here, \hat{H}_s is a system Hamiltonian generating the unitary evolution and \hat{L} is a Lindblad operator making up the dissipative part of the Liouvillian. For simplicity we consider only a single dissipative channel. The generalization to several channels as in Eq. (3.6), realized through the coupling to several baths, is straightforward. Equation (3.138) results from a more general system-bath setting, $\hat{H}_{\text{tot}} = \hat{H}_s + \hat{H}_b + \hat{H}_{sb}$ (\hat{H}_b and \hat{H}_{sb} are a quadratic bath Hamiltonian with a continuum of frequencies and a system-bath Hamiltonian linear in the bath operators, respectively) under the following three assumptions: (i) the system-bath coupling $\sqrt{\gamma(\omega)}$ is weak compared to a typical scale ω_0 in the system (or, by energy conservation, in the bath) indicating, e.g., the level spacing in an atom (Born approximation $\gamma(\omega)/\omega_0 \ll 1$) (ii) the frequency dependence of the system-bath coupling is negligible over the bandwidth ϑ of the bath centered around ω_0 , implying δ -correlations in the time domain (Markov approximation $\gamma(\omega) \approx \text{const.}$), and (iii) the system is *driven with an external field with frequency ν* to bridge the large energy separation of the levels, $(\nu - \omega_0) / (\nu + \omega_0) \ll 1$. This makes it possible to work in the rotating wave approximation, in which only the detuning $\Delta = \nu - \omega_0$ occurs as a physical scale, while all fast terms involving $\nu + \omega_0$ are dropped. From this consideration, it is clear that the master equation is an accurate description of strongly driven systems coupled to an environment. A typical realization in quantum optics is an atom with two relevant levels separated by ω_0 , connected by an external laser drive with frequency ν , which is detuned from resonance by $\Delta = \nu - \omega_0$. Only the laser drive makes the excited level accessible and gives rise to two-level dynamics such as Rabi oscillations, with frequency determined by the laser intensity. The excited level is unstable and can undergo spontaneous emission by coupling to the radiation field, providing for the reservoir – this mechanism is physically completely independent of the coherent dynamics. Alternatively but fully equivalent to the operator formalism, the above approximations can be performed in a Keldysh path integral setting (see below). In this way, the physics of a given quantum master equation becomes amenable to quantum field theoretical approaches, which is particularly useful for bosonic and fermionic driven-dissipative many-body systems. Here the starting point is the Keldysh partition function

$$\mathcal{Z} = \int \mathcal{D}[a^*, a, b^*, b] e^{-i\sigma_{\text{tot}}[a^*, a, b^*, b]}, \quad (3.139)$$

which results from a ‘‘Trotterization’’ of the Hamiltonian dynamics (after normal ordering) acting on the density matrix in the integrated form of the von Neumann equation in the basis of coherent states;

in this process, the second quantized system and bath field operators, \hat{a}_i (the index i denotes both position and internal indices, such as different particle species) and \hat{b}_μ (μ labels the bath modes and will be chosen a continuous index below) respectively, are mapped to time-dependent complex valued fields in the action

$$\sigma_{\text{tot}} = \sum_{\sigma=\pm} \sigma \int dt \left(\sum_i a_{i,\sigma}^*(t) i \partial_t a_{i,\sigma}(t) + \sum_\mu b_{\mu,\sigma}^*(t) i \partial_t b_{\mu,\sigma}(t) - H_{\text{tot},\sigma}(t) \right), \quad (3.140)$$

where $H_{\text{tot},\sigma}(t)$ is a quasilocal polynomial of these fields. The relative minus sign for the evolution on the forward (+) and backward (-) contours clearly reflects the commutator structure in the von Neumann equation of motion for the system-bath density operator above. We have omitted an imaginary regularization term ensuring convergence of the functional integral [75–77] for simplicity, as it does not affect any of the next steps. Integrating out the harmonic bath variables using approximations (i) – (iii) and considering for the moment Lindblad operators \hat{L} which are linear in the system field operators, we arrive at the following effective Markovian dissipative action:

$$\sigma = \sum_{\sigma} \sigma \int dt \left(\sum_i a_{i,\sigma}^*(t) i \partial_t a_{i,\sigma}(t) - H_{s,\sigma}(t) \right) - i\kappa \left[L_+(t) L_-^*(t) - \frac{1}{2} (L_+^*(t) L_+(t) + L_-^*(t) L_-(t)) \right]. \quad (3.141)$$

While the relative minus sign for the system Hamiltonian H_s on the + and - contours preserve the commutator structure, the dissipative terms clearly reflect the temporally local Lindblad structure of Eq. (3.138). We thus arrive at a simple translation rule for bosonic⁶ master equations into the corresponding Keldysh functional integral: (i) the temporal derivative terms can be read off from the last equation; (ii) for all (normal ordered) operators on the right (left) of the density matrix, introduce a contour index + (-) and write down the Markovian dissipative action. The linear Lindblad operators we consider here are not affected by normal ordering. For the more general case of Lindblad operators that are quasilocal polynomials in the system field operators, operator ordering can be tracked by a suitable temporal regularization procedure as elaborated in the next section.

3.A.2 Derivation in the Keldysh setting

Here we present a derivation of the Markovian dissipative action in the \pm basis for arbitrary (non-linear) Lindblad jump operators, which allows for the most direct comparison with the master equation. In particular, we pay special attention to the question how the operator ordering in the master equation is reflected in the path integral formulation. We leave the system action unspecified, requiring only the property that after proper rotating frame transformation the evolution of the system is much slower than the correlation time of the bath $\tau_c = 1/\vartheta$ (broadband bath). The action of the bath is, in the \pm basis,

$$\sigma_b = \sum_{\mu} \int dt dt' (b_{\mu,+}^*(t), b_{\mu,-}^*(t)) \begin{pmatrix} G_{\mu}^{++}(t, t') & G_{\mu}^{+-}(t, t') \\ G_{\mu}^{-+}(t, t') & G_{\mu}^{--}(t, t') \end{pmatrix}^{-1} \begin{pmatrix} b_{\mu,+}(t') \\ b_{\mu,-}(t') \end{pmatrix}. \quad (3.142)$$

⁶For fermions, additional signs arise due to the Grassmann nature of the fermion field, but a similar translation table exists.

The Green's functions for the oscillators of the bath are assumed to be in thermal equilibrium and read

$$\begin{aligned}
G_{\mu}^{+-}(t, t') &= -i\bar{n}(\omega_{\mu})e^{-i\omega_{\mu}(t-t')}, \\
G_{\mu}^{-+}(t, t') &= -i(\bar{n}(\omega_{\mu}) + 1)e^{-i\omega_{\mu}(t-t')}, \\
G_{\mu}^{++}(t, t') &= \theta(t-t')G_{\mu}^{-+}(t, t') + \theta(t'-t)G_{\mu}^{+-}(t, t'), \\
G_{\mu}^{--}(t, t') &= \theta(t'-t)G_{\mu}^{-+}(t, t') + \theta(t-t')G_{\mu}^{+-}(t, t').
\end{aligned} \tag{3.143}$$

The linear coupling between system and the bath is (note that the case of several dissipative channels and local baths as in Eq. (3.6) can be implemented by adding appropriate indices to the L_{σ} and $b_{\mu,\sigma}$ and summing over these indices)

$$\sigma_{sb} = \sum_{\mu} \sqrt{\gamma_{\mu}} \int dt \left(L_{+}^{*}(t)b_{\mu,+}(t) + L_{+}(t)b_{\mu,+}^{*}(t) - L_{-}^{*}(t)b_{\mu,-}(t) - L_{-}(t)b_{\mu,-}^{*}(t) \right), \tag{3.144}$$

where L_{\pm} correspond to the quantum jump operators which are typically quasilocal polynomials of the system's creation and annihilation operators. To be consistent with the derivation of the path integral, we require the jump operators to have been normal ordered before the Trotter decomposition giving rise to the path integral. The partition function is of the general form

$$\mathcal{Z} = \int \mathcal{D}[a^{*}, a, b^{*}, b] e^{i(\sigma_s[a^{*}, a] + \sigma_b[b^{*}, b] + \sigma_{sb}[a^{*}, a, b^{*}, b])}, \tag{3.145}$$

Now we integrate out the bath via completion of the square which results in an effective action σ_{eff} for the system degrees of freedom. The contribution $\sigma_{\text{eff},\mu}$ of the μ th mode to the effective action reads

$$\sigma_{\text{eff},\mu} = \gamma_{\mu} \int dt dt' \left(L_{+}^{*}(t), -L_{-}^{*}(t) \right) \begin{pmatrix} G_{\mu}^{++}(t, t') & G_{\mu}^{+-}(t, t') \\ G_{\mu}^{-+}(t, t') & G_{\mu}^{--}(t, t') \end{pmatrix} \begin{pmatrix} L_{+}(t') \\ -L_{-}(t') \end{pmatrix}. \tag{3.146}$$

The signs for the operators on the $-$ contour comes from the backward integration in time. Thus the mixed terms will occur with an overall $-$ sign, while the $++$ and $--$ terms come with an overall $+$. Summing over all the modes μ we obtain the effective action for the field variables of the subsystem due to the coupling to the bath. We now take the continuum limit of densely lying bath modes, centered around some central frequency ω_0 and with bandwidth ϑ . That is, we substitute the sum over the modes with an integral in the energy Ω weighted by a (phenomenologically introduced) density of states $\nu(\Omega)$ of the bath $\sum_{\mu} \gamma_{\mu} \simeq \int_0^{\infty} d\Omega \gamma(\Omega) \nu(\Omega)$, and obtain

$$\sigma_{\text{eff}} = - \int_{\omega_0 - \vartheta}^{\omega_0 + \vartheta} d\Omega \gamma(\Omega) \nu(\Omega) \int dt d\tau \left(L_{+}^{*}(t), -L_{-}^{*}(t) \right) \begin{pmatrix} G_{\Omega}^{++}(\tau) & G_{\Omega}^{+-}(\tau) \\ G_{\Omega}^{-+}(\tau) & G_{\Omega}^{--}(\tau) \end{pmatrix} \begin{pmatrix} L_{+}(t - \tau) \\ -L_{-}(t - \tau) \end{pmatrix}, \tag{3.147}$$

where in addition we have used the translation invariance of the bath Green's function, $G_{\Omega}^{\alpha\beta}(t, t') = G_{\Omega}^{\alpha\beta}(t - t')$ to suitably shift the integration variables. We consider the various terms separately. In doing the Markov approximation, we use (a) that by assumption it is possible to choose a rotating frame in which the evolution of the system is slow compared to the scales in the bath, $\omega_{\text{sys}} \ll \omega_0, \vartheta$. In this case, a zeroth order temporal derivative approximation for the jump operators is appropriate. This gives rise to a *temporally local* form of the markovian dissipative action. However, for the evaluation of tadpole diagrams for this action, ambiguities due to a temporally local vertex arises. In these diagrams – and only in these – it is then important to specify the proper regularization of the

system's Green's function at equal time arguments. To keep track of this, we indicate the sign of the next time step in the approximated jump operators by $t_{\pm\delta} = t \pm \delta t$. In step (b) below, we assume that the density of states and the coupling of the system to bath are well approximated as constant over the relevant reservoir width,

$$\begin{aligned}
& - \int dt L_+^*(t) \int d\tau \int_{\omega_0 - \vartheta}^{\omega_0 + \vartheta} \frac{d\Omega}{2\pi} \gamma(\Omega) \nu(\Omega) G_{\Omega}^{+-}(\tau) L_-(t - \tau) \\
& = i \int dt L_+^*(t) \int d\tau \int_{\omega_0 - \vartheta}^{\omega_0 + \vartheta} \frac{d\Omega}{2\pi} \gamma(\Omega) \nu(\Omega) \bar{n}(\Omega) e^{-i\Omega\tau} L_-(t - \tau) \\
& \stackrel{(a)}{\approx} i \int dt L_+^*(t) \int d\tau \int_{\omega_0 - \vartheta}^{\omega_0 + \vartheta} \frac{d\Omega}{2\pi} \gamma(\Omega) \nu(\Omega) \bar{n}(\Omega) e^{-i\Omega\tau} L_-(t - \delta) \\
& \stackrel{(b)}{\approx} i \int dt L_+^*(t) \gamma \nu \int d\tau \int_{\omega_0 - \vartheta}^{\omega_0 + \vartheta} \frac{d\Omega}{2\pi} \bar{n}(\Omega) e^{-i\Omega\tau} L_-(t - \delta) \quad (3.148) \\
& \approx i \int dt L_+^*(t) \gamma \nu \int_{-\infty}^{\infty} d\Omega \bar{n}(\Omega) \delta(\Omega - \omega_0) L_-(t - \delta) \\
& = i \kappa \bar{n} \int dt L_+^*(t) L_-(t - \delta),
\end{aligned}$$

where we have shifted the frequency integration domain by $-\omega_0$ and taken the limit $\vartheta \rightarrow \infty$, as well as $\kappa = \gamma\nu$ and $\bar{n} = \bar{n}(\omega_0)$. Further note the relation to the operator formalism $\int_{-\infty}^{\infty} \frac{d\Omega}{2\pi} \bar{n}(\Omega) e^{-i\Omega\tau} = \langle \hat{b}^\dagger(\tau) \hat{b}(0) \rangle$. Similarly,

$$- \int dt L_-^*(t) \int d\tau \int_{\omega_0 - \vartheta}^{\omega_0 + \vartheta} \frac{d\Omega}{2\pi} \gamma(\Omega) \nu(\Omega) G_{\Omega}^{-+}(\tau) L_+(t - \tau) \approx i \kappa (\bar{n} + 1) \int dt L_-^*(t) L_+(t - \delta) \quad (3.149)$$

and $\int_{-\infty}^{\infty} \frac{d\Omega}{2\pi} (\bar{n}(\Omega) + 1) e^{-i\Omega\tau} = \langle \hat{b}(\tau) \hat{b}^\dagger(0) \rangle$. For the terms on the forward contour, we obtain

$$\begin{aligned}
& \int dt L_+^*(t) \int d\tau \int_{\omega_0 - \vartheta}^{\omega_0 + \vartheta} \frac{d\Omega}{2\pi} \gamma(\Omega) \nu(\Omega) G_{\Omega}^{++}(\tau) L_+(t - \tau) \\
& = -i \int dt L_+^*(t) \int d\tau \int_{\omega_0 - \vartheta}^{\omega_0 + \vartheta} \frac{d\Omega}{2\pi} \gamma(\Omega) \nu(\Omega) [\theta(\tau) (\bar{n}(\Omega) + 1) + \theta(-\tau) \bar{n}(\Omega)] e^{-i\Omega\tau} L_+(t - \tau) \\
& \stackrel{(a)}{\approx} -i \int dt L_+^*(t) \int d\tau \int_{\omega_0 - \vartheta}^{\omega_0 + \vartheta} \frac{d\Omega}{2\pi} \gamma(\Omega) \nu(\Omega) [\theta(\tau) (\bar{n}(\Omega) + 1) + \theta(-\tau) \bar{n}(\Omega)] e^{-i\Omega\tau} L_+(t - \delta) \\
& \stackrel{(b)}{\approx} -i \int dt L_+^*(t) \gamma \nu \left[\int d\tau \theta(\tau) \int_{\omega_0 - \vartheta}^{\omega_0 + \vartheta} \frac{d\Omega}{2\pi} (\bar{n}(\Omega) + 1) e^{-i\Omega\tau} + \int d\tau \theta(-\tau) \int_{\omega_0 - \vartheta}^{\omega_0 + \vartheta} \frac{d\Omega}{2\pi} \bar{n}(\Omega) e^{-i\Omega\tau} \right] L_+(t - \delta) \\
& \approx -i \int dt \left\{ \left[\frac{1}{2} \kappa (\bar{n} + 1) - i\delta E_1 \right] L_+^*(t) L_+(t - \delta) + \left(\frac{1}{2} \kappa \bar{n} + i\delta E_2 \right) L_+^*(t) L_+(t + \delta) \right\}. \quad (3.150)
\end{aligned}$$

In the last line we have used

$$\begin{aligned}
\int d\tau \theta(\tau) \int_{\omega_0-\vartheta}^{\omega_0+\vartheta} \frac{d\Omega}{2\pi} (\bar{n}(\Omega) + 1) e^{-i\Omega\tau} L_+(t-\delta) \\
\approx \int_{-\infty}^{\infty} \frac{d\Omega}{2\pi} (\bar{n}(\Omega) + 1) \left(\pi\delta(\Omega - \omega_0) - i\mathcal{P} \frac{1}{\Omega - \omega_0} \right) L_+(t-\delta) \\
= \left[\frac{1}{2}\kappa(\bar{n} + 1) - i\delta E_1 \right] L_+(t-\delta)
\end{aligned} \tag{3.151}$$

and

$$\begin{aligned}
\int d\tau \theta(-\tau) \int_{\omega_0-\vartheta}^{\omega_0+\vartheta} \frac{d\Omega}{2\pi} \bar{n}(\Omega) e^{-i\Omega\tau} L_+(t-\delta) \\
= \int d\tau \theta(\tau) \int_{\omega_0-\vartheta}^{\omega_0+\vartheta} \frac{d\Omega}{2\pi} \bar{n}(\Omega) e^{+i\Omega\tau} L_+(t+\delta) \\
\approx \int_{-\infty}^{\infty} \frac{d\Omega}{2\pi} \bar{n}(\Omega) \left(\pi\delta(\Omega - \omega_0) - i\mathcal{P} \frac{1}{\Omega - \omega_0} \right) L_+(t+\delta) \\
= \left(\frac{1}{2}\kappa\bar{n} + i\delta E_2 \right) L_+(t+\delta).
\end{aligned} \tag{3.152}$$

Importantly, note the sign change in the regularization of the time argument upon reversal of integration direction. This gives a hint which operator “comes first” in the coarse grained evolution where the bath has been integrated out, and reflects the fact that in the corresponding master equation, the “cooling” dissipation terms $\sim (\bar{n} + 1)$ are normal ordered in the jump operators ($\sim \hat{L}^\dagger \hat{L}$), while the “heating” terms $\sim \bar{n}$ are anti-normal ordered ($\sim \hat{L} \hat{L}^\dagger$). Similarly, we obtain on the backward contour,

$$\begin{aligned}
\int dt L_-^*(t) \int d\tau \int_{\omega_0-\vartheta}^{\omega_0+\vartheta} \frac{d\Omega}{2\pi} \gamma(\Omega) \nu(\Omega) G_\Omega^{--}(\tau) L_-(t-\tau) \\
\approx -i \int dt \left\{ \left[\frac{1}{2}\kappa(\bar{n} + 1) + i\delta E_1 \right] L_-^*(t) L_-(t+\delta) + \left[\frac{1}{2}\kappa\bar{n} - i\delta E_2 \right] L_-^*(t) L_-(t-\delta) \right\},
\end{aligned} \tag{3.153}$$

where the changes in the signs relative to the forward term emerge from the reverse signs in the θ -functions. In summary, we obtain the following dissipative contribution to the action:

$$\begin{aligned}
\sigma_d = -ik \int dt \left\{ (\bar{n} + 1) \left[L_-^*(t) L_+(t-\delta) - \frac{1}{2} (L_+^*(t) L_+(t-\delta) + L_-^*(t) L_-(t+\delta)) \right] \right. \\
\left. + \bar{n} \left[L_+^*(t) L_-(t-\delta) - \frac{1}{2} (L_+^*(t) L_+(t+\delta) + L_-^*(t) L_-(t-\delta)) \right] \right\}.
\end{aligned} \tag{3.154}$$

In addition, there is a “Lamb shift” which reads

$$\sigma_L = - \int dt \left[\delta E_1 (-L_+^*(t) L_+(t-\delta) + L_-^*(t) L_-(t+\delta)) + \delta E_2 (L_+^*(t) L_+(t+\delta) - L_-^*(t) L_-(t-\delta)) \right]. \tag{3.155}$$

This gives a contribution to the coherent dynamics which has the same physical origin as the dissipative dynamics. However, typically there is a dominant independent Hamiltonian contribution, such that the effective Hamiltonian parameters after the Lamb shift renormalization are properly regarded as independent of the Liouvillian ones.

3.B Symmetry constraints on the action and truncation for MAR

In this section we derive the action Eq. (3.61) and the truncation Eq. (3.64) for MAR. Our starting point is the truncation Eq. (3.43) appropriate for the driven-dissipative model on which we impose invariance under the equilibrium symmetry transformation Eq. (3.60). This leads to Eq. (3.64) which reduces to the action Eq. (3.61) when we set $k = k_{\text{cg}}$.

In terms of the bare spinors $\bar{\Phi}_\nu$ the truncation for the DDM can be written as

$$\Gamma_k = \int_X \bar{\Phi}_q^\dagger \left[(Z_R \sigma_z - i Z_I \mathbb{1}) i \partial_t \bar{\Phi}_c - \frac{\delta \bar{\mathcal{U}}_H}{\delta \bar{\Phi}_c^*} + i \sigma_z \frac{\delta \bar{\mathcal{U}}_D}{\delta \bar{\Phi}_c^*} + i \frac{\bar{\gamma}}{2} \bar{\Phi}_q \right]. \quad (3.156)$$

We perform the change of basis Eq. (3.59) and obtain for the contributions in the sum $\Gamma_k = \Gamma_{\text{dyn},k} + \Gamma_{H,k} + \Gamma_{D,k} + \Gamma_{\text{reg},k}$ the expressions

$$\Gamma_{\text{dyn},k} = i \frac{\bar{r} Z_R + Z_I}{Z_{R,\text{cg}} - \bar{r} Z_{I,\text{cg}}} \int_X \tilde{\Phi}_q^\dagger \sigma_z \partial_t \tilde{\Phi}_c, \quad (3.157)$$

$$\Gamma_{H,k} = \frac{i}{Z_{R,\text{cg}} - \bar{r} Z_{I,\text{cg}}} \int_X \tilde{\Phi}_q^\dagger \sigma_z \left(\bar{r} \frac{\delta \bar{\mathcal{U}}_D}{\delta \tilde{\Phi}_c^*} - \frac{\delta \bar{\mathcal{U}}_H}{\delta \tilde{\Phi}_c^*} \right), \quad (3.158)$$

$$\Gamma_{D,k} = -\frac{1}{Z_{R,\text{cg}} - \bar{r} Z_{I,\text{cg}}} \int_X \tilde{\Phi}_q^\dagger \left(\frac{\delta \bar{\mathcal{U}}_D}{\delta \tilde{\Phi}_c^*} + \bar{r} \frac{\delta \bar{\mathcal{U}}_H}{\delta \tilde{\Phi}_c^*} \right), \quad (3.159)$$

and

$$\Gamma_{\text{reg},k} = \frac{i}{Z_{R,\text{cg}} - \bar{r} Z_{I,\text{cg}}} \int_X \tilde{\Phi}_q^\dagger \left((Z_R - \bar{r} Z_I) i \partial_t \tilde{\Phi}_c + \frac{1 + \bar{r}^2}{Z_{R,\text{cg}} - \bar{r} Z_{I,\text{cg}}} \frac{\bar{\gamma}}{2} \tilde{\Phi}_q \right). \quad (3.160)$$

Both $\Gamma_{\text{dyn},k}$ and $\Gamma_{D,k}$ are symmetric under the transformation Eq. (3.60). Demanding the remaining contributions $\Gamma_{H,k}$ and $\Gamma_{\text{reg},k}$ to be invariant we find that a term of the form of Eq. (3.158) is actually forbidden by the symmetry, i.e., we must have $\Gamma_{H,k} = 0$, which is satisfied for $\bar{\mathcal{U}}_H = \bar{r} \bar{\mathcal{U}}_D$. For the regularization term $\Gamma_{\text{reg},k}$ we obtain the additional constraint Eq. (3.65). All these requirements are implemented in the truncation Eq. (3.64) which is easily seen to reduce to Eq. (3.61) for $k = k_{\text{cg}}$.

If in addition to the equilibrium symmetry we demand invariance under complex conjugation of the fields Eq. (3.63) as is the case for MA, we find the condition $\Gamma_{\text{dyn},k} = 0$. This is met for all $0 < k < k_{\text{cg}}$ if $\bar{r} = -Z_I/Z_R$.

3.C Non-Equilibrium FRG flow equations

Here we present details of the derivation of the non-equilibrium FRG flow equations in Sec. 3.7. To start with, we rewrite the flow equation (3.42) such that only renormalized quantities appear on the RHS,

$$\partial_t \Gamma_k = \frac{i}{2} \text{Tr} \left[\left(\Gamma_k^{(2)} + R_k \right)^{-1} \tilde{\partial}_t R_k \right]. \quad (3.161)$$

The second functional derivatives appearing under the trace on the RHS are taken with respect to renormalized real fields Eq. (3.50). These can be written in terms of the bare ones as $\chi(Q) = z \bar{\chi}(Q)$, where the matrix z is given by

$$z = \mathbb{1} \oplus \begin{pmatrix} Z_R & -Z_I \\ Z_I & Z_R \end{pmatrix}. \quad (3.162)$$

The linear transformation from bare to renormalized fields implies for functional derivatives the relations

$$\Gamma_k^{(2)} = z^T \Gamma_k^{(2)} z, \quad \bar{R}_k = z^T R_k z, \quad (3.163)$$

and inserting these in the flow equation (3.42) yields Eq. (3.161) if in addition we replace the derivative with respect to t by the differential operator $\tilde{\partial}_t$ which is defined as

$$\tilde{\partial}_t \equiv \partial_t R_{k,\bar{k}} \partial_{R_{k,\bar{k}}} + \partial_t R_{k,\bar{k}}^* \partial_{R_{k,\bar{k}}^*}. \quad (3.164)$$

With this definition we may write $\partial_t \bar{R}_k = \tilde{\partial}_t \bar{R}_k$, which has the advantage that $\tilde{\partial}_t$ commutes with the multiplicative renormalization with Z (note that also Z is a running coupling and depends on t), i.e., we have

$$\tilde{\partial}_t \bar{R}_k = \tilde{\partial}_t (z^T R_k z) = z^T (\tilde{\partial}_t R_k) z. \quad (3.165)$$

Furthermore, since $\tilde{\partial}_t$ acts only on the cutoff and not the inverse propagator $\Gamma_k^{(2)}$, we may rewrite the exact flow equation (3.161) in the simple form

$$\partial_t \Gamma_k = \frac{i}{2} \text{Tr} \tilde{\partial}_t \ln (\Gamma_k^{(2)} + R_k). \quad (3.166)$$

3.C.1 Expansion in fluctuations

According to its definition in Sec. 3.3.3, the effective action is a functional of the field expectation values, and also the flow equation (3.166) can be evaluated for arbitrary field configurations. A particularly useful form of the flow equation can be obtained by decomposing the fields into homogeneous and frequency- and momentum-dependent fluctuation parts as $\chi(Q) = \chi\delta(Q) + \delta\chi(Q)$ and expanding the logarithm on the RHS of Eq. (3.166) to second order in the fluctuations $\delta\chi(Q)$. Then, the zeroth order term determines the flow of the momentum-independent couplings whereas the β -functions for the wave-function renormalization and the gradient coefficient can be obtained from the second order contribution.

We begin by deriving an explicit expression for the full inverse propagator $\Gamma_k^{(2)}$ up to second order in $\delta\chi$. To this end we rewrite the effective action Eq. (3.45) in the form

$$\Gamma_k = \frac{1}{2} \int_Q \chi(-Q)^T D(Q) \chi(Q) - \int_X V, \quad (3.167)$$

where $\int_Q = \int \frac{d\omega d^d \mathbf{q}}{(2\pi)^{d+1}}$. The frequency- and momentum-dependent part of the inverse propagator Eq. (3.49) is denoted by $D(Q) = P(Q) - P(0)$, and the effective potential V that contains all momentum-independent couplings is given by

$$V = U' \rho_{cq} + U'^* \rho_{qc} - i\gamma \rho_q. \quad (3.168)$$

The second functional derivative of the effective action can then be expressed as the sum of two contributions,

$$\Gamma_k^{(2)}(Q, Q') = D(Q) \delta(Q - Q') - \mathcal{V}^{(2)}(Q, Q'), \quad (3.169)$$

where the second term is just the functional derivative of the effective potential,

$$\mathcal{V}_{ij}^{(2)}(Q, Q') = \frac{\delta^2}{\delta\chi_i(-Q)\delta\chi_j(Q')} \int_X V = \int_X e^{i(Q-Q')X} V_{ij}^{(2)}, \quad (3.170)$$

which can be reduced to ordinary (i.e., not functional) partial derivatives with respect to the fields in the time domain and real space,

$$V_{ij}^{(2)} = \frac{\partial^2}{\partial\chi_i\partial\chi_j} V. \quad (3.171)$$

Setting the fluctuation components of the fields to zero in Eq. (3.169) we obtain the inverse propagator in the presence of homogeneous classical and quantum background fields,

$$P_{cq}(Q)\delta(Q-Q') = \Gamma_k^{(2)}(Q, Q')\big|_{\delta\chi=0} = (D(Q) - V_{cq}^{(2)})\delta(Q-Q'). \quad (3.172)$$

Note that the difference between $P_{cq}(Q)$ and the inverse propagator Eq. (3.49) is that in the latter the background fields are set to their stationary values while in the former they remain unspecified. The background fields are all contained in the second contribution $V_{cq}^{(2)}$ which we split into 2×2 blocks according to

$$V_{cq}^{(2)} = \begin{pmatrix} V_{cq}^{(2)H} & V_c^{(2)A} \\ V_c^{(2)R} & V_c^{(2)K} \end{pmatrix}. \quad (3.173)$$

While the upper left block $V_{cq}^{(2)H}$ is linear in the quantum fields (and, therefore, vanishes when we set these to zero, giving rise to the causality structure of the inverse propagator Eq. (3.49)),

$$\begin{aligned} V_{cq,11}^{(2)H} &= [(\rho_{cq} + \rho_{qc})U_H^{(3)} + i(\rho_{cq} - \rho_{qc})U_D^{(3)}]\chi_{c,1}^2 + (\rho_{cq} + \rho_{qc} + 2\chi_{c,1}\chi_{q,1})U_H'' \\ &\quad + i(\rho_{cq} - \rho_{qc} + i2\chi_{c,1}\chi_{q,2})U_D'', \\ V_{cq,12}^{(2)H} &= V_{cq,21}^{(2)H} = (\chi_{c,2}\chi_{q,1} + \chi_{c,1}\chi_{q,2})U_H'' + (\chi_{c,1}\chi_{q,1} - \chi_{c,2}\chi_{q,2})U_D'' \\ &\quad + \chi_{c,1}\chi_{c,2}[(\rho_{cq} + \rho_{qc})U_H^{(3)} + i(\rho_{cq} - \rho_{qc})U_D^{(3)}], \\ V_{cq,22}^{(2)H} &= [(\rho_{cq} + \rho_{qc})U_H^{(3)} + i(\rho_{cq} - \rho_{qc})U_D^{(3)}]\chi_{c,2}^2 + (\rho_{cq} + \rho_{qc} + 2\chi_{c,2}\chi_{q,2})U_H'' \\ &\quad + i(\rho_{cq} - \rho_{qc} - i2\chi_{c,2}\chi_{q,1})U_D'', \end{aligned} \quad (3.174)$$

the retarded and advanced components only contain classical background fields (hence we omit the index q),

$$V_c^{(2)R} = \begin{pmatrix} U_H' + \chi_{c,1}(\chi_{c,2}U_D'' + \chi_{c,1}U_H'') & U_D' + \chi_{c,2}(\chi_{c,2}U_D'' + \chi_{c,1}U_H'') \\ \chi_{c,1}(\chi_{c,2}U_H'' - \chi_{c,1}U_D'') - U_D' & U_H' + \chi_{c,2}(\chi_{c,2}U_H'' - \chi_{c,1}U_D'') \end{pmatrix}, \quad V_c^{(2)A} = (V_c^{(2)R})^\dagger, \quad (3.175)$$

and the Keldysh component is field-independent and given by $V_c^{(2)K} = -i\gamma\mathbb{1}$. In Eq. (3.166), the inverse propagator is supplemented by the cutoff to yield the regularized propagator

$$P_{k,cq}(Q) = P_{cq}(Q) + R_k(q^2), \quad (3.176)$$

which determines the zeroth order contribution in the fluctuation expansion of the flow equation.

We proceed by expanding the inverse propagator Eq. (3.169) to second order in the fluctuations $\delta\chi$. With Eq. (3.172) we may write

$$\Gamma_k^{(2)}(Q, Q') = P_{cq}(Q)\delta(Q-Q') + \mathcal{F}(Q, Q') + O(\delta\chi^3), \quad (3.177)$$

where the matrix \mathcal{F} is given by the sum $\mathcal{F} = \mathcal{F}_1 + \mathcal{F}_2$ with $\mathcal{F}_{1,2}$ being of first and second order in $\delta\chi$. The explicit dependence of these matrices on the fluctuations reads

$$\mathcal{F}_1(Q, Q') = - \sum_i V_i^{(3)} \delta\chi_i(Q - Q'), \quad (3.178)$$

$$\mathcal{F}_2(Q, Q') = - \frac{1}{2} \sum_{ij} V_{ij}^{(4)} \int_P \delta\chi_i(-P) \delta\chi_j(P + Q - Q'). \quad (3.179)$$

Here, for given values of i and j the quantities $V_i^{(3)}$ and $V_{ij}^{(4)}$ are 4×4 matrices defined as the partial derivatives of $V^{(2)}$,

$$V_i^{(3)} = \frac{\partial V^{(2)}}{\partial \chi_i}, \quad V_{ij}^{(4)} = \frac{\partial V^{(2)}}{\partial \chi_i \partial \chi_j}. \quad (3.180)$$

Inserting the decomposition Eq. (3.177) in Eq. (3.166) and expanding the logarithm in the fluctuations $\delta\chi$ yields

$$\partial_t \Gamma_k = \frac{i}{2} \left[\text{Tr} \tilde{\partial}_t \ln P_{k,cq} - \frac{1}{2} \tilde{\partial}_t \text{Tr} (G_{k,cq} \mathcal{F}_1)^2 \right], \quad (3.181)$$

where $G_{k,cq}(Q) = P_{k,cq}(Q)^{-1}$ is the propagator in the presence of classical and quantum background fields. Note that the appearance of $G_{k,cq}^2$ makes the trace in the last term UV-convergent and thereby allowed us to commute $\tilde{\partial}_t$ with Tr. In the expansion Eq. (3.181) we are keeping only terms of zeroth and second order, as these determine, respectively, the flow of the effective potential and the frequency- and momentum-dependent contributions to the inverse propagator. We also omit a term $\tilde{\partial}_t \text{Tr} G_{k,cq} \mathcal{F}_2$ which in our truncation with momentum-independent vertices does not contribute to the flow of Z and \bar{K} .

3.C.2 Flow equation for the effective potential

Equation (3.181) reduces to the flow equation for the effective potential if we set the fluctuations $\delta\chi$ to zero. Then the second term on the RHS vanishes and we have

$$\frac{1}{\Omega} \partial_t \Gamma_{k,cq} = \frac{i}{2} \int_Q \tilde{\partial}_t \ln \det_{cq}(\omega, q^2) \quad (3.182)$$

where $\det_{cq}(\omega, q^2) = \det P_{k,cq}(Q)$ denotes the determinant of the regularized inverse propagator Eq. (3.176) in the presence of classical and quantum background fields. Since our model is symmetric under simultaneous phase rotations $\phi_\nu \rightarrow e^{i\alpha} \phi_\nu$ of the classical and quantum fields, the determinant $\det_{cq}(\omega, q^2)$ can be expressed as a function of the $U(1)$ -invariant field combinations $\rho_c, \rho_{cq}, \rho_{qc}$, and ρ_q . It can not be written as a function of these invariants without ambiguity though, as can be seen by noting that the product of four fields $\phi_c^* \phi_q^* \phi_c \phi_q$ equals both $\rho_c \rho_q$ and $\rho_{cq} \rho_{qc}$. However, the form of the field-dependent contribution Eq. (3.173) to the inverse propagator implies that $\det_{cq}(\omega, q^2)$ contains terms that are at most quadratic in the quantum fields and that there is no contribution that contains $\phi_q^* \phi_q$ but no classical fields. All contributions containing quantum *and* classical fields can be expressed in powers of ρ_c, ρ_{cq} , and ρ_{qc} . Therefore, in the following we will consider $\det_{cq}(\omega, q^2)$ to be a function of this reduced set of invariants. Then, inserting Eq. (3.182) in the definition of ζ' in Eq. (3.81) we find

$$\zeta' = - \frac{i}{2} \int_Q \tilde{\partial}_t \left\{ \frac{1}{\det_c(\omega, q^2)} \left[\partial_{\rho_{cq}} \det_{cq}(\omega, q^2) \right]_{\rho_{cq}=\rho_{qc}=0} \right\}, \quad (3.183)$$

where $\det_c(\omega, q^2) = \det P_{k,c}(Q)$ is the determinant of the regularized propagator with only classical background fields,

$$P_{k,c}(Q) = P_{k,cq}(Q)|_{\phi_q = \phi_q^* = 0}, \quad (3.184)$$

which differs from $P_{k,cq}(Q)$ only in the block $V_{cq}^{(2)H}$ (note that the other blocks in Eq. (3.173) do not contain quantum fields) which vanishes for $\phi_q = \phi_q^* = 0$. Accordingly the inverse propagator $P_{k,c}(Q)$ acquires the causality structure Eq. (3.51) which implies that the determinant $\det_c(\omega, q^2)$ factorizes into retarded and advanced contributions,

$$\det_c(\omega, q^2) = \det_c^R(\omega, q^2) \det_c^A(\omega, q^2). \quad (3.185)$$

These are simply related by a change of the sign of the frequency variable, $\det_c^R(\omega, q^2) = \det_c^A(-\omega, q^2)$. Inserting Eq. (3.185) in Eq. (3.183) we can rewrite the latter as

$$\zeta' = 2v_d \int_0^\infty dx x^{d/2-1} \tilde{\partial}_t \zeta'(x), \quad (3.186)$$

where $v_d = (2^{d+1} \pi^{d/2} \Gamma(d/2))^{-1}$ and we introduced a new integration variable $x = q^2$; the function appearing in the integrand is given by the integral over frequencies

$$\zeta'(q^2) = -\frac{i}{4\pi} \int_{-\infty}^\infty d\omega \frac{[\partial_{\rho_{cq}} \det_{cq}(\omega, q^2)]_{\rho_{cq} = \rho_{qc} = 0}}{\det_c^A(\omega, q^2) \det_c^A(-\omega, q^2)}, \quad (3.187)$$

which can be performed with the aid of Ref. [105], p. 308, 18. (where a factor of $(-1)^{n+1}$ is missing [106]). We omit the rather lengthy result.

Let us proceed by specifying the action of $\tilde{\partial}_t$ in Eq. (3.186). The function $\zeta'(x)$ depends on the cutoff via its dependence on $p_a(x)$ for which we have $\tilde{\partial}_t p_a(x) = -\tilde{\partial}_t R_{k,a}(x)$, see Eq. (3.58), and thus

$$\tilde{\partial}_t \zeta'(x) = - \sum_{a=A,D} \tilde{\partial}_t R_{k,a}(x) \partial_{p_a(x)} \zeta'(x). \quad (3.188)$$

Recalling the definition Eq. (3.164) of the differential operator $\tilde{\partial}_t$ according to which it effectively acts as a scale derivative of the bare cutoff, we find

$$\begin{aligned} \tilde{\partial}_t R_{k,A}(x) &= \text{Re} \left(\partial_t R_{k,\bar{K}}(x) / Z \right), \\ \tilde{\partial}_t R_{k,D}(x) &= \text{Im} \left(\partial_t R_{k,\bar{K}}(x) / Z \right). \end{aligned} \quad (3.189)$$

Inserting here the expression

$$\partial_t R_{k,\bar{K}}(x) = - \left[(2\bar{K} + \partial_t \bar{K}) k^2 - \partial_t \bar{K} x \right] \theta(k^2 - x), \quad (3.190)$$

we end up with

$$\tilde{\partial}_t R_{k,a}(x) = - \left[(2 - \bar{\eta}_a) k^2 + \bar{\eta}_a x \right] a \theta(k^2 - x), \quad (3.191)$$

where we defined

$$\bar{\eta}_A = -\frac{1}{A} \text{Re} \left(\partial_t \bar{K} / Z \right), \quad \bar{\eta}_D = -\frac{1}{D} \text{Im} \left(\partial_t \bar{K} / Z \right). \quad (3.192)$$

Plugging these results in Eq. (3.186) and using that the θ -function restricts the range of integration over x to the interval $[0, k^2]$, where $p_a(x) = ak^2$ (cf. Eq. (3.58)) and therefore $\zeta'(x) = \zeta'(k^2)$ does not depend on x , we get

$$\zeta' = \frac{8v_d k^{d+2}}{d} \sum_a \left(1 - \frac{\bar{\eta}_a}{d+2}\right) a \left[\partial_{p_a(x)} \zeta'(x) \right]_{p_A(x)=Ak^2, p_D(x)=Dk^2}. \quad (3.193)$$

The further evaluation of this expression is most conveniently performed on the computer using MATHEMATICA.

In Sec. 3.7 we specified prescriptions that allow us to obtain flow equations for the complex two- and three-body couplings from the flow equation for the effective potential, cf. Eqs. (3.83) and (3.84). When we switch to MATHEMATICA for an explicit evaluation of the flow equations, however, it is more convenient to work with real couplings. The flow equations for the quartic and sextic couplings are then given by

$$\begin{aligned} \partial_t \lambda &= \beta_\lambda = \eta_{ZR} \lambda - \eta_{ZI} \kappa + \lambda_3 \partial_t \rho_0 + \partial_{\rho_c} \zeta'_H \Big|_{\text{ss}}, \\ \partial_t \kappa &= \beta_\kappa = \eta_{ZR} \kappa + \eta_{ZI} \lambda + \kappa_3 \partial_t \rho_0 + \partial_{\rho_c} \zeta'_D \Big|_{\text{ss}}, \\ \partial_t \lambda_3 &= \beta_{\lambda_3} = \eta_{ZR} \lambda_3 - \eta_{ZI} \kappa_3 + \partial_{\rho_c}^2 \zeta'_H \Big|_{\text{ss}}, \\ \partial_t \kappa_3 &= \beta_{\kappa_3} = \eta_{ZR} \kappa_3 + \eta_{ZI} \lambda_3 + \partial_{\rho_c}^2 \zeta'_D \Big|_{\text{ss}}, \end{aligned} \quad (3.194)$$

where we decompose $\zeta' = \zeta'_H + i\zeta'_D$ and $\eta_Z = \eta_{ZR} + i\eta_{ZI}$ into real and imaginary parts. For completeness we also state the flow equation of ρ_0 in terms of these quantities:

$$\partial_t \rho_0 = \beta_{\rho_0} = -\zeta'_D \Big|_{\text{ss}} / \kappa. \quad (3.195)$$

To conclude this section let us specify the flow equation for γ . Similar to Eq. (3.186) we can express the quantity ζ_γ defined in Eq. (3.87) as

$$\zeta_\gamma = 2v_d \int_0^\infty dx x^{d/2-1} \tilde{\partial}_t \zeta_\gamma(x). \quad (3.196)$$

As anticipated in the paragraph following Eq. (3.182), the determinant $\det_{cq}(\omega, q^2)$ can be expressed in terms of ρ_c, ρ_{cq} , and ρ_{qc} solely. Therefore, the term that is proportional to $\phi_q^* \phi_q$ and determines the flow of γ can then be found taking the derivative

$$\frac{\partial^2}{\partial \phi_q^* \partial \phi_q} = \frac{\partial \rho_{cq}}{\partial \phi_q} \frac{\partial \rho_{qc}}{\partial \phi_q^*} \frac{\partial^2}{\partial \rho_{cq} \partial \rho_{qc}} = \rho_c \frac{\partial^2}{\partial \rho_{cq} \partial \rho_{qc}}, \quad (3.197)$$

and we find for the integrand in Eq. (3.196) the expression

$$\zeta_\gamma(q^2) = \frac{\rho_0}{4\pi} \int_{-\infty}^\infty d\omega \left[\frac{\partial_{\rho_{cq}, \rho_{qc}}^2 \det_{cq}(\omega, q^2)}{\det_c(\omega, q^2)} - \frac{\partial_{\rho_{cq}} \det_{cq}(\omega, q^2) \partial_{\rho_{qc}} \det_{cq}(\omega, q^2)}{\det_c^2(\omega, q^2)} \right]_{\text{ss}}. \quad (3.198)$$

This can be treated in the same way as Eq. (3.187) above.

3.C.3 Flow equation for the inverse propagator

The second term on the RHS of Eq. (3.181) determines the flow of both the wave-function renormalization and the gradient coefficient. It is quadratic in the fluctuations $\delta\chi$, hence we can write it as

$$\text{Tr} \left(G_{k,cq} \mathcal{F}_1 \right) \Big|_{\text{ss}}^2 = -i2 \int_Q \delta\chi(-Q)^T \Sigma(Q) \delta\chi(Q), \quad (3.199)$$

where we set the fields to their stationary values. $\Sigma(Q)$ can be visualized as consisting of one-loop diagrams with four external legs two of which are attached to the condensate (cf. the second diagram on the RHS of Eq. (3.32)) and is given by

$$\Sigma_{ij}(Q) = \frac{i}{2} \int_P \text{tr} \left(G_k(P) V_i^{(3)} G_k(P+Q) V_j^{(3)} \right), \quad (3.200)$$

where $G_k(Q) = P_k(Q)^{-1}$ with the inverse propagator given by Eqs. (3.51) and (3.52) to which the cutoff $R_k(q^2)$ has to be added. For $\phi_c = \phi_c^* = \phi_0$ and $\phi_q = \phi_q^* = 0$ the matrices $V_i^{(3)}$ have the structure

$$V_i^{(3)} = \begin{pmatrix} v_{3,i}^H & v_{3,i}^A \\ v_{3,i}^R & 0 \end{pmatrix}, \quad v_{3,1}^H = v_{3,2}^H = 0, \quad v_{3,3}^{R/A} = v_{3,4}^{R/A} = 0. \quad (3.201)$$

Inserting this expression in Eq. (3.200) above and taking the causality structure of the propagator into account, we can rewrite the integrand in the form ($P_+ = P + Q$)

$$\begin{aligned} \text{tr} \left(G_k(P) V_i^{(3)} G_k(P_+) V_j^{(3)} \right) &= \text{tr} \left(G_k^K(P) v_{3,i}^H G_k^K(P_+) v_{3,j}^H \right) \\ &+ \text{tr} \left(G_k^K(P) v_{3,i}^H G_k^R(P_+) v_{3,j}^R \right) + \text{tr} \left(G_k^R(P) v_{3,i}^R G_k^K(P_+) v_{3,j}^H \right) \\ &+ \text{tr} \left(G_k^K(P) v_{3,i}^A G_k^A(P_+) v_{3,j}^H \right) + \text{tr} \left(G_k^A(P) v_{3,i}^H G_k^K(P_+) v_{3,j}^A \right). \end{aligned} \quad (3.202)$$

Then the second and third equalities in Eq. (3.201) imply that $\Sigma(Q)$ has the same causality structure as the inverse propagator. For the retarded block we find

$$\Sigma_{ij}^R(Q) = \frac{i}{2} \int_P \left[\text{tr} \left(G_k^K(P) v_{3,i+2}^H G_k^R(P_+) v_{3,j}^R \right) + \text{tr} \left(G_k^A(P) v_{3,i+2}^H G_k^K(P_+) v_{3,j}^A \right) \right], \quad (3.203)$$

where now the indices i and j take the values 1, 2, and the Keldysh component is given by

$$\Sigma_{ij}^K(Q) = \frac{i}{2} \int_P \text{tr} \left(G_k^K(P) v_{3,i+2}^H G_k^K(P_+) v_{3,j+2}^H \right). \quad (3.204)$$

The frequency integrals appearing in Eqs. (3.203) and (3.204) can be evaluated by straightforward application of the residue theorem: $G_k^R(Q)$ has simple poles $\omega_{1,2}^R$ given by Eq. (3.54) with Aq^2 and Dq^2 replaced by $p_A(q^2)$ and $p_D(q^2)$ respectively. While the poles of the advanced propagator $\omega_{1,2}^A$ are complex conjugate to the poles of the retarded propagator, $G_k^K(Q)$ has poles at both $\omega_{1,2}^R$ and $\omega_{1,2}^A$. We omit the lengthy expression for $\Sigma(Q)$ after frequency integration.

Combining Eqs. (3.88) and (3.181), the flow equation for frequency- and momentum-dependent part of the the bare inverse propagator can be written as

$$\partial_t \left(\bar{P}(Q) - \bar{P}(0) \right) = -z^T \left(\tilde{\partial}_t \Sigma(Q) \right) z, \quad (3.205)$$

with the matrix z defined in Eq. (3.162). Inserting this expression in the flow equations for the wavefunction renormalization Z and the gradient coefficient \bar{K} , Eqs. (3.91) and (3.90) respectively, we find after some algebra,

$$\eta_Z = -\frac{1}{2}\partial_\omega \text{tr} \left[(\mathbb{1} + \sigma_y) \tilde{\partial}_t \Sigma^R(Q) \right] \Big|_{Q=0}, \quad (3.206)$$

$$\partial_t \bar{K}/Z = \partial_{q^2} \left(\tilde{\partial}_t \Sigma_{22}^R(Q) + i \tilde{\partial}_t \Sigma_{12}^R(Q) \right) \Big|_{Q=0}. \quad (3.207)$$

The real and imaginary parts of the anomalous dimension η_Z , which appear in the flow equations (3.194) of the real quartic and sextic couplings, are then given by

$$\eta_{ZR} = \text{Re } \eta_Z = -\frac{1}{2}\partial_\omega \text{tr} \left(\sigma_y \tilde{\partial}_t \Sigma^R(Q) \right) \Big|_{Q=0}, \quad (3.208)$$

$$\eta_{ZI} = \text{Im } \eta_Z = -\frac{i}{2}\partial_\omega \text{tr} \left(\tilde{\partial}_t \Sigma^R(Q) \right) \Big|_{Q=0}. \quad (3.209)$$

Here we used the relation $\Sigma^R(Q) = \Sigma^R(-Q)^*$ which implies $\partial_\omega \Sigma^R(0) = -\partial_\omega \Sigma^R(0)^*$. To further evaluate η_{ZR} and η_{ZI} we switch to MATHEMATICA. The derivatives with respect to the frequency can be carried out without any difficulty and $\tilde{\partial}_t$ can be calculated as in Eq. (3.188) above. Again the integral over spatial momenta is facilitated by the θ -function contained in $\tilde{\partial}_t R_{k,d}(x)$ and can be carried out analytically.

Finally, for the real and imaginary parts of the renormalized kinetic coefficient $K = \bar{K}/Z = A + iD$ we have

$$\partial_t A = \beta_A = \text{Re } \partial_t K = \eta_{ZR} A - \eta_{ZI} D - \bar{\eta}_A A, \quad (3.210)$$

$$\partial_t D = \beta_D = \text{Im } \partial_t K = \eta_{ZR} D + \eta_{ZI} A - \bar{\eta}_D D, \quad (3.211)$$

where using $\partial_{q^2} \Sigma^R(0) = \partial_{q^2} \Sigma^R(0)^*$ (note that $\Sigma(Q)$ depends only on the norm squared q^2 of the spatial momentum) we may express the quantities $\bar{\eta}_A$ and $\bar{\eta}_D$ defined in Eq. (3.192) as

$$\begin{aligned} \bar{\eta}_A &= -\frac{1}{A} \partial_{q^2} \tilde{\partial}_t \Sigma_{22}^R(Q) \Big|_{Q=0} = -\frac{1}{2A} \partial_q^2 \tilde{\partial}_t \Sigma_{22}^R(Q) \Big|_{Q=0}, \\ \bar{\eta}_D &= -\frac{1}{D} \partial_{q^2} \tilde{\partial}_t \Sigma_{12}^R(Q) \Big|_{Q=0} = -\frac{1}{2D} \partial_q^2 \tilde{\partial}_t \Sigma_{12}^R(Q) \Big|_{Q=0}. \end{aligned} \quad (3.212)$$

We will proceed with the evaluation of these expressions in the next section.

3.C.4 Computation of gradient coefficient anomalous dimensions

As the cutoff Eq. (3.55) is a non-analytic function of the momentum, the evaluation of the derivatives in Eq. (3.212) requires some care. In this section we present two approaches to this problem: The first one was introduced by Wetterich in Ref. [101] and the second one makes use of Morris' lemma [107]. Our starting point is Eq. (3.203) in which we set the external frequency ω to zero. Using the shorthand $\int_{\mathbf{p}} = \int \frac{d^d \mathbf{p}}{(2\pi)^d}$ we may write

$$\Sigma^R(0, \mathbf{q}) = \int_{\mathbf{p}} \sigma^R(p_A, p_D, p_{A+}, p_{D+}). \quad (3.213)$$

Here and in the following for the sake of brevity we will omit the arguments in $p_a \equiv p_a(x)$ and $p_{a\pm} \equiv p_a(x_{\pm})$ for $a = A, D$, $x = q^2$ and $x_{\pm} = |\mathbf{p} \pm \mathbf{q}|^2$. The integrand in the above expression is given by the integral over the frequency component of the internal momentum $P = (v, \mathbf{p})$,

$$\sigma_{ij}^R(p_A, p_D, p_{A+}, p_{D+}) = \frac{i}{2} \int \frac{dv}{2\pi} \left[\text{tr} \left(G_k^K(P) v_{3,i+2}^H G_k^R(P_+) v_{3,j}^R \right) + \text{tr} \left(G_k^A(P) v_{3,i+2}^H G_k^K(P_+) v_{3,j}^A \right) \right]. \quad (3.214)$$

Our notation makes explicit that the momentum dependence of the regularized propagator $G_k(Q)$ is contained in the functions $p_a(q^2)$ introduced in Eq. (3.58). Inserting Eq. (3.214) in the expressions for the anomalous dimensions Eq. (3.212) we find

$$\begin{aligned} \bar{\eta}_A &= -\frac{1}{2A} \partial_q^2 \Big|_{q=0} \int_{\mathbf{p}} \tilde{\partial}_t \sigma_{22}^R(p_A, p_D, p_{A+}, p_{D+}), \\ \bar{\eta}_D &= -\frac{1}{2D} \partial_q^2 \Big|_{q=0} \int_{\mathbf{p}} \tilde{\partial}_t \sigma_{12}^R(p_A, p_D, p_{A+}, p_{D+}). \end{aligned} \quad (3.215)$$

In the following we will discuss the evaluation of $\bar{\eta}_A$ while we will only state the result for $\bar{\eta}_D$. Let us begin by introducing the abbreviations $\partial_a \equiv \partial_{p_a(x)}$ and $\partial_{a\pm} \equiv \partial_{p_a(x_{\pm})}$. In the integrand we omit the arguments and write $\sigma_{22+}^R \equiv \sigma_{22}^R(p_A, p_D, p_{A+}, p_{D+})$ and $\sigma_{22-}^R \equiv \sigma_{22}^R(p_{A-}, p_{D-}, p_A, p_D)$. We recall that the derivative $\tilde{\partial}_t$ acts only on the cutoff, hence we have

$$\bar{\eta}_A = \frac{1}{2A} \partial_q^2 \Big|_{q=0} \int_{\mathbf{p}} \sum_a \tilde{\partial}_t R_{k,a}(x) \partial_a \left(\sigma_{22+}^R + \sigma_{22-}^R \right), \quad (3.216)$$

where we performed a change of integration variables $\mathbf{p} \rightarrow \mathbf{p} - \mathbf{q}$ in the second term.

Wetterich's method

Following Ref. [101] we introduce new variables: With $y = x - k^2$ and $z = (x - k^2)\theta(x - k^2) = y\theta(y)$ we have

$$p_a(x) = a(k^2 + z). \quad (3.217)$$

We now use the fact that an expansion of the integrand in Eq. (3.216) in powers of z_{\pm} is effectively equivalent to an expansion in q^2 : Below we will see that due to the θ -functions contained in z_{\pm} and $\tilde{\partial}_t R_{k,a}(x)$ the integration over \mathbf{p} is restricted to a region that is $O(q)$ for $q \rightarrow 0$. In this region $p \approx k$ and the prefactor of the θ -function in the definition of z_{\pm} , therefore, is also $O(q)$. Hence we may restrict ourselves to the first order in the expansion

$$a \partial_a \sigma_{22\pm}^R = a \partial_a \sigma_{22\pm}^R \Big|_{z_{\pm}=0} + A_{\pm} z_{\pm} + O(z_{\pm}^2), \quad (3.218)$$

where the coefficient of the linear term is

$$A_{\pm} = a \partial_a \sum_b b \partial_b \sigma_{22\pm}^R \Big|_{z_{\pm}=0}. \quad (3.219)$$

The zeroth order term does not depend on q and can be discarded from the expression for $\bar{\eta}_A$ which now becomes

$$\bar{\eta}_A = \frac{1}{2A} \partial_q^2 \Big|_{q=0} \int_{\mathbf{p}} \sum_a \frac{1}{a} \tilde{\partial}_t R_{k,a}(x) (A_+ z_+ + A_- z_-). \quad (3.220)$$

Inserting here the explicit expressions for $z_{\pm} = y_{\pm}\theta(y_{\pm})$ we find

$$\bar{\eta}_A = -\frac{1}{2A}\partial_q^2|_{q=0}(B_+ + B_-), \quad (3.221)$$

where using Eq. (3.191) we have

$$B_{\pm} = \sum_a \int_{\mathbf{p}} [(2 - \bar{\eta}_a)k^2 + \bar{\eta}_a x] \theta(k^2 - x) \theta(y_{\pm}) A_{\pm} y_{\pm}. \quad (3.222)$$

Due to the first θ -function only momenta \mathbf{p} within a circle of radius k centered at the origin contribute to the integral (hence we may set $p_a(x) = ak^2$ in A_{\pm}), while the second θ -function excludes all \mathbf{p} inside a circle of radius k centered at $\mp \mathbf{q}$. In the resulting area of integration – which is itself $O(q)$ as anticipated above – we have $p \approx k$ for $q \rightarrow 0$. Without loss of generality we choose $\mathbf{q} = (q, 0, \dots)$ and decompose the integral as $\int_{\mathbf{p}} = \int_{\mathbf{p}_t} \int_{-\infty}^{\infty} \frac{dp_1}{2\pi}$, where p_1 is the component in the direction of \mathbf{q} , i.e., $\mathbf{p} = (p_1, \mathbf{p}_t)$, and $\mathbf{p}_t \in \mathbb{R}^{d-1}$. The integrand does not depend on the direction of \mathbf{p}_t , hence, using (this relation holds for $d \geq 2$; for $d = 1$ there is no integration over \mathbf{p}_t)

$$\int_{\mathbf{p}_t} f(x_t) = 2v_{d-1} \int_0^{\infty} dx_t x_t^{(d-3)/2}, \quad (3.223)$$

where the integration variable on the RHS is $x_t = p_t^2$, we have

$$B_{\pm} = \int_0^{\infty} dx_t \int_{-\infty}^{\infty} dp_1 \theta(k^2 - x) \theta(y_{\pm}) b_{\pm}, \quad (3.224)$$

where

$$b_{\pm} = \frac{v_{d-1}}{\pi} x_t^{(d-3)/2} \sum_a [(2 - \bar{\eta}_a)k^2 + \bar{\eta}_a x] A_{\pm} y_{\pm}. \quad (3.225)$$

In Eq. (3.224) the θ -functions restrict the range of integration to

$$k^2 - p_1^2 - x_t > 0, \quad (p_1 \pm q)^2 + x_t - k^2 > 0. \quad (3.226)$$

The first of these inequalities allows for a solution for p_1 only if $0 < x_t < k^2$. Then it implies

$$-\alpha < p_1 < \alpha. \quad (3.227)$$

where $\alpha = \sqrt{k^2 - x_t}$. The second inequality is equivalent to

$$p_1 > \alpha \mp q \quad \vee \quad p_1 < -\alpha \mp q. \quad (3.228)$$

For B_+ we have to consider the upper sign. Then Eq. (3.227) and the first inequality Eq. (3.228) have the joint solution

$$\max\{-\alpha, \alpha - q\} < p_1 < \alpha. \quad (3.229)$$

Splitting the integration over x_t into two ranges $0 < x_t < x_{t0}$ where $x_{t0} = k^2 - q^2/4$ and $x_{t0} < x_t < k^2$ we can specify the maximum explicitly as

$$\max\{-\alpha, \alpha - q\} = \begin{cases} \alpha - q & \text{for } 0 < x_t < x_{t0}, \\ -\alpha & \text{for } x_{t0} < x_t < k^2. \end{cases} \quad (3.230)$$

The second inequality Eq. (3.228) and Eq. (3.227) do not have a common region of validity, and we find

$$B_+ = \int_0^{x_{t0}} dx_t \int_{\alpha-q}^{\alpha} dp_1 b_+ + \int_{x_{t0}}^{k^2} dx_t \int_{-\alpha}^{\alpha} dp_1 b_+. \quad (3.231)$$

Let us now consider B_- : Eq. (3.227) and the second inequality Eq. (3.228) are solved by

$$-\alpha < p_1 < \min\{\alpha, -\alpha + q\}. \quad (3.232)$$

where in the same ranges of x_t as above the minimum is

$$\min\{\alpha, -\alpha + q\} = \begin{cases} -\alpha + q & \text{for } 0 < x_t < x_{t0}, \\ \alpha & \text{for } x_{t0} < x_t < k^2. \end{cases} \quad (3.233)$$

The first inequality Eq. (3.228) and Eq. (3.227) can not be fulfilled at the same time. Thus we have

$$B_- = \int_0^{x_{t0}} dx_t \int_{-\alpha}^{-\alpha+q} dp_1 b_- + \int_{x_{t0}}^{k^2} dx_t \int_{-\alpha}^{\alpha} dp_1 b_-. \quad (3.234)$$

Now it is straightforward to carry out the integral over x_t in both B_+ and B_- and we obtain the result

$$B_{\pm} = \frac{4v_d}{d} k^{d+2} q^2 \sum_a A_{\pm}. \quad (3.235)$$

Inserting this in Eq. (3.221) and using that setting $z_{\pm} = 0$ in Eq. (3.219) is the same as setting $q = 0$ and $p = k$ we find

$$\bar{\eta}_A = -\frac{4v_d}{dA} k^{d+2} \sum_{a,b} ab \partial_a \left[\partial_{b+} \sigma_{22+}^R + \partial_{b-} \sigma_{22-}^R \right]_{q=0, p=k}. \quad (3.236)$$

Both terms on the RHS give the same contribution. Then, carrying out a similar analysis for $\bar{\eta}_D$ yields

$$\begin{aligned} \bar{\eta}_A &= -\frac{8v_d}{dA} k^{d+2} \sum_{a,b} ab \partial_a \partial_{b+} \sigma_{22+}^R \Big|_{q=0, p=k}, \\ \bar{\eta}_D &= -\frac{8v_d}{dD} k^{d+2} \sum_{a,b} ab \partial_a \partial_{b+} \sigma_{12+}^R \Big|_{q=0, p=k}, \end{aligned} \quad (3.237)$$

The remaining derivatives can straightforwardly be performed using MATHEMATICA.

Morris' lemma

The same results can also be obtained by a direct evaluation of the derivatives in Eq. (3.216),

$$\begin{aligned} \bar{\eta}_A &= \frac{1}{2A} \int_{\mathbf{p}} \sum_{a,b} \tilde{\partial}_t R_{k,a}(x) \partial_a \left\{ \sum_c \partial_{b+,c+}^2 \sigma_{22+}^R p'_{b+} p'_{c+} (\partial_q x_+)^2 \right. \\ &\quad \left. + \partial_{b+} \sigma_{22+}^R \left[p''_{b+} (\partial_q x_+)^2 + p'_{b+} \partial_q^2 x_+ \right] + (+ \rightarrow -) \right\} \Big|_{q=0} \end{aligned} \quad (3.238)$$

Upon setting $q = 0$ in the terms in braces, x_{\pm} are replaced by x . Then we may drop all terms that include the product $\tilde{\partial}_t R_{k,a}(x)p'_b$ as it contains θ -functions that do not have a common support: According to Eq. (3.191) $\tilde{\partial}_t R_{k,a}(x)$ is proportional to $\theta(k^2 - x)$, while $p'_b(x) = b\theta(x - k^2)$. With $\partial_q x_{\pm}|_{q=0} = \pm 2\mathbf{p} \cdot \hat{\mathbf{q}}$ (here $\hat{\mathbf{q}}$ denotes the vector of unit length in the direction of \mathbf{q}) we find

$$\bar{\eta}_A = \frac{2}{dA} \int_{\mathbf{p}} x \sum_{a,b} \tilde{\partial}_t R_{k,a}(x) p''_b \partial_a \left[\partial_{b+} \sigma_{22+}^R + \partial_{b-} \sigma_{22-}^R \right]_{q=0}, \quad (3.239)$$

where we used

$$\int_{\mathbf{p}} (\mathbf{p} \cdot \hat{\mathbf{q}})^2 f(p) = \frac{1}{d} \int_{\mathbf{p}} p^2 f(p) \quad (3.240)$$

The second derivative $p''_b(x) = b\delta(x - k^2)$ contains a δ -function and, therefore, we set $p = k$ in the terms in brackets. (Note that $p_a(x)$ is continuous at $x = k^2$.) Then, Using Morris' lemma according to which we can replace $\delta(x)\theta(x) \rightarrow \frac{1}{2}\delta(x)$ when this combination is multiplied by a function that is continuous at $x = 0$, we have

$$\tilde{\partial}_t R_{k,a}(x) p''_b(x) = -\frac{abk}{2} \delta(p - k). \quad (3.241)$$

Evaluating the integral over p with the aid of the δ -function reproduces the result Eq. (3.236).

Bibliography

- [1] I. Carusotto and C. Ciuti, *Rev. Mod. Phys.* **85**, 299 (2013).
- [2] K. Baumann, C. Guerlin, F. Brennecke, and T. Esslinger, *Nature* **464**, 1301 (2010).
- [3] F. Brennecke, F. R. Mottl, K. Baumann, R. Landig, T. Donner, and T. Esslinger, *PNAS* **110**, 11763 (2013).
- [4] H. Ritsch, P. Domokos, F. Brennecke, and T. Esslinger, *Rev. Mod. Phys.* **85**, 553 (2013).
- [5] J. Kasprzak, M. Richard, S. Kundermann, A. Baas, P. Jeambrun, J. M. J. Keeling, F. M. Marchetti, M. H. Szymańska, R. Andre, J. L. Staehli, V. Savona, P. B. Littlewood, B. Deveaud, and L. S. Dang, *Nature* **443**, 409 (2006).
- [6] K. G. Lagoudakis, M. Wouters, M. Richard, A. Baas, I. Carusotto, R. Andre, L. S. Dang, and B. Deveaud-Pledran, *Nat. Phys.* **4**, 706 (2008).
- [7] G. Roumpos, M. Lohse, W. H. Nitsche, J. Keeling, M. H. Szymańska, P. B. Littlewood, A. Löffler, S. Höfling, L. Worschech, A. Forchel, and Y. Yamamoto, *PNAS* **109**, 6467 (2012).
- [8] S. A. Moskalenko and D. Snoke, *Bose-Einstein Condensation of Excitons and Biexcitons* (Cambridge Univ. Press, 2000).
- [9] J. Keeling, M. Szymańska, and P. Littlewood, in *Optical Generation and Control of Quantum Coherence in Semiconductor Nanostructures*, NanoScience and Technology, edited by G. Slavcheva and P. Roussignol (Springer Berlin Heidelberg, 2010) pp. 293–329.
- [10] J. Clarke and F. K. Wilhelm, *Nature* **453**, 1031 (2008).

- [11] M. Hartmann, F. Brandao, and M. Plenio, *Laser & Photonics Reviews* **2**, 527 (2008).
- [12] A. A. Houck, H. E. Türeci, and J. Koch, *Nat. Phys.* **8**, 292 (2012).
- [13] J. Koch and S. Schmidt, *Ann. Phys.* **525**, 395 (2013).
- [14] R. Blatt and C. Roos, *Nat. Phys.* **8**, 227 (2012).
- [15] J. W. Britton, B. C. Sawyer, A. C. Keith, C.-C. J. Wang, J. K. Freericks, H. Uys, M. J. Biercuk, and J. J. Bollinger, *Nature* **484**, 489 (2012).
- [16] F. Marquardt and S. M. Girvin, *Physics* **2**, 40 (2009).
- [17] D. E. Chang, A. H. Safavi-Naeini, M. Hafezi, and O. Painter, *New J. Phys.* **13**, 023003 (2011).
- [18] M. Ludwig and F. Marquardt, *Phys. Rev. Lett.* **111**, 073603 (2013).
- [19] L. M. Sieberer, S. D. Huber, E. Altman, and S. Diehl, *Phys. Rev. Lett.* **110**, 195301 (2013).
- [20] S. Utsunomiya, L. Tian, G. Roumpos, C. W. Lai, N. Kumada, T. Fujisawa, M. Kuwata-Gonokami, A. Löffler, S. Höfling, A. Forchel, and Y. Yamamoto, *Nat. Phys.* **4**, 700 (2008).
- [21] A. Mitra, S. Takei, Y. B. Kim, and A. J. Millis, *Phys. Rev. Lett.* **97**, 236808 (2006).
- [22] S. Diehl, A. Micheli, A. Kantian, B. Kraus, H. P. Büchler, and P. Zoller, *Nat. Phys.* **4**, 878 (2008).
- [23] S. Diehl, A. Tomadin, A. Micheli, R. Fazio, and P. Zoller, *Phys. Rev. Lett.* **105**, 015702 (2010).
- [24] E. G. Dalla Torre, E. Demler, T. Giamarchi, and E. Altman, *Nat. Phys.* **6**, 806 (2010).
- [25] E. G. D. Torre, S. Diehl, M. D. Lukin, S. Sachdev, and P. Strack, *Phys. Rev. A* **87**, 023831 (2013).
- [26] B. Öztıp, M. Bordyuh, Özgür E Müstecaplıođlu, and H. E. Türeci, *New J. Phys.* **14**, 085011 (2012).
- [27] M. Wouters and I. Carusotto, *Phys. Rev. B* **74**, 245316 (2006).
- [28] A. Mitra and T. Giamarchi, *Phys. Rev. Lett.* **107**, 150602 (2011).
- [29] A. Mitra and T. Giamarchi, *Phys. Rev. B* **85**, 075117 (2012).
- [30] R. Graham, in *Quantum Statistics in Optics and Solid-State Physics*, Springer Tracts in Modern Physics, Vol. 66 (Springer-Verlag, Berlin, 1973) pp. 1–97.
- [31] U. Decker and F. Haake, *Phys. Rev. A* **11**, 2043 (1975).
- [32] P. C. Hohenberg and B. I. Halperin, *Rev. Mod. Phys.* **49**, 435 (1977).
- [33] U. C. Täuber, V. K. Akkineni, and J. E. Santos, *Phys. Rev. Lett.* **88**, 045702 (2002).
- [34] U. C. Täuber, in *Ageing and the Glass Transition*, Lecture Notes in Phys., Vol. 716, edited by M. Henkel, M. Pleimling, and R. Sanctuary (Springer-Verlag, Berlin, 2007) pp. 295–348.

- [35] B. Schmittmann and R. Zia, in *Statistical Mechanics of Driven Diffusive System*, Phase Transitions and Critical Phenomena, Vol. 17, edited by B. Schmittmann and R. K. P. Zia (Academic Press, 1995) pp. 3 – 214.
- [36] M. Doi, *Journal of Physics A: Mathematical and General* **9**, 1465 (1976).
- [37] L. Peliti, *J. Phys.* **46**, 1469 (1985).
- [38] J. Cardy and U. C. Täuber, *Phys. Rev. Lett.* **77**, 4780 (1996).
- [39] L. Canet, *Journal of Physics A: Mathematical and General* **39**, 7901 (2006).
- [40] S. Obukhov, *Physica A: Statistical Mechanics and its Applications* **101**, 145 (1980).
- [41] H. Hinrichsen, *Advances in Physics* **49**, 815 (2000).
- [42] H. J. Jensen, *Self Organized Criticality* (Cambridge University Press, Cambridge, 1998).
- [43] M. Kardar, G. Parisi, and Y.-C. Zhang, *Phys. Rev. Lett.* **56**, 889 (1986).
- [44] T. Halpin-Healy and Y.-C. Zhang, *Phys. Rep.* **254**, 215 (1995).
- [45] L. Canet, H. Chaté, B. Delamotte, and N. Wschebor, *Phys. Rev. Lett.* **104**, 150601 (2010).
- [46] T. Kloss, L. Canet, and N. Wschebor, *Physical Review E* **86**, 051124 (2012).
- [47] C. Ates, B. Olmos, J. P. Garrahan, and I. Lesanovsky, *Phys. Rev. A* **85**, 043620 (2012).
- [48] B. Olmos, D. Yu, and I. Lesanovsky, arXiv:1308.3967 (2013).
- [49] T. E. Lee, S. Gopalakrishnan, and M. D. Lukin, *Phys. Rev. Lett.* **110**, 257204 (2013).
- [50] S. De Sarkar, R. Sensarma, and K. Sengupta, arXiv:1308.4689 (2013).
- [51] A. Janot, T. Hyart, P. R. Eastham, and B. Rosenow, arXiv:1307.1407 (2013).
- [52] J. Berges, A. Rothkopf, and J. Schmidt, *Phys. Rev. Lett.* **101**, 041603 (2008).
- [53] C. Scheppach, J. Berges, and T. Gasenzer, *Phys. Rev. A* **81**, 033611 (2010).
- [54] J. Schole, B. Nowak, and T. Gasenzer, *Phys. Rev. A* **86**, 013624 (2012).
- [55] M. Karl, B. Nowak, and T. Gasenzer, arXiv:1307.7368 (2013).
- [56] C. Wetterich, *Phys. Lett. B* **301**, 90 (1993).
- [57] U. C. Täuber and S. Diehl, *Physical Review X* **4**, 021010 (2014).
- [58] M. Wouters and I. Carusotto, *Phys. Rev. Lett.* **99**, 140402 (2007).
- [59] J. Keeling, P. R. Eastham, M. H. Szymańska, and P. B. Littlewood, *Phys. Rev. Lett.* **93**, 226403 (2004).
- [60] M. H. Szymańska, J. Keeling, and P. B. Littlewood, *Phys. Rev. Lett.* **96**, 230602 (2006).

- [61] J. Keeling and N. G. Berloff, *Phys. Rev. Lett.* **100**, 250401 (2008).
- [62] M. Wouters and I. Carusotto, *Phys. Rev. Lett.* **105**, 020602 (2010).
- [63] M. Wouters, T. C. H. Liew, and V. Savona, *Phys. Rev. B* **82**, 245315 (2010).
- [64] S. Coleman and E. Weinberg, *Phys. Rev. D* **7**, 1888 (1973).
- [65] B. I. Halperin, T. C. Lubensky, and S.-k. Ma, *Phys. Rev. Lett.* **32**, 292 (1974).
- [66] E. Altman, L. M. Sieberer, L. Chen, S. Diehl, and J. Toner, arXiv:1311.0876 (2013).
- [67] N. Goldenfeld, *Lectures on Phase Transitions and the Renormalization Group*, Frontiers in Physics (Perseus Books, Reading, Massachusetts, 1992).
- [68] J. T. Stewart, J. P. Gaebler, and D. S. Jin, *Nature* **454**, 744 (2008).
- [69] J. Berges, N. Tetradis, and C. Wetterich, *Phys. Rept.* **363**, 223 (2002).
- [70] M. Salmhofer and C. Honerkamp, *Progress of Theoretical Physics* **105**, 1 (2001).
- [71] J. M. Pawłowski, *Annals of Physics* **322**, 2831 (2007).
- [72] B. Delamotte, in *Renormalization Group and Effective Field Theory Approaches to Many-Body Systems SE - 2*, Lecture Notes in Physics, Vol. 852, edited by A. Schwenk and J. Polonyi (Springer Berlin Heidelberg, 2012) pp. 49–132.
- [73] O. J. Rosten, *Physics Reports* **511**, 177 (2012).
- [74] I. Boettcher, J. M. Pawłowski, and S. Diehl, *Nuclear Physics B - Proceedings Supplements* **228**, 63 (2012).
- [75] A. Kamenev and A. Levchenko, *Adv. Phys.* **58**, 197 (2009).
- [76] A. Kamenev, *Field Theory on Non-Equilibrium Systems*, 1st ed. (Cambridge University Press, Cambridge, 2011).
- [77] A. Altland and B. Simons, *Condensed Matter Field Theory*, 2nd ed. (Cambridge University Press, Cambridge, 2010).
- [78] D. J. Amit and V. Martin-Mayor, *Field Theory, the Renormalization Group, and Critical Phenomena*, 3rd ed. (World Scientific, Singapore, 2005).
- [79] H. Kleinert and V. Schulte-Frohlinde, *Critical Properties of ϕ^4 -Theories*, 1st ed. (World Scientific, Singapore, 2001).
- [80] J. Zinn-Justin, *Quantum Field Theory and Critical Phenomena*, 4th ed., International Series of Monographs on Physics No. 113 (Oxford University Press, Oxford, 2002).
- [81] A. C. Y. Li, F. Petruccione, and J. Koch, arXiv:1311.3227 (2013).
- [82] E. M. Lifshitz and L. P. Pitaevskii, *Statistical Physics, Part 2: Theory of the Condensed State*, 2nd ed., Course of Theoretical Physics, Vol. 9 (Pergamon Press, New York, 1980).

- [83] T. Gasenzer and J. M. Pawłowski, Phys. Lett. B **670**, 135 (2008).
- [84] J. Berges and G. Hoffmeister, Nucl. Phys. B **813**, 383 (2009).
- [85] J. Berges and D. Mesterházy, Nuclear Physics B - Proceedings Supplements **228**, 37 (2012).
- [86] D. Mesterházy, J. H. Stockemer, L. F. Palhares, and J. Berges, Phys. Rev. B **88**, 174301 (2013).
- [87] R. Gezzi, T. Pruschke, and V. Meden, Phys. Rev. B **75**, 045324 (2007).
- [88] S. G. Jakobs, V. Meden, and H. Schoeller, Phys. Rev. Lett. **99**, 150603 (2007).
- [89] C. Karrasch, S. Andergassen, M. Pletyukhov, D. Schuricht, L. Borda, V. Meden, and H. Schoeller, EPL **90**, 30003 (2010).
- [90] L. Canet, H. Chaté, and B. Delamotte, J. Phys. A: Math. Theor. **44**, 495001 (2011).
- [91] J. Cardy, *Scaling and Renormalization in Statistical Physics* (Cambridge University Press, Cambridge, 1996).
- [92] N. Tetradis and C. Wetterich, Nucl. Phys. B **422**, 541 (1994).
- [93] U. C. Täuber, *Critical Dynamics – A field theory approach to equilibrium and non-equilibrium scaling behavior* (Cambridge University Press, Cambridge, to appear in 2014).
- [94] H. Janssen, in *Dynamical Critical Phenomena and Related Topics*, Lecture Notes in Physics, Vol. 104, edited by C. Enz (Springer-Verlag, Berlin, 1979) pp. 25–47.
- [95] C. Aron, G. Biroli, and L. F. Cugliandolo, J. Stat. Mech. **2010**, P11018 (2010).
- [96] D. F. Litim, Phys. Lett. B **486**, 92 (2000).
- [97] U. C. Täuber, Nuclear Physics B - Proceedings Supplements **228**, 7 (2012).
- [98] R. Dashen and D. J. Gross, Phys. Rev. D **23**, 2340 (1981).
- [99] R. Guida and J. Zinn-Justin, Journal of Physics A: Mathematical and General **31**, 8103 (1998).
- [100] D. F. Litim, Nuclear Physics B **631**, 128 (2002).
- [101] C. Wetterich, Phys. Rev. B **77**, 064504 (2008).
- [102] L. Canet and H. Chaté, Journal of Physics A: Mathematical and Theoretical **40**, 1937 (2007).
- [103] N. V. Antonov and A. N. Vasil'ev, Theoretical and Mathematical Physics **60**, 671 (1984).
- [104] D. Porras and J. I. Cirac, Phys. Rev. Lett. **92**, 207901 (2004).
- [105] A. P. Prudnikov, Y. A. Brychkov, and O. I. Marichev, *Integrals and Series, Volume 1: Elementary Functions*, 4th ed. (Taylor & Francis, London, 1998).
- [106] S. G. Hofer, private communication (2013).
- [107] T. R. Morris, International Journal of Modern Physics A **09**, 2411 (1994).

Part II

Universality in Driven-Dissipative Systems in Reduced Dimensions

CHAPTER 4

PUBLICATION

Two-dimensional superfluidity of exciton-polaritons requires strong anisotropy[†]

Phys. Rev. X, **5**, 011017 (2015)

E. Altman,¹ L. M. Sieberer,² L. Chen,³ S. Diehl,^{2,4} and J. Toner⁵

¹*Department of Condensed Matter Physics, Weizmann Institute of Science, Rehovot 76100, Israel*

²*Institute for Theoretical Physics, University of Innsbruck, A-6020 Innsbruck, Austria*

³*College of Science, China University of Mining and Technology, Xuzhou Jiangsu, 221116, PR China*

⁴*Institute of Theoretical Physics, TU Dresden, D-01062 Dresden, Germany*

⁵*Department of Physics and Institute of Theoretical Science, University of Oregon, Eugene OR, 97403, USA*

Fluids of exciton-polaritons, excitations of two dimensional quantum wells in optical cavities, show collective phenomena akin to Bose condensation. However, a fundamental difference from standard condensates stems from the finite life-time of these excitations, which necessitate continuous driving to maintain a steady state. A basic question is whether a two dimensional condensate with long range algebraic correlations can exist under these non-equilibrium conditions. Here we show that such driven two-dimensional Bose systems cannot exhibit algebraic superfluid order except in low-symmetry, strongly anisotropic systems. Our result implies, in particular, that recent apparent evidence for Bose condensation of exciton-polaritons must be an intermediate scale crossover phenomenon, while the true long distance correlations fall off exponentially. We obtain these results through a mapping of the long-wavelength condensate dynamics onto the anisotropic Kardar-Parisi-Zhang equation.

4.1 Introduction

One of the most striking discoveries to emerge from the study of non-equilibrium systems is that they sometimes exhibit ordered states that are impossible in their equilibrium counterparts. For example, it

[†]The author of the thesis contributed to the understanding of the distinction between driven-dissipative condensate dynamics and equilibrium dynamical models, and to the comparison with experimental findings. He was also actively involved in preparing the manuscript together with the other authors.

has been shown [1] that a two-dimensional “flock” - that is, a collection of moving, self-propelled entities - can develop long-ranged orientational order in the presence of finite noise (the non-equilibrium analog of temperature), and in the absence of both rotational symmetry breaking fields and long ranged interactions. In contrast, a two-dimensional *equilibrium* system with short-ranged interactions (e.g., a two-dimensional ferromagnet) cannot order at finite temperature; this is the Mermin-Wagner theorem [2].

In this paper, we report an example of the opposite phenomenon: A *driven*, two-dimensional Bose system, such as a gas of polariton excitations in a two-dimensional isotropic quantum well [3], cannot exhibit off-diagonal algebraic correlations (i.e., two-dimensional superfluidity).¹ In the polariton gas, the departure from thermal equilibrium is due to the incoherent pumping needed to counteract the intrinsic losses and maintain a constant excitation density.

The critical properties of related driven quantum systems have been the subject of numerous theoretical studies; in certain cases it can be shown that the low frequency correlation functions induced by driving are identical to those in equilibrium systems at an effective temperature set by the driving [7–11]. Such emergent equilibrium behavior occurs in three dimensional bosonic systems, although non-equilibrium effects *can* change the *dynamical* critical behavior [11, 12]. Here, we show that the non-equilibrium conditions imposed by the driving have a much more dramatic effect on *two-dimensional* Bose systems: effective equilibrium is never established in the generic isotropic case; instead, the non-equilibrium nature of the fluctuations inevitably destroys the condensate at long scales. We emphasize that dissipation alone, e.g., due to coupling to an dissipative equilibrium bath, would not have an adverse effect on the condensate. Rather, it is crucial to have both dissipation and driving, giving rise to a true non-equilibrium steady-state situation.

This conclusion follows from the known [13–16] connection between the Complex Ginzburg-Landau equation (CGL) (which describes the long wavelength dynamics of a driven condensate) and the Kardar-Parisi-Zhang (KPZ) equation [17], or, in the anisotropic case, the anisotropic KPZ equation [18], which were originally formulated to describe randomly growing interfaces. The non-equilibrium fluctuations generated by the drive translate into the non-linear terms of the KPZ equation.

Our results suggest that recent experiments [19–24] done with isotropic semiconductor quantum wells purporting to show evidence for the long sought [25] Bose condensation of polariton excitations are in fact observing an intermediate length scale crossover phenomenon, and not the true long-distance behavior of correlations. This is true despite the weak anisotropy, present in these experiments due to the splitting of transverse electric and transverse magnetic cavity modes [3, 26], which proves to be far too weak to create sufficient anisotropy at reasonable laser driving power. We remark that earlier work, which predicted long range algebraic order in two-dimensional driven condensates [27], relied on a linear (Bogoliubov) theory. Although this may be valid on intermediate scales, our analysis shows that it fails at long distances due to the relevant non-linearity.

On the other hand, performing the same mapping on the *anisotropic* CGL leads, as noted by Grinstein et al. [15, 16], to the *anisotropic* KPZ equation. This suggests, as also noted by those authors,

¹We will throughout this paper follow the literature on the *equilibrium* Kosterlitz-Thouless transition [4, 5] and refer to an algebraically ordered phase as a “superfluid phase,” even though the nature of its response (i.e., whether or not it has a well-defined superfluid density) remains an open question for future investigation. We note, however, that it has been shown by J. Keeling [6] that, within the Gaussian approximation, superfluid response persists in the presence of drive and dissipation in two dimensions, concomitant with algebraically decaying correlations in the same approximation. Since the anisotropic KPZ equation approaches a Gaussian fixed point in the algebraically ordered phase, it seems reasonable to expect superfluid response in this phase.

that algebraic order can prevail if the system is anisotropic, in the sense that the non-linear coupling parameters are different in different directions. Then the transition from this algebraically ordered phase to the disordered phase occurs by a standard equilibrium-like Kosterlitz-Thouless transition. This requires very strong anisotropy, which may seem unnatural in the case of exciton-polaritons in two dimensional quantum wells. However, mapping a realistic model of such a system to the anisotropic KPZ equation shows that the anisotropy of the KPZ non-linearities is a function of the driving laser power. Surprisingly, we find that even if the intrinsic anisotropy of the system is moderate, the effective anisotropy increases with pump power and eventually passes the threshold allowing for an effective equilibrium description. Then, not only does an algebraically ordered phase occur, but it does so in a *reentrant* manner: the phase is entered, and then left, as the driving laser power is increased.

We emphasize that the results reported here are *universal*, in the sense that they apply to all driven open quantum systems with phase rotation symmetry in two dimensions. They are thus of relevance to a variety of experiments in which competition between coherent and driven-dissipative dynamics occur, such as microcavity arrays [28, 29] or ultracold atoms [30]. However, at present ensembles of exciton-polaritons stand out as the most promising realization of this physics, as the ability to tune laser power provides a crucial "knob" which can be "turned" to make the system more non-equilibrium. (Note that this goal is opposite to that of some recent work, which has strived to reach the equilibrium limit [24].) In particular, below we present parameter estimates which demonstrate that our predictions should be in reach with current technology.

4.2 Model

The dynamics of a driven-dissipative system like a polariton condensate is determined both by coherent processes, such as the dispersion and scattering between polaritons, and independent dissipative processes induced by loss and the pumping field. A model of the condensate dynamics that incorporates these processes is

$$\partial_t \psi(\mathbf{x}, t) = -\frac{\delta H_d}{\delta \psi^*} - i \frac{\delta H_c}{\delta \psi^*} + \zeta(\mathbf{x}, t). \quad (4.1)$$

Here, ψ is the scalar complex order parameter, which describes the incipient condensate of linearly polarized polaritons [3]. The effective Hamiltonians H_ℓ ($\ell = c, d$) that generate the coherent and dissipative dynamics respectively read

$$H_\ell = \int_{x,y} \left[r_\ell |\psi|^2 + K_\ell^x |\partial_x \psi|^2 + K_\ell^y |\partial_y \psi|^2 + \frac{1}{2} u_\ell |\psi|^4 \right]. \quad (4.2)$$

The last term $\zeta(\mathbf{x}, t)$ in Eq. (4.1) is a zero mean Gaussian white noise with short-ranged spatiotemporal correlations: $\langle \zeta^*(\mathbf{x}, t) \zeta(\mathbf{x}', t') \rangle = 2\sigma \delta^d(\mathbf{x} - \mathbf{x}') \delta(t - t')$, $\langle \zeta(\mathbf{x}, t) \zeta(\mathbf{x}', t') \rangle = 0$.

Eq. (4.1) is widely known as the complex Ginzburg-Landau equation [31, 32], or in the context of polariton condensates, as the dissipative Gross-Pitaevskii equation [33, 34], although usually only the isotropic (i.e., $K_\ell^x = K_\ell^y$), noise free ($\zeta = 0$) case is considered (but see [35]). Modifications of this equation, e.g., including higher powers of ψ and ζ , higher derivatives, or combinations of the two, can readily be shown to be irrelevant in the Renormalization Group (RG) sense: they have no effect

on the long-distance, long-time scaling properties of either the ordered phase, or the transition into it².

Each of the parameters appearing in the model has a clear physical origin, as we now review. The coefficient r_d is the single particle loss rate γ_l (spontaneous decay) offset by the pump rate γ_p , that is, $r_d = \gamma_l - \gamma_p$. We consider a situation in which both loss and pump processes are spatially homogeneous. The effective chemical potential r_c is *completely arbitrary*. Indeed, it can be adjusted by a temporally local gauge transformation $\psi(\mathbf{x}, t) = \psi'(\mathbf{x}, t)e^{i\omega t}$, such that $r'_c = r_c - \omega$. In the following, we choose r_c so that, in the absence of noise, the equation of motion has a stationary, spatially uniform solution.

The term proportional to u_c is the pseudo-potential which describes the elastic scattering of two polaritons, whereas u_d is the non-linear loss or, alternatively, a reduction of the pump rate with density, that ensures saturation of particle number. The coefficients $K_c^{x,y} = 1/(2m_{x,y})$ (units are chosen such that $\hbar = 1$), where $m_{x,y}$ are the eigenvalues of the effective polariton mass tensor, with principal axes x, y . Under typical circumstances, the diffusion-like term K_d is expected to be small, but is allowed by symmetry, and so will always be generated [36, 37]. Finally, the noise is given by the total rate of particles entering and leaving the system. In polariton condensates, where u_d reflects a non-linear reduction of the pumping rate rather than an additional loss mechanism (see appendix 4.B), the noise strength at steady state is simply set by the single particle loss, i.e. $2\sigma = 2\gamma_l$.³

Before proceeding, it is important to clarify under what conditions Eq. (4.1) describes an effective thermal equilibrium at *all* wavelengths. Imposing the additional condition that the field follows a thermal Gibbs distribution at steady state translates to the simple requirement $H_d = RH_c$, where R is a multiplicative constant [35, 38–40]. This condition can also be seen as a symmetry of the dynamics which ensures detailed balance [11, 12] and is realized in dynamical systems which relax to thermal equilibrium [41, 42]. In contrast, in a driven system, the relation $H_d = RH_c$ is not satisfied in general, because the dissipative and coherent parts of the dynamics are generated by independent processes. This relation *can*, however, arise as an emergent symmetry at low frequencies and long wavelengths as was shown to be the case for a three-dimensional driven condensate [11, 12]. Below we shall derive the hydrodynamic long-wavelength description of a two-dimensional driven condensate and determine if it flows to effective thermal equilibrium.

4.3 Mapping to a KPZ equation

In the long-wavelength limit, Eq. (4.1) generically reduces to a KPZ equation [17] for the phase variable [15]. In the dissipationless case $H_d = 0$, the dynamics becomes totally different, and exhibits the usual propagating long wavelength Bogoliubov quasiparticles. We discuss this point further in the Supplemental Materials, after equation (4.17). As in equilibrium, in a hydrodynamic description of the condensate the order-parameter field is written in the amplitude-phase representation as $\psi(\mathbf{x}, t) = (M_0 + \chi(\mathbf{x}, t))e^{i\theta(\mathbf{x}, t)}$. Integrating out the gapped amplitude mode, and keeping only terms which are not

²The gradient terms shown are the only ones at second order in gradients allowed in systems which have inversion symmetry about either the x or the y axis; we will restrict our discussion here to such systems.

³In reality the system might be coupled also to a particle conserving bath, such as phonons in the solid, which we have not included. While such a coupling is irrelevant in the RG sense, if it is strong and induces fast relaxation toward the bath equilibrium, it may renormalize the parameters of the stochastic equation of motion (4.1). However, such a bath will not restore detailed balance, and none of the universal results presented here will change.

irrelevant in the sense of the renormalization group, we obtain a closed equation for θ (see appendix 4.A)

$$\partial_t \theta = D_x \partial_x^2 \theta + D_y \partial_y^2 \theta + \frac{\lambda_x}{2} (\partial_x \theta)^2 + \frac{\lambda_y}{2} (\partial_y \theta)^2 + \bar{\zeta}(\mathbf{x}, t), \quad (4.3)$$

with $(\alpha = x, y)$:

$$D_\alpha = K_d^\alpha \left[1 + \frac{K_c^\alpha u_c}{K_d^\alpha u_d} \right], \quad (4.4)$$

$$\lambda_\alpha = 2K_c^\alpha \left[\frac{K_d^\alpha u_c}{K_c^\alpha u_d} - 1 \right].$$

and noise strength (replacing σ in the noise correlations above)

$$\Delta = \frac{(u_d^2 + u_c^2) \gamma_l}{2u_d(\gamma_p - \gamma_l)}. \quad (4.5)$$

Eq. (4.3) is the anisotropic KPZ equation, originally formulated to describe the roughness of a growing surface due to random deposition of particles on it [17, 18], in which case θ is the height of the interface. It reduces to the *isotropic* KPZ equation when $D_x = D_y$ and $\lambda_x = \lambda_y$. This reduction can also be achieved by a trivial rescaling of lengths if $\Gamma \equiv \frac{\lambda_y D_x}{\lambda_x D_y} = 1$. Thus, when $\Gamma \neq 1$, the system is anisotropic.

Crucially, the presence of the non-linearity directly reflects non-equilibrium conditions⁴. Indeed, the coefficients λ_x, λ_y that measure the deviation from thermal equilibrium vanish identically when the conditions

$$K_c^x / K_d^x = K_c^y / K_d^y = u_c / u_d, \quad (4.6)$$

which follow from the equilibrium requirement that $H_d = RH_c$, are met.

It is furthermore important to note that our KPZ model differs from that formulated for a description of randomly growing interfaces [17] in that the analog of the interface height variable in our model is actually a compact phase; hence, topological defects in this field are possible. This difference with the conventional KPZ equation also arises in “Active Smectics” [44].

Analysis of Eq. (4.3) in the absence of vortices is the analogue of the low temperature spin-wave (linear phase fluctuation) theory of the equilibrium XY model. Indeed, without the non-linear terms, the KPZ equation reduces to linear diffusion, which would bring the field to an effective thermal equilibrium with power-law off-diagonal correlations (in $d = 2$). A transition to the disordered phase in this equilibrium situation can occur only as a Kosterlitz-Thouless (KT) transition through proliferation of topological defects in the phase field.

In a driven condensate, the non-linear terms are in general present, and in two dimensions have the same canonical scaling dimension as the linear terms. A more careful RG analysis is therefore required to determine how the system behaves at long scales even without defect proliferation. Such an analysis has been done in Refs. [18] and [44] for the anisotropic KPZ equation. In this case, the

⁴ More precisely, the KPZ equation describes non-equilibrium conditions in $d > 1$. In fact, in one dimension, it can be mapped “accidentally” onto the noisy Burgers equation, and thus may occur also in an equilibrium context. An explicit example has been identified in [43].

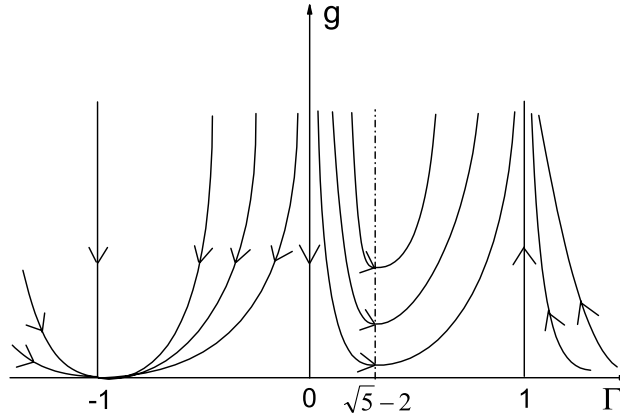


Figure 4.1. *The RG flow in the Γ - g parameter space for anisotropic driven BEC in $d = 2$. For $\Gamma < 0$ and $g > 0$, all flow lines go to a stable fixed point $(-1, 0)$; for $\Gamma > 0$ and $g > 0$, all flow lines go to infinity, and approach the isotropic limit $\Gamma = 1$.*

flow is closed in the two parameter space of scaled non-linearity $g \equiv \frac{\lambda_x^2 \Delta}{D_x^2 \sqrt{D_x D_y}}$ and scaled anisotropy $\Gamma \equiv \frac{\lambda_y D_x}{\lambda_x D_y}$, and is given, to leading order in g , by:

$$\begin{aligned} \frac{dg}{dl} &= \frac{g^2}{32\pi} (\Gamma^2 + 4\Gamma - 1), \\ \frac{d\Gamma}{dl} &= \frac{\Gamma g}{32\pi} (1 - \Gamma^2). \end{aligned} \quad (4.7)$$

These flows are illustrated in Fig. 4.1. We see that in an isotropic system, $\Gamma = 1$, and the nonlinear coupling g , which embodies the non-equilibrium fluctuations, is relevant. Moreover, for a wide range of anisotropies (namely, all $\Gamma > 0$) the flow is attracted to the isotropic line: the system flows to strong coupling, with emergent rotational symmetry. On the other hand, if the anisotropy is sufficiently strong, so that $\Gamma < 0$, the non-linearity becomes irrelevant and the system can flow to an effective equilibrium state at long scales. We emphasize that by "strong anisotropy" we mean only that the KPZ non-linearities $\lambda_{x,y}$ have opposite signs; the diffusion constants $D_{x,y}$ must both be positive for reasons of stability. Furthermore, we do not assume strong anisotropy between D_x and D_y ; our predictions apply even when these are comparable in magnitude, or, indeed, even if they are equal. The linear spatial extents of the system $L_{x,y}$ are also assumed to be comparable. That is, in no sense are we considering a "nearly one-dimensional" system.

We will now discuss the physics of these two regimes, starting with the isotropic case, which is most relevant to current experiments with polariton condensates.

4.4 Isotropic systems

As noted above, rotational symmetry is emergent at long scales if the anisotropy is not too strong at the outset. This is also the regime in which current experimental quantum well polaritons lie. We

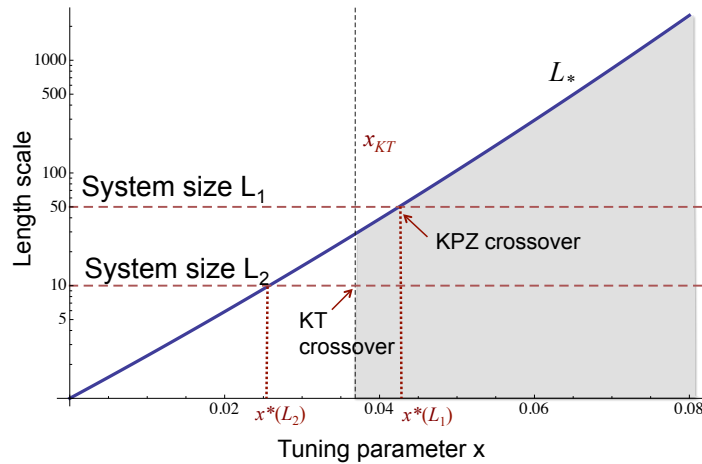


Figure 4.2. *Dependence of the emergent KPZ length scale L_* (in units of the microscopic healing length) on the tuning parameter $x = \gamma_p/\gamma_l - 1$. This curve was obtained by inserting the expression Eq. (4.9) for the bare coupling g_0 into Eq. (4.8) for L_* . While L_* is exponentially large when $x > \bar{u}\bar{\gamma}^2/2\pi$, it goes to a microscopic value ξ_0 at the mean field transition $x = 0^+$. The shaded region marks the scales at which a system would exhibit algebraic correlations. Upon decreasing the tuning parameter x , a finite system will lose its algebraic order in one of two ways: (1) When L_* falls below system size, as in the case of system L_1 shown, or (2) in a KT transition before L_* falls below system size, as in the case of system L_2 . Here we have used $\bar{\gamma} = 0.8$, $\bar{u} = 0.14$.*

therefore consider this case first.

On the line $\Gamma = 1$, the scaling of the non-linear coupling $dg/dl = g^2/8\pi$ drives $g \rightarrow \infty$; in the growing surface problem the system goes to the “rough” state, with height fluctuations scaling algebraically with length. The analogous behavior in the phase field θ would lead to stretched exponentially decaying order parameter correlations. However, the fact that the phase field is compact implies that topological defects (vortices) in this field exist. Our expectation, based on analogy with equilibrium physics (which admittedly may be an untrustworthy analogy), is that vortices will unbind at the strong coupling fixed point of the KPZ equation. If this happens, it will lead to simple exponential correlations. Testing this expectation will be the object of future work.

We have thus established that the non-linearity, no matter how weak, destroys the condensate at long distances, leading to either stretched or simple exponential decay of correlations throughout the isotropic regime. However, the effects of the nonlinearity only become apparent when g gets to be of order one. Solving the scaling equation we see that this occurs at the characteristic “RG time” $l_* = 8\pi/g_0$; the corresponding length scale is:

$$L_* = \xi_0 e^{l_*} = \xi_0 e^{8\pi/g_0}, \quad (4.8)$$

where ξ_0 is the mean field healing length of the condensate. If the bare value of g_0 is small, then the scale L_* can be huge. On length scales smaller than L_* , the system is governed by the linearized isotropic KPZ equation, which, as noted earlier, is the same as an equilibrium XY model. Thus, all of

the equilibrium physics associated with two-dimensional BEC, including power law correlations and a Kosterlitz-Thouless defect unbinding transition, can appear in a sufficiently small system.

As parameters, such as the pump power, are changed, the system can lose its apparent algebraic order in one of two ways: (i) the KPZ length L_* is gradually reduced below the system size, or (ii) L_* remains large while the correlations within the system size L are destroyed by unbinding of vortex anti-vortex pairs at the scale L . The latter type of crossover would appear as a KT transition broadened by the finite size. Of course, for any given set of system parameters, a sufficiently large system ($L > L_*$) will always be disordered.

We shall now discuss how the system parameters determine what type of crossover, if any, will be seen in an experiment. We assume that the main tuning parameter is the pump power γ_p , and it will be convenient to track the behavior as a function of a dimensionless tuning parameter $x = \gamma_p/\gamma_l - 1$, and set $K_d = 0$ since this parameter is thought to be small in current experimental realizations. In appendix 4.B we derive the parameters of the KPZ equation for a realistic model of a polariton condensate that is coupled to an excitonic reservoir. In particular, we obtain an expression for the bare dimensionless coupling constant g_0 in this model, which measures the bare deviation from equilibrium:

$$g_0 = \frac{\Delta\lambda^2}{D^3} = 2\bar{u}\bar{\gamma}^2 \left(\frac{\bar{\gamma}^2 + (1+x)^2}{x(1+x)^3} \right). \quad (4.9)$$

Here $\bar{u} \equiv u_c/K_c$ is the dimensionless interaction constant, and $\bar{\gamma} \sim \gamma_l$ the dimensionless loss rate as defined in appendix 4.B. Note that g_0 diverges as we approach the mean field transition at $x \rightarrow 0^+$, while it decays as $1/x^2$ as $x \rightarrow \infty$ at very high pump power.

Hence, in the latter regime the KPZ length scale $L_* = \xi_0 \exp(8\pi/g_0)$ is certainly much larger than any reasonable system size. As the pump power is decreased, and the system approaches the mean field transition at $x = 0$, L_* drops sharply to a microscopic healing length $L_* \approx \xi_0$. L_* drops below the system size when $x \lesssim x_*$, where

$$\frac{x_*(1+x_*)^3}{\bar{\gamma}^2 + (1+x_*)^2} \approx \frac{\bar{u}\bar{\gamma}^2}{4\pi} \ln(L/\xi_0). \quad (4.10)$$

For pump powers corresponding to $x > x_*$, the system will appear to be at effective equilibrium, and, hence, may sustain power law order within its confines, whereas for pump power $x < x_*$, the non-equilibrium fluctuations become effective and destroy the algebraic correlations at the scale of the system size. However, it is possible that this crossover at x_* is preceded by unbinding of vortices at values of $x = x_{KT} > x_*$, while the finite system is still at effective equilibrium. This crossover behavior is depicted in Fig. 4.2.

To determine which crossover occurs in a particular system, let us estimate the value of the tuning parameter x_{KT} at which the putative Kosterlitz-Thouless transition *would* occur if the non-linear term λ vanished, or was negligible. Then Eq. (4.3) obeys a fluctuation-dissipation relation with a temperature set by the noise $T = \Delta$. The KT transition would occur for an equilibrium XY model approximately at the point where $\Delta/D = \pi$. Expressing both Δ and D in terms of the tuning parameter x , we obtain the equation for the critical value x_{KT} at which the Kosterlitz-Thouless transition will appear to occur:

$$\frac{x_{KT}(1+x_{KT})}{\bar{\gamma}^2 + (1+x_{KT})^2} \approx \frac{\bar{u}}{2\pi}. \quad (4.11)$$

These equations (4.10) and (4.11) for x_* and x_{KT} simplify when the interactions are weak: $\bar{u} \ll 2\pi$, and the system is not too big: $(\bar{u}/4\pi)\bar{\gamma}^2 \ln(L/\xi_0) \ll 1$. In this limit, which proves to hold in current experiments, x_* and x_{KT} are given approximately by $x_* \approx (\bar{u}/4\pi)\bar{\gamma}^2(1 + \bar{\gamma}^2) \ln(L/\xi_0)$, and $x_{KT} \approx (\bar{u}/4\pi)(1 + \bar{\gamma}^2)$.

Under these conditions, we expect to see a crossover controlled by vortex unbinding through the KT mechanism, i.e., $x_{KT} > x_*$, if the system size is $L < \xi_0 \exp(2/\bar{\gamma}^2)$. For larger system sizes, the crossover will be controlled by the nonlinearities of the KPZ equation.

In which regime do experiments on Polariton condensates lie? In Ref. [45] parameter values for typical experimental systems have been deduced for the effective two band polariton model described in appendix 4.B. Based on this analysis we find $\bar{u}_c \approx 0.14$, and $\bar{\gamma} \approx 0.1$. With these parameters the KT transition would be expected at $x_{KT} \sim 0.02$ and the bare healing length at this point is $\xi_0 \sim 2\mu m$. Since the system size (spot size) is no more than $\sim 100\mu m$ in any current experiments, these values satisfy the conditions for the simplified expressions for x_* and x_{KT} discussed above. In addition, the small value of $\bar{\gamma}$ implies that the crossover will be dominated by KT physics; the non-linear effects we have treated here will not be visible in these experiments. However, it should not be difficult to raise $\bar{\gamma}$ by reducing the cavity Q (note that this will require a concomitant increase of the laser power at threshold). A moderate increase of $\bar{\gamma}$ to 0.75 will make it possible to enter the KPZ dominated regime at attainable system sizes.

Several recent experiments in the field of exciton-polariton physics [46–48] have come nearly as close to equilibrium conditions as cold atom experiments by realizing increasingly long polariton lifetimes (i.e., lowering $\bar{\gamma}$). From the perspective of the findings presented in this work it may be viewed as an outstanding feature of exciton-polaritons that both close-to-equilibrium conditions and the regime required to investigate the genuine non-equilibrium aspects predicted here are accessible in these systems.

4.5 Strong anisotropy

If the bare value of the anisotropy parameter is negative $\Gamma < 0$, then the RG equations (4.7) lead to a fixed point at $g = 0$. Because the non-linear $\lambda_{x,y}$ terms in (4.3) are irrelevant in this region of parameter space, the linear (and, hence, equilibrium) version of the theory applies. Hence it is possible, for $\Gamma < 0$, to obtain both a power law phase and a KT defect unbinding transition out of it.

To estimate the extent of this phase, we can utilize the RG flow of the anisotropic KPZ equation for $\Gamma < 0$ analyzed in Ref. [44]. In principle, we should add to these recursion relations terms coming from the vortices. Instead, we will follow reference [44] and assume that the vortex density is low enough that vortices only become important on length scales far longer than those at which the KPZ nonlinearities λ_α have become unimportant (i.e., those at which the scaled non-linearity g has flowed to nearly zero). If this is the case, then we can use the recursion relations Eq. (4.7) for our problem, despite the fact that they were derived neglecting vortices.

Our strategy is then to use those recursion relations to flow to the linear regime, which, as noted earlier, is equivalent to an equilibrium XY model. In this regime, vortex unbinding is controlled by the (bare) parameters of equation (4.3) through the dimensionless noise strength $\kappa_0 \equiv \Delta/\sqrt{D_x D_y}$ and scaled anisotropy $\Gamma_0 = \lambda_y D_x/(\lambda_x D_y)$. Following [44], the critical point for vortex unbinding can be estimated by solving for the renormalized scaled noise $\kappa(l \rightarrow \infty) \equiv \kappa(\infty)$ as a function of

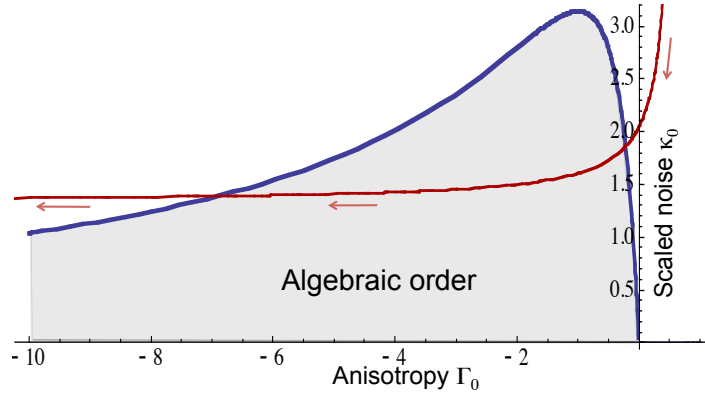


Figure 4.3. Phase diagram of a generic anisotropic system exhibiting reentrance. The thin line marks the natural trajectory in an experiment in which only the pump-power is varied. The arrows mark the direction of increasing pump power. Such an experiment will see a reentrant behavior, where the system starts in a disordered state, enters the power-law superfluid and then goes back to a disordered state. Here we have used the two band model of appendix 4.B with $\bar{\gamma} = 1/2$, $\bar{u} = 2$, $\nu_x = 1/8$ and $\nu_y = 1/4$.

the bare value using the RG equations of the non-compact KPZ equation; this involves additional recursion relations for D_α and Δ as well as Eq. (4.7); for details see reference [44]. This gives $\kappa(\infty) = -\kappa_0(1 - \Gamma_0)^2 / (4\Gamma_0)$. The KT transition occurs at the point where this renormalized value $\kappa(\infty)$ of κ reaches π . Hence the phase boundary in the κ_0 - Γ_0 plane is a locus in the plane of bare scaled noise and anisotropy parameters given by [44]

$$\kappa_0 = -\frac{4\pi\Gamma_0}{(1 - \Gamma_0)^2}. \quad (4.12)$$

The assumption in deriving this curve was that the dominant contribution to the stiffness renormalization comes from the non-linear fluctuations, rather than from bound vortex-antivortex pairs, which have been neglected.

There is a broad range of parameters for which a system enters a regime $\Gamma_0 = (D_x\lambda_y)/(D_y\lambda_x) < 0$, in which true power-law order and a KT transition exist. Using the effective (two band) polariton model in appendix 4.B we find the trajectory a realistic system would follow in the κ_0, Γ_0 plane as with increasing pump power as a function of its microscopic parameters, see Fig. 4.3. This is given by

$$\Gamma_0 = \frac{[\nu_y(1+x) - \bar{\gamma}][\nu_x\bar{\gamma} + 1+x]}{[\nu_x(1+x) - \bar{\gamma}][\nu_y\bar{\gamma} + 1+x]}, \quad (4.13)$$

$$\kappa_0 = \frac{\bar{u}}{2x} \frac{[\bar{\gamma}^2 + (1+x)^2]}{\sqrt{[\nu_y\bar{\gamma} + (1+x)][\nu_x\bar{\gamma} + (1+x)]}}, \quad (4.14)$$

with the ratios of the dissipative to coherent phase stiffnesses along the two directions, $\nu_\alpha = K_d^\alpha / K_c^\alpha$. Now consider gradually increasing the pump power, and hence x , from the mean field threshold $x = 0$. For system parameters $\bar{\gamma} > \nu_y > \nu_x$, $\Gamma_0(x)$ starts out positive at $x = 0$, is reduced to negative values

as x is increased past $x = \frac{\bar{\gamma}}{\nu_y} - 1$, and eventually runs off to $\Gamma_0 = -\infty$ at a finite value of x (namely, $x = \frac{\bar{\gamma}}{\nu_x} - 1$). If at the same time \bar{u} is sufficiently small, then the experimental trajectory in the $\kappa_0 - \Gamma_0$ plane is guaranteed to cross the dome marking the condensate (algebraic order) phase as determined in Eq. (4.12). The condition on \bar{u} for this crossing to occur is

$$\bar{u} < 2\pi \frac{(\bar{\gamma} - \nu_y)}{\bar{\gamma}\nu_y(1 + \nu_y^2)}. \quad (4.15)$$

Thus, we not only naturally achieve the ordered phase in this anisotropic system by varying the driving, but we do so in a *reentrant* manner: we enter the phase, and then leave it again, as the driving is increased. The analysis for $\gamma > \nu_y > \nu_x$ is the same if we take $\Gamma \rightarrow 1/\Gamma$.

We note that momentum-dependent splitting of transverse electric and transverse magnetic modes in typical exciton-polariton experiments induces a slight anisotropy in the coherent mass terms in these systems [3, 26], while the dissipative mass terms K_d^α are typically very small because they are generated as second order effects in the interactions [11, 12]. Under these conditions the regime of strong anisotropy cannot be reached with reasonable pump power.

4.6 Outlook

Our analysis can be extended to three dimensions. There, for weak deviations from equilibrium, i.e. a small bare value of the KPZ non-linearity, it predicts a true Bose condensate which may be established through the dynamical phase transition described in Ref. [11], even in the isotropic case. However, beyond a critical strength of the deviation from equilibrium, there may be a different, non-equilibrium transition controlled by a strong coupling fixed point of the three dimensional KPZ equation [49]. This opens up the possibility of a new non-equilibrium phase of matter with short-ranged order, distinct from the usual uncondensed state in that vortex loops do not proliferate. This will be explored in future work. Other directions for future research are investigation of the interplay of the KPZ physics uncovered here with more realistic microscopic models of exciton-polariton condensates. This involves taking into account both the polariton polarization inherited from the driving light [50, 51], and the effects of disorder on phases and phase transitions [52] (see also Refs. [3, 53] and references therein for further aspects of disorder in exciton-polaritons), which is unavoidable in real experimental systems. It is worth noting that a recent analysis of the dissipative Ginzburg-Landau equation in the presence of static disorder without noise found that the mean field condensate is destroyed, through a completely different mechanism [54].

4.7 Acknowledgements

Illuminating discussions with Daniel Podolsky and Anatoli Polkovnikov are gratefully acknowledged. We thank Austen Lamacraft for insightful comments on the manuscript. JT thanks Dung-hai Lee and the Physics Department of the University of California, Berkeley, CA, and the MPIPKS, Dresden, Germany, for their support (financial and otherwise) and hospitality while this work was being done. EA likewise thanks the Miller Institute at UC Berkeley and the Aspen Center for Physics under NSF Grant # 1066293. LC also thanks the MPIPKS for support and hospitality, and acknowledges support

by the National Science Foundation of China (under Grant No. 11474354). We also thank the US NSF for support by awards # EF-1137815 and 1006171; and the Simons Foundation for support by award #225579 (JT), ERC grant UQUAM, and the ISF (EA), and the Austrian Science Fund (FWF) through the START Grant No. Y 581-N16 and the SFB FoQuS (FWF Project No. F4006- N16) (LMS, SD).

4.A Mapping to the Kardar-Parisi-Zhang equation

Here we review the mapping [15], in the long-wavelength limit, between the model (4.1) and an anisotropic KPZ equation [17, 18]. We work in the amplitude-phase representation $\psi(\mathbf{x}, t) = (M_0 + \chi(\mathbf{x}, t))e^{i\theta(\mathbf{x}, t)}$, with M_0 , χ , and θ all real. Here M_0 is determined by requiring that $\chi = 0$, $\theta = 0$ is a static uniform solution of Eq. (4.1) in the absence of fluctuations ($\zeta(\mathbf{x}, t) = 0$). The real and imaginary parts of Eq. (4.1) then give $M_0^2 = -r_d/u_d$ and $r_c = -u_c M_0^2$, respectively. We can satisfy the second condition by exploiting the freedom to choose r_c mentioned in the main text. As explained there, by varying the strength of the pump laser, one can experimentally control r_d , which determines the amplitude M_0 . The mean field transition occurs at the point $r_d = 0$ (i.e., when $\gamma_p = \gamma_l$), where the amplitude M_0 vanishes. For later convenience we define the dimensionless tuning parameter $x \equiv \gamma_p/\gamma_l - 1$.

Plugging the amplitude-phase representation of ψ into Eq. (4.1), and linearizing in the amplitude fluctuations χ , we obtain the pair of equations

$$\partial_t \chi = -2u_d M_0^2 \chi - K_c^x M_0 \partial_x^2 \theta - K_c^y M_0 \partial_y^2 \theta - K_d^x M_0 (\partial_x \theta)^2 - K_d^y M_0 (\partial_y \theta)^2 + \text{Re} \zeta, \quad (4.16)$$

$$M_0 \partial_t \theta = -2u_c M_0^2 \chi + K_d^x M_0 \partial_x^2 \theta + K_d^y M_0 \partial_y^2 \theta - K_c^x M_0 (\partial_x \theta)^2 - K_c^y M_0 (\partial_y \theta)^2 + \text{Im} \zeta, \quad (4.17)$$

where we have used the freedom discussed earlier to choose $r_c = -u_c M_0^2$ to simplify this expression.

Note that if we have no dissipation ($H_d = 0$), so that $u_d = 0$, both χ and θ are ‘‘slow’’ variables, in the sense of evolving at rates that vanish as the wavevector goes to zero. In this case we can substitute Eq. (4.16) into the time derivative of Eq. (4.17) to obtain a wave equation for θ supplemented by irrelevant non-linear corrections. This gives the linear dispersion of the undamped Goldstone modes characteristic of a lossless condensate with exact particle number conservation. In contrast, without particle number conservation (i.e., in the presence of loss and drive), $u_d \neq 0$, and we can therefore neglect the $\partial_t \chi$ term (which vanishes as frequency $\omega \rightarrow 0$) on the left hand side of Eq. (4.16) relative to the $2u_d M_0^2 \chi$ on the right hand side for any ‘‘hydrodynamic mode’’ (i.e., in the low frequency limit). Doing so turns Eq. (4.16) into a simple linear algebraic equation relating χ to spatial derivatives of θ . Substituting the solution for χ of this equation into Eq. (4.17) gives Eq. (4.3), a closed equation for θ . The noise variable in that equation is related to the original noise through $\bar{\zeta} = (\text{Im} \zeta - u_c \text{Re} \zeta / u_d) / M_0$, and hence $\langle \bar{\zeta}(\mathbf{x}, t) \bar{\zeta}(\mathbf{x}', t') \rangle = 2\Delta \delta^d(\mathbf{x} - \mathbf{x}') \delta(t - t')$ with Δ given in Eq. (4.5). The stochastic equation for θ includes all terms that are marginal and relevant by canonical power-counting, while neglecting irrelevant terms like $\partial_t^2 \theta$, $\partial_t \nabla^2 \theta$, and $\partial_t (\nabla \theta)^2$, and terms with even more derivatives.

4.B Polariton condensate model with reservoir

In the main text we worked with a complex Ginzburg-Landau equation describing the incipient condensate in the lower polariton band. Such a model clearly gives the correct universal physics. How-

ever, in order to find how the parameters of the anisotropic KPZ equation change as actual experimental parameters are varied requires to start from a more microscopic model of the polariton degrees of freedom.

The standard model for describing these systems is a two fluid model which treats the excitonic range of the lower polariton band as a reservoir with local density n_R for the condensate which forms at zero momentum in the lower polariton band [3]. Here we generalize the model slightly in order to include dissipative mass terms and anisotropy:

$$\begin{aligned}\partial_t \psi &= \left[\sum_{\alpha=x,y} (iK_c^\alpha + K_d^\alpha) \partial_\alpha^2 - ir_c - \gamma_l - iu_c |\psi|^2 + Rn_R \right] \psi + \zeta, \\ \partial_t n_R &= P - Rn_R |\psi|^2 - \gamma_R n_R,\end{aligned}\quad (4.18)$$

where $\langle \zeta^*(\mathbf{x}, t) \zeta(\mathbf{x}', t') \rangle = 2\sigma \delta(\mathbf{x} - \mathbf{x}') \delta(t - t')$. It is usually assumed that the reservoir relaxation time γ_R is faster than all other scales. Hence we may solve the reservoir density independently assuming it is time independent

$$n_R = \frac{P}{\gamma_R + R|\psi|^2}.\quad (4.19)$$

Substituting this in the equation for ψ we obtain

$$\partial_t \psi = \left[\sum_{\alpha} (iK_c^\alpha + K_d^\alpha) \partial_\alpha^2 - ir_c - \gamma_l - iu_c |\psi|^2 + \frac{P}{\eta + |\psi|^2} \right] \psi + \zeta,\quad (4.20)$$

where we have eliminated R and γ_R for the single parameter $\eta = \gamma_R/R$. We note that the amplitude of the white noise is given by the total loss rate (γ_l) and gain, and since in steady state the loss and gain must be equal we simply have $\sigma = \gamma_l$ in this case.

In the following, as in the main text we work in the phase-amplitude representation $\psi(\mathbf{x}, t) = (M_0 + \chi(\mathbf{x}, t))e^{i\theta(\mathbf{x}, t)}$ and expand around the homogeneous mean field solution. Let us therefore first solve for the mean field steady state. The real part of the equation gives $\gamma_l = P/(\eta + M_0^2)$ from which we can deduce the condensate density $M_0^2 = P/\gamma_l - \eta$. The imaginary part of the equation is $r_c = -u_c M_0^2$. It is also worth noting that loss comes only from the term γ_l , since there is no two-particle loss term in this model (instead saturation is reached due to the non-linear reduction of the pump term). Hence in steady state, when loss is equal to gain, the noise term is simply $\sigma = \gamma_l$.

We now proceed to write the equations of motion for χ and θ to linear order in χ . This gives

$$\begin{aligned}M_0^{-1} \partial_t \chi &= -2\gamma_l^2 P^{-1} M_0 \chi - K_c^\alpha \partial_\alpha^2 \theta - K_d^\alpha (\partial_\alpha \theta)^2 + M_0^{-1} \text{Re} \zeta, \\ \partial_t \theta &= -2u_c \chi + K_d^\alpha \partial_\alpha^2 \theta - K_c^\alpha (\partial_\alpha \theta)^2 - M_0^{-1} \text{Im} \zeta.\end{aligned}\quad (4.21)$$

Now as in the main text we can eliminate χ to obtain the KPZ equation for θ , where $\alpha = x, y$ is summed over and

$$\partial_t \theta = D_\alpha \partial_\alpha^2 \theta + \frac{1}{2} \lambda_\alpha (\partial_\alpha \theta)^2 + \bar{\zeta},\quad (4.22)$$

where

$$\bar{\zeta} = M_0^{-1} \left(\text{Re} \zeta - \frac{u_c P}{\gamma_l^2} \text{Im} \zeta \right).\quad (4.23)$$

The noise parameter in $\langle \bar{\zeta}^*(\mathbf{x}, t) \bar{\zeta}(\mathbf{x}', t') \rangle = 2\Delta \delta(\mathbf{x} - \mathbf{x}') \delta(t - t')$ is here given by:

$$\begin{aligned} \Delta &= \frac{\gamma_l^2/2}{P - \eta\gamma_l} \left(1 + \frac{u_c^2 P^2}{\gamma_l^4} \right) = \left(1 + \frac{u_c^2 \eta^2 \gamma_p^2}{\gamma_l^4} \right) \frac{\gamma_l^2/2\eta}{\gamma_p - \gamma_l} \\ &= \frac{u_c \bar{\gamma}}{2x} \left(1 + \frac{(1+x)^2}{\bar{\gamma}^2} \right), \end{aligned} \quad (4.24)$$

where we have defined $\gamma_p \equiv P/\eta$, the dimensionless tuning parameter $x = \gamma_p/\gamma_l - 1$ and the dimensionless loss parameter $\bar{\gamma} \equiv \gamma_l/(\eta u_c)$. Below we will also need the dimensionless interaction strength $\bar{u} \equiv u_c/\sqrt{K_c^x K_c^y}$ and the ratios $\nu_\alpha = K_d^\alpha/K_c^\alpha$. The parameters of the anisotropic KPZ equation may now be written as:

$$\begin{aligned} D_\alpha &= K_c^\alpha \left(\frac{K_d^\alpha}{K_c^\alpha} + \frac{u_c P}{\gamma_l^2} \right) = K_c^\alpha \left(\nu^\alpha + \frac{1+x}{\bar{\gamma}} \right), \\ \lambda_\alpha &= 2K_c^\alpha \left(\frac{K_d^\alpha u_c P}{K_c^\alpha \gamma_l^2} - 1 \right) = 2K_c^\alpha \left(\nu^\alpha \frac{1+x}{\bar{\gamma}} - 1 \right). \end{aligned} \quad (4.25)$$

In order to make contact to the main text, we note that the expressions for the diffusion constants D_α and non-linear coefficients λ_α can be obtained from the predictions Eq. (4.25) for the complex Ginzburg-Landau model Eq. (1) of the main text, if we make the replacement

$$u_d = \frac{\gamma_l^2}{P} = \frac{u_c \bar{\gamma}}{1+x}. \quad (4.26)$$

The parameter K_d is thought to be small in isotropic two-dimensional quantum wells. If we take $K_d = 0$, then $D = K_c u_c / u_d = K_c (1+x) / \bar{\gamma}$, and $\lambda = -2K_c$. Eq. (4.9) in the main text corresponds to this special case $K_d = 0$.

Finally, to facilitate estimating the scales on which the phenomena discussed here can be observed in current experiments, we summarize the relations between the dimensionless quantities used in the main text and the parameters of the commonly used theoretical model of isotropic exciton-polariton systems. There the diffusion constant K_d is taken to be zero (although in some cases such a term is included effectively in a complex prefactor $(1 + i\Omega) \partial_t \psi = \dots$ on the right-hand side of Eq. (4.18) which models frequency-dependent pumping [37] or energy relaxation [36]); the coefficient $K_c = \hbar^2/(2m_{LP})$ is related to the effective mass of the polariton branch; then the mean field healing length can be expressed in terms of the experimental parameters in Eq. (4.18) as

$$\xi_0 = \frac{\hbar}{\sqrt{2m_{LP} u_c \left(\frac{P}{\gamma_l} - \frac{\gamma_R}{R} \right)}}. \quad (4.27)$$

The healing length sets a natural scale for the KPZ crossover length L_* (4.8). In order to compare the latter to spatial extent L of the condensate (as explained in the main text, only for $L > L_*$ can the KPZ crossover be observed), we have to express the bare dimensionless non-linearity g_0 (4.9) in terms of the parameters of the microscopic model. This can be achieved by inserting the relations

$$\begin{aligned} \bar{u} &= \frac{2m_{LP} u_c}{\hbar^2}, \\ \bar{\gamma} &= \frac{R\gamma_l}{\gamma_R u_c}, \\ x &= \frac{PR}{\gamma_R \gamma_l} - 1, \end{aligned} \quad (4.28)$$

in Eq. (4.9).

Bibliography

- [1] J. Toner and Y. Tu, Phys. Rev. Lett. **75**, 4326 (1995).
- [2] N. Mermin and H. Wagner, Phys. Rev. Lett. **17**, 1133 (1966).
- [3] I. Carusotto and C. Ciuti, Rev. Mod. Phys. **85**, 299 (2013).
- [4] V. Berezinskii, Sov. Phys. JETP **34**, 610 (1972).
- [5] J. M. Kosterlitz and D. J. Thouless, Journal of Physics C: Solid State Physics **6**, 1181 (1973).
- [6] J. Keeling, Phys. Rev. Lett. **107**, 080402 (2011).
- [7] A. Mitra, S. Takei, Y. Kim, and A. Millis, Phys. Rev. Lett. **97**, 1 (2006).
- [8] S. Gopalakrishnan, B. L. Lev, and P. M. Goldbart, Phys. Rev. A **82**, 043612 (2010).
- [9] E. Dalla Torre, E. Demler, T. Giamarchi, and E. Altman, Phys. Rev. B **85**, 184302 (2012).
- [10] E. G. D. Torre, S. Diehl, M. D. Lukin, S. Sachdev, and P. Strack, Phys. Rev. A **87**, 023831 (2013).
- [11] L. M. Sieberer, S. D. Huber, E. Altman, and S. Diehl, Phys. Rev. Lett. **110**, 195301 (2013).
- [12] L. M. Sieberer, S. D. Huber, E. Altman, and S. Diehl, Physical Review B **89**, 134310 (2014).
- [13] G. Sivashinsky, Acta Astronautica **4**, 1177 (1977).
- [14] Y. Kuramoto, *Chemical Oscillations, Waves, and Turbulence*, springer series in synergetics ed. (Springer, Berlin, 1984).
- [15] G. Grinstein, D. Mukamel, R. Seidin, and C. Bennett, Phys. Rev. Lett. **70**, 3607 (1993).
- [16] G. Grinstein, C. Jayaprakash, and R. Pandit, Physica D: Nonlinear Phenomena **90**, 96 (1996).
- [17] M. Kardar, G. Parisi, and Y.-C. Zhang, Phys. Rev. Lett. **56**, 889 (1986).
- [18] D. Wolf, Physical review letters **67**, 1783 (1991).
- [19] J. Kasprzak, M. Richard, S. Kundermann, A. Baas, P. Jeambrun, J. M. J. Keeling, F. M. Marchetti, M. H. Szymanska, R. Andre, J. L. Staehli, V. Savona, P. B. Littlewood, B. Deveaud, and L. S. Dang, Nature **443**, 409 (2006).
- [20] R. Balili, V. Hartwell, D. Snoke, L. Pfeiffer, and K. West, Science (New York, N.Y.) **316**, 1007 (2007).
- [21] H. Deng, G. Solomon, R. Hey, K. Ploog, and Y. Yamamoto, Phys. Rev. Lett. **99**, 126403 (2007).

- [22] G. Roumpos, M. Lohse, W. H. Nitsche, J. Keeling, M. H. Szymanska, P. B. Littlewood, A. Löffler, S. Höfling, L. Worschech, A. Forchel, and Y. Yamamoto, Proc. Natl. Acad. Sci. U.S.A. **109**, 6467 (2012).
- [23] V. Belykh, N. Sibeldin, V. Kulakovskii, M. Glazov, M. Semina, C. Schneider, S. Höfling, M. Kamp, and A. Forchel, Phys. Rev. Lett. **110**, 137402 (2013).
- [24] W. H. Nitsche, N. Y. Kim, G. Roumpos, C. Schneider, M. Kamp, S. Hoefling, A. Forchel, and Y. Yamamoto, arXiv:1401.0756 (2014).
- [25] A. Imamoglu, R. Ram, S. Pau, and Y. Yamamoto, Phys. Rev. A **53**, 4250 (1996).
- [26] I. A. Shelykh, A. V. Kavokin, Y. G. Rubo, T. C. H. Liew, and G. Malpuech, Semiconductor Science and Technology **25**, 013001 (2010).
- [27] A. Chiocchetta and I. Carusotto, EPL (Europhysics Letters) **102**, 67007 (2013).
- [28] M. Hartmann, F. Brandao, and M. Plenio, Laser & Photonics Reviews **2**, 527 (2008).
- [29] A. A. Houck, H. E. Tureci, and J. Koch, Nature Physics **8**, 292 (2012).
- [30] I. Bloch, J. Dalibard, and W. Zwerger, Rev. Mod. Phys. **80**, 885 (2008).
- [31] M. Cross and P. Hohenberg, Rev. Mod. Phys. **65**, 851 (1993).
- [32] I. Aranson and L. Kramer, Rev. Mod. Phys. **74**, 99 (2002).
- [33] M. Wouters and I. Carusotto, Phys. Rev. Lett. **99**, 140402 (2007).
- [34] J. Keeling and N. G. Berloff, Phys. Rev. Lett. **100**, 250401 (2008).
- [35] R. Graham and T. Tel, Phys. Rev. A **42** (1990).
- [36] M. Wouters, T. C. H. Liew, and V. Savona, Phys. Rev. B **82**, 245315 (2010).
- [37] M. Wouters and I. Carusotto, Phys. Rev. Lett. **105**, 020602 (2010).
- [38] R. Graham, in *Quantum Statistics in Optics and Solid-State Physics*, Springer Tracts in Modern Physics, Vol. 66 (Springer-Verlag, Berlin, 1973) pp. 1–97.
- [39] U. Decker and F. Haake, Phys. Rev. A **11**, 2043 (1975).
- [40] U. C. Täuber, in *Ageing and the Glass Transition*, Lecture Notes in Phys., Vol. 716, edited by M. Henkel, M. Pleimling, and R. Sanctuary (Springer-Verlag, Berlin, 2007) pp. 295–348.
- [41] P. Hohenberg and B. Halperin, Rev. Mod. Phys. **49**, 435 (1977).
- [42] B. V. S. G. V. Kagan, Yu. M.; Svistunov, JETP **75**, 387 (1992).
- [43] M. Kulkarni and A. Lamacraft, Physical Review A **88**, 021603 (2013).
- [44] L. Chen and J. Toner, Phys. Rev. Lett. **111**, 088701 (2013).

-
- [45] K. G. Lagoudakis, M. Wouters, M. Richard, A. Baas, I. Carusotto, R. André, L. S. Dang, and B. Deveaud-Plédran, *Nature Physics* **4**, 706 (2008).
- [46] B. Nelsen, G. Liu, M. Steger, D. W. Snoke, R. Balili, K. West, and L. Pfeiffer, *Physical Review X* **3**, 041015 (2013).
- [47] T. Jacqmin, I. Carusotto, I. Sagnes, M. Abbarchi, D. D. Solnyshkov, G. Malpuech, E. Galopin, A. Lemaître, J. Bloch, and A. Amo, *Phys. Rev. Lett.* **112**, 116402 (2014).
- [48] A. Dreismann, P. Cristofolini, R. Balili, G. Christmann, F. Pinsker, N. G. Berloff, Z. Hatzopoulos, P. G. Savvidis, and J. J. Baumberg, *Proceedings of the National Academy of Sciences of the United States of America* **111**, 8770 (2014).
- [49] M. P. A. Fisher and G. Grinstein, *Phys. Rev. Lett.* **69**, 2322 (1992).
- [50] D. Krizhanovskii, D. Sanvitto, I. Shelykh, M. Glazov, G. Malpuech, D. Solnyshkov, A. Kavokin, S. Ceccarelli, M. Skolnick, and J. Roberts, *Physical Review B* **73**, 073303 (2006).
- [51] L. Klotowski, M. Martín, A. Amo, L. Viña, I. Shelykh, M. Glazov, G. Malpuech, A. Kavokin, and R. André, *Solid State Communications* **139**, 511 (2006).
- [52] G. Malpuech, D. Solnyshkov, H. Ouerdane, M. Glazov, and I. Shelykh, *Phys. Rev. Lett.* **98**, 206402 (2007).
- [53] V. Savona, *Journal of physics. Condensed matter : an Institute of Physics journal* **19**, 295208 (2007).
- [54] A. Janot, T. Hyart, P. Eastham, and B. Rosenow, *Phys. Rev. Lett.* **111**, 230403 (2013).

CHAPTER 5

ADDITIONAL MATERIAL

Superfluidity in Driven-Dissipative Systems[†]

The Mermin-Wagner theorem [1] states that two-dimensional systems with short-range interactions and rotational symmetry cannot exhibit long-range order at any finite temperature. Nevertheless, such systems can undergo the BKT transition to a low-temperature superfluid phase with algebraically decaying correlations. Contrary to that, in systems that are taken out of equilibrium by imposing external drive and dissipation as is the case in fluids of exciton-polaritons, even such quasi-long-range order is destroyed on asymptotically large scales [2]. Here we show that in spite of the absence of algebraic order a finite superfluid density, which we identify through the retarded current-current response, may still survive under non-equilibrium conditions. We obtain this result by mapping the long-wavelength condensate dynamics to the Kardar-Parisi-Zhang equation. Our approach is valid when the density of topological defects in the condensate field is sufficiently low.

5.1 Introduction

The issue of superfluidity in two-dimensional (2D) driven-dissipative systems can most clearly be stated by first considering a related problem which does not suffer from the increased complexity that arises in reduced dimensions and when a system is driven out of equilibrium; i.e., let us consider Bose-Einstein condensation (BEC), e.g., of a cold atomic gas with short-range interactions, in thermodynamic equilibrium and in three spatial dimensions. In such a system the condensation transition marks the establishment of off-diagonal long-range order of the single-particle density matrix, and the spontaneous breaking of the $U(1)$ symmetry under phase rotations, which is associated with the conservation of particle number, by the order parameter ψ : the latter, which might be regarded as the wave function of the condensate, is a complex number and thus singles out a specific value of the phase. Long-wavelength fluctuations of the phase around this value are the low-lying excitations of the system, and the superfluid density determines the increase in free energy that is due to a spatially non-uniform configuration of the phase of ψ [3]. Contrary to what these considerations might suggest,

[†]The author of the present thesis carried out all of the calculations presented in this chapter and wrote the text. This chapter forms the basis of a publication that is currently being written.

superfluidity (i.e., a finite superfluid density) does not only occur in systems with spontaneously broken phase rotation symmetry. A specific example is BEC in two spatial dimensions: as stated by the Mermin-Wagner theorem [1], in this case phase rotation symmetry persists at any finite temperature. Nevertheless, there is a low-temperature phase with a finite superfluid density, and in which correlations decay algebraically instead of approaching a constant value at large distances as in 3D. This quasi-long-range order in 2D and the true long-range order in 3D condensates have in common, that they lead to non-analytic behavior when correlation functions are transformed to momentum space, and due to the obedience of specific fluctuation-dissipation relations (FDRs) in thermodynamic equilibrium, which establish an immediate link between correlation functions and corresponding response functions, the same non-analyticities also show up in the response of the system to external perturbations. In particular, the retarded current-current response function of a superfluid system contains a term that is in momentum space proportional to $q_i q_j / q^2$, where q_i and q_j are components of the momentum \mathbf{q} , and the coefficient of this term is immediately related to the superfluid density that measures the free energy cost of long-wavelength order parameter phase fluctuations as described above, thereby providing us with an alternative definition of the superfluid density. This definition of the superfluid density in terms of the current-current response function, which is reviewed in detail in Sec. 5.2, can be generalized to systems out of equilibrium, where the notion of a free energy is missing.

To be specific, in the following we consider a bosonic many-body system that is driven out of equilibrium by coupling it to several baths with which it can exchange particles, such that a steady state is established when the rates of particles entering and leaving the system exactly cancel each other. This scenario is realized in experiments with exciton-polaritons [4–8]. When the replenishment of particles occurs by an incoherent pump processes, these systems possess a $U(1)$ phase rotation symmetry even in the absence of particle number conservation, as is discussed in Sec. 5.3.2, and thus the question arises whether quasi-long-range order and superfluidity can also be realized out of equilibrium. In Ref. [2] it was shown that algebraic decay of correlations persists in driven-dissipative systems only up to a characteristic scale, above which it is followed by stretched-exponential or even faster decay. This indicates that there are no non-analyticities in the momentum space representation of correlation functions, however, due to the violation of equilibrium FDRs by the combination of drive and dissipation, we must not conclude that the same holds true also for the response. Under these conditions, an exotic phase with short-range correlations but a finite superfluid density is conceivable. Here we provide theoretical evidence that such a phase might actually be realized in 2D driven-dissipative systems, and that its properties are governed by the strong-coupling fixed point (SCFP) of the Kardar-Parisi-Zhang (KPZ) equation in 2D [9]. The relation between the complex Ginzburg-Landau equation, which describes the dynamics of the condensate field in driven-dissipative systems, and the KPZ equation was noticed in Refs. [10–13] and discussed in the context of exciton-polaritons in Refs. [2, 14–16]. Using this connection, we find that the superfluid density is given by

$$\rho_s = \rho_0 \left(\frac{u_c}{2m\nu_* u_d} L^{-\chi} + \frac{\ln 2}{8\pi} g_* \right). \quad (5.1)$$

Here, ρ_0 is the mean-field condensate density, u_c and u_d are the elastic two-body interaction and two-body loss coefficients, respectively, and m is the mass of bosonic quasiparticles; $\nu \sim \nu_* L^\chi$ is the scaling form of the diffusion coefficient in the KPZ equation at the SCFP. In particular, ν_* is a non-universal constant, $\chi \approx 0.4$ is the so-called roughness exponent (its value in 2D has been determined, e.g., using renormalization group (RG) methods [17–19] or numerically [20–25]), and L is the linear

size of the system. g_* denotes the universal value of the dimensionless KPZ non-linearity at the SCFP; a rough estimate based on Ref. [17], where the value of g_*v_2 with $v_2^{-1} = 2^3\pi\Gamma(1) = 8\pi$ is shown as a function of the spatial dimension in Fig. 1, gives $g_* \approx 1.4/v_2 \approx 35.2$, leading to $\rho_s \approx \rho_0$ in the thermodynamic limit $L \rightarrow \infty$.

In Ref. [26] the superfluid density of a 2D driven-dissipative system has been calculated in a perturbative expansion in fluctuations around the mean-field condensate. This approach does not fully account for the crucial role played by the non-equilibrium fluctuations of the phase at the KPZ SCFP, and hence yields a result that is different from the one reported in Eq. (5.1). It is expected to apply in systems that are smaller than the characteristic scale identified in Ref. [2], beyond which KPZ scaling sets in.

In thermodynamic equilibrium, at high temperatures the superfluid density is destroyed by the proliferation of topological defects. The pendant of thermal fluctuations in a non-equilibrium system is Markovian noise, which might create topological defects also in a driven-dissipative system. At present it is not clear how the presence of topological defects might affect the result for the superfluid density in Eq. (5.1). In fact, if vortices proliferate at any value of the noise strength, then we expect it to be valid only in systems that are smaller than the average distance between vortices. On the other hand, if the BKT scenario with a low-temperature/low-noise phase in which free vortices are absent applies also out of equilibrium, then the superfluid density in this phase would be given by ρ_s in Eq. (5.1) even in the thermodynamic limit $L \rightarrow \infty$. Clarification of this point, which we discuss further in Sec. 5.5, could be achieved by performing numerical simulations of the driven-dissipative order parameter dynamics, i.e., of the stochastic complex Ginzburg-Landau equation, or by performing an RG analysis of the KPZ equation that fully takes into account the compactness of the phase field.

The remainder of this chapter is organized as follows: In Sec. 5.2 we review the definition of the superfluid density in terms of the current-current response function, and contrast it with other definitions. We specify the model we consider in Sec. 5.3, and discuss its relevance for exciton-polariton systems and its relation to the models of Hohenberg and Halperin [27–29] of dynamical criticality in thermodynamic equilibrium. The notion of a current in a system without particle number conservation (i.e., without a continuity equation) is introduced in Sec. 5.3.2: first, in Sec. 5.3.2 we give a motivation on physical grounds, and then, in Sec. 5.3.2, we derive the expression for the current from a symmetry-based argument. In order to explicitly evaluate the superfluid density we employ a hydrodynamic description, which is introduced in Sec. 5.3.3. There we derive the long-wavelength Keldysh action for the phase of a driven-dissipative condensate. (We illustrate this method further in Appendix 5.C with the example of a weakly interacting Bose gas.) The calculation of the superfluid density leading to the result reported in Eq. (5.1) is presented in Sec. 5.4. Finally, in Sec. 5.5, we conclude with a discussion of the possible influence of topological defects on the phase diagram of 2D driven-dissipative systems.

5.2 Superfluidity in systems without particle number conservation

Superfluidity is a notion that integrates a plethora of exotic phenomena, many of which have been successfully described by the so-called two-fluid model [30]. In this model the system is decomposed into a normal component, which behaves as an ordinary liquid, and a superfluid component, that is

liable for the remarkable observations that have been made in the study of superfluid systems. Prominent among these is the complete absence of viscosity in the motion of the superfluid component, and thus the dramatically reduced viscosity of the system as a whole at low temperatures, where there is still a finite density of the normal component, which flows with non-zero friction. However, a more fundamental difference distinguishing the superfluid from the normal component is that the circulation of the flow of the former around an arbitrarily chosen point is quantized to be a multiple of 2π . As a result, the superfluid component cannot rotate as a whole [31], but only by forming vortices, which are topological excitations and thus long-lived. Indeed, even in an annular geometry, in which the core of a vortex lies outside of the system itself, metastable circular currents of the superfluid component can exist. On the other hand, when one takes a superfluid at rest and attempts to set it into motion by rotating the vessel in which it is contained, there is a critical angular velocity for the formation of vortices below which the superfluid fraction will cease to rotate. This observation can be turned into a rigorous definition of the superfluid component: it is precisely that part of the system, which stays at rest if the system is exposed to a weak rotational force or, stated differently, only the normal component starts to flow in response to such a force. Apparently the superfluid and normal components can be distinguished by studying the response of the system and, in particular, the relevant information is encoded in the retarded current-current response function, which is defined as

$$\chi_{ij}(t - t', \mathbf{x} - \mathbf{x}') = i\theta(t - t')\langle [j_i(t, \mathbf{x}), j_j(t', \mathbf{x}')] \rangle, \quad (5.2)$$

where $j_i(t, \mathbf{x})$ are the Cartesian components of the current operator. In a system without particle number conservation, the rate at which the number of particles within a given volume changes is not completely determined by the flow of particles into this volume, but rather has an additional contribution due to the exchange of particles with the baths surrounding the system. Subtleties in the definition of a current in an open system are discussed in Sec. 5.3.2 below.

In an isotropic system the current-current response function defined in Eq. (5.2) can be brought to a form in which the responses to potential and rotational – or, in other words, longitudinal and transverse – forces are clearly distinguished. To achieve this we have to take the Fourier transform of Eq. (5.2): then, in frequency and momentum space, the current-current response function can be decomposed into longitudinal and transverse components [32–34], $\chi_l(\omega, \mathbf{q})$ and $\chi_t(\omega, \mathbf{q})$ respectively, which are scalars and depend only on the magnitude of the momentum \mathbf{q} and not on its direction,

$$\chi_{ij}(\omega, \mathbf{q}) = \chi_l(\omega, \mathbf{q}) \frac{q_i q_j}{q^2} + \chi_t(\omega, \mathbf{q}) \left(\delta_{ij} - \frac{q_i q_j}{q^2} \right). \quad (5.3)$$

If the applied force is longitudinal, i.e., its Fourier transform $\mathbf{f}_l(\omega, \mathbf{q})$ is parallel to the direction of the momentum \mathbf{q} , then the same is true for the induced current, which is in the linear response regime given by $\langle \mathbf{j}(\omega, \mathbf{q}) \rangle = \chi(\omega, \mathbf{q}) \mathbf{f}_l(\omega, \mathbf{q}) = \chi_l(\omega, \mathbf{q}) \mathbf{f}_l(\omega, \mathbf{q})$; instead, for the case of a rotational or transverse force $\mathbf{f}_t(\omega, \mathbf{q})$ that is perpendicular to \mathbf{q} , the induced current is determined by the transverse part of the current-current response function, $\langle \mathbf{j}(\omega, \mathbf{q}) \rangle = \chi_t(\omega, \mathbf{q}) \mathbf{f}_t(\omega, \mathbf{q})$. We can make the above definition of the superfluid component precise as follows: superfluidity corresponds to a reduced response $\chi_t(0, \mathbf{q})$ to a static transverse force in the limit $\mathbf{q} \rightarrow \mathbf{0}$, as compared to the response of a normal fluid. In fact, in the latter case the current is expected to be parallel to the force, which implies that the off-diagonal elements of $\chi_{ij}(0, \mathbf{q})$ vanish for $\mathbf{q} \rightarrow \mathbf{0}$ and hence $\lim_{\mathbf{q} \rightarrow \mathbf{0}} (\chi_l(0, \mathbf{q}) - \chi_t(0, \mathbf{q})) = 0$. A deviation from this relation can be attributed to the presence of superfluidity. In particular, we may define the superfluid density as [32–34]

$$\rho_s/m = \lim_{\mathbf{q} \rightarrow \mathbf{0}} (\chi_l(0, \mathbf{q}) - \chi_t(0, \mathbf{q})). \quad (5.4)$$

In a system with particle number conservation the longitudinal component is determined by the total density ρ according to the so-called f -sum rule [34], which can be stated as $\rho/m = \chi_l(0, \mathbf{q})$ and holds for any value of the momentum \mathbf{q} . This observation together with Eq. (5.4) motivates the identification of $\chi_l(0, \mathbf{q})$ in the limit $\mathbf{q} \rightarrow \mathbf{0}$ with the normal density ρ_n , such that Eq. (5.4) can be written as $\rho = \rho_s + \rho_n$, in accordance with the two-fluid picture. If the number of particles in the system is not conserved, the f -sum rule does not hold any more. Nevertheless, we can still divide the right-hand side (RHS) of Eq. (5.4) by $\chi_l(0, \mathbf{q})$ to define the superfluid fraction *ad hoc* as $f_s = \lim_{\mathbf{q} \rightarrow \mathbf{0}} (\chi_l(0, \mathbf{q}) - \chi_t(0, \mathbf{q})) / \chi_l(0, \mathbf{q})$. Then the normal fraction is just the difference of f_s from unity, i.e., $f_n = 1 - f_s = \lim_{\mathbf{q} \rightarrow \mathbf{0}} \chi_t(0, \mathbf{q}) / \chi_l(0, \mathbf{q})$.

The definition of the superfluid density in Eq. (5.4) has a clear physical motivation that is still meaningful if one considers a system out of thermodynamic equilibrium and in the absence of particle number conservation. However, it is certainly not the only definition of superfluidity that has been devised in the past. For example, the Landau criterion [31] provides an argument that is based on energy conservation for the absence of dissipation in superfluid flow. In particular, it states that an impurity may move through the system without friction as long as the motion occurs at a speed that is lower than a critical value. This criterion has been extended to driven-dissipative systems [35, 36], and tested in experiments with exciton-polaritons [37, 38], and a sudden onset of scattering from the defect at the critical velocity has indeed been observed. However, this effect strongly depends on the precise shape of the defect: while small defects experience drag due to the emission of sound waves, vortices and/or solitons are created in the wake of an extended defect [39–42]. On the other hand, the definition of the superfluid density in Eq. (5.4) relates to the low-frequency and long-wavelength limit, and thus is expected to be insensitive to microscopic details. In a similar spirit and as described in Sec. 5.1, in equilibrium one can define the superfluid density (in this context one also speaks of the helicity modulus) as a measure for the change of the free energy due to long-wavelength fluctuations of the phase of the order parameter [3], imposed by a twist in the boundary conditions. While this definition coincides in equilibrium with the one in Eq. (5.4) given in terms of the current-current response function [43], it cannot be generalized straightforwardly to non-equilibrium conditions, for the simple reason that a quantity analogous to the free energy is missing. (One alternative would be to choose the oscillation frequency of the driven-dissipative condensate instead [44].) Finally, another strongly related [45, 46] notion in equilibrium is the superfluid stiffness, i.e., the coefficient of the term $\int_{\mathbf{x}} (\nabla\theta)^2$ in the long-wavelength phase-only action. This is in fact the quantity that determines the critical temperature for the equilibrium BKT-transition in 2D, which is driven by the unbinding of vortex-antivortex pairs. While as pointed out above the observation of metastable vortices is clearly another hallmark of superfluidity and has been extensively studied in exciton-polaritons [47–49], it is still unclear whether there is a transition in which topological defects proliferate in two-dimensional driven-dissipative systems in the thermodynamic limit, even though recently there has been numerical evidence that it actually exists in finite size systems [50].

In the present chapter we take Eq. (5.4) as the basic definition of the superfluid density of a 2D driven-dissipative systems in the absence of particle number conservation. We evaluate the current-current response in Sec. 5.4 in the limit of vanishing frequency of the external perturbation and for long-wavelength excitation, ignoring the possible occurrence of topological defects. This approach can be considered as analogous to the spin-wave theory for the 2D XY-model in thermodynamic equilibrium, and thus we expect our result to be valid at least at low noise level and concomitant low density of topological defects (out of equilibrium, the strength of Markovian noise is the counterpart of a finite temperature), in a finite-size system, such that the probability for a vortex to occur within

the confines of the system is small. If it turns out that even in an infinite system at low noise level there exists a phase in which topological defects occur only in bound pairs, analogous to the low-temperature BKT phase in equilibrium, then our results should apply in this phase. This issue is discussed further in Sec. 5.5.

5.3 Model

In this section we specify the open system dynamics we consider in terms of a quantum master equation for a bosonic many-body system and a corresponding dissipative Keldysh action. We discuss the relation of this model to exciton-polariton condensates and equilibrium dynamical models [27–29] with (model F) and without (model A*) particle number conservation. The issue of defining a current in an open system is considered in Sec. 5.3.2, and in Sec. 5.3.3 we specify how a hydrodynamic description of the open system in which the *phase* of the bosonic field, which determines the current through its gradient, is a fundamental degree of freedom.

5.3.1 Quantum master equation and Keldysh action

In the following we consider the model of bosons with single-particle loss and gain and two-body loss discussed in Refs. [51, 52], however, here we turn our attention to the case of two spatial dimensions. The dynamics of this model can be described by the master equation in Lindblad form

$$\partial_t \rho = \mathcal{L}\rho = -i[H, \rho] + \gamma_p \mathcal{D}[\psi^\dagger]\rho + \gamma_l \mathcal{D}[\psi]\rho + u_d \mathcal{D}[\psi^2]\rho, \quad (5.5)$$

where the dissipative terms are given by

$$\mathcal{D}[\Gamma]\rho = \int_{\mathbf{x}} \left(\Gamma(\mathbf{x})\rho\Gamma^\dagger(\mathbf{x}) - \frac{1}{2}\{\Gamma^\dagger(\mathbf{x})\Gamma(\mathbf{x}), \rho\} \right), \quad (5.6)$$

and the Hamiltonian reads

$$H = \int_{\mathbf{x}} \left(-\psi^\dagger(\mathbf{x}) \frac{\nabla^2}{2m} \psi(\mathbf{x}) + \frac{u_c}{2} \psi^\dagger(\mathbf{x})^2 \psi(\mathbf{x})^2 \right). \quad (5.7)$$

In Eq. (5.5), γ_p , γ_l , and u_d are the rates of single-particle pumping, single-particle loss, and two-body loss, respectively. The parameters appearing in the Hamiltonian are the mass m and the coupling constant u_c of elastic two-body interactions.

As we are interested in the steady-state properties of the system described by Eq. (5.5), we may alternatively use a formulation in terms of a Keldysh functional integral with the dissipative Keldysh action [51, 52] (we denote the collection of time and space variables by capital letters, $X = (t, \mathbf{x})$)

$$S = \int_X \left[\phi_q^* (i\partial_t + K_c \nabla^2) \phi_c + \text{c.c.} - V \right], \quad (5.8)$$

$$V = (r_c - ir_d) \phi_q^* \phi_c + (u_c - iu_d) \left(\phi_q^* \phi_c^* \phi_c^2 + \frac{1}{4} \phi_q^* \phi_c^* \phi_q^2 \right) + \text{c.c.} - i2(\gamma + u_d \phi_c^* \phi_c) \phi_q^* \phi_q,$$

where the potential V incorporates elastic interactions as well as the spatially homogeneous particle loss and source terms. Additionally, we introduced a “chemical potential” r_c , the value of which,

however, is arbitrary, as it can be adjusted by a gauge transformation $\phi_{c,q} \mapsto \phi_{c,q} e^{-i\omega t}$ which corresponds to $r_c \mapsto r_c - \omega$. The other parameters in the Keldysh action are $K_c = 1/(2m)$ and, in the dissipative quadratic part of the Keldysh action, we have the effective loss rate, $r_d = (\gamma_l - \gamma_p)/2$, which is the difference between the single-particle loss and pump rates, and their sum $\gamma = (\gamma_l + \gamma_p)/4$. Finally, the classical and quantum fields are defined as the sum and difference of fields on the forward and backward branches of the closed time path, respectively,

$$\begin{aligned}\phi_c &= \frac{\psi_+ + \psi_-}{2}, \\ \phi_q &= \psi_+ - \psi_-.\end{aligned}\tag{5.9}$$

In a mean-field approximation, where the steady-state expectation value $\phi_0 = \langle \phi_c \rangle$ of the classical field is determined by the classical field equation $\delta S / \delta \phi_q^* = 0$, a transition to a condensed phase is induced by increasing the single-particle pump rate γ_p above the corresponding loss rate γ_l such that $r_d = (\gamma_l - \gamma_p)/2 < 0$. Then we have $|\phi_0|^2 = -r_d/u_d = -r_c/u_c$ (note that the last equality can always be satisfied by means of a gauge transformation as discussed above), while $\phi_0 = 0$ for $r_d > 0$.

Relation to exciton-polariton models

In Refs. [51, 52] it was shown that the model described by the quantum master equation (5.5) or the corresponding Keldysh action (5.8) belongs to the same universality class as exciton-polaritons in semiconductor quantum wells, i.e., it exhibits the same universal long-wavelength and long-time behavior in 3D [51–53] (keeping in mind, however, that this case can be explored in exciton-polaritons only theoretically, as these systems are restricted to one or two spatial dimensions), as well as in 2D [2], and 1D [14–16]. The simplest model to describe the latter system theoretically employs a dissipative Gross-Pitaevskii equation [54], which can be supplemented with a Markovian noise source to account for the fluctuations that are induced by the loss and pump processes. Then the Gross-Pitaevskii equation takes the form of a Langevin equation which by the MSR construction [55, 56] can be expressed as the classical limit of a Keldysh action. On the other hand, starting from the Keldysh action Eq. (5.8) and focusing on the physics at long scales we can restrict ourselves to the most relevant contributions in the RG sense, which turns out to be equivalent to taking the classical limit of the Keldysh action [51, 52]. In particular, we may discard the so-called quantum vertices, i.e., the vertices that are of quadratic and higher order in the quantum fields. Note that while both approaches yield the same Keldysh action, which we specify below in Eq. (5.10), they are quite different in spirit: the former may actually be regarded as a simplistic phenomenological model for the microscopic physics of exciton-polariton condensation, while the latter is an effective theory for the long-wavelength physics in the sense of a Ginzburg-Landau-Wilson approach [29, 57–59]. In both cases the Keldysh action takes the form

$$\begin{aligned}S &= \int_X \left\{ \phi_q^* \left[i\partial_t + (K_c - iK_d) \nabla^2 \right] \phi_c + \text{c.c.} - V \right\}, \\ V &= (r_c - ir_d) \phi_q^* \phi_c + (u_c - iu_d) \phi_q^* \phi_c^* \phi_c^2 + \text{c.c.} - i2\gamma \phi_q^* \phi_q,\end{aligned}\tag{5.10}$$

where in addition to omitting the quantum vertices we introduced an effective diffusion constant K_d which is generated by integrating out high-frequency fluctuations (e.g., in the course of RG transformations; we note that omitting irrelevant contributions amounts to a first coarse-graining step, i.e.,

the parameters in the above action should be interpreted as renormalized and not bare ones) and thus has to be included to properly describe the universal long-scale physics. (A complex wave-function renormalization can be absorbed in a redefinition of the basic fields [51, 52].) As indicated above, this action corresponds to a simple model of exciton-polaritons with saturable pump, discarding the excitonic reservoir and with the non-linear pump term expanded to first order in $|\psi|^2$ [54]. In these models the diffusion term $iK_d \nabla^2 \psi$ is sometimes introduced effectively via a complex prefactor of the derivative of ψ with respect to time. Such a complex prefactor models frequency-dependent pumping [36] or energy relaxation [60–62].

Relation to thermodynamic equilibrium models

Condensation of exciton-polaritons is different from “conventional” Bose-Einstein condensation in two important aspects, which are first that the number of particles is not conserved, and second that the stationary state of the system is not thermodynamic equilibrium but rather characterized by the balance between non-linear loss and linear gain mechanisms.¹ Remarkably, both properties can be attributed to the absence of a symmetries in the action Eq. (5.8): for the case of particle number conservation this is the symmetry under global phase rotations, which we discuss in detail in Sec. 5.3.2 below, and the symmetry that distinguishes equilibrium from non-equilibrium stationary states is specified in Refs. [67–70] and discussed in detail in Appendix 5.A.

Systems with both particle number conservation and a thermal Gibbs ensemble stationary state belong to the universality class of model F of Hohenberg and Halperin [27–29], whereas equilibrium critical dynamics without particle number conservation correspond to the universality class of model A* [71]. While in general the action Eq. (5.10) describes condensation under non-equilibrium conditions, for a specific choice of parameters [29, 72–74], which is given by

$$K_c/K_d = u_c/u_d, \quad (5.11)$$

it satisfies the equilibrium symmetry mentioned above, and then it reduces to model A*. We note that this condition does not involve the ratio r_c/r_d , as the latter can be tuned at will by means of a rotating frame transformation as explained in Sec. 5.3. The consequences of deviations from the equilibrium condition (5.11) for the dynamical critical behavior in 3D driven-dissipative condensates have been discussed in Ref. [51–53], and for the coherence properties of 2D and 1D systems in [2] and [14–16], respectively. The purpose of the present chapter is to infer how violations of the equilibrium condition affect the superfluid density.

5.3.2 Current in open systems

In Sec. 5.2 we specified how the current-current response function (5.2) determines the superfluid fraction. However, up to now we have not yet given the very definition of the current that enters Eq. (5.2). This is the purpose of the present section.

If a system is perfectly isolated from its environment, then the temporal change of the number of particles in a given volume Ω is equal to the current of particles $J_{\partial\Omega}$ passing through the boundary $\partial\Omega$. This is illustrated in panel (a) of Fig. 5.1. In an open system, on the other hand, as is depicted in panel

¹We note that while this distinction applies to idealized systems it does not always conform to experimental reality: cold atomic systems suffer from losses [63] (which are, however, often negligible on experimental timescales) while longer and longer lifetimes of exciton-polaritons are reached [64–66], bringing these systems closer to thermodynamic equilibrium.

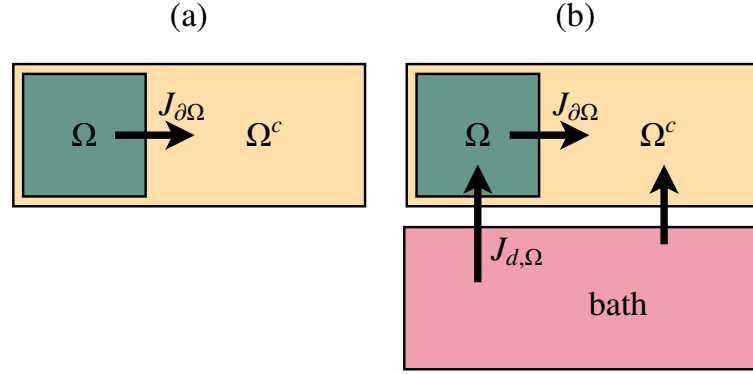


Figure 5.1. *Notions of current in closed and open systems. (a) In a closed system the single contribution to the current from a volume Ω to its complement Ω^c is due to particles moving through the boundary $\partial\Omega$. We denote this current as $J_{\partial\Omega}$ and it is given by Eq. (5.20). (b) Exchange of particles between the system and the bath results in an additional dissipative current $J_{d,\Omega}$, cf. Eq. (5.21), present only in open systems.*

(b) of the same figure, there is an additional contribution to the current out of Ω due to the exchange of particles between the system and the baths to which it is coupled. Following Refs. [75, 76] we call this contribution the dissipative current $J_{d,\Omega}$, and it has to be carefully distinguished from the coherent current $J_{\partial\Omega}$: only the latter involves the actual movement of particles within the system. We define the current-current response function (5.2) in terms of the coherent current, and as we show below in Sec. 5.3.2, the corresponding current density operator is given by

$$\mathbf{j}(\mathbf{x}) = \frac{1}{i2m} : (\psi^\dagger(\mathbf{x})\nabla\psi(\mathbf{x}) - \psi(\mathbf{x})\nabla\psi^\dagger(\mathbf{x})) :, \quad (5.12)$$

where the colons denote normal ordering. For the evaluation of the current-current response function Eq. (5.2) we switch in Sec. 5.4 below to a formulation in terms of a Keldysh functional integral. The formalism of quantum field theory is particularly well suited for studying symmetries, and we develop an alternative perspective on the notions of currents in closed and open systems, based on a discussion of phase rotation symmetries of the Keldysh action, in Sec. 5.3.2. As a very step, this requires an appropriate representation of the current operator in Eq. (5.12) in terms of fields on the closed time path. This representation can be obtained simply by replacing the field operators in Eq. (5.12) by fields ψ_\pm , which yields currents \mathbf{j}_\pm on the forward and backward branches of the closed time path, respectively. As in the definition Eq. (5.9) of classical and quantum fields, we form the sum and difference of the currents \mathbf{j}_\pm and in this way define classical and quantum *currents*,

$$\mathbf{j}_c = \frac{1}{2} (\mathbf{j}_+ + \mathbf{j}_-) = \frac{1}{i2m} \left(\phi_c^* \nabla \phi_c + \frac{1}{4} \phi_q^* \nabla \phi_q - \text{c.c.} \right), \quad (5.13)$$

$$\mathbf{j}_q = \mathbf{j}_+ - \mathbf{j}_- = \frac{1}{i2m} \left(\phi_c^* \nabla \phi_q + \phi_q^* \nabla \phi_c - \text{c.c.} \right). \quad (5.14)$$

In terms of these currents we can write the retarded current-current response function (5.2) as (see Appendix 5.B for a detailed discussion of the translation of the operator expression (5.2) to the Keldysh formalism)

$$\chi_{ij}(X - X') = i \langle j_{ci}(X) j_{qj}(X') \rangle. \quad (5.15)$$

This expression is the starting point for the evaluation of the superfluid density in Sec. 5.4.

Coherent and dissipative currents

Let us now make precise the notions of current in an open system introduced at the beginning of this section and illustrated in Fig. 5.1, and thereby clarify the motivation for using the expression for the current (5.12) in the definition of the current-current response function. In this section we proceed along the lines of Ref. [76] and argue within the operator formalism and based on physical intuition. Then, in Sec. 5.3.2, we will take a more formal viewpoint and discuss currents in an open system from a symmetry-based perspective, which is conveniently done in the functional integral formalism.

In Fig. 5.1 we consider a subsystem in space, i.e., a subvolume, Ω and its complement Ω^c and define the total current J_Ω out of Ω as the rate of change of the number of particles within the subsystem, $J_\Omega = \dot{N}_\Omega$. Our goal is to decompose the total current as $J_\Omega = J_{\partial\Omega} + J_{d,\Omega}$ into contributions describing the coherent current $J_{\partial\Omega}$ from the subsystem to its complement Ω^c , and the so-called dissipative current $J_{d,\Omega}$ from the subsystem to the bath. In fact, the existence of this dissipative current can be traced back to be a consequence of coarse-graining in time involved in the Markov approximation [75].

The number of particles in the subsystem defined by a spatial region Ω is $N_\Omega = \int_{\mathbf{x} \in \Omega} n(\mathbf{x})$, where $n(\mathbf{x}) = \psi^\dagger(\mathbf{x})\psi(\mathbf{x})$ is the local density. From the master equation $\dot{\rho} = \mathcal{L}\rho$ with Liouvillian \mathcal{L} in Lindblad form given in Eq. (5.5), it follows that the time evolution of N_Ω in Heisenberg representation is given by $\dot{N}_\Omega = \mathcal{L}^* N_\Omega$ with the adjoint Liouvillian defined by $\text{tr}(A\mathcal{L}B) = \text{tr}(B\mathcal{L}^*A)$, i.e., we have

$$\partial_t N_\Omega = i[H, N_\Omega] + \gamma_p \mathcal{D}^*[\psi^\dagger] N_\Omega + \gamma_l \mathcal{D}^*[\psi] N_\Omega + u_d \mathcal{D}^*[\psi^2] N_\Omega, \quad (5.16)$$

where (note that $\mathcal{D}^*[\Gamma]$ differs from $\mathcal{D}[\Gamma]$ in Eq. (5.6) only in that Γ and Γ^\dagger are exchanged in the first term)

$$\mathcal{D}^*[\Gamma] N_\Omega = \int_{\mathbf{x}} \left(\Gamma^\dagger(\mathbf{x}) N_\Omega \Gamma(\mathbf{x}) - \frac{1}{2} \{ \Gamma^\dagger(\mathbf{x}) \Gamma(\mathbf{x}), N_\Omega \} \right). \quad (5.17)$$

An explicit expression for the equation of motion for N_Ω in Eq. (5.16) can be obtained by starting from the one for local density $n(\mathbf{x}) = \psi^\dagger(\mathbf{x})\psi(\mathbf{x})$, which reads

$$\partial_t n(t, \mathbf{x}) = -\nabla \cdot \mathbf{j}(t, \mathbf{x}) + \gamma_p \psi(t, \mathbf{x}) \psi^\dagger(t, \mathbf{x}) - \gamma_l n(t, \mathbf{x}) - 2u_d \psi^\dagger(t, \mathbf{x})^2 \psi(t, \mathbf{x})^2, \quad (5.18)$$

where first term encodes coherent dynamics and corresponds to the Heisenberg commutator $i[H, n(\mathbf{x})]$, whereas the remaining contributions incorporate the dissipative parts stemming from the terms involving \mathcal{D}^* in Eq. (5.16). Integrating Eq. (5.18) over a the volume Ω we obtain the extended continuity equation in the form

$$\partial_t N_\Omega = J_{\partial\Omega} + J_{d,\Omega}, \quad (5.19)$$

where we identified the coherent and dissipative currents as

$$J_{\partial\Omega}(t) = - \int_{\partial\Omega} d\mathbf{s} \cdot \mathbf{j}(t, \mathbf{x}), \quad (5.20)$$

$$J_{d,\Omega}(t) = \int_{\Omega} d\mathbf{x} \left(\gamma_p \psi(t, \mathbf{x}) \psi^\dagger(t, \mathbf{x}) - \gamma_l n(t, \mathbf{x}) - 2u_d \psi^\dagger(t, \mathbf{x})^2 \psi(t, \mathbf{x})^2 \right). \quad (5.21)$$

Note that the coherent current is indeed located at the boundary between the subsystem Ω and its complement, and its density is given by \mathbf{j} , which we already anticipated in Eq. (5.12).

Phase rotation symmetries and Noether currents

The number of particles in a closed system is conserved—by Noether’s theorem, this conservation law is equivalent to the symmetry of the action describing the system under global phase rotations. More precisely, Noether’s theorem states that any global symmetry entails the existence of a $d + 1$ -component current with components j^μ , which obeys a continuity equation, $\langle \partial_\mu j^\mu \rangle = 0$, where $\partial_0 = \partial_t$ and $\partial_{1,2,\dots,d}$ are derivatives with respect to Cartesian coordinates, so that the integral over space $Q = \int_{\mathbf{x}} j^0$ gives a conserved quantity, i.e., we have $\langle dQ/dt \rangle = 0$. The *global* phase rotation symmetry associated with particle number conservation can be made a *local* one by introducing a gauge field in the action that couples to the Noether current j^μ . Then the current-current response function determines the current that is induced in linear response due to the presence of precisely this gauge field.

In the model we introduced in Sec. 5.3.1, the number of particles is clearly not conserved. However, as we discuss in the following, the corresponding Keldysh action still is symmetric under phase rotations of a specific kind, and this symmetry is spontaneously broken in the ordered phase with $\langle \phi_c \rangle \neq 0$. The existence of different types of phase rotations is related to the doubling of degrees of freedom in the Keldysh formalism, where there are fields ψ_\pm on the forward and backward branches of the closed time contour, as compared to the equilibrium Matsubara formalism with only a single field that is a function of imaginary time τ taking values from 0 to the inverse temperature $1/T$. In fact, the Keldysh formalism for single-component complex bosons allows for exactly two independent kinds of phase rotations: (i) A first one, which we denote by U_c , that shifts the phases of fields ψ_\pm on the forward and backward branches of the closed time path by the same amount α_c , i.e., $\psi_\pm \mapsto U_c \psi_\pm = \psi_\pm e^{i\alpha_c}$, and (ii) a second one $\psi_\pm \mapsto U_q \psi_\pm = \psi_\pm e^{\pm i\alpha_q}$, such that the phase shifts take opposite signs on the forward and backward branches.

As we show in the following, the second type of phase rotations, U_q , if it is a symmetry of the Keldysh action, implies particle number conservation and hence obviously cannot leave the action (5.8) for a system with incoherent particle loss and gain invariant. Instead, phase rotations U_c of type (i) *are* a symmetry of the action even in this case (this can be seen straightforwardly in the representation of the Keldysh action Eq. (5.8) in terms of fields ψ_\pm [52]), and consequently there exists an associated Noether current. This current, however, is just the quantum current Eq. (5.14) (complemented by the $\mu = 0$ component $j_q^0 = \rho_+ - \rho_- \equiv \rho_q$, where $\rho_\pm = \psi_\pm^* \psi_\pm$ are the local densities on the forward and backward branches), and the continuity equation $\langle \partial_\mu j_q^\mu \rangle = 0$ is trivially satisfied, since already the expectation value $\langle j_q^\mu \rangle = 0$ vanishes and – obviously – so does its divergence. The last statement is, in fact, always true, since a non-vanishing average value $\langle j_q^\mu \rangle \neq 0$ would imply a violation of causality.² In other words, we see that while the type (i) phase rotation symmetry under transformations U_c clearly has physical consequences in that it distinguishes the disordered phase of the model introduced in Sec. 5.3.1 with $\langle \psi_+ \rangle = \langle \psi_- \rangle = \langle \phi_c \rangle = 0$ from the ordered phase in which these expectation values are finite and thus the phase rotation symmetry is spontaneously broken, leading to the appearance of a Goldstone mode as discussed in Sec. 5.3.3 below, it does not imply a non-trivial conservation law. The latter is the case only for the phase rotation symmetry of the second kind, which implies $\langle \partial_\mu j_c^\mu \rangle = 0$, with $j_c^0 = (\rho_+ + \rho_-)/2 \equiv \rho_c$ and spatial components \mathbf{j}_c given by

²In the Keldysh formalism, “causality” or the “causality structure of the action” [55, 56] means the property that the time evolution on the forward and backward branches of the closed time contour is generated by the same Liouvillian. Then for any observable A it does not matter on which branch its expectation is evaluated, i.e. we have $\langle A_+ \rangle = \langle A_- \rangle = \langle A_c \rangle$, where $A_c = (A_+ + A_-)/2$, and therefore $\langle A_q \rangle = 0$ for $A_q = A_+ - A_-$.

Eq. (5.13).

For the gauge fields associated with the phase rotation symmetries of type (i) and (ii) the situation is in a sense reversed: the gauge field that has to be introduced in order to make phase rotations U_c of type (i) *local* symmetries is in fact a *physical* external source, in the sense that its components A_\pm satisfy $A_+ = A_- \equiv A_c$ in accordance with causality. In contrast to that, the gauge field that makes the type (ii) phase rotation symmetry under U_q , which implies particle number conservation, local, is *unphysical* and violates causality. To summarize, the current-current response function Eq. (5.15) determines the *physical* current $\langle \mathbf{j}_c(X) \rangle = \langle \mathbf{j}_+(X) \rangle = \langle \mathbf{j}_-(X) \rangle$ – which is conserved only for invariance under phase rotations U_q of type (ii) – that is induced by the *physical* gauge field A_c . The latter couples in the action to the current j_q which is always conserved due to causality and is the Noether current associated with phase rotations U_c of type (i).

Let us now proceed to prove the above statements, i.e., to derive the Noether currents and associated gauge fields for symmetries under global phase rotations U_c and U_q , of type (i) and (ii), respectively. A straightforward way to do this [77] is to perform in the Keldysh functional integral a change of integration variables that corresponds a *local* phase transformation. Such a change of integration variables leaves the value of the functional integral invariant, and therefore, if we expand the transformed functional integral in a power series in the local phase shifts, each term in this series has to vanish individually. The linear contributions yield the continuity equations for the Noether currents.

Thus we consider transformations $\psi_\pm \mapsto U_c \psi_\pm = e^{i\alpha_c} \psi_\pm$ and $\psi_\pm \mapsto U_q \psi_\pm = e^{\pm i\alpha_q} \psi_\pm$, where $\alpha_{c,q} = \alpha_{c,q}(X)$ are local (i.e., position- and time-dependent) phase shifts. It is straightforward to check that these transformations leave the functional integration measure invariant, $\mathcal{D}[\Psi] = \mathcal{D}[U_{c,q}\Psi]$, and hence a change of integration variables in the Keldysh partition function and subsequent expansion of the action in α_ν , where $\nu = c, q$, leads to

$$Z = \int \mathcal{D}[\Psi] e^{iS[\Psi]} = \int \mathcal{D}[\Psi] e^{iS[U_\nu \Psi]} = Z + i \int_X \alpha_\nu(X) \left\langle \frac{\delta S[U_\nu \Psi]}{\delta \alpha_\nu(X)} \Big|_{\alpha_\nu=0} \right\rangle + O(\alpha_\nu^2). \quad (5.22)$$

In the expansion in powers of $\alpha_{c,q}$ each term has to vanish individually, and as we show now, the expectation value in the linear contribution gives the continuity equations for classical and quantum currents. In order to find these continuity equations, we have to evaluate the change in the action induced by a local transformation $U_{c,q}$. It is given by the expressions

$$S[U_c \Psi] = S[\Psi] + \int_X \alpha_c \sum_{\sigma=\pm} \sigma (\partial_t \rho_\sigma + \nabla \cdot \mathbf{j}_\sigma) + O(\alpha_c^2), \quad (5.23)$$

$$S[U_q \Psi] = S[\Psi] + \int_X \alpha_q \sum_{\sigma=\pm} \left[\partial_t \rho_\sigma + \nabla \cdot \mathbf{j}_\sigma - \gamma_p \psi_+^* \psi_- + \gamma_l \psi_-^* \psi_+ + 2u_d (\psi_-^* \psi_+)^2 \right] + O(\alpha_q^2). \quad (5.24)$$

Inserting Eq. (5.23) in the expectation value in Eq. (5.22) immediately yields the continuity equation for the quantum current, $\langle \partial_\mu J_q^\mu \rangle = 0$. On the other hand, Eq. (5.24) leads to the extended continuity equation for the classical current,

$$\langle \partial_\mu J_c^\mu \rangle - \gamma_p \langle \psi_+^* \psi_- \rangle + \gamma_l \langle \psi_-^* \psi_+ \rangle + 2u_d \langle (\psi_-^* \psi_+)^2 \rangle = 0, \quad (5.25)$$

which is just the expectation value of the equation of motion (5.18) for the local density, including the contributions from the dissipative current defined in Eq. (5.21). In order to see this one has to use

the relations between expectation values in the Keldysh and operator formalisms, which follow from Eq. (5.92) in Appendix 5.B for $t = t'$,

$$\begin{aligned}\langle \psi_+^*(X)\psi_+(X) \rangle &= \langle \psi_-^*(X)\psi_-(X) \rangle = \langle \psi_-^*(X)\psi_+(X) \rangle = \langle n(X) \rangle, \\ \langle \mathbf{j}_+(X) \rangle &= \langle \mathbf{j}_-(X) \rangle = \langle \mathbf{j}(X) \rangle, \\ \langle \psi_+^*(X)\psi_-(X) \rangle &= \langle \psi(X)\psi^\dagger(X) \rangle, \\ \langle (\psi_-^*(X)\psi_+(X))^2 \rangle &= \langle \psi^{\dagger 2}(X)\psi^2(X) \rangle.\end{aligned}\tag{5.26}$$

Having found the continuity equation for j_q , which is implied by the symmetry of the action (5.8) under global phase rotations U_c of type (i), let us now derive the gauge field that has to be introduced in the action in order to turn the global symmetry into a local one. For a local symmetry the expansion in Eq. (5.23) has to terminate after the zeroth order contribution $S[\Psi]$. Cancellation of the terms at linear order can be achieved by adding to the Keldysh action a contribution $\int_X A_{c,\mu} j_q^\mu$, in which the current couples to a vector potential A_c : assuming that under local gauge transformations of type U_c the latter transforms as $A_c \mapsto A'_c$, we have

$$S[U_c\Psi, A'_c] = S[\Psi, A_c] + \int_X (A'_{c,\mu} - A_{c,\mu} - \partial_\mu\alpha_c) j_q^\mu + O(\alpha_c^2),\tag{5.27}$$

which is invariant to linear order if $A'_{c,\mu} = A_{c,\mu} + \partial_\mu\alpha_c$. Full symmetry of the action under local U_c gauge transformation requires adding another contribution $-\frac{1}{2m} \int_X \mathbf{A}_c^2 \rho_q$, which is quadratic in the vector potential and when combined with the term that is linear in the quantum current, amounts to the so-called minimal substitution, replacing ordinary derivatives by covariant ones,

$$\partial_t \rightarrow \partial_t - iA_{c,0}, \quad \nabla \rightarrow \nabla - i\mathbf{A}_c.\tag{5.28}$$

Let us emphasize that this construction is indeed physical: in fact, the modifications of the Keldysh action due to the minimal substitution Eq. (5.28) correspond to adding to the Hamiltonian in Eq. (5.7) a term

$$H_{A_c}(t) = - \int_{\mathbf{x}} \left[\left(A_{c,0}(t, \mathbf{x}) - \frac{1}{2m} \mathbf{A}_c^2(t, \mathbf{x}) \right) n(\mathbf{x}) + \mathbf{A}_c(t, \mathbf{x}) \cdot \mathbf{j}(\mathbf{x}) \right].\tag{5.29}$$

To linear order in \mathbf{A}_c , such a contribution induces a current $\langle \mathbf{j}(t, \mathbf{x}) \rangle$ which can be written in terms of the current-current response function Eq. (5.2) as

$$\langle \mathbf{j}(t, \mathbf{x}) \rangle = \int_{t', \mathbf{x}'} \chi(t - t', \mathbf{x} - \mathbf{x}') \mathbf{A}_c(t', \mathbf{x}').\tag{5.30}$$

Finally, these considerations should be contrasted with the analogous derivation of a gauge potential for the case of phase rotations U_q of type (ii), which are a symmetry of systems with particle number conservation. Again this symmetry can be made local by means of a minimal substitution as in Eq. (5.28), however, the gauge field A_q has to be introduced with different signs on the forward and backward branches of the closed time contour, i.e., one has to replace derivatives with respect to time and space by

$$\partial_t \rightarrow \partial_t - i\sigma A_{q,0}, \quad \nabla \rightarrow \nabla - i\sigma \mathbf{A}_q,\tag{5.31}$$

where $\sigma = \pm$ is the contour index. Evidently the gauge field A_q violates causality and hence cannot be represented as a contribution in the Hamiltonian similarly to Eq. (5.29).

5.3.3 Density-phase representation of the Keldysh action

As pointed out in Sec. 5.2, the definition of the superfluid density stated in Eq. (5.4) is related to the *static* current-current response *at long wavelengths*. In this section we derive an effective action for the relevant low-frequency and low-momentum degrees of freedom, starting from the microscopic Keldysh action Eq. (5.8).

At large scales the properties of 2D condensates are vitally influenced by fluctuations of the Goldstone mode, e.g., both in and out of equilibrium these lead to a suppression of long range correlations. In Ref. [2] an effective long-wavelength description of a driven-dissipative condensate with the condensate phase as the single dominant gapless degree of freedom has been formulated starting from the equations of motion of the complex order parameter. Below we achieve the same within the Keldysh functional integral formalism [55, 56], thereby avoiding the detour from the Keldysh functional integral in terms of which the microscopic theory of a bosonic many-body system with particle loss and gain can be formulated [51, 52], over a Langevin equation that effectively captures the physics on a mesoscopic scale and on the level of which amplitude fluctuations can be eliminated leading to the KPZ equation for the phase, back to an MSR functional integral formulation of the KPZ equation that serves as a convenient starting point for approaching the longest scales in a renormalization group analysis. In this sense we establish a closer link between microscopic and mesoscopic theories, which is both appealing from a theoretical point of view and brings about a number of technical advantages. For example, physical observables are usually represented by quantum mechanical operators or equivalently in terms of fields in a Keldysh functional integral description of the microscopic theory; Here our approach comes in handy as it yields the effective long-wavelength form of generating functionals for expectation values and correlation functions of these observables which can then be evaluated further utilizing established approximation strategies.

Apart from specific applications, the derivation of the action for the Goldstone mode presented here deepens our understanding of general properties of the Keldysh formalism with regard to phase rotation symmetries. The crucial point is that phase rotations of type (i) introduced in Sec. 5.3.2 are a symmetry of the Keldysh action both in a closed system and in the presence of terms that describe incoherent pumping and losses, and the spontaneous breaking of this symmetry is sufficient to ensure the appearance of a Goldstone mode that corresponds to fluctuations of the phase of the order parameter [78, 79] (note, however, that the conservation of particle number entails the existence of an additional slow mode in model F of Hohenberg and Halperin [27–29]). In the basis of classical and quantum fields $\phi_{c,q}$ such phase rotations of type (i) become $\phi_{c,q} \mapsto \phi_{c,q} e^{i\alpha_c}$ with $\alpha_c = \alpha_+ = \alpha_-$, showing that the Goldstone mode corresponds to joint phase fluctuations of both the classical and the quantum fields. Therefore, in order to derive the action for the Goldstone boson we represent the fields in the form

$$\begin{aligned}\phi_c &= \sqrt{\rho} e^{i\theta}, \\ \phi_q &= \zeta e^{i\theta},\end{aligned}\tag{5.32}$$

where the density ρ is real whereas ζ is a complex variable. For a system with particle number conservation both types of phase rotations introduced in Sec. 5.3.2 are symmetries of the action and both are broken in the condensed phase. As we illustrate in Appendix 5.C with the example of a weakly interacting Bose gas, the Goldstone boson corresponds to the phase θ in Eq. (5.32) also in this case.

Let us now discuss how the low-energy effective action for the Goldstone boson θ in a driven-dissipative system can be derived by integrating out fluctuations of the density ρ in Eq. (5.32) in the Keldysh partition function with action S given by Eq. (5.8),

$$Z = \int \mathcal{D}[\phi_c, \phi_c^*, \phi_q, \phi_q^*] e^{iS} = \int \mathcal{D}[\rho, \theta, \zeta, \zeta^*] e^{iS}. \quad (5.33)$$

The equality of the integrals over complex classical and quantum fields and the variables introduced in the transformation Eq. (5.32) follows from the fact that this transformation leaves the integration measure invariant, i.e., we have $\mathcal{D}[\phi_c, \phi_c^*, \phi_q, \phi_q^*] = \mathcal{D}[\rho, \theta, \zeta, \zeta^*]$. Note that this would not be the case if instead of the density we introduced the amplitude of ϕ_c as a degree of freedom. Our goal is then to treat the integrals over ρ and ζ in Eq. (5.33) in a saddle-point approximation, which as we show below is justified since fluctuations of the density are gapped in the ordered phase with $r_d < 0$ and hence expected to be small. The first step is thus to find the saddle point, i.e., the solutions to the classical field equations

$$\frac{\delta S}{\delta \rho} = 0, \quad \frac{\delta S}{\delta \zeta} = 0. \quad (5.34)$$

For $r_d < 0$, spatially homogeneous solutions are given by $\rho = \rho_0 = -r_d/u_d = -r_c/u_c$ (note that the last equality can always be satisfied by performing a gauge transformation to adjust the value of r_c as described in Sec. 5.3.1) and $\zeta = 0$, and we proceed to expand the action Eq. (5.8) to second order in fluctuations of ρ and ζ around the saddle point. Note that the quantum vertex in the potential V in the action Eq. (5.8) that is cubic in the quantum fields does not contribute at this order. Denoting the density fluctuations as $\pi = \rho - \rho_0$ we find

$$S = 2 \int_X \left(\sqrt{\rho_0} \left\{ -\zeta_1 \left[\partial_t \theta + K_c (\nabla \theta)^2 \right] + K_c \zeta_2 \nabla^2 \theta - (u_c \zeta_1 - u_d \zeta_2) \pi \right\} + i(\gamma + u_d \rho_0) |\zeta|^2 \right), \quad (5.35)$$

where ζ_1 and ζ_2 are, respectively, real and imaginary parts of ζ . Here, of all terms involving the products of fluctuations $\zeta_1 \pi$ and $\zeta_2 \pi$ we only keep the dominant ones in the long-wavelength limit, i.e., we neglect contributions containing temporal derivatives $\zeta_2 \partial_t \pi$, $\zeta_1 \pi \partial_t \theta$, and spatial derivatives $\zeta_1 \nabla^2 \pi$, $\zeta_2 \nabla \pi \cdot \nabla \theta$, and $\zeta_1 \pi (\nabla \theta)^2$ which are both small as compared to the mass-like contributions $u_c \zeta_1 \pi$ and $u_d \zeta_2 \pi$ in Eq. (5.35) for the Goldstone mode θ for which $\omega \rightarrow 0$ for $\mathbf{q} \rightarrow \mathbf{0}$. Note that terms of higher order in π and ζ are contained in the original action Eq. (5.8) both in contributions involving derivatives and in the coherent and dissipative vertices. The validity of the saddle-point approximation, therefore, is restricted to the low-frequency and low-momentum sector in a weakly interacting system.

The action (5.35) resulting from this expansion is linear in π and hence integration over this variable is trivial and yields a δ -functional which in turn facilitates integration over the imaginary part ζ_2 of ζ ,

$$Z = \int \mathcal{D}[\pi, \theta, \zeta_1, \zeta_2] e^{iS} = \int \mathcal{D}[\theta, \zeta_1, \zeta_2] \delta[u_c \zeta_1 - u_d \zeta_2] e^{iS'} = \int \mathcal{D}[\theta, \tilde{\theta}] e^{iS_{\text{KPZ}}}, \quad (5.36)$$

where at each step a normalization factor is implicitly included in the integration measure, ensuring $Z = 1$ [55, 56]. In the last equality we replaced ζ_1 by the KPZ response field $\tilde{\theta} = i2 \sqrt{\rho_0} \zeta_1$, and the KPZ action S_{KPZ} is given by

$$S_{\text{KPZ}} = \int_X \tilde{\theta} \left[\partial_t \theta - \nu \nabla^2 \theta - \frac{\lambda}{2} (\nabla \theta)^2 - \Delta \tilde{\theta} \right], \quad (5.37)$$

where the diffusion constant, non-linear coupling, and noise strength, respectively, are expressed in terms of the microscopic parameters in the original action Eq. (5.8) as

$$\nu = K_c \frac{u_c}{u_d}, \quad \lambda = -2K_c, \quad \Delta = \frac{\gamma + u_d \rho_0}{2\rho_0} \left(1 + \frac{u_c^2}{u_d^2} \right). \quad (5.38)$$

Usually, the KPZ action is derived as the MSR functional integral representation [29, 55, 56] of the KPZ equation, which reads

$$\partial_t \theta = \nu \nabla^2 \theta + \frac{\lambda}{2} (\nabla \theta)^2 + \eta, \quad (5.39)$$

where the stochastic noise η has zero mean, $\langle \eta(X) \rangle = 0$, and is Gaussian with second moment $\langle \eta(X) \eta(X') \rangle = 2\Delta \delta(X - X')$.

At this point, let us come back to the statement made in Sec. 5.3.1, saying that the action in Eq. (5.8) and the model for exciton-polaritons Eq. (5.10) entail the same universal long-wavelength physics. Indeed, taking the latter model as the starting point to integrate out density fluctuations leads us again to the KPZ action Eq. (5.37), however, with parameters [2]

$$\nu = K_c \left(\frac{K_d}{K_c} + \frac{u_c}{u_d} \right), \quad \lambda = -2K_c \left(1 - \frac{K_d u_c}{K_c u_d} \right), \quad \Delta = \frac{\gamma}{2\rho_0} \left(1 + \frac{u_c^2}{u_d^2} \right). \quad (5.40)$$

Note that if we set $K_d = 0$ both ν and λ reduce to the corresponding expressions in Eq. (5.38). On the other hand, the quantum vertex that is proportional to $\phi_c^* \phi_c \phi_q^* \phi_q$ in the action in Eq. (5.8) leads to the tree-level shift $\propto u_d \rho_0$ of the noise strength Δ in Eq. (5.38), which is absent in Eq. (5.40). Nevertheless, the fact that both can be mapped to the KPZ action confirms that the action Eq. (5.10) for exciton-polaritons describes the same universal long-wavelength physics as our microscopic model of bosons with loss and gain given by Eq. (5.8). There is, however, one caveat: in the special case that $K_c/K_d = u_c/u_d$, the KPZ non-linearity λ in Eq. (5.40) vanishes. Then the phase-only action reduces to simple diffusive Edwards-Wilkinson dynamics [80], corresponding to an effective thermal equilibrium at all wavelengths [29, 72–74] as discussed in Sec. 5.3.1 and detailed in Appendix 5.A. This situation, which corresponds to a fine tuning of parameters that is absolutely non-generic for driven-dissipative systems, can obviously not be realized in the microscopic model Eq. (5.8) where $K_d = 0$. Still it might arise asymptotically at low frequencies and long wavelengths, which is indeed the case for three-dimensional driven-dissipative condensates [51, 52]. In two spatial dimensions, though, the non-linear term in the KPZ equation is relevant in the RG sense and, therefore, grows under renormalization and strongly influences the physics at the largest scales.

What does this mean for the universal physics in two-dimensional driven-dissipative condensates? It is governed by the SCFP of the KPZ equation, which is genuinely non-perturbative. In particular, it has been shown in Ref. [81] that the SCFP is out of reach of perturbative RG at arbitrary order. This fixed point is fully attractive in 2D whereas the Gaussian equilibrium fixed point at which $\lambda = 0$ is repulsive, hence generically correlation functions will show non-trivial scaling behavior. From the point of view of performing practical calculations this implies that more elaborate methods than mean-field and perturbation theory are required – at least if one wishes to consider phenomena on asymptotically large scales. In fact, it is possible to estimate the length scale beyond which perturbative methods break down [2]. In this discussion it should be kept in mind that the phase field in the KPZ equation (5.39) is a compact variable, in contrast to the fluctuation height field the KPZ equation was originally devised to describe [9]. A compact field contains topological defects, which might thus

strongly influence the long-wavelength physics of 2D driven-dissipative systems, as has been shown to be the case in finite size systems in Ref. [50]. Here we neglect topological defects for the time being and comment on their role in Sec. 5.5.

To conclude this section let us comment on the relation of the approach presented here to Bogoliubov theory. The latter corresponds to integrating out Gaussian fluctuations of the complex fields ϕ_c and ϕ_q in a saddle-point approximation, i.e., eliminating *four* independent degrees of freedom at once instead of *three* (as one does when integrating out π and ζ), even though strictly speaking the saddle-point approximation is not valid for low-momentum modes in the Goldstone direction since the latter are not gapped, and consequently the classical equation of motion (or saddle-point equation) for the Goldstone mode θ involves only derivative terms and is thus solved by any spatially and temporally homogeneous configuration. We can recover the Bogoliubov result from our approach by expanding the transformation Eq. (5.32) about the arbitrarily chosen value $\theta = 0$, which yields

$$\begin{aligned}\phi_c &= \sqrt{\rho_0} + \frac{\pi}{2\sqrt{\rho_0}} + i\sqrt{\rho_0}\theta, \\ \phi_q &= \zeta.\end{aligned}\tag{5.41}$$

In the KPZ action Eq. (5.37) such an expansion in θ would amount to neglecting the non-linearity. Without the non-linearity, however, the KPZ action describes a free field coupled to a thermal bath. In other words, by performing a Bogoliubov approximation the non-equilibrium character that is intrinsic to the microscopic model with action (5.8) is lost in the long-wavelength limit.

5.4 Superfluid density of a driven-dissipative condensate

In this section we derive the result in Eq. (5.1) for the superfluid density. First we describe how the expectation value in Eq. (5.15) for the current-current response function can be evaluated in a saddle-point approximation, which results in an expression for the current-current response function that contains correlation functions of the phase variable θ and the response field $\tilde{\theta}$ introduced in the KPZ action (5.37) in the previous section. Then we use exact relations between these correlation functions and irreducible vertex functions in order to express the former in terms of low-frequency and low-momentum approximations to the latter, the form of which is determined by symmetries of the KPZ equation.

As stated in Sec. 5.2, the superfluid and normal densities are determined by the response current that is induced by a static force varying slowly in space. Since the physics on long scales is dominated by fluctuations of the massless Goldstone mode, we utilize in the following the hydrodynamic approach presented in Sec. 5.3.3 to calculate the current-current response function to lowest order in the saddle-point approximation for the integrals over ρ and ζ , while at the same time retaining unrestricted fluctuations of the phase. The first step is to express the classical and quantum currents in Eq. (5.15) in terms of the hydrodynamic variables ρ and θ . With the representation Eq. (5.32) of the complex fields, the classical and quantum currents, Eqs. (5.13) and (5.14) respectively, become

$$\begin{aligned}\mathbf{j}_c &= \frac{1}{m} \left[\rho \nabla \theta + \frac{1}{4} (\zeta_1 \nabla \zeta_2 - \zeta_2 \nabla \zeta_1 + |\zeta|^2 \nabla \theta) \right], \\ \mathbf{j}_q &= \frac{1}{m} \left[\sqrt{\rho} (\nabla \zeta_2 + 2\zeta_1 \nabla \theta) - \frac{1}{2\sqrt{\rho}} \zeta_2 \nabla \rho \right].\end{aligned}\tag{5.42}$$

Note, in particular, that \mathbf{j}_q is linear in the quantum fields and hence vanishes at the saddle point where $\zeta = 0$, i.e., a straightforward evaluation of the expectation value in the expression for the current-current response function in Eq. (5.15) in a saddle-point approximation yields zero. Let us illustrate the problem by drawing an analogy to a one-dimensional integral: then the product of classical and quantum fields in Eq. (5.15) is replaced by a function $f(x)$, and instead of performing a functional integral over the density and the quantum field ζ we wish to integrate over $x \in \mathbb{R}$. Specifically, we consider an integral of the form $I = \int_{-\infty}^{\infty} dx f(x) e^{-g(x)}$, where $g(x)$ corresponds to the Keldysh action Eq. (5.8) for the driven-dissipative system. In a saddle-point approximation one would evaluate $f(x)$ at the saddle point x_0 of $g(x)$, where $g'(x_0) = 0$, and expand $g(x)$ to quadratic order around x_0 , leading to $I \approx \int_{-\infty}^{\infty} dx f(x_0) e^{-g(x_0) - g''(x_0)(x-x_0)^2/2}$. However, as pointed out above, \mathbf{j}_q is linear in the quantum fields and vanishes at the saddle point, which corresponds to $f(x_0) = 0$ in our one-dimensional analogy and hence $I \approx 0$ in our simple approximation. Then finding the leading order approximation to the integral I requires us to expand $f(x)$ around x_0 [82]. Due to the symmetry of the integrand the first order expansion still gives $I \approx 0$ and one has to go to second order. In the case of the functional integral, however, we obtain a non-trivial result already for an expansions of \mathbf{j}_c and \mathbf{j}_q to lowest non-vanishing order in ζ ,

$$\begin{aligned}\mathbf{j}_c &= \frac{\rho_0}{m} \nabla \theta, \\ \mathbf{j}_q &= \frac{\sqrt{\rho_0}}{m} (\nabla \zeta_2 + 2\zeta_1 \nabla \theta).\end{aligned}\tag{5.43}$$

These expressions do not involve density fluctuations and, therefore, in the expectation value in Eq. (5.15) the integral over π can be evaluated as in Eq. (5.36), leading to a δ -functional that allows us to express ζ_2 in terms of ζ_1 . Replacing the latter by the KPZ response field $\tilde{\theta} = i2\sqrt{\rho_0}\zeta_1$ we obtain the following expression for the current-current response function:

$$\chi_{ij}(X - X') = \chi_{ij}^{(1)}(X - X') + \chi_{ij}^{(2)}(X - X'),\tag{5.44}$$

with two contributions involving, respectively, two and three-point correlation functions of the phase variable, where averages are taken with respect to the KPZ action Eq. (5.37),

$$\chi_{ij}^{(1)}(X - X') = \frac{u_c \rho_0}{2m^2 u_d} \langle \partial_i \theta(X) \partial_j \tilde{\theta}(X') \rangle,\tag{5.45}$$

$$\chi_{ij}^{(2)}(X - X') = \frac{\rho_0}{m^2} \langle \partial_i \theta(X) \partial_j \theta(X') \tilde{\theta}(X') \rangle.\tag{5.46}$$

Let us first consider the contribution Eq. (5.45), which after Fourier transformation and at vanishing external frequency becomes

$$\chi_{ij}^{(1)}(Q) = \frac{u_c \rho_0}{2m^2 u_d} q_i q_j G(Q),\tag{5.47}$$

where $G(Q)$ is the retarded response function

$$G(Q) \delta(Q + Q') = \int_X e^{i(QX + Q'X')} \langle \theta(X) \tilde{\theta}(X') \rangle = \langle \theta(Q) \tilde{\theta}(Q') \rangle.\tag{5.48}$$

Similarly, Fourier transformation of Eq. (5.46) involving the three-point function yields

$$\chi_{ij}^{(2)}(Q) = -\frac{\rho_0}{m^2} q_i \int_{Q'} q'_j G_{112}(Q, Q').\tag{5.49}$$

Our notation, which we choose for later convenience, indicates that G_{112} is the average value of a product of fields involving twice the phase field $\theta_1 = \theta$ and once the response field $\theta_2 = \tilde{\theta}$. Moreover, as in Eq. (5.48) we have singled out a δ -function, which expresses invariance under spacial and temporal translations and hence fixes the third argument in the Fourier transform of G_{112} ,

$$G_{112}(Q_1, Q_2)\delta(Q_1 + Q_2 + Q_3) = \langle \theta(Q_1)\theta(Q_2)\tilde{\theta}(Q_3) \rangle. \quad (5.50)$$

Let us recall the discussion in Sec. 5.2, which showed that the superfluid density is determined by the contribution to the current-current response function which is proportional to $q_i q_j$, whereas the coefficient of δ_{ij} is the normal density. Thus by inspection of the momentum dependence in Eqs. (5.47) and (5.49) we see that the normal density vanishes at the present level of approximation. In fact, the present approach of completely neglecting excitations of density fluctuations is analogous to keeping only the zero-loop diagram in Fig. 1 of Ref. [26] – which still gives a non-trivial result due to the non-equilibrium fluctuations of the phase at the SCFP of the KPZ equation. The leading contribution to the normal density, however, is encoded in diagrams involving fluctuations of the density at one-loop order.

Note that evaluating Eqs. (5.47) and (5.49) in a Gaussian approximation would lead to a result for the superfluid density that is completely different from the one reported in Eq. (5.1). The Gaussian approximation consists in neglecting the non-linear term in the KPZ action (5.37) or, on the level of complex bosonic fields in the original action (5.8), to a Bogoliubov expansion in fluctuations $\delta\phi_c = \phi_c - \phi_0$ and $\delta\phi_q = \phi_q$ around the mean-field values of the classical and quantum fields. Then the expectation values in Eqs. (5.47) and (5.49) can be evaluated straightforwardly: since all odd moments of Gaussian distributed variables vanish, the contribution (5.49) to the current-current response function evaluates to zero, while the retarded response function in Eq. (5.47) reduces to its bare value

$$G_0(Q) = \frac{i}{\omega + i\nu_0 q^2}, \quad (5.51)$$

where we have added a subscript in ν_0 to emphasize that we mean the microscopic value of this quantity, $\nu_0 = K_c u_c / u_d$, reported in Eq. (5.38), which, in particular, does not scale with system size like the renormalized quantities appearing in Eq. (5.1). Inserting the bare retarded response function in Eq. (5.47) and with Eq. (5.4) we find the superfluid density in the Gaussian approximation,

$$\rho_{s,0} = \frac{u_c \rho_0}{2m u_d \nu_0}. \quad (5.52)$$

As pointed out in Ref. [26], the crucial point leading to a finite value of the superfluid density in the Gaussian approximation is the scaling of the bare retarded response function with momentum as $G_0(0, \mathbf{q}) \sim 1/q^2$, which should be contrasted with the KPZ result $G(0, \mathbf{q}) \sim 1/q^{2-\chi}$, obtained from scaling analysis as described below around Eq. (5.53), or from the explicit expression Eq. (5.69) upon identifying the smallest possible momentum with the inverse system size $q \sim 1/L$. Remarkably, if the expectation values in Eqs. (5.47) and (5.49) are evaluated with the KPZ action (5.37) as we do in the following, it turns out that the mechanism leading to a non-vanishing superfluid density in Eq. (5.1) in the thermodynamic limit is an entirely different one: In fact, the contribution from the response function in Eq. (5.47) vanishes for $L \rightarrow \infty$, while the three-point function in Eq. (5.49) can be related to the characteristic non-linear term in the KPZ action (5.37), which is already hinted at by the observation that both have exactly the same structure of derivatives and fields. The coupling λ of the non-linear vertex in Eq. (5.37) is protected from renormalization by symmetries of the KPZ

equation [18, 19, 29, 55]. Then, the precise combination of λ with powers of the renormalized values of the diffusion constant ν and the noise strength Δ that appear in the evaluation of Eq. (5.49) gives just the dimensionless KPZ coupling $g = \lambda^2 \Delta / \nu^3$, which takes a universal value g_* at the SCFP, leading to the second term in the expression for the superfluid density (5.1), which remains finite even in the thermodynamic limit. In other words, whereas in the Gaussian approximation the contribution to the superfluid density due to Eq. (5.47) is finite while the one from the three-point function in Eq. (5.49) vanishes for $L \rightarrow \infty$, non-equilibrium fluctuations at the SCFP of the KPZ equation lead to exactly the opposite conclusion.

In fact, before going into the details of the derivation of the expression for the superfluid density in Eq. (5.1), let us show that this conclusion can already be drawn from a simple scaling analysis for the two terms in the current-current response function in Eq. (5.44). Crucially, the superfluid density follows from the current-current response function for zero frequency and for $\mathbf{q} \rightarrow \mathbf{0}$, which is precisely the limit in which scaling analysis applies. Note that these considerations – as well as the detailed calculation of ρ_s presented below – rely on a knowledge of the value of the roughness exponent χ at the SCFP. This value has to be determined by resorting to renormalization group methods [17–19] or numerics [20–25]. Indeed it is nothing but the scaling dimension of the phase, i.e., we have $[\theta(X)] = -\chi$. Here we are counting momentum dimensions such that $[q] = 1$ and for the integration measures of time and space we find $[dt] = -z$ and $[d\mathbf{x}] = -d$ with the dynamical exponent z . The scaling dimension of the response field is $[\tilde{\theta}(X)] = -\tilde{\chi}$. Then the Fourier transform of the contribution to the current-current response function in Eq. (5.45) scales as

$$[\chi_{ij}^{(1)}(0, \mathbf{q})] = -z - d + 2 - \chi - \tilde{\chi} = \chi, \quad (5.53)$$

where we used that $[\partial/\partial x] = [q] = 1$ and the second equality follows from the scaling relations $d + \chi + \tilde{\chi} = 0$ and $\chi + z = 2$ [55] which in turn follow from symmetries of the KPZ equation. Thus we obtain precisely the finite size scaling of the first term in Eq. (5.1) (note that $[L] = [1/q] = -1$ so that in fact Eq. (5.53) implies $\chi_{ij}^{(1)}(0, \mathbf{q}) \sim L^{-\chi}$). Let us proceed to show that also the scale-invariance of the second term in this equation can be deduced using scaling arguments. Indeed, for the Fourier transform of the contribution to the current-current response function in Eq. (5.46) we find

$$[\chi_{ij}^{(2)}(0, \mathbf{q})] = -z - d + 2 - 2\chi - \tilde{\chi} = 0, \quad (5.54)$$

where we used the same scaling relations as above. We note that the contributions to \mathbf{j}_c in Eq. (5.42), which we neglect in the saddle-point approximation, contain additional powers of $\tilde{\theta}$, scaling quickly to zero as $L^{-\chi-d}$, and hence omitting these terms is consistent with the scaling analysis. These considerations shows that scaling analysis allows us to correctly predict the dependence of the superfluid density on the size of the system – however, to obtain the precise form of prefactors in the expression for ρ_s in Eq. (5.1), we have to evaluate explicitly the expectation values in Eqs. (5.47) and (5.49).

The main obstacle we are facing in this endeavor is due to the fact that the fluctuations over which we have to average are governed by the SCFP of the KPZ equation, which makes it difficult to perform analytical calculations as pointed out above at the end of Sec. 5.3.3. One of the few methods that allows one to make progress even under strong-coupling conditions without resorting to numerics from the very beginning (note that the averages we are interested in contain the response field $\tilde{\theta}$, i.e., they are even not accessible to a direct simulation of the KPZ equation (5.39) without introducing additional source terms and performing a demanding linear response analysis) is the functional renormalization group [83–87], which has been adopted to the KPZ equation in Refs. [17–19]. The

functional renormalization group is based on an exact RG flow equation, the solution of which corresponds to continuously including fluctuations, starting from a microscopic scale and proceeding up to the largest relevant scale in the problem, which is typically determined by the size of the system L . Approximate solutions to this flow equation have to possess the symmetries of the underlying microscopic model, which are in fact conserved in the RG flow. A very thorough discussion of the symmetries of the KPZ equation can be found in Ref. [18]. For our present purposes, the attractiveness of such an approach lies in the fact, that beyond giving the phase diagram and scaling behavior at fixed points, the resultant approximate expression for the effective action encodes information on arbitrary correlation and vertex functions. To be precise, the effective action is the generating functional of irreducible vertex functions [57–59, 88], for which exact relations with correlation functions exist [88]. In the following we review the derivation of such relations that allow us to express the two-point and three-point functions in Eqs. (5.48) and Eq. (5.50) in terms of irreducible vertices. Then it remains to find approximate expressions for these irreducible vertices. In order to do so we will rely on the same guiding principles that lead to the ansatz for the effective action in Refs. [17–19], i.e., the symmetries of the KPZ equation. This ansatz yielded not only quantitatively reasonable values of the scaling exponents in the strong-coupling phase of the KPZ equation in physical dimensions ($d = 1, 2, 3$), but also remarkably good results for scaling functions and amplitude ratios [18, 19, 89], which hence gives us confidence in the validity of our approximation. The latter effectively amounts to retaining only the leading contributions in the limit of low frequencies and momenta in the expressions for the irreducible vertex functions, as appropriate for the evaluation of the current-current response at zero frequency and in the limit $\mathbf{q} \rightarrow \mathbf{0}$. Below we show that these leading contributions follow straightforwardly from the Ward identities associated with the various symmetries of the KPZ equation.

Let us now proceed to find the explicit form of the correlation functions in Eqs. (5.48) and (5.50). Our strategy is to first relate these correlation functions to irreducible vertex functions and then approximate the latter by their low frequency and momentum expansions, which are essentially determined by symmetries of the KPZ equation. Starting point for the derivation of exact relations between correlation and vertex functions [88] is the generating functional for correlation functions,

$$Z[h, \tilde{h}] = \int \mathcal{D}[\theta, i\tilde{\theta}] e^{-S + \int_x (h\theta + \tilde{h}\tilde{\theta})}. \quad (5.55)$$

(We note that with this convention for coupling external sources h and \tilde{h} to the phase θ and response field $\tilde{\theta}$ a physical source field would be denoted by \tilde{h} whereas h corresponds to an causality violating, i.e., unphysical, field. This is different from the convention usually used in the Keldysh formalism [55, 56], according to which a classical field couples to a “quantum source” and vice versa.) Connected correlation functions can then be derived by taking derivatives of the functional $W = \ln Z$ with respect to the sources. In particular, we have for the expectation values of θ and the response field $\tilde{\theta}$ (note that these expectation values are taken in the presence of the auxiliary fields h and \tilde{h} ; we do not indicate this explicitly in the notation),

$$\begin{aligned} \varphi(X) = \langle \theta(X) \rangle &= \frac{\delta W}{\delta h(X)}, \\ \tilde{\varphi}(X) = \langle \tilde{\theta}(X) \rangle &= \frac{\delta W}{\delta \tilde{h}(X)}. \end{aligned} \quad (5.56)$$

To make the notation more compact in the following we introduce indices to distinguish between θ and the response field $\tilde{\theta}$, i.e., we set $\theta_1 = \theta, \theta_2 = \tilde{\theta}$ (and correspondingly for the expectation values

φ and $\tilde{\varphi}$ and the sources h and \tilde{h}), and use numbers to indicate both the field index $\alpha = 1, 2$ and coordinates, e.g., $1 \equiv (\alpha_1, X_1)$ such that $\theta(1) = \theta_{\alpha_1}(X_1)$ and $\int_1 \equiv \sum_{\alpha_1=1,2} \int_{X_1}$. Moreover, for functional derivatives we use the shorthand notation

$$\begin{aligned} \frac{\delta^n Z}{\delta h(1)\delta h(2)\cdots\delta h(n)} &= \langle \theta(1)\theta(2)\cdots\theta(n) \rangle = G(1, 2, \dots, n), \\ \frac{\delta^n W}{\delta h(1)\delta h(2)\cdots\delta h(n)} &= W(1, 2, \dots, n), \\ \frac{\delta^n \Gamma}{\delta \varphi(1)\delta \varphi(2)\cdots\delta \varphi(n)} &= \Gamma(1, 2, \dots, n). \end{aligned} \quad (5.57)$$

The functional Γ in the last equation is the effective action, which generates one-particle irreducible vertex functions, and is the Legendre transform of the generating functional W ,

$$\Gamma = -W + \int_1 h(1)\varphi(1). \quad (5.58)$$

We obtain the basic relation between correlation functions and vertex functions (or, in other words, between derivatives of W and Γ), from which all others can be derived by taking functional derivatives, from the following sequence of equalities:

$$\begin{aligned} \delta(1-2) &= \frac{\delta \varphi(1)}{\delta \varphi(2)} = \frac{\delta^2 W}{\delta h(1)\delta \varphi(2)} = \int_3 \frac{\delta^2 W}{\delta h(1)\delta h(3)} \frac{\delta h(3)}{\delta \varphi(2)} \\ &= \int_3 \frac{\delta^2 W}{\delta h(1)\delta h(3)} \frac{\delta^2 \Gamma}{\delta \varphi(3)\delta \varphi(2)} = \int_3 W(1, 3)\Gamma(3, 2). \end{aligned} \quad (5.59)$$

In the second equality we used Eq. (5.56), the third one is just the chain rule and in the fourth one we replaced the source $h(3)$ by $h(3) = \Gamma(3)$. The latter relation which follows from Eq. (5.58). Note that since functional derivatives commute the order of arguments of W and Γ is arbitrary. Differentiating the basic relation (5.59) – which in fact is just the statement that the irreducible vertex $\Gamma(3, 2)$ is the inverse of the connected correlation function $W(1, 3)$ – with respect to $\varphi(3)$ yields

$$\int_{4,5} W(1, 4, 5)\Gamma(5, 3)\Gamma(4, 2) = - \int_4 \Gamma(2, 3, 4)W(4, 1). \quad (5.60)$$

This equation can be solved for the connected three-point function by multiplying it with $W(3, 6)W(2, 7)$ and taking the integral over 2 and 3. Using Eq. (5.59), this results in

$$W(1, 2, 3) = - \int_{4,5,6} \Gamma(4, 5, 6)W(1, 4)W(5, 2)W(6, 3). \quad (5.61)$$

The relations (5.59) and (5.61) hold for arbitrary values of the external sources h and \tilde{h} . Setting them both to zero, we may assume without loss of generality that the expectation values Eq. (5.56) vanish and consequently the connected two-point and three-point functions become equal to the disconnected ones, which can be obtained by taking functional derivatives of Z (cf. the first line in Eq. (5.57)), i.e., we have

$$\begin{aligned} W(1, 2) &= G(1, 2) = G_{\alpha_1\alpha_2}(X_1, X_2) = \langle \theta_{\alpha_1}(X_1)\theta_{\alpha_2}(X_2) \rangle, \\ W(1, 2, 3) &= G(1, 2, 3) = G_{\alpha_1\alpha_2\alpha_3}(X_1, X_2, X_3) = \langle \theta_{\alpha_1}(X_1)\theta_{\alpha_2}(X_2)\theta_{\alpha_3}(X_3) \rangle. \end{aligned} \quad (5.62)$$

Thus Eqs. (5.59) and (5.61) are in fact the desired relations between vertex and correlation functions. In the present form, however, they are not very transparent, so let us proceed to make them more explicit by specifying the field indices. Then we can rewrite Eq. (5.59) as

$$\int_{X_3} \begin{pmatrix} C(X_1 - X_3) & G(X_1 - X_3) \\ G(X_3 - X_1) & 0 \end{pmatrix} \begin{pmatrix} 0 & \Gamma_{12}(X_3 - X_2) \\ \Gamma_{12}(X_2 - X_3) & \Gamma_{22}(X_3 - X_2) \end{pmatrix} = \delta(X_1 - X_2) \mathbb{1}, \quad (5.63)$$

where we exploited the fact that due to temporal and spatial translational invariance the correlation and vertex functions depend only on differences of coordinates. Here and in the following we denote the two-point response and correlation functions by G and C , respectively,

$$\begin{aligned} G(X - X') &= G_{12}(X, X') = \langle \theta_1(X) \theta_2(X') \rangle = \langle \theta(X) \tilde{\theta}(X') \rangle, \\ C(X - X') &= G_{11}(X, X') = \langle \theta_1(X) \theta_1(X') \rangle = \langle \theta(X) \theta(X') \rangle. \end{aligned} \quad (5.64)$$

Note that both G_{22} and Γ_{11} vanish due to causality [55, 56]. The matrix equation (5.63) can be inverted straightforwardly after taking the Fourier transform, which yields

$$\begin{pmatrix} C(Q) & G(Q) \\ G(-Q) & 0 \end{pmatrix} = \begin{pmatrix} -\Gamma_{22}(Q)/(\Gamma_{12}(Q)\Gamma_{12}(-Q)) & 1/\Gamma_{12}(-Q) \\ 1/\Gamma_{12}(Q) & 0 \end{pmatrix}. \quad (5.65)$$

From this relation we obtain approximate expressions for the response and correlation functions by inserting for the vertex functions the respective low-frequency and low-momentum expansions. These follow directly from the Ward identity associated with the shift-gauged symmetry of the KPZ equation [18, 19]: indeed this symmetry entails that the coefficient of the term $\int_X \tilde{\theta} \partial_t \theta$ in the KPZ action (5.37) is not renormalized, i.e., exactly the same term appears also in the effective action and we have

$$\Gamma_{12}(\omega, \mathbf{0}) = i\omega. \quad (5.66)$$

Rotational invariance implies that the lowest order contribution to an expansion in powers of \mathbf{q} is proportional to q^2 . This leads to

$$\Gamma_{12}(\omega, \mathbf{q}) = i\omega + \nu q^2 + O(\omega^2, \omega q^2, q^4). \quad (5.67)$$

At the strong-coupling fixed point the coefficient ν obeys the finite-size scaling $\nu \sim \nu_* L^\chi$ [55], where ν_* is a non-universal constant. For the Γ_{22} vertex there is no restriction from the shift-gauged symmetry and, therefore, its leading contribution in the limit of vanishing frequency and momentum is just a constant,

$$\Gamma_{22}(\omega, \mathbf{q}) = -2\Delta + O(\omega, q^2), \quad (5.68)$$

which scales with system size as $\Delta \sim \Delta_* L^{3\chi+d-2}$ [55]. Plugging Eqs. (5.67) and (5.68) into Eq. (5.65) yields the low-frequency and low-momentum scaling forms of the response and correlation functions

$$\begin{aligned} G(Q) &= \frac{i}{\omega + i\nu q^2}, \\ C(Q) &= 2\Delta |G(Q)|^2 = \frac{2\Delta}{\omega^2 + \nu^2 q^4}. \end{aligned} \quad (5.69)$$

Having found the two-point functions, we proceed by specifying the field indices in Eq. (5.61) for the three-point function to the values required in the current-current response function Eq. (5.49), i.e., $\alpha_1 = \alpha_2 = 1$ and $\alpha_3 = 2$. Then we find

$$G_{112}(X_1, X_2, X_3) = - \sum_{\alpha_4, \alpha_5} \int_{X_4, X_5, X_6} \Gamma_{\alpha_4 \alpha_5 1}(X_4, X_5, X_6) G_{1\alpha_4}(X_1, X_4) G_{1\alpha_5}(X_2, X_5) G_{21}(X_3, X_6), \quad (5.70)$$

where we used again that due to causality $G_{22} = 0$, which fixes the value of α_6 to 1. Performing the remaining sums over α_4 and α_5 and taking the Fourier transform of the resulting expression we obtain

$$G_{112}(Q, Q') = -(\Gamma_{122}(-Q - Q', Q)G(Q)G(Q') + \Gamma_{112}(-Q - Q', Q)C(Q)G(Q') + \Gamma_{112}(Q', -Q - Q')C(Q')G(Q))G(Q + Q'). \quad (5.71)$$

Here we adopt the notation of Refs. [17–19]: in Fourier space we omit the third argument of the three-point function and the irreducible vertices, which is determined by frequency and momentum conservation. In order to make progress with Eq. (5.71) we have to specify the vertex functions. Let us restrict ourselves to the lowest order in frequency and momentum and consider the following ansatz,

$$\Gamma_{112}(\omega, \mathbf{q}, \omega', \mathbf{q}') = \gamma_1 + \gamma_2(\omega + \omega') + \gamma_3 \mathbf{q} \cdot \mathbf{q}' + \gamma_4(q^2 + q'^2), \quad (5.72)$$

which incorporates rotational invariance and symmetry of $\Gamma_{112}(Q, Q')$ under exchange of its arguments, as follows from the commutativity of the functional derivatives with respect to $\varphi(Q)$ and $\varphi(Q')$. The shift-gauged symmetry of the KPZ action implies [18, 19]

$$\Gamma_{112}(\omega, \mathbf{0}, \omega', \mathbf{q}') = \gamma_1 + \gamma_2(\omega + \omega') + \gamma_4 q'^2 = 0, \quad (5.73)$$

leading to $\gamma_1 = \gamma_2 = \gamma_4 = 0$. We are left with a single parameter γ_3 , which is in fact determined by another symmetry of the KPZ action: the ansatz (5.72) leads to the first equality in

$$\gamma_3 = \frac{1}{d} \nabla_{\mathbf{q}} \cdot \nabla_{\mathbf{q}'} \Gamma_{112}(Q, Q') \Big|_{Q=Q'=0} = -i\lambda \frac{\partial}{\partial \omega} \Gamma_{12}(\omega, \mathbf{0}) \Big|_{\omega=0} = \lambda, \quad (5.74)$$

whereas in the second one we used the Ward identity associated with the Galilean symmetry of the KPZ equation [18, 19] in order to express the derivatives with respect to momenta of the vertex Γ_{112} in terms of a derivative with respect to frequency of the lower order vertex function Γ_{12} , for which we then inserted Eq. (5.66). Thus we have

$$\Gamma_{112}(\omega, \mathbf{q}, \omega', \mathbf{q}') = \lambda \mathbf{q} \cdot \mathbf{q}', \quad (5.75)$$

which is again just the bare vertex already present in the action (5.37). Renormalization of this vertex might occur only at higher orders in an expansion in powers of frequency and momentum. An analogous treatment for the vertex Γ_{122} leads us to

$$\Gamma_{122}(\omega, \mathbf{q}, \omega', \mathbf{q}') = \kappa q^2. \quad (5.76)$$

Again, the absence of a constant term and of terms proportional to the frequency and to q'^2 follows from the shift-gauged symmetry. However, this vertex is not symmetric with respect to exchange of its arguments and, therefore, the presence of a term $\propto q^2$ with an unknown coefficient κ cannot be excluded. Nevertheless, applying the same logic that lead to $\gamma_3 = \lambda$ in Eq. (5.74), shows that there is no contribution $\propto \mathbf{q} \cdot \mathbf{q}'$ in Γ_{122} .

With the expressions for the response, correlation, and vertex functions, we proceed to evaluate the two contributions to the current-current response function, Eqs. (5.47) and (5.49), at vanishing frequency. We find

$$\chi_{ij}^{(1)}(0, \mathbf{q}) = \frac{u_c \rho_0}{2m^2 u_d \nu} \frac{q_i q_j}{q^2}, \quad (5.77)$$

leading to a contribution to the superfluid density

$$\rho_s^{(1)} = \frac{u_c \rho_0}{2m u_d \nu} \sim \frac{u_c \rho_0}{2m u_d \nu_*} L^{-\chi}, \quad (5.78)$$

which vanishes in the thermodynamic limit $L \rightarrow \infty$. Note that precisely this contribution involving the two-point response function remains finite in a Gaussian approximation in which $G_0(0, \mathbf{q}) \sim 1/q^2$. Let us turn now to the evaluation of Eq. (5.49), which can be rewritten as

$$\begin{aligned} \chi_{ij}^{(2)}(0, \mathbf{q}) = \frac{\rho_0}{m^2} q_i \int_{Q'} q'_j \left[\kappa |\mathbf{q} - \mathbf{q}'|^2 G(0, \mathbf{q}) G(\omega', \mathbf{q}') \right. \\ \left. - \lambda (\mathbf{q} + \mathbf{q}') \cdot (\mathbf{q} C(0, \mathbf{q}) G(\omega', \mathbf{q}') + \mathbf{q}' G(0, \mathbf{q}) C(\omega', \mathbf{q}')) \right] G(\omega', \mathbf{q} + \mathbf{q}'). \end{aligned} \quad (5.79)$$

The integral over ω' of the product $G(\omega', \mathbf{q}') G(\omega', \mathbf{q} + \mathbf{q}')$ vanishes since the integrand has poles only in the lower half-plane; hence there is no contribution $\propto \kappa$ and also the first term $\propto \lambda$ does not contribute to the current-current response function. For the remaining integral over frequency we find

$$\int_{\omega'} C(\omega', \mathbf{q}') G(\omega', \mathbf{q} + \mathbf{q}') = \frac{\Delta}{v^2 q'^2} \frac{1}{q'^2 + |\mathbf{q} + \mathbf{q}'|^2}. \quad (5.80)$$

The integral over the momentum \mathbf{q}' can be carried out exactly in 2D and we obtain

$$\chi_{ij}^{(2)}(0, \mathbf{q}) = -\frac{\ln 2}{8\pi} \frac{\lambda \Delta \rho_0}{m^2 \nu^3} \frac{q_i q_j}{q^2}, \quad (5.81)$$

which yields the contribution to the superfluid density

$$\rho_s^{(2)} = -\frac{\ln 2}{8\pi} \frac{\lambda \Delta \rho_0}{m \nu^3} \sim \frac{\ln 2}{8\pi} g_* \rho_0, \quad (5.82)$$

where we used $m = -1/\lambda$ (cf. Eq. (5.38)) and expressed the final result in terms of the universal value g_* of the dimensionless KPZ coupling $g = \lambda^2 \Delta / \nu^3$ [18, 19, 55]. The sum of Eqs. (5.78) and (5.82) yields the final result (5.1) stated in Sec. 5.1.

5.5 The influence of topological defects

The calculation of the superfluid density presented in Sec. 5.4 neglects the influence of topological defects that might occur in the compact phase field θ . At present it is not known to us what the precise limitations of the validity of this approach are, and in this section we only briefly discuss the issue based on several scenarios for the possible behavior of vortices in 2D driven-dissipative systems. The difficulty with rigorously incorporating vortices in our treatment is rooted in the fact that the KPZ equation (5.39) is non-linear. Indeed, setting the non-linearity λ to zero, the KPZ equation reduces to purely diffusive dynamics, which describes relaxation to a thermodynamic equilibrium at a temperature set by the noise strength Δ . In order to evaluate time-independent observables in the stationary equilibrium state, in this case it is sufficient to consider the thermodynamic partition function $Z = \int \mathcal{D}[\theta] e^{-S}$, where the functional integral is over static configurations $\theta = \theta(\mathbf{x})$ of the phase field and the action is given by $S = \frac{\nu}{\Delta} \int_{\mathbf{r}} (\nabla \theta)^2$. Close to the BKT transition, the crucial contributions to the partition function come from configurations of the phase field which solve the classical field

equation $\delta S/\delta\theta = 0$ and contain vortices [58, 90]. Due to the linearity of the field equation, one can form superpositions of the single-vortex solution and therefore the relevant field configurations can be parameterized simply by listing the positions of vortex cores. Then the functional integral in the partition function can be approximated by a sum over all possible numbers of vortices and ordinary integrals over the vortex positions. On the other hand, for a finite value of λ in the KPZ equation (5.39), the stationary probability distribution of the phase field is not known (in particular, it is not simply the Boltzmann weight as in the equilibrium case), and therefore one has to consider dynamical configurations of the phase $\theta = \theta(t, \mathbf{x})$, i.e., solutions to the field equation $\delta S_{\text{KPZ}}/\delta\theta = 0$ with the KPZ action (5.37), containing several vortices (in fact, due to the complex structure of vortices in the complex Ginzburg-Landau equation [91], it might even be necessary to resort to the original action Eq. (5.8)). However, the KPZ equation is non-linear, so that linear superpositions of dynamical single-vortex configurations do not yield solutions to the field equation. Hence the approach taken in equilibrium cannot be extended to the driven-dissipative case straightforwardly. Let us, therefore, take what is known about the BKT transition in equilibrium as the starting point and content ourselves with speculations on how this scenario might change for small values of the bare dimensionless KPZ non-linearity $g = \lambda^2\Delta/\nu^3$.

If the critical temperature Δ_c of the BKT transition is approached from larger values $\Delta > \Delta_c$, the correlation length diverges as $\xi \sim \xi_0 \exp(b/\sqrt{\Delta - \Delta_c})$, where ξ_0 is a microscopic length scale and b is a non-universal number, i.e., at high temperatures correlations are strongly suppressed at distances $r > \xi$ due to the presence of free vortices. For a small value $g \ll 1$ of the bare dimensionless KPZ non-linearity, this picture applies still if the correlation length ξ is smaller than the characteristic KPZ length $L_* \sim \xi'_0 \exp(a/\Delta)$ which was identified in Ref. [2], and where again ξ'_0 is a microscopic length scale and the parameter $a = 8\pi\nu^3/\lambda$ is determined by the bare values of ν and λ given in Eq. (5.38). Here we consider ξ and L_* as functions of the noise strength Δ , however, in experiments with exciton-polaritons the natural tuning parameter is the pump rate γ_p , which enters the noise strength Δ given in Eq. (5.38) via its dependence on the mean-field density $\rho_0 = -r_d/u_d = (\gamma_p - \gamma_l)/(2u_d)$. Universal scaling behavior governed by the SCFP of the KPZ equation in 2D sets in at length scales above L_* , hence the regime of interest for us is $L_* < \xi$. The latter is obviously realized for $\Delta < \Delta_c$. Then the renormalized value of g becomes sizable and we expect that the dynamics of vortices will be influenced by the fluctuations of the non-topological part of the phase field, which are governed by the KPZ equation. Let us assume that under these conditions vortices lead to exponential decay of correlations and invalidate KPZ scaling on length scales larger than a characteristic scale L_ν , which might be different from the correlation length ξ in equilibrium. How would the existence of such a scale affect the validity of the result (5.1) for the superfluid density? Several options, which are listed below and illustrated in Fig. 5.2, are possible.

- (a) $L_\nu \approx L_*$, i.e., vortices proliferate at the scale where the strong coupling regime of the KPZ equation is reached. Then in a large system $L > L_\nu$ correlations of the order parameter field would decay exponentially and the superfluid density would vanish as in the high-temperature phase of a 2D system in equilibrium.
- (b) $L_* < L_\nu < \infty$, so that in systems with size L that satisfies $L_* < L < L_\nu$ stretched-exponential decay of correlations would be observed, and the superfluid density would indeed be given by Eq. (5.1) for this specific range of system sizes. However, in large systems $L > L_\nu$ the superfluid density would again drop to zero.

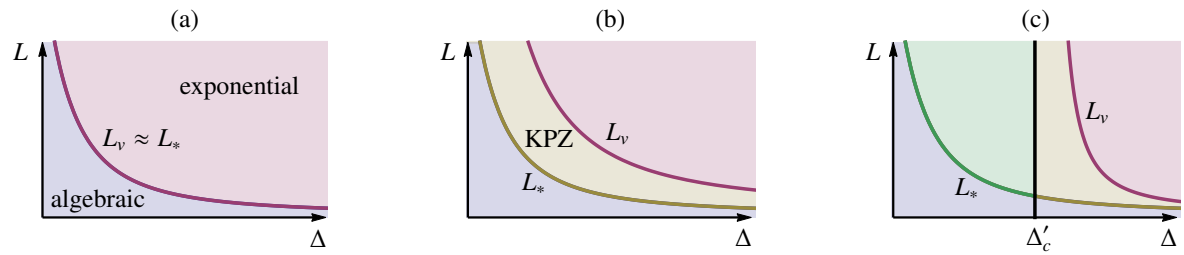


Figure 5.2. Possible phase diagrams of a 2D driven-dissipative system in terms of the noise strength Δ and the system size L (both are measured in arbitrary units): (a) The scale L_v at which vortices proliferate coincides with the characteristic KPZ scale L_* , which thus marks the transition from algebraic to exponential decay of correlations. (b) For $L_* < L_v < \infty$ there is a range of system sizes in which KPZ universality prevails, i.e., order parameter correlations decay stretched-exponentially and the superfluid density is given by Eq. (5.1). (c) Non-equilibrium BKT transition at $\Delta = \Delta'_c$: the low-noise phase is governed by the SCFP of the KPZ equation up to macroscopic scales. Above Δ'_c the situation is as described in (b).

- (c) The most intriguing case, however, would be the existence of a non-equilibrium BKT transition, i.e., the existence of a critical value Δ'_c of the noise strength such that $L_v \rightarrow \infty$ for $\Delta < \Delta'_c$. Then our result Eq. (5.1) for the superfluid density would be valid in the low-noise phase, where it would be accompanied by stretched-exponential decay of correlations.

Finding out which of these scenarios is realized in 2D driven-dissipative systems will be the objective of further studies. Note that the recent numerical work reported in Ref. [50] is not indicative of the answer to this question, since there system sizes $L < L_*$, corresponding to a choice of parameters that is relevant for present experimental setups, have been considered.

5.A Equilibrium symmetry in the density-phase representation

As stated in Sec. 5.3.1, there is a specific symmetry that distinguishes thermodynamic equilibrium from non-equilibrium stationary states. In particular, the response functional for a classical dynamical system [29, 55, 56, 58, 67], or the classical limit of a Keldysh action that describes the dynamics of a corresponding quantum system, possesses this symmetry only if the system resides in equilibrium. This is the case, e.g., for model A^* , which we mentioned as the special instance of the Keldysh action Eq. (5.10) that is realized if the parameters appearing in the action satisfy the condition stated in Eq. (5.11). In a driven-dissipative system, where coherent and dissipative contributions to the Keldysh action have clearly distinct physical origins, this condition amounts to an unphysical fine-tuning and is generically violated, resulting in the appearance of the characteristic KPZ non-linearity proportional to λ , which is given in Eq. (5.40), in the action for the condensate phase.

While the equilibrium symmetry transformation has been specified for classical and quantum fields, in terms of which model A^* and Eq. (5.10) are formulated, in Refs. [52, 67–70], here we derive a representation that can be applied directly to the action for the phase of the classical field, i.e., the order parameter, which allows us to demonstrated that the appearance of the non-linear term in the

KPZ action (5.37) is indicative of non-equilibrium conditions. This is of particular interest in the case of a one-dimensional system, where the KPZ equation “accidentally” satisfies detailed balance [29] – which can again be seen as following from a specific symmetry given in Eq. (5.90) below – and hence can occur also in thermodynamic equilibrium (see, e.g., Ref. [92]). Then the form of the equilibrium symmetry transformation Eq. (5.89) we derive below shows that the 1D KPZ equation, if it emerges as the dynamical equation for the phase of a driven-dissipative condensate, should indeed be regarded as describing non-equilibrium conditions.

The Keldysh action in the classical limit for a system with coherent and dissipative dynamics describes thermodynamic equilibrium at a temperature T , if there exists a real parameters r , the meaning of which is specified below, such that the following transformation [52] is a symmetry of the action:

$$\begin{aligned}\mathcal{T}\Phi_c(t, \mathbf{x}) &= \sigma_x \Phi_c(-t, \mathbf{x}), \\ \mathcal{T}\Phi_q(t, \mathbf{x}) &= (r\mathbb{1} - i\sigma_z) \sigma_x \left(\frac{r\mathbb{1} + i\sigma_z}{1 + r^2} \Phi_q(-t, \mathbf{x}) + \frac{i}{T} \partial_t \Phi_c(-t, \mathbf{x}) \right).\end{aligned}\quad (5.83)$$

Here we collect fields and their complex conjugates in spinors, $\Phi_\nu = (\phi_\nu, \phi_\nu^*)^T$, with $\nu = c, q$ indicating classical and quantum fields; σ_x and σ_z are Pauli matrices. The action in Eq. (5.10) (which can be obtained from the model specified in Eq. (5.8) by taking the classical limit and adding the diffusion terms proportional to K_d) possess this symmetry if it obeys the equilibrium condition Eq. (5.11), so that it reduces to model A^* , and the parameter r is chosen to be $r = K_c/K_d = u_c/u_d$. This parameter also enters the expression for the effective temperature, which is given by $T = \gamma(1 + r^2)$. As a first step towards deriving the symmetry transformation for the phase field θ , we rewrite Eq. (5.83) in terms of the variables introduced in the density-phase representation (5.32),

$$\begin{aligned}\mathcal{T}\theta(t, \mathbf{x}) &= -\theta(-t, \mathbf{x}), \\ \mathcal{T}\rho(t, \mathbf{x}) &= \rho(-t, \mathbf{x}), \\ \mathcal{T}\zeta_1(t, \mathbf{x}) &= \frac{1}{1 + r^2} \left[(r^2 - 1) \zeta_1(-t, \mathbf{x}) - 2r\zeta_2(-t, \mathbf{x}) \right] + \frac{i}{T} \left(\frac{r\partial_t \rho(-t, \mathbf{x})}{2\sqrt{\rho(-t, \mathbf{x})}} - \sqrt{\rho(-t, \mathbf{x})} \partial_t \theta(-t, \mathbf{x}) \right), \\ \mathcal{T}\zeta_2(t, \mathbf{x}) &= -\frac{1}{1 + r^2} \left[(r^2 - 1) \zeta_2(-t, \mathbf{x}) + 2r\zeta_1(-t, \mathbf{x}) \right] - \frac{i}{T} \left(r\sqrt{\rho(-t, \mathbf{x})} \partial_t \theta(-t, \mathbf{x}) + \frac{\partial_t \rho(-t, \mathbf{x})}{2\sqrt{\rho(-t, \mathbf{x})}} \right).\end{aligned}\quad (5.84)$$

Note that under the transformation \mathcal{T} the real and imaginary parts of ζ , denoted by ζ_1 and ζ_2 respectively, explicitly acquire imaginary contributions. This is not surprising since the complex fields ϕ_q and ϕ_q^* are transformed independently, i.e., $\mathcal{T}\phi_q^*$ is not the complex conjugate of $\mathcal{T}\phi_q$. The transformation rules (5.84) mix phase and density fields and are, therefore, not a direct mean to test whether the phase-only action describes an equilibrium situation. We can still make progress by noting that the symmetry transformation Eq. (5.84) can be used to derive the equilibrium FDR for the phase. In the correlation and response functions that appear in this relation and which are defined in Eq. (5.64), we may integrate out density fluctuations using the procedure described in Sec. 5.3.3, and read off an effective transformation prescription involving only the phase and the response field $\tilde{\theta}$ from the resulting relation. Reversing the argument we can then say that a sufficient condition for the validity of the FDR is that the phase-only action is invariant with respect to this effective transformation. The

FDR follows from the relations, valid in thermodynamic equilibrium,

$$\begin{aligned}\langle\theta(t, \mathbf{x})\zeta_1(t', \mathbf{x}')\rangle &= \langle\mathcal{T}\theta(t, \mathbf{x})\mathcal{T}\zeta_1(t', \mathbf{x}')\rangle, \\ \langle\theta(t, \mathbf{x})\zeta_2(t', \mathbf{x}')\rangle &= \langle\mathcal{T}\theta(t, \mathbf{x})\mathcal{T}\zeta_2(t', \mathbf{x}')\rangle.\end{aligned}\quad (5.85)$$

Inserting here the explicit expressions Eq. (5.84) and the decomposition $\rho = \rho_0 + \pi$ of the density into its average value and fluctuations, we proceed to omit all but the leading order contributions in a saddle-point approximation (cf. the discussion following Eq. (5.42)). Then, in the correlation functions that do not involve π , the integration over this variable yields a δ -functional $\delta[u_c\zeta_1 - u_d\zeta_2]$ as in Eq. (5.36), which allows us to replace ζ_2 by $r\zeta_1$. As a result we have

$$\begin{aligned}\langle\theta(t, \mathbf{x})\zeta_1(t', \mathbf{x}')\rangle &= \langle\theta(-t, \mathbf{x})\zeta_1(-t', \mathbf{x}')\rangle \\ &\quad - \frac{i}{T} \left(\frac{r}{2\sqrt{\rho_0}} \langle\theta(-t, \mathbf{x})\partial_t\pi(-t', \mathbf{x}')\rangle - \sqrt{\rho_0} \langle\theta(-t, \mathbf{x})\partial_t\theta(-t', \mathbf{x}')\rangle \right), \\ r\langle\theta(t, \mathbf{x})\zeta_1(t', \mathbf{x}')\rangle &= r\langle\theta(-t, \mathbf{x})\zeta_1(-t', \mathbf{x}')\rangle \\ &\quad + \frac{i}{T} \left(r\sqrt{\rho_0} \langle\theta(-t, \mathbf{x})\partial_t\theta(-t', \mathbf{x}')\rangle + \frac{1}{2\sqrt{\rho_0}} \langle\theta(-t, \mathbf{x})\partial_t\pi(-t', \mathbf{x}')\rangle \right).\end{aligned}\quad (5.86)$$

These two relations can be combined to eliminate the correlation function $\langle\theta(-t, \mathbf{x})\partial_t\pi(-t', \mathbf{x}')\rangle$ from the RHS. Finally, replacing ζ_1 by the response field $\tilde{\theta} = i2\sqrt{\rho_0}\zeta_1$ we find

$$\langle\theta(t, \mathbf{x})\tilde{\theta}(t', \mathbf{x}')\rangle = \langle\theta(-t, \mathbf{x})\tilde{\theta}(-t', \mathbf{x}')\rangle - \frac{1}{\Delta} \langle\theta(-t, \mathbf{x})\partial_t\tilde{\theta}(-t', \mathbf{x}')\rangle, \quad (5.87)$$

with the noise strength Δ given by Eq. (5.40). This relation can readily be seen to be just the equilibrium FDR by noting that the response function defined in Eq. (5.64) vanishes for $t > t'$ [29]. Therefore, upon multiplying Eq. (5.87) with the step function $\theta(t - t')$ we obtain the classical FDR in the time and frequency domains,

$$\begin{aligned}G(t - t', \mathbf{x} - \mathbf{x}') &= -\frac{1}{\Delta} \theta(t - t') \partial_t C(t - t', \mathbf{x} - \mathbf{x}'), \\ C(\omega, \mathbf{q}) &= \frac{2\Delta}{\omega} \text{Im} G(\omega, \mathbf{q}).\end{aligned}\quad (5.88)$$

In order to obtain the effective equilibrium transformation of the response field $\tilde{\theta}$, in analogy with Eq. (5.85) we identify the RHS of the relation Eq. (5.87) with $\langle\mathcal{T}\theta(t, \mathbf{x})\mathcal{T}\tilde{\theta}(t', \mathbf{x}')\rangle$. Then in addition to the transformation in Eq. (5.84) for the phase θ we obtain for the response field $\tilde{\theta}$ the transformation prescription

$$\mathcal{T}\tilde{\theta}(t, \mathbf{x}) = -\tilde{\theta}(-t, \mathbf{x}) + \frac{1}{\Delta} \partial_t \theta(-t, \mathbf{x}), \quad (5.89)$$

i.e., the fields θ and $\tilde{\theta}$ transform as generic real variables with dissipative dynamics [68–70]. The symmetry of the action under this transformation is sufficient not only to establish the FDR for two-point functions but also for arbitrary higher correlation functions [68–70]. We note that the parameter r that determines the relative strength of coherent and dissipative dynamics appears here only implicitly in the effective temperature set by the noise strength Δ .

It is straightforward to check that the non-linear term in the KPZ action (5.37) is not symmetric under the action of \mathcal{T} , specified in Eqs. (5.84) and (5.89), while the remaining parts of the action,

which describe purely diffusive dynamics of the phase realized in model A^* , are. We remark that the violation of the symmetry by the non-linear term occurs in any spatial dimension and, in particular, in 1D where the KPZ equation has a Gaussian thermal Gibbs distribution as stationary state [29, 55]. This is due to the fact that the 1D KPZ equation *does* indeed have an equilibrium-like symmetry, if instead of the transformation Eq. (5.89) one uses [17–19]

$$\mathcal{T}\tilde{\theta}(t) = \tilde{\theta}(-t) + \frac{\nu}{2\Delta}\nabla^2\theta(-t). \quad (5.90)$$

5.B Retarded response functions in the Keldysh formalism

In this appendix we derive the Keldysh functional integral representation of two-time correlation functions such as the retarded current-current response function Eq. (5.2), for the case that the dynamics of the system is described by a quantum master equation in Lindblad form. Then, according to the quantum regression theorem [93], the correlation function of operators A and B at times $t > t'$, can be written as

$$\langle A(t)B(t') \rangle = \text{tr} (Ae^{\mathcal{L}(t-t')}Be^{\mathcal{L}t'}\rho_0), \quad (5.91)$$

where $\rho(t) = e^{\mathcal{L}t}\rho_0$ is the formal solution to the master equation $\partial_t\rho = \mathcal{L}\rho$, with the initial condition $\rho(0) = \rho_0$. Note that \mathcal{L} , which is specified in Eq. (5.5), is a superoperator that acts on its argument both from the LHS and the RHS. The same is true for the exponential $e^{\mathcal{L}t}$, which thus describes evolution on the forward *and* the backward branches of the closed time path. Hence, the expression in the trace on the RHS of Eq. (5.91) should be read as follows: starting at $t = 0$ with ρ_0 , time evolution proceeds on the forward and backward branches up to the time t' , where the operator B is inserted on the forward branch; Then time evolution continues from t to t' , and finally A is again evaluated on the forward branch. However, using the cyclicity of the trace, the operator A can equally be shifted to the very right of the sequence of operators in the trace in Eq. (5.91), i.e., it can also be evaluated on the backward branch. These considerations lead to the following expression for the two-time correlation function in terms of Keldysh functional integrals for $t > t'$:

$$\langle A(t)B(t') \rangle = \langle A_+(t)B_+(t') \rangle = \langle A_-(t)B_+(t') \rangle. \quad (5.92)$$

Let us now turn to the retarded response function for operators A and B , which is defined as

$$\chi_{AB}(t-t') = i\theta(t-t')\langle [A(t), B(t')] \rangle, \quad (5.93)$$

i.e., it is the sum of two two-time correlation functions. Due to the θ -function appearing in this definition we have to evaluate the RHS only for $t > t'$. Then the first term in the commutator can be written as in Eq. (5.91), while the second one is given by

$$\langle B(t')A(t) \rangle = \langle B_-(t')A_+(t) \rangle = \langle B_-(t')A_-(t) \rangle. \quad (5.94)$$

Equations (5.92) and (5.94) show that there is no unique expression for the response function if the operators A and B are evaluated either on the forward or on the backward branch. This ambiguity vanishes when we form superpositions corresponding to the classical and quantum components, $A_c = (A_+ + A_-)/2$ and $A_q = A_+ - A_-$, respectively. Then we have [94]

$$\langle A_q(t)B_q(t') \rangle = 0, \quad \langle A_c(t)B_q(t') \rangle \propto \theta(t-t'), \quad \langle A_q(t)B_c(t') \rangle \propto \theta(t'-t), \quad (5.95)$$

and we find the unique expression for the retarded response function

$$\chi_{AB}(t-t') = i\langle A_c(t)B_q(t') \rangle. \quad (5.96)$$

5.C Density-phase representation for a weakly interaction Bose gas

Here we describe how the action for the phase of the order parameter in a weakly interacting Bose gas in thermodynamic equilibrium can be derived within the Keldysh formalism. As in Sec. 5.3.3, where we considered the case of a driven-dissipative condensate, the functional integrals over density fluctuations and the quantum field are solved by expanding the action around the classical saddle point. We start from the Keldysh action (omitting infinitesimal dissipative regularization terms [55, 56])

$$S = \int_X [\phi_q^* (i\partial_t + K_c \nabla^2) \phi_c + \text{c.c.} - V], \quad (5.97)$$

where the potential V is given by (note that in contrast to the potential in Eq. (5.8) for the driven-dissipative case this expression is invariant under phase rotations U_q introduced in Sec. 5.3.2; this symmetry implies particle number conservation)

$$V = r_c (\phi_q^* \phi_c + \text{c.c.}) + u_c (\phi_q^* \phi_c^* \phi_c^2 + 4\phi_q^* \phi_c^* \phi_q^2 + \text{c.c.}). \quad (5.98)$$

Inserting here the representation Eq. (5.32) of the classical and quantum fields and keeping only terms up to second order in products of density fluctuations $\pi = \rho - \rho_0$ and the quantum field ζ , which we decompose into its real and imaginary parts, ζ_1 and ζ_2 respectively, we find for the potential

$$V \approx 2u_c \sqrt{\rho_0} \zeta_1 \pi. \quad (5.99)$$

This gives a mass-like contribution in sector that involves the fields ζ_1 and π , and in order to obtain a low-energy effective description we will integrate out exactly these two fields. After the expansion in π and ζ the full action reads

$$S = -\frac{1}{\sqrt{\rho_0}} \int_X \left((\pi, \zeta_1) \begin{pmatrix} \partial_t \zeta_2 \\ 2\rho_0 \partial_t \theta \end{pmatrix} + u_c \rho_0 (\pi, \zeta_1) \sigma_x \begin{pmatrix} \pi \\ \zeta_1 \end{pmatrix} - 2K_c \rho_0 \zeta_2 \nabla^2 \theta \right), \quad (5.100)$$

where we neglected three terms $\zeta_1 \nabla^2 \pi$, $\zeta_1 \pi \partial_t \theta$, and $\zeta_1 \pi (\nabla \theta)^2$ which are dominated by the mass term Eq. (5.99); Moreover we neglected $\zeta_1 (\nabla \theta)^2 \ll \zeta_1 \partial_t \theta$ as well as $\zeta_2 \nabla \pi \cdot \nabla \theta$ and $\zeta_2 \pi \nabla^2 \theta$ which are small as compared to $\zeta_2 \partial_t \pi$ since the dynamical exponent is $z = 1$ as we will verify below. We now perform the Gaussian integral over π and ζ_1 (alternatively we could proceed as in Eq. (5.36), i.e., in a first step carry out the integral over π which yields a δ -functional that can be used to solve the integral over ζ_1) to obtain the action for the phase θ ,

$$Z = \int \mathcal{D}[\theta, \pi, \zeta_1, \zeta_2] e^{iS} = \int \mathcal{D}[\theta, \tilde{\theta}] e^{iS_\theta}. \quad (5.101)$$

In the last equality we expressed the imaginary part of the quantum field as $\zeta_2 = -u_c \sqrt{\rho_0} \tilde{\theta}$. The action for the phase reads

$$S_\theta = \int_X \tilde{\theta} (\partial_t^2 \theta - c^2 \nabla^2 \theta), \quad (5.102)$$

where $c = \sqrt{2K_c u_c \rho_0}$ is the speed of sound, and describes the dissipationless propagation of sound waves with linear dispersion $\omega = cq$.

Bibliography

- [1] N. D. Mermin and H. Wagner, *Phys. Rev. Lett.* **17**, 1133 (1966).
- [2] E. Altman, L. M. Sieberer, L. Chen, S. Diehl, and J. Toner, *Phys. Rev. X* **5**, 011017 (2015).
- [3] M. Fisher, M. Barber, and D. Jasnow, *Phys. Rev. A* **8**, 1111 (1973).
- [4] J. Kasprzak, M. Richard, S. Kundermann, A. Baas, P. Jeambrun, J. M. J. Keeling, F. M. Marchetti, M. H. Szymanska, R. André, J. L. Staehli, V. Savona, P. B. Littlewood, B. Deveaud, and L. S. Dang, *Nature* **443**, 409 (2006).
- [5] R. Balili, V. Hartwell, D. Snoke, L. Pfeiffer, and K. West, *Science* **316**, 1007 (2007).
- [6] H. Deng, G. Solomon, R. Hey, K. Ploog, and Y. Yamamoto, *Phys. Rev. Lett.* **99**, 126403 (2007).
- [7] G. Roumpos, M. Lohse, W. H. Nitsche, J. Keeling, M. H. Szymanska, P. B. Littlewood, A. Löffler, S. Höfling, L. Worschech, A. Forchel, and Y. Yamamoto, *Proc. Natl. Acad. Sci. U. S. A.* **109**, 6467 (2012).
- [8] V. Belykh, N. Sibeldin, V. Kulakovskii, M. Glazov, M. Semina, C. Schneider, S. Höfling, M. Kamp, and A. Forchel, *Phys. Rev. Lett.* **110**, 137402 (2013).
- [9] M. Kardar, G. Parisi, and Y.-C. Zhang, *Phys. Rev. Lett.* **56**, 889 (1986).
- [10] G. Grinstein, D. Mukamel, R. Seidin, and C. Bennett, *Phys. Rev. Lett.* **70**, 3607 (1993).
- [11] G. Grinstein, C. Jayaprakash, and R. Pandit, *Phys. D Nonlinear Phenom.* **90**, 96 (1996).
- [12] G. Sivashinsky, *Acta Astronaut.* **4**, 1177 (1977).
- [13] Y. Kuramoto, *Chemical Oscillations, Waves, and Turbulence* (Springer, Berlin, 1984).
- [14] L. He, L. M. Sieberer, E. Altman, and S. Diehl, *arXiv:1412.5579* (2014).
- [15] V. N. Gladilin, K. Ji, and M. Wouters, *Phys. Rev. A* **90**, 023615 (2014).
- [16] K. Ji, V. N. Gladilin, and M. Wouters, *Phys. Rev. B* **91**, 045301 (2015).
- [17] L. Canet, H. Chaté, B. Delamotte, and N. Wschebor, *Phys. Rev. Lett.* **104**, 150601 (2010).
- [18] L. Canet, H. Chaté, B. Delamotte, and N. Wschebor, *Phys. Rev. E* **84**, 061128 (2011).
- [19] L. Canet, *Phys. Rev. E* **86**, 019904(E) (2012).
- [20] J. Kim and J. Kosterlitz, *Phys. Rev. Lett.* **62**, 2289 (1989).
- [21] V. G. Miranda and F. D. A. Aarão Reis, *Phys. Rev. E* **77**, 031134 (2008).
- [22] E. Marinari, A. Pagnani, and G. Parisi, *Journal of Physics A: Mathematical and General* **33**, 8181 (2000).
- [23] S. Ghaisas, *Phys. Rev. E* **73**, 022601 (2006).

- [24] C.-S. Chin and M. den Nijs, *Phys. Rev. E* **59**, 2633 (1999).
- [25] L.-H. Tang, B. Forrest, and D. Wolf, *Phys. Rev. A* **45**, 7162 (1992).
- [26] J. Keeling, *Phys. Rev. Lett.* **107**, 080402 (2011).
- [27] P. Hohenberg and B. Halperin, *Rev. Mod. Phys.* **49**, 435 (1977).
- [28] R. Folk and G. Moser, *Journal of Physics A: Mathematical and General* **39**, R207 (2006).
- [29] U. C. Täuber, *Critical Dynamics: A Field Theory Approach to Equilibrium and Non-Equilibrium Scaling Behavior* (Cambridge University Press, Cambridge, 2014).
- [30] A. Leggett, *Rev. Mod. Phys.* **71**, S318 (1999).
- [31] E. M. Lifshitz and L. P. Pitaevskii, *Statistical Physics, Part 2: Theory of the Condensed State*, 2nd ed. (Pergamon Press, New York, 1980).
- [32] A. Griffin, *Excitations in a Bose-Condensed Liquid* (Cambridge University Press, Cambridge, 1994).
- [33] P. Hohenberg and P. Martin, *Annals of Physics* **34**, 291 (1965).
- [34] L. Pitaevskii and S. Stringari, *Bose-Einstein Condensation* (Oxford University Press, Oxford, 2003).
- [35] I. Carusotto and C. Ciuti, *Phys. Rev. Lett.* **93**, 166401 (2004).
- [36] M. Wouters and I. Carusotto, *Phys. Rev. Lett.* **105**, 020602 (2010).
- [37] A. Amo, D. Sanvitto, F. P. Laussy, D. Ballarini, E. del Valle, M. D. Martin, A. Lemaître, J. Bloch, D. N. Krizhanovskii, M. S. Skolnick, C. Tejedor, and L. Viña, *Nature* **457**, 291 (2009).
- [38] A. Amo, J. Lefrère, S. Pigeon, C. Adrados, C. Ciuti, I. Carusotto, R. Houdré, E. Giacobino, and A. Bramati, *Nat. Phys.* **5**, 805 (2009).
- [39] S. Pigeon, I. Carusotto, and C. Ciuti, *Phys. Rev. B* **83**, 144513 (2011).
- [40] A. Amo, S. Pigeon, D. Sanvitto, V. G. Sala, R. Hivet, I. Carusotto, F. Pisanello, G. Leménager, R. Houdré, E. Giacobino, C. Ciuti, and A. Bramati, *Science* **332**, 1167 (2011).
- [41] G. Grosso, G. Nardin, F. Morier-Genoud, Y. Léger, and B. Deveaud-Plédran, *Phys. Rev. Lett.* **107**, 245301 (2011).
- [42] G. Nardin, G. Grosso, Y. Léger, B. Pitka, F. Morier-Genoud, and B. Deveaud-Plédran, *Nat. Phys.* **7**, 635 (2011).
- [43] P. Minnhagen and G. Warren, *Phys. Rev. B* **24**, 2526 (1981).
- [44] A. Janot, T. Hyart, P. Eastham, and B. Rosenow, *Phys. Rev. Lett.* **111**, 230403 (2013).
- [45] J. Machta and R. A. Guyer, *Journal of Low Temperature Physics* **74**, 231 (1989).
- [46] N. Prokofev and B. Svistunov, *Phys. Rev. B* **61**, 11282 (2000).

- [47] M. Wouters and V. Savona, *Phys. Rev. B* **81**, 054508 (2010).
- [48] K. G. Lagoudakis, M. Wouters, M. Richard, A. Baas, I. Carusotto, R. André, L. S. Dang, and B. Deveaud-Plédran, *Nat. Phys.* **4**, 706 (2008).
- [49] D. Sanvitto, F. M. Marchetti, M. H. Szymanska, G. Tosi, M. Baudisch, F. P. Laussy, D. N. Krizhanovskii, M. S. Skolnick, L. Marrucci, A. Lemaître, J. Bloch, C. Tejedor, and L. Viña, *Nat. Phys.* **6**, 527 (2010).
- [50] G. Dagvadorj, J. M. Fellows, S. Matyjaskiewicz, F. M. Marchetti, I. Carusotto, and M. H. Szymanska, arXiv:1412.7361 (2014).
- [51] L. M. Sieberer, S. D. Huber, E. Altman, and S. Diehl, *Phys. Rev. Lett.* **110**, 195301 (2013).
- [52] L. M. Sieberer, S. D. Huber, E. Altman, and S. Diehl, *Phys. Rev. B* **89**, 134310 (2014).
- [53] U. C. Täuber and S. Diehl, *Phys. Rev. X* **4**, 021010 (2014).
- [54] I. Carusotto and C. Ciuti, *Rev. Mod. Phys.* **85**, 299 (2013).
- [55] A. Kamenev, *Field Theory of Non-Equilibrium Systems* (Cambridge University Press, Cambridge, 2011).
- [56] A. Altland and B. Simons, *Condensed Matter Field Theory*, 2nd ed. (Cambridge University Press, Cambridge, 2010).
- [57] D. J. Amit and V. Martin-Mayor, *Field Theory, the Renormalization Group, and Critical Phenomena*, 3rd ed. (World Scientific, Singapore, 2005).
- [58] J. Zinn-Justin, *Quantum Field Theory and Critical Phenomena*, 4th ed., International Series of Monographs on Physics No. 113 (Oxford University Press, Oxford, 2002).
- [59] H. Kleinert and V. Schulte-Frohlinde, *Critical Properties of ϕ^4 -Theories*, 1st ed. (World Scientific, Singapore, 2001).
- [60] M. Wouters, T. C. H. Liew, and V. Savona, *Phys. Rev. B* **82**, 245315 (2010).
- [61] E. Wertz, A. Amo, D. D. Solnyshkov, L. Ferrier, T. C. H. Liew, D. Sanvitto, P. Senellart, I. Sagnes, A. Lemaître, A. V. Kavokin, G. Malpuech, and J. Bloch, *Phys. Rev. Lett.* **109**, 216404 (2012).
- [62] D. Tanese, H. Flayac, D. Solnyshkov, A. Amo, A. Lemaître, E. Galopin, R. Braive, P. Senellart, I. Sagnes, G. Malpuech, and J. Bloch, *Nature communications* **4**, 1749 (2013).
- [63] I. Bloch and W. Zwerger, *Rev. Mod. Phys.* **80**, 885 (2008).
- [64] B. Nelsen, G. Liu, M. Steger, D. W. Snoke, R. Balili, K. West, and L. Pfeiffer, *Phys. Rev. X* **3**, 041015 (2013).
- [65] T. Jacqmin, I. Carusotto, I. Sagnes, M. Abbarchi, D. D. Solnyshkov, G. Malpuech, E. Galopin, A. Lemaître, J. Bloch, and A. Amo, *Phys. Rev. Lett.* **112**, 116402 (2014).

- [66] A. Dreismann, P. Cristofolini, R. Balili, G. Christmann, F. Pinsker, N. G. Berloff, Z. Hatzopoulos, P. G. Savvidis, and J. J. Baumberg, *Proceedings of the National Academy of Sciences of the United States of America* **111**, 8770 (2014).
- [67] H. K. Janssen, in *Dynamical Critical Phenomena and Related Topics*, Lecture Notes in Physics, Vol. 104, edited by C. Enz (Springer-Verlag, Berlin, 1979) pp. 25–47.
- [68] A. Andreanov, G. Biroli, and A. Lefèvre, *Journal of Statistical Mechanics: Theory and Experiment* **2006**, P07008 (2006).
- [69] C. Aron, G. Biroli, and L. F. Cugliandolo, *Journal of Statistical Mechanics: Theory and Experiment* **2010**, P11018 (2010).
- [70] C. Aron, D. G. Barci, L. F. Cugliandolo, Z. G. Arenas, and G. S. Lozano, arXiv:1412.7564 (2014).
- [71] C. De Dominicis, E. Brézin, and J. Zinn-Justin, *Phys. Rev. B* **12**, 4945 (1975).
- [72] R. Graham, in *Quantum Statistics in Optics and Solid-State Physics*, Springer Tracts in Modern Physics, Vol. 66 (Springer-Verlag, Berlin, 1973) pp. 1–97.
- [73] U. Decker and F. Haake, *Phys. Rev. A* **11**, 2043 (1975).
- [74] R. Graham and T. Tél, *Phys. Rev. A* **42**, 4661 (1990).
- [75] R. Gebauer and R. Car, *Phys. Rev. Lett.* **93**, 160404 (2004).
- [76] J. E. Avron, M. Fraas, and G. M. Graf, *Journal of Statistical Physics* **148**, 800 (2012).
- [77] M. E. Peskin and D. V. Schroeder, *An Introduction to Quantum Field Theory* (Westview Press, Boulder, 1995).
- [78] M. Wouters and I. Carusotto, *Phys. Rev. Lett.* **99**, 140402 (2007).
- [79] M. Szymanska, J. Keeling, and P. Littlewood, *Phys. Rev. Lett.* **96**, 230602 (2006).
- [80] S. F. Edwards and D. R. Wilkinson, *Proceedings of the Royal Society A: Mathematical, Physical and Engineering Sciences* **381**, 17 (1982).
- [81] K. J. Wiese, *Journal of Statistical Physics* **93**, 143 (1998).
- [82] C. M. Bender and S. A. Orszag, *Advanced Mathematical Methods for Scientists and Engineers I* (Springer New York, New York, NY, 1999).
- [83] J. Berges, N. Tetradis, and C. Wetterich, *Physics Reports* **363**, 223 (2002).
- [84] B. Delamotte, in *Renormalization Group and Effective Field Theory Approaches to Many-Body Systems SE - 2*, Lecture Notes in Physics, Vol. 852, edited by A. Schwenk and J. Polonyi (Springer Berlin Heidelberg, 2012) pp. 49–132.
- [85] J.-P. Blaizot, R. Méndez-Galain, and N. Wschebor, *Physics Lett. B* **632**, 571 (2006).
- [86] J. M. Pawłowski, *Annals of Physics* **322**, 2831 (2007).

- [87] I. Boettcher, J. M. Pawłowski, and S. Diehl, *Nuclear Physics B - Proceedings Supplements* **228**, 63 (2012).
- [88] J. W. Negele and H. Orland, *Quantum Many-Particle Systems* (Westview Press, Boulder, 1998).
- [89] T. Kloss, L. Canet, and N. Wschebor, *Phys. Rev. E* **86**, 051124 (2012).
- [90] V. N. Popov, *Functional Integrals in Quantum Field Theory and Statistical Physics* (D. Reidel Publishing Company, Dordrecht, 1983).
- [91] I. Aranson and L. Kramer, *Rev. Mod. Phys.* **74**, 99 (2002).
- [92] M. Kulkarni and A. Lamacraft, *Phys. Rev. A* **88**, 021603 (2013).
- [93] S. Swain, *J. Phys. A: Math. Gen.* **14**, 2577 (1981).
- [94] S. G. Jakobs, M. Pletyukhov, and H. Schoeller, *Journal of Physics A: Mathematical and Theoretical* **43**, 103001 (2010).

CHAPTER 6

PUBLICATION

Scaling properties of one-dimensional driven-dissipative condensates[†]

arXiv:1412.5579 (2014)

L. He,¹ L. M. Sieberer,¹ E. Altman,² and S. Diehl^{1,3}

¹*Institute for Theoretical Physics, University of Innsbruck, A-6020 Innsbruck, Austria*

²*Department of Condensed Matter Physics, Weizmann Institute of Science, Rehovot 76100, Israel*

³*Institute for Theoretical Physics, Technical University Dresden, D-01062 Dresden, Germany*

We numerically investigate the scaling properties of a one-dimensional driven-dissipative condensate described by a stochastic complex Ginzburg-Landau equation (SCGLE). We directly extract the static and dynamical scaling exponents from the dynamics of the condensate's phase field, and find that both coincide with the ones of the one-dimensional Kardar-Parisi-Zhang (KPZ) equation. We furthermore calculate the spatial and the temporal two-point correlation functions of the condensate field itself. The decay of the temporal two-point correlator assumes a stretched-exponential form, providing further quantitative evidence for an effective KPZ description. Moreover, we confirm the observability of this non-equilibrium scaling for typical current experimental setups with exciton-polariton systems, if cavities with a reduced Q factor are used.

6.1 Introduction

Physical systems driven far away from thermal equilibrium can show intrinsically different properties from their equilibrium counterparts. One prototypical example is the growing interface, whose long-wavelength dynamics, described by the so-called Kardar-Parisi-Zhang (KPZ) equation [1], does not belong to the Halperin-Hohenberg classification of near thermal equilibrium dynamical behavior [2]. Recent experimental progress in realizing Bose-Einstein condensation of exciton-polaritons in pumped semiconductor heterostructures [3–5] holds the promise of developing such systems into laboratories for non-equilibrium statistical mechanics. Microscopically, these systems exhibit coherent

[†]The author of the thesis contributed to this publication through discussions on the interpretation of the results, and worked out the precise relation to experiments with exciton-polaritons, including the appropriately rescaled stochastic complex Ginzburg-Landau equation and the experimental parameter values. Furthermore he was involved in preparing the manuscript.

and driven-dissipative dynamics on an equal footing, and therefore explicitly violate detailed balance characteristic of an equilibrium system. This phenomenology can have drastic consequences for the macrophysics of such systems. Indeed, for the case of driven-dissipative condensates of exciton-polaritons in two dimensions (2D), it was pointed out recently [6] that quasi-long-range order can not exist in the long-wavelength limit, in stark contrast to the familiar properties of 2D equilibrium condensates. This conclusion was drawn from a connection between the stochastic complex Ginzburg-Landau equation (SCGLE) and the KPZ equation in the long-wave length limit [6, 7], as also noticed in 1D [8]. However, direct numerical evidence of this connection is still missing.

As a first step to fill this gap, here we investigate the long-wavelength behavior of the dynamics of a driven-dissipative condensate in 1D. Our first goal is to study whether scaling properties of the condensate's phase field dynamics, in particular static and dynamical exponents, indeed coincide with those implied by the KPZ equation. The second goal is to directly study both the spatial and temporal correlation function of the bosonic field for the condensate itself to see whether they match the prediction from the KPZ picture.

We achieve our goals via direct numerical simulations of the SCGLE which governs the dynamics of driven-dissipative condensates. We directly extract both the static and dynamical critical exponents of the system from the dynamics of the condensate's phase field. Within numerical error, we indeed find that the critical exponents of the SCGLE coincide with the ones of the KPZ equation (see Figs. 6.1, 6.5, and 6.6), and we estimate the crossover time scale (see Fig. 6.2) beyond which the KPZ scaling behavior can be observed. We further find that the scaling properties of the condensate field dynamics (see Figs. 6.3 and 6.4) match the expectation from the effective description in terms of the KPZ equation. Finally, we demonstrate that the KPZ scaling can be seen in current experimental setups with exciton-polaritons, if cavities with a reduced Q factor are used (see Fig. 6.4).

The paper is organized as follows: In Sec. 6.2, we specify the system and model under study, and the theoretical approach used. In Sec. 6.3, we present a detailed discussion of the scaling properties of the phase field correlations. This contains in particular the static and dynamical exponents of the condensate's phase field dynamics. In Sec. 6.4, we discuss the scaling properties of two-point correlation functions of the condensate field itself. In Sec. 6.5, we investigate the experimental observability of the scaling properties discussed in Sec. 6.4 in exciton-polariton condensate experiments. We conclude and give an outlook in Sec. 6.6.

6.2 Model and Theoretical Approach

The dynamics of driven-dissipative condensates, which have been realized in experiments with exciton-polariton systems [3–5], can be modeled by the SCGLE with a complex Gaussian white noise (units are chosen such that $\hbar = 1$) which reads in 1D as [6, 9]

$$\frac{\partial}{\partial t} \tilde{\psi} = \left[\tilde{r} + \tilde{K} \frac{\partial^2}{\partial \tilde{x}^2} + \tilde{u} |\tilde{\psi}|^2 \right] \tilde{\psi} + \tilde{\zeta} \quad (6.1)$$

with $\tilde{r} = -\tilde{r}_d - i\tilde{r}_c$, $\tilde{K} = \tilde{K}_d + i\tilde{K}_c$, $\tilde{u} = -\tilde{u}_d - i\tilde{u}_c$, $\langle \tilde{\zeta}(\tilde{x}, \tilde{t}) \tilde{\zeta}(\tilde{x}', \tilde{t}') \rangle = 0$, $\langle \tilde{\zeta}^*(\tilde{x}, \tilde{t}) \tilde{\zeta}(\tilde{x}', \tilde{t}') \rangle = 2\tilde{\sigma} \delta(\tilde{x} - \tilde{x}') \delta(\tilde{t} - \tilde{t}')$. The second moment of the noise $\tilde{\sigma} = \tilde{\gamma}_l$ with $\tilde{\gamma}_l$ being the single particle loss, while $\tilde{r}_d = \tilde{\gamma}_l - \tilde{\gamma}_p$ is the difference between the single particle loss and pump. For the existence of a condensate in the mean field steady state solution, \tilde{r}_d has to be negative, i.e., the single-particle pump

rate has to be larger than the loss rate. \tilde{u}_d is the positive two-particle loss rate; $K_c = 1/(2m_{\text{LP}})$ with m_{LP} being the mass of polaritons and K_d is an effective diffusion constant. For convenience, we use the following rescaled form of Eq. (6.1),

$$\frac{\partial}{\partial t} \psi = \left[r + K \frac{\partial^2}{\partial x^2} + u|\psi|^2 \right] \psi + \zeta, \quad (6.2)$$

where

$$t = |\tilde{r}_d| \tilde{t}, \quad x = \sqrt{\frac{|\tilde{r}_d|}{\tilde{K}_d}} \tilde{x}, \quad \psi = \sqrt{\frac{\tilde{u}_d}{|\tilde{r}_d|}} \tilde{\psi}, \quad \zeta = \sqrt{\frac{\tilde{u}_d}{|\tilde{r}_d|^3}} \tilde{\zeta}, \quad (6.3)$$

$$r_c = \frac{\tilde{r}_c}{|\tilde{r}_d|}, \quad K_c = \frac{\tilde{K}_c}{\tilde{K}_d}, \quad u_c = \frac{\tilde{u}_c}{\tilde{u}_d}, \quad r = 1 - ir_c, \quad K = (1 + iK_c), \quad u = (-1 - iu_c) \quad (6.4)$$

and the second moment of the rescaled Gaussian white noise $\zeta(x, t)$ is $\sigma = \tilde{\sigma} \tilde{u}_d |\tilde{r}_d|^{-3/2} \tilde{K}_d^{-1/2}$.

Adopting the amplitude-phase representation of the complex bosonic field $\psi(x, t) = \rho(x, t)e^{i\theta(x, t)}$, it was shown [6–8] that, assuming that spatial-temporal fluctuations of the amplitude field $\rho(x, t)$ are small, the dynamical equation of the phase field $\theta(x, t)$ assumes in the low-frequency and long-wavelength limit the form of the KPZ equation, which reads

$$\partial_t \theta(x, t) = D \partial_x^2 \theta(x, t) + \frac{\lambda}{2} (\partial_x \theta(x, t))^2 + \eta(x, t), \quad (6.5)$$

where $\eta(x, t)$ is an effective Gaussian white noise, with mean $\langle \eta(x, t) \rangle = 0$, and correlations

$$\langle \eta(x, t) \eta(x', t') \rangle = 2\sigma_{\text{KPZ}} \delta(x - x') \delta(t - t').$$

Here $\sigma_{\text{KPZ}} = (\tilde{u}_d^2 + \tilde{u}_c^2) \tilde{\gamma}_l / (2\tilde{u}_d (\tilde{\gamma}_p - \tilde{\gamma}_l))$ is the effective noise strength, $D = \tilde{K}_d (1 + \tilde{K}_c \tilde{u}_c / \tilde{K}_d \tilde{u}_d)$ is the diffusion constant, and $\lambda = 2\tilde{K}_c (\tilde{K}_d \tilde{u}_c / \tilde{K}_c \tilde{u}_d - 1)$ is the non-linear coupling strength [6]. With a simple rescaling, i.e., $\theta = \Theta \sqrt{2\sigma_{\text{KPZ}}/D}$, $t = \tau/D$, $\eta = \xi \sqrt{2\sigma_{\text{KPZ}}D}$, the KPZ equation Eq. (6.5) can be recast into a form where only one dimensionless parameter, the non-linear coupling strength g , enters, i.e.

$$\partial_\tau \Theta(x, \tau) = \partial_x^2 \Theta(x, \tau) + g (\partial_x \Theta(x, \tau))^2 + \xi(x, \tau), \quad (6.6)$$

where

$$g = \lambda \sqrt{\frac{\sigma_{\text{KPZ}}}{2D^3}}, \quad (6.7)$$

and $\langle \xi(x, \tau) \xi(x', \tau') \rangle = \delta(x - x') \delta(\tau - \tau')$. Importantly, the magnitude of g directly characterizes how far the dynamics of the complex field ψ is driven away from thermal equilibrium. More precisely, $g = 0$ is guaranteed by symmetry in a thermal equilibrium system which obeys global detailed balance [10, 11], in which case Eq. (6.6) reduces to the so-called Edwards-Wilkinson (EW) dynamical equation [12], while $g \neq 0$ indicates that the system is driven away from thermal equilibrium.

In the following, we investigate the scaling properties of various correlation functions of the phase field $\theta(x, t)$, in particular the static and dynamical critical exponent, as well as the correlation properties of the complex bosonic field $\psi(x, t)$ which are of most direct physical interest for experiments.

To put our investigation in a more general context, here we mention a few situations where similar dynamical equations appear. Without the noise term in (6.2), the above equation reduces to the *deterministic* complex Ginzburg-Landau equation (CGLE). One key feature of the latter is the existence

of a so-called Benjamin-Feir unstable parameter region [13] specified by $1 + K_c u_c < 0$, where the dynamics described by the deterministic CGLE develops spatiotemporal chaotic behavior (see e.g. [14]) which has been extensively studied in the literature [15, 16]. As we are interested in the parameter regime with both K_c and u_c being positive, the Benjamin-Feir unstable region is not relevant for the current investigation. However, it can be relevant if one is interested in turbulence of the bosonic fluid in the presence of external noise [17]. Moreover, a similar stochastic dynamical equation, the so-called stochastic Gross-Pitaevskii equation [18, 19], is used to describe, e.g. the BEC formation dynamics of alkali atoms at finite temperature. Here, however, the constraints resulting from detailed balance in stationary state are built in. Finally, we mention that recently in Ref. [8] a higher order spatial derivative term was included in the effective description of the 1D SCGLE. This study focuses on the static correlation properties of the system, where a crossover in the spatial correlation function at intermediate scale is identified.

We finally give some general information concerning our numerical simulations. We use the semi-implicit algorithm developed in [20] to solve the stochastic partial differential equation (6.2) numerically. In all the simulations spatial periodic boundary conditions of the complex field $\psi(x, t)$ are assumed and the winding number of the phase field $\theta(x, t)$ across the whole system is chosen to be zero. We work in the low noise regime, where we find defects of the phase field to be absent. If not specified in text, we use $N_{\text{Traj}} = 10^2$ stochastic trajectories to perform ensemble averages.

6.3 Scaling properties of the phase correlations

6.3.1 KPZ exponents

In order to characterize the phase dynamics we extract the phase field $\theta(x, t)$ from the simulations of the condensate field $\psi(x, t)$. We then investigate the following correlation function associated with the phase field:

$$w(L, t) \equiv \left\langle \frac{1}{L} \int_x \theta^2(x, t) - \left(\frac{1}{L} \int_x \theta(x, t) \right)^2 \right\rangle, \quad (6.8)$$

where L is the linear size of the system and “ $\langle \rangle$ ” indicates ensemble average over stochastic trajectories. In the context of the KPZ equation, $w(L, t)$ is usually referred to as “roughness function”. Regarding $\theta(x, t)$ as the crystal height variable as in the conventional KPZ equation, $w(L, t)$ measures the spatial fluctuations of that height. Later we discuss subtleties involved in the definition of $w(L, t)$ due to the fact that the phase field θ is in fact compact, i.e. defined on the circle. Measuring the scaling properties of $w(L, t)$ allows to extract both static and dynamic exponents and thus establish a connection to KPZ universality (see e.g. [21]):

1. In a large system we expect to see a wide range of time-scales over which $w(L, t) \propto t^{2\beta}$, where the dynamical exponent β is usually referred to as growth exponent in the KPZ context. It relates to the conventional dynamical exponent z according to $\beta = \alpha/z$, with α being the roughness exponent to be explained in the following.
2. Because of the finite system size, the roughness function will saturate at $w_s(L)$ beyond a saturation time. We expect the saturation value to scale as $w_s(L) \sim L^{2\alpha}$, where the static exponent α is called the roughness exponent in the KPZ context.

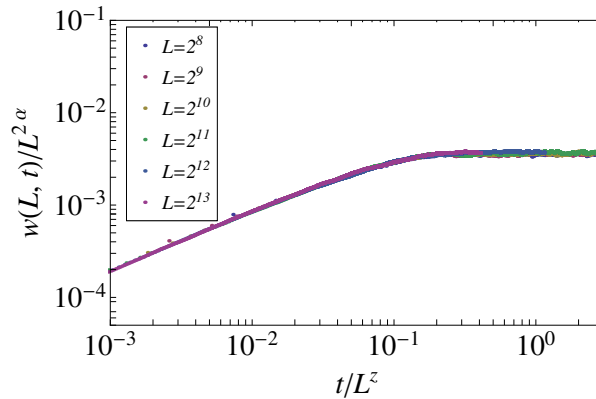


Figure 6.1. (Color online) Finite-size scaling collapse of $w(L, t)$ in the 1D KPZ universality class with $\alpha = 1/2$ and $z = 3/2$. Ensemble averages were performed over a number of $N_{\text{Traj}} = 1000$ stochastic trajectories. Values of the parameters used in the simulations are $r_c = -0.1$, $u_c = 0.1$, $\sigma = 0.1$, $K_c = 3.0$.

3. The roughness function reaches its saturation value $w_s(L)$ at a time T_s , which thus separates the growth period 1. from the long time regime 2. This saturation time scales with system size as $T_s \sim L^z$.

These scaling features are demonstrated by the finite-size scaling of $w(L, t)$ shown in Fig. 6.1. Perfect data collapse is obtained using the 1D KPZ exponents $\alpha = 1/2$ and $z = 3/2$. During the growth period the roughness increases nearly linearly on the log-log scale, which indicates power-law growth $w(L, t) \propto t^{2\beta}$. For different system sizes saturation is reached at the same point on the rescaled time axis, confirming the scaling behavior $T_s \sim L^z$. Finally, the saturation values $w_s(L)$ of the roughness function collapse upon rescaling $w(L, t)$ with $L^{2\alpha}$.

A more precise numerical determination of the exponents α and β , which confirms that their values are given by the ones of the KPZ equation, i.e. $\alpha = 1/2$ and $\beta = 1/3$, is presented in the appendix. This provides us with strong evidence that the phase field dynamics of a driven-dissipative condensate is indeed described by the KPZ equation, in contrast to the thermal equilibrium case, in which the dynamics of the phase is purely diffusive and thus belongs to the EW universality class [22]. The corresponding dynamical exponent $\beta = 1/4$ is different from KPZ universality, however, the value of the static roughness exponent, $\alpha = 1/2$, is exactly the same in both cases. This is due to a symmetry of the KPZ equation that is present only in one spatial dimension, and which allows one to show that the static correlations in stationary state are Gaussian [23]. On the other hand, the dynamical exponent β (or equivalently z) witnesses quantitatively the difference between KPZ and EW universality.

Before we proceed, let us emphasize an important difference between the phase of a complex field we consider here and the crystal height: The phase is a compact field variable defined on a circle. Without loss of generality the value of $\theta(x, t)$ is in fact bounded to the interval $(-\pi, \pi]$. Consequently, the value of $w(L, t)$ is also bounded from above by $4\pi^2$, which inevitably invalidates the static scaling behavior $w_s(L) \sim L^{2\alpha}$ if α is positive as expected from the conventional KPZ scenario. However, as long as the field amplitude remains nonvanishing we can let the value of ψ be defined on the Riemann

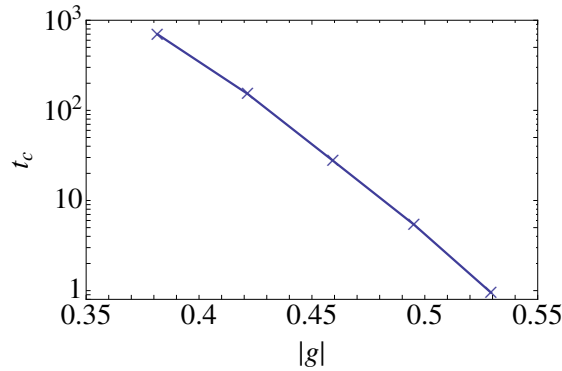


Figure 6.2. (Color online) Dependence of the crossover time t_c on the non-equilibrium strength $|g|$. t_c decreases pronouncedly as $|g|$ increases. In the numerical results presented here, $|g|$ is tuned by changing $K_c = 2.4, 2.2, 2.0, 1.8, 1.6$ while keeping the other parameters unchanged. Their values are $L = 2^{15}$, $r_c = -0.1$, $u_c = 0.1$, $\sigma = 0.1$.

surface, where the value of θ is in the interval $(-\infty, +\infty)$. With this choice there is no upper bound imposed on $w_s(L)$. In numerical simulations, we ensure the requirement $|\psi(x, t)| > 0$ by working with low noise. In this regime phase defects do not occur within the spatio-temporal range of our simulations. $\theta(x, t)$ is constructed from $\psi(x, t)$'s complex argument by requiring the phase difference between neighboring space-time points to be less than π .

6.3.2 Crossover time scale

In the above subsection we have established that the phase field dynamics indeed belong to the KPZ universality class. However, it is important to notice that the scaling behavior of $w(L, t) \propto t^{2\beta}$, where $\beta = 1/3$ is the KPZ growth exponent, is reached only after a crossover time t_c . In particular, for weak nonlinearity (i.e. $|g| \ll 1$) the KPZ renormalization group equations lead to a crossover time that scales as $t_c \approx t_0 |g|^{-4}$ [24], where t_0 is a microscopic time scale. Scaling behavior of $w(L, t)$ before t_c is expected to be governed by the EW growth exponent $\beta = 1/4$. In Fig. 6.2, we investigate the $|g|$ dependence of the crossover time t_c at moderate values of $|g|$ (the numerical scheme for the extraction of t_c can be found in App. 6.A.2), since extraction of t_c in the near equilibrium case, $|g| \ll 1$, is numerically very demanding and t_c quickly exceeds the accessible simulation runtimes. We observe that t_c increases pronouncedly as $|g|$ decreases (but not yet according to the weak coupling scaling pointed out above). The rapid decrease of t_c with increasing non-equilibrium strength is promising for the experimental observation of KPZ scaling behavior, rather than transient EW-like dynamics, before finite size effects set in. We discuss possible experimental settings for observing these phenomena in Sec. 6.5.

6.4 Scaling of the condensate field correlations

In the previous section we have demonstrated numerically that the dynamics of the phase of a one-dimensional polariton condensate follows universal KPZ scaling. In this section we investigate how

this scaling manifests in directly observable correlations of the condensate field. Specifically, we consider the correlation functions

$$\begin{aligned} C_x(x_1, x_2; t) &\equiv \langle \psi^*(x_1, t) \psi(x_2, t) \rangle, \\ C_t(x; t_1, t_2) &\equiv \langle \psi^*(x, t_1) \psi(x, t_2) \rangle, \end{aligned} \quad (6.9)$$

i.e. the equal time two-point correlation function in space and the temporal autocorrelation function, respectively. These are directly accessible in experiments with exciton-polaritons: Both spatial and temporal coherence can be probed by interference measurements, on the photoluminescence emitted from different regions of the exciton-polariton condensate [3, 5] and by combining two images of the condensate taken at different times using, e.g., a Mach-Zehnder interferometer [25], respectively. The visibility of interference fringes yields the correlation functions. Assuming spatial translational invariance of the correlation functions, we calculate the following spatially averaged correlation functions, which are equivalent to the corresponding correlation functions above but in practice help to reduce the statistical error

$$\begin{aligned} \bar{C}_x(x_1, x_2, t) &\equiv \frac{1}{L} \int dy \langle \psi^*(x_1 + y, t) \psi(x_2 + y, t) \rangle, \\ \bar{C}_t(t_1, t_2) &\equiv \frac{1}{L} \int dx \langle \psi^*(x, t_1) \psi(x, t_2) \rangle. \end{aligned} \quad (6.10)$$

6.4.1 Spatial correlations

We start with the spatial correlation function $\bar{C}_x(x_1, x_2, t)$. In Fig. 6.3 we show the dependence of $|\bar{C}_x(x_1, x_2, t)|$ on the distance $|x_1 - x_2|$ at time $t > T_s$, from which we clearly identify exponential decay on the semi-logarithmic scale plot. This coincides with the prediction from the effective KPZ description in 1D, and with previous numerical results [8]. However, as anticipated in Sec. 6.3, this static signature would in fact be compatible with thermal equilibrium dynamics of the field ψ and does not unambiguously demonstrate KPZ physics.

6.4.2 Temporal correlations

In contrast to the time-independent spatial correlation function discussed in the previous section, the temporal correlation function shows distinct properties depending on whether the system is in thermal equilibrium or not: indeed, based on the effective long-wavelength description of the out-of-equilibrium condensate dynamics in terms of the KPZ equation, we expect stretched-exponential decay of the autocorrelation function, i.e., $|\bar{C}_t(t_1, t_2)| = A e^{-B|t_1 - t_2|^{2\beta}}$, with the KPZ growth exponent $\beta = 1/3$ and non-universal numbers A and B . On the other hand, the purely diffusive EW dynamics of the phase of a condensate in equilibrium entails simple exponential decay, corresponding to $\beta = 1/2$. Hence both cases lead to linear growth of $-\log(|\bar{C}_t(t_1, t_2)| / |\bar{C}_t(t_2, t_2)|)$ with a slope of 2β in the double-logarithmic scale used in Fig. 6.4, which is clearly visible for the upper (at large $|t_1 - t_2|$) curves shown in blue and yellow. Performing linear fits to the data points with $|t_1 - t_2| \in [10^2, 10^3]$ we find $\beta = 0.311$ and $\beta = 0.317$, respectively, in reasonable agreement with the KPZ prediction of $\beta = 1/3$ and evidently distinct from the value $\beta = 1/2$ for a condensate in equilibrium. For these curves KPZ scaling sets in after a short crossover time difference t_c , which is due to the relatively

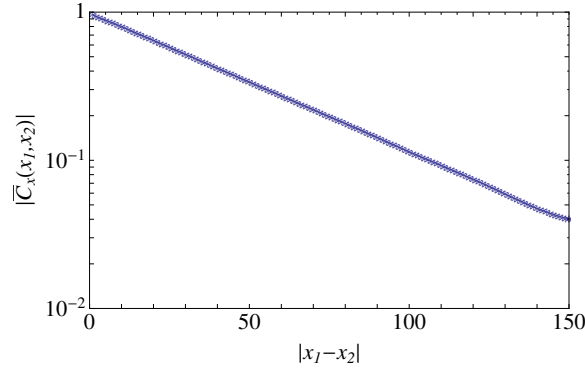


Figure 6.3. (Color online) Behavior of the translation invariant two-point function $\bar{C}_x(x_1, x_2, t = 2.9 \times 10^5 > T_s)$ at linear system size $L = 2^{12}$ on a semi-logarithmic scale. $N_{\text{Traj}} = 800$ stochastic trajectories are used to perform the ensemble average. Values of other parameters used here are $r_c = -0.1$, $u_c = 0.1$, $\sigma = 0.1$, $K_c = 3.0$. The exponential decay of $|\bar{C}_x(x_1, x_2, t)|$ with respect to $|x_1 - x_2|$ can be clearly identified from this plot.

large value of the effective non-linear coupling strength $|g|$ in both cases. On the contrary, for the parameters that yield the lowermost (red) curve, the value of $|g|$ is small, and as a result in this case universal scaling behavior is approached only at the largest time differences shown. A fit with $|t_1 - t_2|$ lying in the last half decade of the data shown in the Figure gives $\beta = 0.307$, and we expect a value closer to $\beta = 1/3$ at time differences larger than those that are accessible within the temporal range of our simulations. The parameters leading to the two lower (red and yellow) curves shown in Fig. 6.4 are relevant for current experiments with exciton-polaritons as is discussed in the following section.

6.5 Predictions for experimental observation

In the preceding sections we studied the SCGLE as an effective description of the long-wavelength dynamics of a generic driven-dissipative condensate. The microscopic model for the specific case of exciton-polaritons [9] differs from the SCGLE in that the diffusion constant is essentially absent and instead of an explicit two-body loss term the pump itself is assumed to be non-linear and saturates at high densities. Slightly above the condensation threshold the saturable pump term can be expanded in the polariton field and we recover the SCGLE, which then reads in dimensionless form

$$\partial_t \psi = \left[i \partial_x^2 + (i + u_d) \left(\frac{p}{u_d} - |\psi|^2 \right) \right] \psi + \zeta. \quad (6.11)$$

Here the effective dimensionless two-body loss coefficient u_d and the dimensionless pump strength p are given by

$$u_d = \frac{\hbar \tilde{\gamma}_l R}{2 \gamma_R \tilde{u}_c} (1 + 2p), \quad p = \frac{1}{2} \left(\frac{P}{P_{\text{th}}} - 1 \right), \quad (6.12)$$

with P and $P_{\text{th}} = \tilde{\gamma}_l \gamma_R / R$ being pump rate of the excitonic reservoir and its value at threshold, respectively; R is the condensate amplification rate and γ_R denotes the relaxation rate of the reservoir. Finally, $\tilde{\gamma}_l$ is the inverse lifetime of polaritons and \tilde{u}_c their interaction strength. Here we measure time

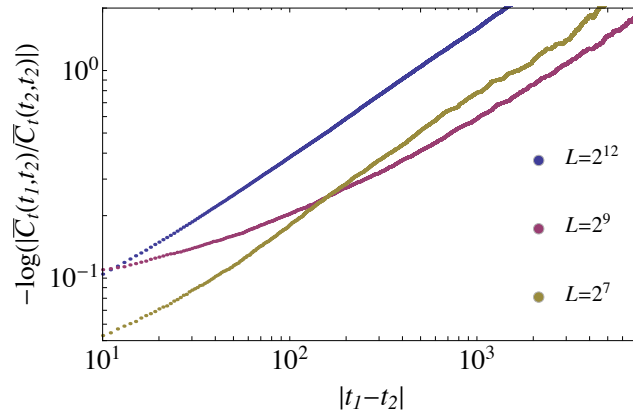


Figure 6.4. (Color online) The dependence of $-\log\left(\frac{|\bar{C}_t(t_1, t_2)|}{|\bar{C}_t(t_2, t_2)|}\right)$ on $|t_1 - t_2|$ for three different sets of parameters in the SCGLE and system sizes. The system size and the parameters for the uppermost (blue) curve are the same as those used in Fig. 6.3. For the lowermost (at large time differences) curve shown in red, the dimensionless linear system size is 2^9 , and the parameters are chosen to match typical values in current experiments with exciton-polaritons (see Sec. 6.5 for details). Finally, assuming that a cavity with reduced Q factor is used we obtain the parameters for the middle (yellow) curve, which corresponds to a system size of 2^7 . KPZ behavior is revealed by performing linear fits to the data points: with $|t_1 - t_2| \in [10^2, 10^3]$ we find $\beta = 0.311$ and $\beta = 0.317$ for the blue and yellow curves, respectively, while for the red curve a fit with $|t_1 - t_2|$ lying in the last half decade in the above plot, gives rise to $\beta = 0.307$. These values should be compared with the KPZ prediction $\beta = 1/3$. For all curves $N_{\text{Traj}} = 10^3$ stochastic trajectories are used.

and space in units of $\tilde{\gamma}_l^{-1}$ and $\sqrt{\hbar/2m_{\text{LP}}\tilde{\gamma}_l}$ respectively with m_{LP} being the effective mass of lower polaritons. The strength of the dimensionless noise field ζ is $\sigma = \tilde{u}_c \sqrt{2m_{\text{LP}}/\hbar^3\tilde{\gamma}_l}$. Typical values of experimental parameters in 1D exciton-polariton systems are (see, e.g., Ref. [26]),

$$m_{\text{LP}} = 4 \times 10^{-5} m_e, \quad \tilde{u}_c = 5 \times 10^{-4} \text{ meV } \mu\text{m}, \quad \tilde{\gamma}_l = 0.03 \text{ ps}^{-1}, \quad R = 3 \mu\text{m ps}^{-1}, \quad \gamma_R = 0.06 \text{ ps}^{-1}, \quad (6.13)$$

where m_e is the mass of the electron.

The lowermost (red) curve in Fig. 6.4 shows the temporal correlation function $\bar{C}_t(t_1, t_2)$ in the stationary state for the values given in Eq. (6.13) and at a dimensionless pump power of $p = 0.3$. Due to fact that the corresponding $|g|$ is relatively small, the red curve approaches linear growth characteristic of KPZ scaling only after a large crossover time difference t_c . As already mentioned in the previous section, a linear fit to the data points with $|t_1 - t_2|$ lying in the last half decade in Fig. 6.4 yields $\beta = 0.307$, indicating that signatures of KPZ physics are nevertheless observable. However, we note that the physical system size corresponding to the dimensionless linear system size of $L = 2^9$ chosen in this simulation is $\sim 3 \times 10^3 \mu\text{m}$, which is considerably larger than the typical scale $\sim 10^2 \mu\text{m}$ of current experiments.

Here we propose to make the KPZ physics observable with current experimental system sizes by reducing the cavity Q factor. To this end, we note that KPZ scaling is still observable when, while reducing the *physical* system size, the *dimensionless effective system* size can be kept large. A convenient knob to achieve this goal is indeed a reduction of the cavity Q (and thus increase of the decay rate $\tilde{\gamma}_l$), which leads to a decrease of the unit of length. (We note that this also facilitates observation of KPZ scaling behavior in equal-time spatial correlations in 2D [6].) The middle (yellow) curve in Fig. 6.4 shows $\bar{C}_t(t_1, t_2)$ for $\tilde{\gamma}_l = 1 \text{ ps}^{-1}$ and a dimensionless linear system size of $L = 2^7$, corresponding in physical units to $\sim 1.5 \times 10^2 \mu\text{m}$. In addition to the increase of $\tilde{\gamma}_l$, for this simulation we chose a larger value of 6 for the dimensionless prefactor in u_d in Eq. (6.12) instead of ~ 1 which we obtain for the parameters given in Eq. (6.13). This choice magnifies the effective KPZ non-linearity and corresponds to a moderate variation of the experimental parameters only. In fact, the latter are often determined only indirectly via fitting simulations to experimental measurements, and are thus not known with very high precision. In this setting, the exponent of $\beta = 0.317$ obtained from the middle (yellow) curve in Fig. 6.4 indicates that it is promising to search for signatures of KPZ physics in the first-order temporal coherence of 1D exciton-polariton systems when the lifetime of polaritons is rather short, so that the intrinsic non-equilibrium nature is strongly pronounced.

6.6 Conclusions and Outlook

We investigated scaling properties of the long-wavelength dynamics of 1D driven-dissipative condensate via direct numerical simulations of the SCGLE, and numerically established the connection to 1D KPZ universality. We further numerically confirmed the experimental observability of the non-equilibrium scaling properties of the first order temporal coherence within the typical current experimental setups of exciton-polariton condensates if cavities with a reduced Q factor are used. Similar investigations will be extended to higher dimensions in the future. Moreover, it is intriguing to investigate the dynamics of the driven-dissipative condensates at higher noise level, where in particular phase defects, e.g. phase slips in 1D or vortices in 2D, are expected to play a role in determining the long-wave length scaling properties of the system's dynamics.

Note added– Upon completion of this manuscript, we became aware of the work by K. Ji et al. reporting similar results [27].

Acknowledgments

We thank I. Boettcher for useful discussions. This work was supported by the Austrian Science Fund (FWF) through the START grant Y 581-N16, the SFB FoQuS (FWF Project No. F4006-N16), the Austrian Ministry of Science BMWF as part of the UniInfrastrukturprogramm of the Focal Point Scientific Computing at the University of Innsbruck, and by German Research Foundation (DFG) through ZUK 64.

6.A Extraction of α, β , and t_c

In this appendix we present a more precise determination of the static roughness exponent α and the dynamical growth exponent β , and describe how the crossover time scale t_c is extracted in numerical simulations.

6.A.1 Static roughness exponent α

We extract α from the finite-size scaling of $w_s(L)$. For given system size L , we monitor the value of $w(L, t)$ during a simulation and wait until it reaches a stable value up to statistical fluctuations at the saturation time T_s . After T_s , we continue simulating the dynamics to the final time point T_f with $T_f - T_s$ at least two times larger than T_s . Afterwards $w_s(L)$ is extracted according to $w_s(L) = (T_f - T_s)^{-1} \int_{T_s}^{T_f} dt w(L, t)$. In Fig. 6.5 we show the finite size scaling of $w_s(L)$ from the direct simulations of the SCGLE. The extracted roughness exponent is $\alpha = 0.499$, which is in good agreement with the roughness exponent α_{KPZ} of the KPZ dynamics being $\alpha_{\text{KPZ}} = 1/2$ in 1D [22].

6.A.2 Dynamical growth exponent β and cross over time scale t_c

We extract β from the time dependent roughness function $w(L, t)$. As pointed before, this exponent is related to the dynamical exponent z and the roughness exponent α via the relation $\beta = \alpha/z$. Its value is expected to be $1/3$ and $1/4$ for effective KPZ and EW dynamics, respectively [22].

In order to reliably extract the exponent β it is important to note that $w(L, t) \propto t^{2\beta}$ is reached only after the initial crossover time scale t_c discussed in Sec. 6.3.2. In practice we fit $w(L, t)$ to a power law over a long time window $t \in [t_e, t_e + T]$. We identify the asymptotic scaling by observing how the exponent depends on the lower cutoff time t_e . As shown in Fig. 6.6, the fitted exponent β first grows with t_e but then rapidly reaches a plateau. The value at this plateau represents the asymptotic scaling behavior. We note however that for this scheme to reflect the KPZ scaling, the upper cutoff time $t_e + T$ should not reach the finite size saturation time $T_s \sim L^z$ of the roughness function. If it does, then we expect the extracted exponent β to start decreasing again. Thus we extract β from the maximum value of the fitted exponent $\beta(t_e)$. This gives the estimate $\beta = 0.335$ consistent with KPZ dynamics, for which $\beta = 1/3$.

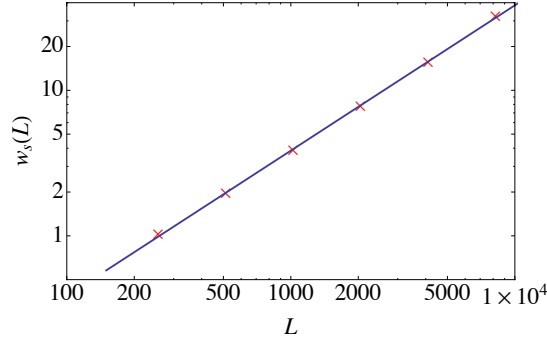


Figure 6.5. (Color online) Finite size scaling of $w_s(L)$. Points marked by “ \times ” denote the numerical value of $w_s(L)$ for system sizes $L = 2^8, 2^9, 2^{10}, 2^{11}, 2^{12}, 2^{13}$. The blue line is a linear fit to the data on the log-log scale, from which we extract the roughness exponent $\alpha = 0.499$. This is in good agreement with the roughness exponent α_{KPZ} of the KPZ dynamics in 1D, $\alpha_{\text{KPZ}} = 1/2$. Values of parameters used in the simulations are $r_c = -0.1, u_c = 0.1, \sigma = 0.1, K_c = 3.0$.

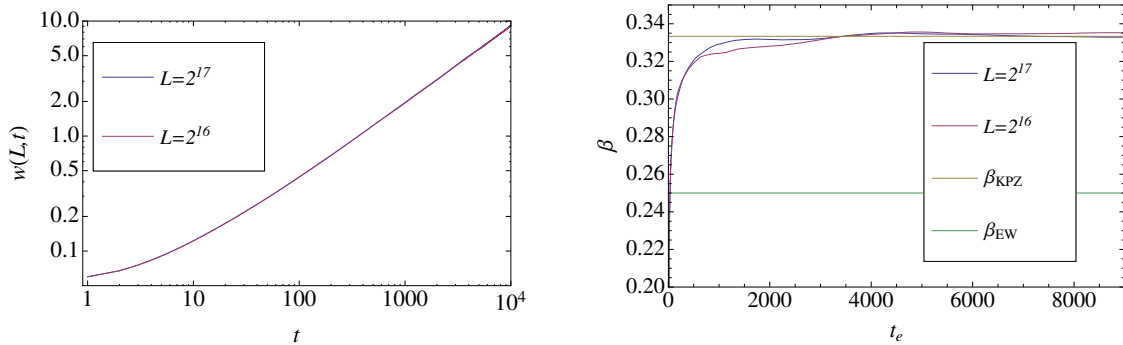


Figure 6.6. (Color online) Left panel: Time dependence of $w(L, t)$ of different system sizes $L = 2^{16}, 2^{17}$ with $r_c = -0.1, u_c = 0.1, \sigma = 0.1, K_c = 3.0$, on logarithmic scales. Right panel: t_e dependence of extracted β at different system sizes $L = 2^{16}, 2^{17}$. The growth exponent of EW dynamics β_{EW} and KPZ dynamics β_{KPZ} are indicated by two lines in the plot to facilitate direct comparison. From the results at system size $L = 2^{17}$, we obtain the dynamical exponent $\beta = 0.335$ from the maximum value of $\beta(t_e)$, which is in good agreement with $\beta_{\text{KPZ}} = 1/3$.

To extract the crossover time t_c from the simulations we use the following scheme. At given system size L , we fit the time dependent roughness function $w(L, t)$ to a double scaling function $c_{\text{EW}}t^{1/2} + c_{\text{KPZ}}t^{2/3}$ in a time interval that extends from zero until a final time t_f well before the finite system size effects set in, i.e. $t_f \ll T_s$. We then identify t_c as the time point where the two scaling functions have the same contribution to the roughness function, i.e. $c_{\text{EW}}t_c^{1/2} = c_{\text{KPZ}}t_c^{2/3}$, giving rise to $t_c = (c_{\text{EW}}/c_{\text{KPZ}})^6$.

Bibliography

- [1] M. Kardar, G. Parisi, and Y.-C. Zhang, Phys. Rev. Lett. **56**, 889 (1986).
- [2] P. Hohenberg and B. Halperin, Rev. Mod. Phys. **49**, 435 (1977).
- [3] J. Kasprzak, M. Richard, S. Kundermann, A. Baas, P. Jeambrun, J. M. J. Keeling, F. M. Marchetti, M. H. Szymanska, R. André, J. L. Staehli, V. Savona, P. B. Littlewood, B. Deveaud, and L. S. Dang, Nature **443**, 409 (2006).
- [4] K. G. Lagoudakis, M. Wouters, M. Richard, A. Baas, I. Carusotto, R. André, L. S. Dang, and B. Deveaud-Plédran, Nat. Phys. **4**, 706 (2008).
- [5] G. Roumpos, M. Lohse, W. H. Nitsche, J. Keeling, M. H. Szymanska, P. B. Littlewood, A. Löffler, S. Höfling, L. Worschech, A. Forchel, and Y. Yamamoto, Proc. Natl. Acad. Sci. U. S. A. **109**, 6467 (2012).
- [6] E. Altman, L. M. Sieberer, L. Chen, S. Diehl, and J. Toner, Phys. Rev. X **5**, 011017 (2015).
- [7] G. Grinstein, D. Mukamel, R. Seidin, and C. Bennett, Phys. Rev. Lett. **70**, 3607 (1993).
- [8] V. N. Gladilin, K. Ji, and M. Wouters, Phys. Rev. A **90**, 023615 (2014).
- [9] I. Carusotto and C. Ciuti, Rev. Mod. Phys. **85**, 299 (2013).
- [10] L. M. Sieberer, S. D. Huber, E. Altman, and S. Diehl, Phys. Rev. Lett. **110**, 195301 (2013), 1301.5854 .
- [11] L. M. Sieberer, S. D. Huber, E. Altman, and S. Diehl, Phys. Rev. B **89**, 134310 (2014).
- [12] S. F. Edwards and D. R. Wilkinson, Proc. R. Soc. A Math. Phys. Eng. Sci. **381**, 17 (1982).
- [13] T. B. Benjamin and J. E. Feir, J. Fluid Mech. **27**, 417 (2006).
- [14] G. Grinstein, C. Jayaprakash, and R. Pandit, Phys. D Nonlinear Phenom. **90**, 96 (1996).
- [15] M. Cross and P. Hohenberg, Rev. Mod. Phys. **65**, 851 (1993).
- [16] I. Aranson and L. Kramer, Rev. Mod. Phys. **74**, 99 (2002).
- [17] S. Mathey, T. Gasenzer, and J. M. Pawłowski, arXiv:1405.7652 (2014).
- [18] H. T. C. Stoof, J. Low Temp. Phys. **114**, 11 (1999).
- [19] P. Blakie, A. Bradley, M. Davis, R. Ballagh, and C. Gardiner, Adv. Phys. **57**, 363 (2008).

- [20] M. Werner and P. Drummond, *J. Comput. Phys.* **132**, 312 (1997).
- [21] E. Marinari, A. Pagnani, and G. Parisi, *J. Phys. A: Math. Gen.* **33**, 8181 (2000).
- [22] T. Halpin-Healy and Y.-C. Zhang, *Phys. Rep.* **254**, 215 (1995).
- [23] U. C. Täuber, *Critical Dynamics: A Field Theory Approach to Equilibrium and Non-Equilibrium Scaling Behavior* (Cambridge University Press, Cambridge, 2014).
- [24] T. Nattermann and L.-H. Tang, *Phys. Rev. A* **45**, 7156 (1992).
- [25] A. P. D. Love, D. N. Krizhanovskii, D. M. Whittaker, R. Bouchekioua, D. Sanvitto, S. A. Rizeiqi, R. Bradley, M. S. Skolnick, P. R. Eastham, R. André, and L. S. Dang, *Phys. Rev. Lett.* **101**, 067404 (2008).
- [26] E. Wertz, A. Amo, D. D. Solnyshkov, L. Ferrier, T. C. H. Liew, D. Sanvitto, P. Senellart, I. Sagnes, A. Lemaître, A. V. Kavokin, G. Malpuech, and J. Bloch, *Phys. Rev. Lett.* **109**, 216404 (2012).
- [27] K. Ji, V. N. Gladilin, and M. Wouters, *Phys. Rev. B* **91**, 045301 (2015).

Part III

Thermodynamic Equilibrium as a Symmetry of the Keldysh Action

CHAPTER 7

ADDITIONAL MATERIAL

Thermodynamic Equilibrium as a Symmetry of the Keldysh Action[†]

L. M. Sieberer,¹ A. Chiocchetta,² A. Gambassi,² U. C. Täuber,³ S. Diehl⁴

¹*Institute for Theoretical Physics, University of Innsbruck, A-6020 Innsbruck, Austria*

²*SISSA — International School for Advanced Studies and INFN, Via Bonomea 265, 34136 Trieste, Italy*

³*Department of Physics (MC 0435), Robeson Hall, 850 West Campus Drive, Virginia Tech, Blacksburg, Virginia 24061, USA*

⁴*Institute for Theoretical Physics, Technical University Dresden, D-01062 Dresden, Germany*

The time evolution of an extended quantum system can be theoretically described in terms of the Keldysh functional integral formalism, whose action conveniently encodes the information about the dynamics. We show here that the action of quantum systems evolving in thermal equilibrium is invariant under a symmetry transformation which distinguishes them from generic open systems. A unitary or dissipative dynamics having this symmetry naturally leads to the emergence of a Gibbs thermal stationary state. Moreover, the fluctuation-dissipation relations characterizing the linear response of an equilibrium system to external perturbations can be derived as the Ward-Takahashi identities associated with this symmetry. Accordingly, the symmetry unveiled here provides an efficient check for the onset of thermodynamic equilibrium and it makes testing the validity of fluctuation-dissipation relations unnecessary. Remarkably, in the classical limit, this symmetry renders the one which is known to characterize equilibrium in the stochastic dynamics of classical systems coupled to thermal baths, described by Langevin equations.

7.1 Introduction

In recent years, the question under which conditions and how a quantum many-body system thermalizes has received ever-growing attention. This interest has been primarily triggered by the increasing ability to prepare and manipulate such systems, which might be either *isolated* [1, 2] — as it is typically the case of experiments with cold atoms [3, 4] — or in contact with an environment (*open*), e.g., a thermal bath, and therefore subject to losses and driving. Examples for the latter case include exciton-polaritons [5–8] or photons [9, 10] in semiconductor or non-linear microcavities. In general

[†]The author of the thesis performed the main calculations presented in this chapter and wrote substantial parts of the manuscript. This chapter is the basis of a preprint that is currently being written.

it is unclear, *a priori*, by which physical mechanism an effective temperature is possibly established in these systems and, in case, what determines its value. In isolated systems, for instance, thermalization of local quantities might not eventually take place because of the presence of an extensive amount of conserved quantities induced by integrability [11–15] or many-body localization [16–19]. Although it is possible to define a variety of effective temperatures based on the static [20–22] and dynamic properties [23, 24] of the system, the lack of thermal behavior is witnessed by the fact that these temperatures do not assume all the same thermodynamic value. In open systems, instead, an effective temperature can be set by the level of noise induced by the environment [25–31]. In these cases effective thermalization often occurs only in the low-energy degrees of freedom. Alternatively, a completely different mechanisms such as dephasing due to interactions [26] can effectively determine the value of the temperature. All these examples show clearly that, on the one hand, the presence of effective thermodynamic equilibrium (which might be established only in a subsystem) is often by no means obvious while, on the other, it is not straightforward to give a precise instruction on how to act on a system in order to drive it into a non-equilibrium stationary state *at all scales*.

Before addressing the question of whether a certain system thermalizes or not, it is imperative to identify criteria which allow a clear-cut detection of thermodynamic equilibrium. In this direction it is important to consider of the system not only the properties of the density matrix which describes its stationary state, but also the dynamics which might or might not be compatible with equilibrium. In turn, from the theoretical point of view, the time evolution of statistical systems (both classical and quantum) is often conveniently studied in terms of the so-called dynamical functionals which are used in order to generate expectation values of physical observables in the form of functional integrals over a suitable set of fields. It is then natural to address the issue of thermalization by investigating the properties of the corresponding dynamical functional. In the case of classical statistical systems evolving under the effect of an external stochastic noise of thermal origin, this issue has been discussed to a certain level of detail in the past [32–37] and, in fact, it was found that the dynamical functional acquires a certain symmetry in equilibrium. Remarkably, the fluctuation-dissipation theorem which connects dynamical responses to correlation functions in equilibrium can be actually derived as a consequence of this symmetry. For quantum systems, instead, we are not aware of any analogous derivation based on the symmetries of the corresponding dynamical functional, which takes the form of the so-called Schwinger-Keldysh action (see, e.g., Refs. [38–40]).

The aim of the present work is to fill in this gap by showing that the Schwinger-Keldysh dynamical functional of a quantum system in thermal equilibrium is characterized by a *symmetry* which may be considered as the generalization of the classical one, to which it reduces in a suitable classical limit. In particular: (i) this symmetry holds for any Schwinger-Keldysh action associated to a time-independent Hamiltonian which generates the unitary dynamics of a closed quantum system, while (ii) it constraints the form of possible dissipative contributions to this action emerging, e.g., from a coupling with a thermal bath. For bosonic systems, we show that requiring the symmetry to be realized naturally leads to the emergence of the equilibrium Bose-Einstein distribution. Accordingly, this symmetry distinguishes between the unitary or dissipative dynamics leading to a stationary state of thermal equilibrium and those which do not.

Some of the consequences of this symmetry can be worked out rather conveniently within the field theoretical formalism: for example, the Ward-Takahashi identities associated with the symmetry constitute a hierarchy of generalized quantum fluctuation-dissipation relations (FDRs) for multi-time correlation functions of arbitrary order; in turn, these FDRs were shown to be equivalent to a combination of the quantum mechanical time reversal transformation [41] and the Kubo-Martin-Schwinger

(KMS) condition [42, 43]. Heuristically, this condition expresses the fact that the Hamiltonian ruling the time evolution of a system is the same as the one determining the density matrix of the canonical ensemble which characterizes the system when it is weakly coupled to a thermal bath. Hence a key conceptual step forward we take in this paper is to provide a compact formulation of the KMS condition (or, alternatively, of the equivalent hierarchy of FDRs) in terms of a single symmetry transformation. This is of great practical value, as it reduces answering the question about the possible presence of thermodynamic equilibrium to verifying a symmetry of the Schwinger-Keldysh action instead of having to check explicitly the validity of all FDRs. In particular, we show that the Markovian quantum dynamics described by a Lindblad master equation [44, 45] explicitly violates the symmetry. This reflects the driven nature of the system — indeed, the Lindblad equation may be viewed as resulting from the coarse graining of the evolution of an underlying time-dependent system-bath Hamiltonian, where the time dependence is dictated by coherent external driving fields.

The existence of this symmetry, beyond unifying the quantum and classical description of equilibrium systems, may play a crucial role in the study of the effective thermalization in non-equilibrium quantum statistical systems, for which the Schwinger-Keldysh formalism is a rather natural approach; in fact, the latter allows one to take advantage of a number of very powerful and efficient renormalization-group techniques for studying the possible emergence of collective behaviors, and for monitoring how the effective description of a statistical system depends on the length and time scale at which it is analyzed. The possible scale-dependence of the restoration/violation of the equilibrium symmetry could shed light on the mechanism underlying the thermalization of extended systems.

The rest of the presentation is organized as follows: in Sec. 7.2 we specify the symmetry transformation, collect various representations, and list a number of properties, which are then detailed in Sec. 7.3. In particular, in Sec. 7.3.1 we discuss the invariance of an Hamiltonian (unitary) evolution, while in Sec. 7.3.2 we consider possible dissipative terms which are invariant under the transformation, and show that any system governed by a quantum master equation in the Lindblad form violates it, due to the driven nature underlying the rotating wave and Markov approximations. In Sec. 7.3.3 we show that the quantum symmetry reduces to the one known in classical stochastic system in the limit $\hbar \rightarrow 0$. In Sec. 7.4 we show that the symmetry unveiled here can be interpreted as a practical implementation on the Schwinger-Keldysh functional integral of the KMS conditions [42, 43], which in Ref. [46] were instead formulated as identities within the full hierarchy of time-ordered correlation functions. Finally, Sec. 7.5 presents two applications of the equilibrium symmetry: in Sec. 7.5.1 we derive the single-particle fluctuation-dissipation relation, while in Sec. 7.5.2 we show that the steady states of a simple quantum master equation violates the symmetry.

7.2 Symmetry transformation

As we anticipated above, a convenient framework for the theoretical description of the time evolution of interacting quantum many-body systems is provided by the Keldysh functional integral formalism [38, 39]. In fact, it offers full flexibility in describing both non-equilibrium dynamics and equilibrium as well as non-equilibrium stationary states, which is not possible, e.g., within the finite-temperature Matsubara technique [47]. In addition, it is amenable to the well-established toolbox of quantum field theory. The simplest way to illustrate the basic ingredients of the Keldysh formalism is to consider the functional integral representation of the so-called Keldysh partition function Z . For a system with unitary dynamics generated by the Hamiltonian H and initialized in a state described by

the density matrix ρ_0 , this function is given by $Z = \text{tr} \left(e^{-iHt} \rho_0 e^{iHt} \right)$. (Note that, as it stands, $Z = 1$; however, it is convenient to think of its structure independently of its actual value.) In this expression, time evolution is interpreted as occurring along a closed path: starting in the state described by ρ_0 , the exponential e^{-iHt} to the left of ρ_0 corresponds to a “forward” evolution up to the time t , while the exponential e^{iHt} to its left corresponds to an evolution going “backward” in time. The trace $\text{tr}(\dots)$ connects, at time t , the forward with the backward branch of the time path and therefore it produces a closed path-time integral. Along each of these two branches, the temporal evolution can be represented in a standard way as a functional integral of an exponential weight e^{iS} over suitably introduced (generally complex) integration variables, i.e., fields, $\psi_+(t, \mathbf{x})$ and $\psi_-(t, \mathbf{x})$ on the forward and backward branches, respectively. The Keldysh action S is a functional of these two fields and it is generally obtained as a temporal integral along the close path in time of a Lagrangian density. (Explicit forms of S will be discussed further below, but they are not relevant for the present discussion.) By introducing different (time-dependent) sources J_\pm for the fields ψ_\pm on the two branches, the partition function $Z[J_+, J_-]$ is no longer identically equal to 1 and its functional derivatives can be used in order to generate various time-dependent correlation functions (see, e.g., Refs. [38–40]).

Within the formalism recalled above, the transformation \mathcal{T}_β which is a symmetry of the action S is specified by the way it acts on the fields along the closed time path, which are conveniently collected into two spinors $\Psi_\sigma(t, \mathbf{x}) = (\psi_\sigma(t, \mathbf{x}), \psi_\sigma^*(t, \mathbf{x}))^T$ with $\sigma = +$ and $-$ indicating the forward and backward branch, respectively. In the following we focus on the case of a single complex bosonic field which is simple enough but, at the same time general enough to introduce and illustrate all the basic ideas. The transformation \mathcal{T}_β is actually composed of a complex conjugation of the field components ψ_\pm , an inversion of the sign of the time variable, as well as a translation of the time variable into the complex plane by an amount $i\sigma\beta/2$ where β is a real parameter. In fact it acts on the fields $\psi_\sigma(t, \mathbf{x})$ and $\psi_\sigma^*(t, \mathbf{x})$ as

$$\begin{aligned} \mathcal{T}_\beta \psi_\sigma(t, \mathbf{x}) &= \psi_\sigma^*(-t + i\sigma\beta/2, \mathbf{x}), \\ \mathcal{T}_\beta \psi_\sigma^*(t, \mathbf{x}) &= \psi_\sigma(-t + i\sigma\beta/2, \mathbf{x}). \end{aligned} \quad (7.1)$$

For convenience and future reference we provide a representation of the action of \mathcal{T}_β both in the time and real space domain (t, \mathbf{x}) as well as in frequency-momentum domain (ω, \mathbf{q}) . The convention for the Fourier transforms of the fields is the following:

$$\Psi_\sigma(t, \mathbf{x}) = \int \frac{d^d \mathbf{q}}{(2\pi)^d} \int_{-\infty}^{+\infty} \frac{d\omega}{2\pi} e^{i(\mathbf{q}\cdot\mathbf{x} - \omega t)} \Psi_\sigma(\omega, \mathbf{q}), \quad (7.2)$$

where field spinors are defined as $\Psi_\sigma(\omega, \mathbf{q}) = (\psi_\sigma(\omega, \mathbf{q}), \psi_\sigma^*(-\omega, -\mathbf{q}))^T$ and d is the spatial dimensionality of the problem. In these terms, the symmetry \mathcal{T}_β reads, alternatively:

$$\begin{aligned} \mathcal{T}_\beta \Psi_\sigma(t, \mathbf{x}) &= \Psi_\sigma^*(-t + i\sigma\beta/2, \mathbf{x}) = \sigma_x \Psi_\sigma(-t + i\sigma\beta/2, \mathbf{x}), \\ \mathcal{T}_\beta \Psi_\sigma(\omega, \mathbf{q}) &= e^{-\sigma\beta\omega/2} \Psi_\sigma^*(\omega, -\mathbf{q}) = e^{-\sigma\beta\omega/2} \sigma_x \Psi_\sigma(-\omega, \mathbf{q}). \end{aligned} \quad (7.3)$$

Here we introduced the standard Pauli matrix $\sigma_x = \begin{pmatrix} 0 & 1 \\ 1 & 0 \end{pmatrix}$. The transformation in real time requires evaluating the fields for complex values of the time argument, which in principle is not defined; however, the complementary representation in Fourier space indicates how this can be done in practice: in fact, in frequency space the shift of time by an imaginary part $i\sigma\beta/2$ amounts to a multiplication by a prefactor $e^{-\sigma\beta\omega/2}$. In Sec. 7.3 we will show that while a Keldysh action S describing coherent (i.e.,

unitary) time evolution is invariant under \mathcal{T}_β independently of the value of the parameter β , dissipative contributions to the action do not break such a symmetry only if β is identified with the inverse temperature, $\beta = 1/T$ (see Sec. 7.3). As usual within the Keldysh formalism, it is convenient to introduce the classical and quantum fields defined as the symmetric and antisymmetric superpositions, respectively, of fields on the forward and backward branches:

$$\phi_c = \frac{1}{\sqrt{2}} (\psi_+ + \psi_-), \quad \phi_q = \frac{1}{\sqrt{2}} (\psi_+ - \psi_-), \quad (7.4)$$

which can also be combined in the spinors $\Phi_\nu(\omega, \mathbf{q}) = (\phi_\nu(\omega, \mathbf{q}), \phi_\nu^*(-\omega, -\mathbf{q}))^T$, where the index $\nu = c, q$ distinguishes classical and quantum fields. In these terms, the transformation \mathcal{T}_β becomes

$$\begin{aligned} \mathcal{T}_\beta \Phi_c(\omega, \mathbf{q}) &= \sigma_x \left(\cosh(\beta\omega/2) \Phi_c(-\omega, \mathbf{q}) - \sinh(\beta\omega/2) \Phi_q(-\omega, \mathbf{q}) \right), \\ \mathcal{T}_\beta \Phi_q(\omega, \mathbf{q}) &= \sigma_x \left(-\sinh(\beta\omega/2) \Phi_c(-\omega, \mathbf{q}) + \cosh(\beta\omega/2) \Phi_q(-\omega, \mathbf{q}) \right), \end{aligned} \quad (7.5)$$

which we report here for future convenience.

Here we anticipate and summarize a number of properties of the equilibrium transformation \mathcal{T}_β which are going to be discussed in detail in Secs. 7.3 and 7.4:

1. The transformation is discrete, and involutive, i.e., $\mathcal{T}_\beta^2 = \mathbb{1}$. This property follows straightforwardly from Eqs. (7.1) or (7.3).
2. \mathcal{T}_β can be written as a composition $\mathcal{T}_\beta = \mathbb{T} \circ \mathcal{K}_\beta$ of a time reversal transformation \mathbb{T} and an additional transformation \mathcal{K}_β , which we will identify in Sec. 7.4.3 as the implementation of the KMS condition within the Keldysh functional integral formalism.
3. \mathcal{T}_β is not uniquely defined, due to a certain freedom in implementing the time-reversal transformation within the Keldysh functional integral formalism, as discussed in Sec. 7.4.2. However, without loss of generality we stick to the definition provided in Eq. (7.1) and comment on the alternative forms in Sec. 7.4.2.
4. The transformation \mathcal{T}_β leaves the functional measure invariant, i.e., the absolute value of the Jacobian determinant associated with \mathcal{T}_β is equal to one, as we show in Sec. 7.4.4.
5. The various forms of the transformation \mathcal{T}_β presented above apply to the case of a system of bosons with vanishing chemical potential μ . In the presence of $\mu \neq 0$, Eq. (7.1) becomes

$$\begin{aligned} \mathcal{T}_\beta \psi_\sigma(t, \mathbf{x}) &= e^{\sigma\beta\mu/2} \psi_\sigma^*(-t + i\sigma\beta/2, \mathbf{x}), \\ \mathcal{T}_\beta \psi_\sigma^*(t, \mathbf{x}) &= e^{-\sigma\beta\mu/2} \psi_\sigma(-t + i\sigma\beta/2, \mathbf{x}), \end{aligned} \quad (7.6)$$

with a consequent modification of Eq. (7.3), which can be easily worked out. After transformation to the basis of classical and quantum fields in Eq. (7.4) this modification amounts to shifting the frequency ω in the arguments of the hyperbolic functions in Eq. (7.5) according to $\omega \rightarrow \omega - \mu$.

6. In taking the Fourier transforms in Eqs. (7.3) and (7.5) one implicitly assumes that the initial state of the system was prepared at time $t = -\infty$, while its evolution extends to $t = \infty$. In the following we will work under this assumption, commenting briefly on the role of an initial condition imposed at a finite time in Sec. 7.3.3.

7.3 Invariance of Keldysh action

As we demonstrate further below, a system is in thermodynamic equilibrium if its Keldysh action S is invariant under the transformation \mathcal{T}_β , i.e.,

$$S[\Psi] = \tilde{S}[\mathcal{T}_\beta\Psi], \quad (7.7)$$

where, for convenience of notation, $\Psi = (\Psi_+, \Psi_-)^T = (\psi_+, \psi_+^*, \psi_-, \psi_-^*)^T$ collects all the fields introduced in the previous section into a single vector. The tilde in \tilde{S} indicates that the parameters in S which are related to external fields have been replaced by their corresponding time-reversed values (e.g., the signs of magnetic fields is inverted), while in the absence of these parameters the tilde may be dropped. In Sec. 7.3.1, we demonstrate the invariance of the action associated with time-independent Hamiltonian dynamics. We then take the point of view that the *microscopic* dynamics of a system can always be thought as being generated by such a Hamiltonian, appropriate for a closed quantum system. In a renormalization group picture, such a setting does not exclude the possibility that dissipative contributions to the effective low-frequency and long-wavelength dynamics are generated upon coarse graining. The system may act as its own reservoir, as witnessed by the phenomenon of thermalization, or the finite lifetimes of low-energy single particle excitations in many-body systems. Indeed, in Sec. 7.3.2 we explicitly construct dissipative terms which comply with the thermal symmetry \mathcal{T}_β of the microscopic dynamics. In particular, we find that the noise components associated with these dissipative terms must necessarily have the form of the equilibrium Bose-Einstein distribution function, as appropriate to the bosonic fields which we are presently focussing on. This fact is often implicitly used in the very construction of the Keldysh action S of a certain system, especially when the interest is in the long-time stationary dynamics. In order to avoid keeping track of the initial state ρ_0 of the system at time t_0 , it is convenient to imagine that such a state was prepared in the remote past and to add even infinitesimally small dissipative terms [38, 39] compatible with the symmetry \mathcal{T}_β to the Keldysh action of the system. In fact, in the limit $t_0 \rightarrow -\infty$ they ensure that the dynamics of the system is the equilibrium one independently of the specific choice of ρ_0 , which can therefore be omitted in S . From a practical point of view, the requirement of invariance under \mathcal{T}_β provides stringent constraints on the possible form of a low-energy effective action in thermal equilibrium, such that it captures properly both static and dynamic properties of system. Conversely, given a generic effective action S_{eff} , one can decide whether it gives rise to an equilibrium dynamics or not solely on the basis of \mathcal{T}_β being a symmetry of S_{eff} or not, without the need to verify if the fluctuation-dissipation relations typical of equilibrium are satisfied.

7.3.1 Invariance of Hamiltonian dynamics

The microscopic Keldysh action associated to time-local, time independent Hamiltonian dynamics generated by H can be written as (for integrals we use the shorthand $\int_t \equiv \int_{-\infty}^{\infty} dt$, $\int_{\mathbf{x}} = \int d^d \mathbf{x}$; in the following $\sigma_z = \begin{pmatrix} 1 & 0 \\ 0 & -1 \end{pmatrix}$ is the standard Pauli matrix)

$$S = S_{\text{dyn}} + S_{\mathcal{H}}, \quad (7.8)$$

$$S_{\text{dyn}} = \frac{1}{2} \int_{t,\mathbf{x}} \left(\Psi_+^\dagger i\sigma_z \partial_t \Psi_+ - \Psi_-^\dagger i\sigma_z \partial_t \Psi_- \right), \quad (7.9)$$

$$S_{\mathcal{H}} = - \int_{t,\mathbf{x}} (\mathcal{H}_+ - \mathcal{H}_-) \quad (7.10)$$

We show below that the invariance of microscopic Keldysh action is directly related to the fact that it can be written as the sum of terms containing, respectively, only fields on the forward and backward branches. For concreteness, from now on we consider the Keldysh action for a bosonic many-body system with contact interactions, i.e., the Hamiltonian density in Eq. (7.10) is given by

$$\mathcal{H}_\sigma = \frac{1}{2m} |\nabla\psi_\sigma|^2 + \tau |\psi_\sigma|^2 + \lambda |\psi_\sigma|^4. \quad (7.11)$$

Here m is the mass of bosons, τ sets the minimal energy of single particles, and λ parametrizes two-body interactions. We choose this model for the sake of convenience: it is sufficiently general to illustrate all basic concepts associated with the thermal symmetry and, moreover, in the classical limit it allows for a direct comparison to dynamical equilibrium models [48, 49], where $\phi_c = (\psi_+ + \psi_-) / \sqrt{2}$ takes the role of a bosonic order parameter field.

Dynamical term

To begin with, here we show that the dynamical contribution Eq. (7.9) to the Keldysh action is invariant under the equilibrium transformation \mathcal{T}_β , i.e., we have $S_{\text{dyn}}[\mathcal{T}_\beta\Phi] = S_{\text{dyn}}[\Phi]$, where $\Phi = (\Phi_c, \Phi_q)^T = (\phi_c, \phi_c^*, \phi_q, \phi_q^*)^T$. Rewriting the contribution S_{dyn} in the Keldysh basis and in frequency-momentum space we obtain ($\int_{\omega, \mathbf{q}} \equiv \int \frac{d\omega d^d \mathbf{q}}{(2\pi)^{d+1}}$)

$$S_{\text{dyn}}[\mathcal{T}_\beta\Phi] = \int_{\omega, \mathbf{q}} \omega \left[\cosh^2(\beta\omega/2) \Phi_q^\dagger(\omega, \mathbf{q}) \sigma_z \Phi_c(\omega, \mathbf{q}) - \sinh^2(\beta\omega/2) \Phi_c^\dagger(\omega, \mathbf{q}) \sigma_z \Phi_q(\omega, \mathbf{q}) \right. \\ \left. + \sinh(\beta\omega/2) \cosh(\beta\omega/2) \left(\Phi_c^\dagger(\omega, \mathbf{q}) \sigma_z \Phi_c^\dagger(\omega, \mathbf{q}) - \Phi_q^\dagger(\omega, \mathbf{q}) \Phi_q(\omega, \mathbf{q}) \right) \right]. \quad (7.12)$$

The combination $\Phi_v^\dagger(\omega, \mathbf{q}) \sigma_z \Phi_v(\omega, \mathbf{q}) = \phi_v^*(\omega, \mathbf{q}) \phi_v(\omega, \mathbf{q}) - \phi_v(-\omega, -\mathbf{q}) \phi_v^*(-\omega, -\mathbf{q})$ with $v = c, q$ is an odd function of (ω, \mathbf{q}) , whereas $\omega \cosh(\beta\omega/2) \sinh(\beta\omega/2)$ is even, and the integral over the product of these terms, therefore, vanishes. Then with some simple manipulations of the first line in Eq. (7.12) invariance of S_{dyn} follows straightforwardly. We note that this property is independent of the value of β in the equilibrium transformation \mathcal{T}_β .

Hamiltonian contribution

We proceed to consider the transformation properties of the Hamiltonian contribution Eq. (7.10) under the thermal symmetry. First we argue that the strictly local terms (i.e., does that do not contain derivatives) in the Hamiltonian density (7.11) obey the symmetry, and then generalize the reasoning to the case of quasilocal terms such as the kinetic energy contribution or even non-local interactions. Hence let us consider an expression of the form

$$\mathcal{V}[\Psi] = \int_{t, \mathbf{x}} (v_+(t, \mathbf{x}) - v_-(t, \mathbf{x})), \quad (7.13)$$

where $v_\sigma(t, \mathbf{x}) = (\psi_\sigma^*(t, \mathbf{x}) \psi_\sigma(t, \mathbf{x}))^N$. For $N = 2$ this is just the contact interaction of Eq. (7.11). Since $v_\sigma(t, \mathbf{x})$ is real, under the equilibrium transformation only its time argument is shifted according to

$\mathcal{T}_\beta v_\sigma(t, \mathbf{x}) = v_\sigma(-t + i\sigma\beta/2, \mathbf{x})$, and taking the Fourier transform with respect to time of this relation yields

$$\mathcal{T}_\beta v_\sigma(\omega, \mathbf{x}) = e^{-\sigma\beta\omega/2} v_\sigma(-\omega, \mathbf{x}). \quad (7.14)$$

The vertex (7.13), then, is invariant under \mathcal{T}_β : it is local in time and, therefore, in a diagrammatic representation where fields $\psi_\sigma(t, \mathbf{x})$ are represented by ingoing lines and complex conjugates $\psi_\sigma^*(t, \mathbf{x})$ by outgoing lines, it obeys frequency conservation for in- and outgoing lines, as can be seen by taking the Fourier transform of each of the fields in $v_\sigma(t, \mathbf{x})$ individually. In particular, the frequency variable ω appearing in Eq. (7.14) corresponds to the difference of the sums of in- and outgoing frequencies respectively, and only the $\omega = 0$ component contributes to Eq. (7.13). This component, however is evidently invariant under \mathcal{T}_β , and hence the same is true for the vertex, $\mathcal{V}[\mathcal{T}_\beta\Psi] = \mathcal{V}[\Psi]$. Clearly, the invariance of the coherent interaction vertex (and also of the dynamical term Eq. (7.9)) relies on the fact that time-local vertices obey frequency conservation, and this invariance is realized for any value of the parameter β . From this we conclude that any contribution to the Hamiltonian which is local in time and does not explicitly depend on time is invariant. Thus the derivation presented here for the vertex Eq. (7.13) can straightforwardly be generalized to expressions containing derivatives such as the kinetic energy in Eq. (7.11) and even non-local interactions. Note that these considerations do not rule out the emergence of time-nonlocal terms upon renormalization, as long as they are consistent with the symmetry.

Enhanced symmetry for simple integrable systems

In the form presented in Sec. 7.2 the equilibrium transformation \mathcal{T}_β contains a single parameter β . While this form is appropriate for systems in thermodynamic equilibrium, where (as we show below) $\beta = 1/T$ is the inverse temperature, an enhanced form of the symmetry is realized in simple integrable systems which have single-particle states as eigenmodes. The stationary state of such systems is a generalized Gibbs ensemble [13, 50–57], determined (in the cases we consider) by the extensive amount of conserved eigenmode occupation numbers. Here we provide an example where the Lagrangian multipliers associated with these conserved occupations correspond to parameters in a generalization of the equilibrium transformation Eq. (7.3) or, more specifically, to inverse temperatures of the individual eigenmodes of the system. In the non-integrable case the eigenstates of the system Hamiltonian are not single-particle states and the symmetry is realized only with a single parameter β .

As an example of a non-integrable system, let us consider bosons on a d -dimensional lattice with hopping and on-site interactions, such that the Hamiltonian is given by

$$\begin{aligned} H &= H_{\text{kin}} + H_{\text{int}}, \\ H_{\text{kin}} &= -T \sum_{\langle \mathbf{I}, \mathbf{I}' \rangle} a_{\mathbf{I}}^\dagger a_{\mathbf{I}'}, \\ H_{\text{int}} &= \frac{U}{2} \sum_{\mathbf{I}} a_{\mathbf{I}}^\dagger a_{\mathbf{I}} (a_{\mathbf{I}}^\dagger a_{\mathbf{I}} - 1), \end{aligned} \quad (7.15)$$

where $a_{\mathbf{I}}$ is the annihilation operator for bosons on the lattice site \mathbf{I} ; T is the hopping matrix element between site \mathbf{I} and its nearest neighbors \mathbf{I}' , and finally U determines the strength of on-site interactions. The kinetic energy contribution to the Hamiltonian is diagonal in momentum space and the corresponding eigenmodes are the Bloch states. In the non-interacting limit $U = 0$ the occupation

numbers of Bloch states become conserved quantities, making the model integrable. Then the contribution from each individual quasi-momentum \mathbf{q} and band index n to the Keldysh action corresponding to the kinetic energy

$$H_{\text{kin}} = \sum_{\mathbf{q},n} \epsilon_{\mathbf{q},n} a_{\mathbf{q},n}^\dagger a_{\mathbf{q},n}, \quad (7.16)$$

where $a_{\mathbf{q},n}$ is the annihilation operator for a particle in the Bloch state with quantum numbers \mathbf{q} and n , is invariant under the transformation (cf. Eq. (7.3); here $A_{\mathbf{q},n,\sigma}(\omega) = (a_{\mathbf{q},n,\sigma}(\omega), a_{-\mathbf{q},n,\sigma}^*(-\omega))^T$)

$$\mathcal{T}_{\beta_{\mathbf{q},n}} A_{\mathbf{q},n,\sigma}(\omega) = e^{-\sigma\beta_{\mathbf{q},n}\omega/2} A_{-\mathbf{q},n,\sigma}^*(\omega), \quad (7.17)$$

where crucially $\beta_{\mathbf{q},n}$ can be chosen to depend on the state indices, indicating that to each eigenmode of the system can be assigned an individual “temperature” $T_{\mathbf{q},n} = 1/\beta_{\mathbf{q},n}$ such that the mean occupation number of the state \mathbf{q}, n is determined by a Bose distribution with precisely this “temperature.”

Let us now consider the opposite limit in which the hopping amplitude vanishes, $J = 0$, while the interaction strength remains finite. The interaction energy in Eq. (7.15) is diagonal in the basis of Wannier states localized at specific lattice sites and occupation numbers of these sites are conserved, hence also in this case the system is integrable. The proper generalized symmetry transformation is obtained from Eq. (7.17) by replacing the quasi-momentum and band index by the lattice site index \mathbf{l} or, in other words, there are local “temperatures” $T_{\mathbf{l}} = 1/\beta_{\mathbf{l}}$.

In the generic case, when both hopping and interactions are non-zero, the system is not integrable. Then neither the generalized transformation Eq. (7.17) nor the variant with local “temperatures” are symmetries of the corresponding Keldysh action, showing that this case allows only for one single global temperature determining mean occupation numbers of single-particle states.

7.3.2 Dissipative contributions in equilibrium

The functional integral with action (7.8) is not convergent but can be made so by supplying infinitesimal imaginary or, in other words, dissipative contributions [38, 39]. In a renormalization group picture, these *infinitesimal* imaginary parts may be seen as the microscopic initial values of *finite* dissipative contributions which are obtained upon coarse graining by means of the renormalization group flow, and result in, e.g., finite lifetimes of excitations of the effective low-energy degrees of freedom. The precise form of the effective low-energy action and, in particular, its dissipative contributions, is strongly constrained by the presence of the equilibrium symmetry at the microscopic starting point: terms which violate the symmetry will not be generated in the renormalization group flow. Therefore, by identifying dissipative contributions to the Keldysh action which possess the symmetry in the following sections, we are able to anticipate the structure of the low-energy effective action.

Finite dissipative terms even at a microscopic scale can be due to, e.g., coupling the system to a bath. Below we consider two examples for this case: in Sec. 7.5.2 we show that the equilibrium symmetry is broken explicitly if the system is coupled to Markovian baths and driven – a situation described by a quantum master equation. Another specific example in which the equilibrium symmetry is obeyed is the particle number non-conserving coupling of the Keldysh action Eq. (7.8) to an Ohmic bath. This situation, which we discuss in Sec. 7.3.3, is of particular interest since it leads in the classical limit to the dynamical model A [48] with reversible mode couplings (termed model A* in Ref. [49]), allowing us to establish the connection to the known equilibrium symmetry of the classical generating functional.

Single particle sector

Dissipative contributions to the single-particle sector that are compatible with the symmetry take the form

$$S_d = i \int_{\omega, \mathbf{q}} h(\omega, \mathbf{q}) \left(\phi_q^*(\omega, \mathbf{q}) \phi_c(\omega, \mathbf{q}) - \phi_q(\omega, \mathbf{q}) \phi_c^*(\omega, \mathbf{q}) + 2 \coth(\beta\omega/2) \phi_q^*(\omega, \mathbf{q}) \phi_q(\omega, \mathbf{q}) \right) \quad (7.18)$$

with a real function $h(\omega, \mathbf{q})$ that transforms under time reversal as $\tilde{h}(\omega, \mathbf{q}) = h(\omega, -\mathbf{q})$. The typical choice made in regularizations of the Keldysh functional integral is $h(\omega, \mathbf{q}) = \epsilon$ [38, 39] with $\epsilon \rightarrow 0$ and ensures that the bare Green's functions, i.e., those that are obtained by ignoring the influence of interactions, satisfy a fluctuation-dissipation relation (we postpone the detailed discussion of the FDR to Sec. 7.5.1). Crucially, the function $\coth(\beta\omega/2)$ is *uniquely* fixed by the requirement of invariance under the symmetry, as can be verified following the subsequent discussion. In particular, S_d with a certain value of β in the argument of $\coth(\beta\omega/2)$ is invariant under $\mathcal{T}_{\beta'}$ if and only if $\beta' = \beta$. This shows that the thermodynamic equilibrium Bose distribution function $n(\omega)$ at a temperature $T = 1/\beta$ appearing implicitly in $\coth(\beta\omega/2) = 2n(\omega) + 1$ can be traced back to the symmetry. The appearance of the Bose distribution function $n(\omega)$ is entirely due to the required invariance under the equilibrium transformation! Note that here for simplicity we consider only the case of vanishing chemical potential. For finite μ , the frequency in the argument of the hyperbolic cotangent in Eq. (7.18) should be shifted according to $\omega \rightarrow \omega - \mu$.

We proceed by showing the invariance of S_d as given by Eq. (7.18). This is most conveniently done by assuming that the function $h(\omega, \mathbf{q})$ has definite parity and considering separately the cases of odd and even parity in frequency, $h_o(-\omega, \mathbf{q}) = -h_o(\omega, \mathbf{q})$ and $h_e(-\omega, \mathbf{q}) = h_e(\omega, \mathbf{q})$, respectively. The general case follows straightforwardly by linear combination. Thus we consider

$$S_d = i\epsilon \int_{\omega, \mathbf{q}} \Phi_q^\dagger(\omega, \mathbf{q}) \left\{ \begin{array}{l} h_o(\omega, \mathbf{q}) \\ h_e(\omega, \mathbf{q}) \sigma_z \end{array} \right\} \left(\Phi_c(\omega, \mathbf{q}) + \coth(\beta\omega/2) \Phi_q(\omega, \mathbf{q}) \right). \quad (7.19)$$

Inserting here the transformed fields, Eq. (7.5), where for the moment we assume that the parameter in the transformation takes the value β' which is different from the β in Eq. (7.19), we obtain

$$\begin{aligned} S_d[\mathcal{T}_{\beta'}\Phi] = i\epsilon \int_{\omega, \mathbf{q}} & \left(\sinh(\beta'\omega/2) \Phi_c^\dagger(-\omega, \mathbf{q}) + \cosh(\beta'\omega/2) \Phi_q^\dagger(-\omega, \mathbf{q}) \right) \sigma_x \left\{ \begin{array}{l} h_o(\omega, \mathbf{q}) \\ h_e(\omega, \mathbf{q}) \sigma_z \end{array} \right\} \sigma_x \\ & \times \left[\cosh(\beta'\omega/2) \Phi_c(-\omega, \mathbf{q}) - \sinh(\beta'\omega/2) \Phi_q(-\omega, \mathbf{q}) \right. \\ & \left. + \coth(\beta\omega/2) \left(-\sinh(\beta'\omega/2) \Phi_c(-\omega, \mathbf{q}) + \cosh(\beta'\omega/2) \Phi_q(-\omega, \mathbf{q}) \right) \right]. \quad (7.20) \end{aligned}$$

Note that only for $\beta' = \beta$ the terms in the second and third lines involving the classical field spinor Φ_c cancel each other. Otherwise, terms $\sim \Phi_c^\dagger \Phi_c$ remain, violating causality. For $\beta' = \beta$ instead, using the identities for Pauli matrices $\sigma_x^2 = \mathbb{1}$ and $\sigma_x \sigma_z \sigma_x = -\sigma_z$, and performing a change of integration variables $\omega \rightarrow -\omega$ (keeping in mind the parity of $h_o(\omega, \mathbf{q})$ and $h_e(\omega, \mathbf{q})$) we find

$$\begin{aligned} S_d[\mathcal{T}_\beta\Phi] = -i\epsilon \int_{\omega, \mathbf{q}} & \left(-\sinh(\beta\omega/2) \Phi_c^\dagger(\omega, \mathbf{q}) + \cosh(\beta\omega/2) \Phi_q^\dagger(\omega, \mathbf{q}) \right) \left\{ \begin{array}{l} h_o(\omega, \mathbf{q}) \\ h_e(\omega, \mathbf{q}) \sigma_z \end{array} \right\} \\ & \times (\sinh(\beta\omega/2) - \coth(\beta\omega/2) \cosh(\beta\omega/2)) \Phi_q(\omega, \mathbf{q}). \quad (7.21) \end{aligned}$$

Finally, using the hyperbolic identity

$$\sinh(x) - \coth(x) \cosh(x) = -1/\sinh(x), \quad (7.22)$$

after some straightforward algebraic manipulations we find $S_d[\mathcal{T}_\beta\Phi] = S_d[\Phi]$.

Dissipative vertices

Dissipative contributions in the quadratic part of the Keldysh action discussed in the previous section occur, e.g., when the system is coupled to a thermal bath such that the system-bath interaction is linear in the system field operators. This type of coupling explicitly breaks particle number conservation, which is not the case if instead the bath couples to a system operator which commutes with the total number of particles, e.g., the local density $n(\mathbf{x}) = \psi^\dagger(\mathbf{x})\psi(\mathbf{x})$. In other words, to ensure particle number conservation it is necessary that the coupling terms are quadratic or of higher order in the system operators. Then dissipative *vertices* appear after integrating out the bath degrees of freedom, and the requirement of invariance under the equilibrium symmetry allows us to infer *a priori* what the structure of such vertices might be. In particular, we find a frequency-independent number-conserving quartic vertex (i.e., the direct dissipative counterpart to the two-body interaction in the Hamiltonian Eq. (7.11)) is forbidden by the thermal symmetry. We note, however, that below in Sec. 7.3.3 we will encounter a case where this type of vertex emerges effectively in the classical limit.

A general number-conserving time-local quartic vertex is given by (for notational convenience we suppress the spatial arguments of fields)

$$S_d = -i \int_{\omega_1, \dots, \omega_4} \delta(\omega_1 - \omega_2 + \omega_3 - \omega_4) (f_1(\omega_1, \omega_2, \omega_3, \omega_4) \psi_+(\omega_1) \psi_+(\omega_2) \psi_+(\omega_3) \psi_+(\omega_4) \\ + f_2(\omega_1, \omega_2, \omega_3, \omega_4) \psi_-(\omega_1) \psi_-(\omega_2) \psi_-(\omega_3) \psi_-(\omega_4) \\ + f_3(\omega_1, \omega_2, \omega_3, \omega_4) \psi_+(\omega_1) \psi_+(\omega_2) \psi_-(\omega_3) \psi_-(\omega_4)), \quad (7.23)$$

where $f_{1,2,3}$ are real functions. Conservation of particle number is ensured in each term separately by the appearance of an equal number of fields and complex conjugate fields with the same contour index; The δ -function enforces locality in time. Without loss of generality we may assume that f_1 and f_2 are invariant under a simultaneous exchange of ω_1 with ω_3 and ω_2 with ω_4 , respectively. Causality then implies that the contribution S_d to the action must vanish for $\psi_+ = \psi_-$, i.e.,

$$f_1(\omega_1, \omega_2, \omega_3, \omega_4) + f_2(\omega_1, \omega_2, \omega_3, \omega_4) + \frac{1}{2} (f_3(\omega_1, \omega_2, \omega_3, \omega_4) + f_3(\omega_2, \omega_1, \omega_4, \omega_3)) = 0. \quad (7.24)$$

Note that only the part of f_3 that is symmetric with respect to the exchange of frequencies mentioned above enters this condition. Now let us consider Eq. (7.23) with transformed fields $\mathcal{T}_\beta \Psi_\sigma$. Requiring invariance, we find the conditions

$$\begin{aligned} f_1(\omega_1, \omega_2, \omega_3, \omega_4) &= f_1(\omega_2, \omega_1, \omega_4, \omega_3), \\ f_2(\omega_1, \omega_2, \omega_3, \omega_4) &= f_2(\omega_2, \omega_1, \omega_4, \omega_3), \\ f_3(\omega_1, \omega_2, \omega_3, \omega_4) &= e^{\beta[\omega_1 - \omega_2 - (\omega_3 - \omega_4)]/2} f_3(\omega_2, \omega_1, \omega_4, \omega_3), \end{aligned} \quad (7.25)$$

where it is implicitly assumed that frequency is conserved according to the δ -function in Eq. (7.23). To begin with we investigate the possibility of a frequency-independent solution. Then the system of equations (7.24) and (7.25) is solved by

$$f_1 = -f_2 = \text{const.}, \quad f_3 = 0. \quad (7.26)$$

This solution, however, is unphysical and can hence be ruled out for the following reasons: inserting (7.26) in Eq. (7.23) yields a vertex that is equal to the two-body interaction in Eq. (7.11) apart

from an overall factor of i , i.e., such a vertex would originate from an *imaginary* two-body coupling in a Hamiltonian, clearly violating hermiticity. In addition, this term, which could be written as iH' with Hermitean $H'^{\dagger} = H'$, would change sign under the time reversal transformation that is included in Eq. (7.7): $TiH'T^{\dagger} = -iH'$. Equations (7.25) should then be replaced by

$$f_i = -f_i, \quad i = 1, 2, \quad (7.27)$$

which is solved by $f_i = 0$. While this demonstrates that a frequency-independent number-conserving quartic vertex is not compatible with equilibrium conditions, Eqs. (7.24) and (7.25) *do* allow for solutions f_i that depend on frequency. One particular solution is given by

$$\begin{aligned} f_3(\omega_1, \omega_2, \omega_3, \omega_4) &= -4(\omega_1 - \omega_2)(n(\omega_1 - \omega_2) + 1), \\ f_1(\omega_1, \omega_2, \omega_3, \omega_4) &= f_2(\omega_1, \omega_2, \omega_3, \omega_4) = (\omega_1 - \omega_2) \coth(\beta(\omega_1 - \omega_2)/2). \end{aligned} \quad (7.28)$$

with the Bose distribution function $n(\omega)$. It is interesting to note that in the basis of classical and quantum fields this corresponds to a generalization of Eq. (7.18) with $h(\omega, \mathbf{q}) = \omega$ in which the fields are replaced by the respective densities defined as $\rho_c = \psi_+^* \psi_+ + \psi_-^* \psi_-$ and $\rho_q = \psi_+^* \psi_+ - \psi_-^* \psi_-$. The functions f_i in Eq. (7.28) approach a constant value as the difference $\omega_1 - \omega_2$ goes to zero, and therefore this solution gives the leading dissipative contribution to the action of a number-conserving system in the low-frequency limit.

7.3.3 Classical limit, detailed balance and microreversibility

An analogous equilibrium symmetry was previously derived for the stochastic evolution of classical statistical systems in contact with an environment which acts as a source of noise, within the response functional formalism [32, 34, 35, 58–61]. This formalism allows one to determine expectation values of relevant quantities as a functional integral with a certain “action” known as response functional, which can also be derived from a suitable classical limit of the Keldysh action for quantum systems [38, 39].

Here, we show that the classical limit of \mathcal{T}_β yields exactly the transformation which implements the equilibrium symmetry known for classical systems [36]. In order to consider the classical limit within the Keldysh formalism it is convenient to express the Keldysh action in Eq. (7.8) in terms of the classical and quantum fields defined in Eq. (7.4), while reinstating the Planck constant according to [38, 39]

$$S \rightarrow S/\hbar, \quad \coth(\beta\omega/2) \rightarrow \coth(\beta\hbar\omega/2), \quad \phi_q \rightarrow \hbar\phi_q \quad (7.29)$$

for $\hbar \rightarrow 0$. Then the action can be formally expanded in powers of \hbar . The classical part of the Keldysh action is then given by the contribution which remains for $\hbar = 0$. Note that the same formal simplifications apply at finite temperatures in the vicinity of a critical point, $m/T \rightarrow 0$, where m is the mass scale in the retarded Green’s function, by applying power counting arguments (see, e.g., [31]). This conforms with the expectation that quantum fluctuations generically play only a subdominant role at high temperatures.

In order to see the emergence of a stochastic dynamics driven by incoherent (thermal) noise from a quantum coherent dynamics, we supplement the Keldysh action in Eq. (7.8) describing the latter with dissipative terms arising from its coupling to a bath. For simplicity, we assume this bath to be characterized by an ohmic spectral density. This physical situation can be formally implemented

based on Eq. (7.77) under the assumption that $\gamma(\omega)\nu(\omega) = 2\kappa\omega$ is linear in the frequency, and by choosing $L_\sigma(\omega) \rightarrow \psi_\sigma(\omega, \mathbf{q})$ (note that we now consider a multimode system). The thermal bath is thus assumed to act independently on each momentum mode [39]. Then, in the classical limit with $\coth(\beta\omega/2) \sim 2T/\omega$ we find

$$S = \int_{t,\mathbf{x}} \Phi_q^\dagger \left\{ \left[(\sigma_z + i\kappa\mathbb{1}) i\partial_t + \frac{1}{2m} \nabla^2 \right] \Phi_c + i2\kappa T \Phi_q \right\} - \lambda \int_{t,\mathbf{x}} (\phi_c^{*2} \phi_c \phi_q + \text{c.c.}). \quad (7.30)$$

The action in Eq. (7.30) is of the form of the equilibrium dynamical models considered in Ref. [48]: it includes a contribution which is linear and one which is quadratic in the quantum field. After having transformed the latter quadratic term into a linear one via the introduction of an auxiliary field (which is eventually interpreted as a Gaussian additive noise), the quantum field can be integrated out and one is left with an effective constraint on the dynamics of the classical field which takes the form of a Langevin equation, namely

$$(i - \kappa) \partial_t \phi_c = \left(-\frac{1}{2m} \nabla^2 + \lambda |\phi_c|^2 \right) \phi_c + \eta, \quad (7.31)$$

where $\eta = \eta(\mathbf{x}, t)$ is a Gaussian stochastic variable which satisfies

$$\langle \eta(\mathbf{x}, t) \rangle = 0, \quad \langle \eta(\mathbf{x}, t) \eta^*(\mathbf{x}', t') \rangle = \kappa T \delta(t - t') \delta^{(d)}(\mathbf{x} - \mathbf{x}'), \quad \langle \eta(\mathbf{x}, t) \eta(\mathbf{x}', t') \rangle = 0. \quad (7.32)$$

This equation describes the dynamics of the non-conserved (complex scalar) field Φ_c without additional conserved densities, which is known in the literature as *model A* [48]. However, as it can be seen from the complex prefactor of the time derivative in Eq. (7.30), the dynamics is not purely relaxational as in model A but it has additional coherent contributions, also known as *reversible mode couplings* [61]. The fact that the simultaneous appearance of dissipative and coherent dynamics can be described by a complex prefactor of the time derivative is specific to thermal equilibrium – dividing Eq. (7.31) by it, one may think of reversible and irreversible generators of the Langevin dynamics which are not independent of each other, but whose coupling constants share a common ratio [34, 35, 62]. In a more general non-equilibrium situation, these reversible and irreversible generators result from different microscopic origins and no common ratio thus exists. In the present equilibrium context, however, the action Eq. (7.30) corresponds to *model A** in the notation of Ref. [49], and the form of the equilibrium symmetry appropriate for this case was given in Ref. [31]. Here we show that this equilibrium symmetry emerges as the classical limit of the equilibrium transformation \mathcal{T}_β . In fact, for $\beta \rightarrow 0$ and neglecting the contribution of the quantum fields in the transformation of the classical fields (i.e., at the leading order in \hbar), Eq. (7.5) becomes

$$\begin{aligned} \mathcal{T}_\beta \Phi_c(t, \mathbf{x}) &= \sigma_x \Phi_c(-t, \mathbf{x}), \\ \mathcal{T}_\beta \Phi_q(t, \mathbf{x}) &= \sigma_x \left(\Phi_q(-t, \mathbf{x}) + \frac{i}{2T} \partial_t \Phi_c(-t, \mathbf{x}) \right), \end{aligned} \quad (7.33)$$

after a transformation back to the time and space domains. Upon identifying the classical field Φ_c with the physical field and Φ_q with the response field $\tilde{\Phi}$, according to $\Phi_q = i\tilde{\Phi}$, Eq. (7.33) takes the form of the classical symmetry introduced in Ref. [36]. Note, however, that the transformation (7.33) is not the only form in which the equilibrium symmetry in the classical context can be expressed. In fact, the transformation of the response field can also be expressed [34, 35] in terms of a functional derivative of the equilibrium distribution rather than of the time derivative of the classical field as in Eq. (7.33).

The existence of these different but equivalent transformations might be related to the freedom in the definition of the response field, which is introduced in the theory as an auxiliary variable in order to enforce the dynamical constraint represented by the Langevin equation [34, 35, 61, 63]. This has the well-known consequence [63] that the related action acquires the so-called Slavnov-Taylor symmetry. As far as we know, the consequences of this symmetry have not been thoroughly investigated in the classical case and its role in the quantum case surely represents an intriguing issue for future studies.

We emphasize the fact that the derivation of the symmetry in the classical case involves explicitly the equilibrium probability density [34, 35]. In fact, the response functional contains also the probability distribution of the value of the fields at the initial time, after which the dynamics is considered. This term breaks, in general, the time translational invariance of the theory [34, 35], unless the probability distribution is the equilibrium one. Therefore, when the classical equilibrium symmetry \mathcal{T}_β is derived under the assumption of time-translational invariance, the equilibrium distribution is explicitly taken into account in calculations. In the quantum case, time-translational symmetry was implicitly imposed by extending the time integration in the action from $-\infty$ to $+\infty$, which is equivalent to the explicit inclusion of the initial condition (in the form of an initial density matrix) and makes the analysis simpler, though less transparent from a physical standpoint.

Although in classical systems this equilibrium symmetry takes (at least) two different but equivalent forms due to some arbitrariness in the definition of the response functional, it can always be traced back to the condition of detailed balance [34–36]. Within this context, detailed balance is defined as the request that the probability of observing a certain (stochastic) realization of the dynamics of the system equals the probability of observing the time-reversed realization, and therefore it encodes the notion of *microreversibility*. This condition guarantees the existence and validity of fluctuation-dissipation relations, which can be proved on the basis of this symmetry. In addition, detailed balance constrains the form that the response functional can take as well as the form of the equilibrium probability distribution for this stochastic process.

The situation in the quantum case appears to be significantly less clear. In fact, a precise notion of *quantum detailed balance* and *quantum microreversibility* is seemingly still lacking. The first attempt to introduce a principle of quantum detailed balance dates back to Ref. [64], where it was derived from a condition of microreversibility in the context of Markovian quantum dynamics described by a Lindblad master equation. The mathematical properties of this conditions were subsequently studied in detail (see, e.g., Refs. [65–69]) and were shown to constrain the form of the Lindblad super-operator in order to admit a Gibbs-like stationary density matrix. However, these Lindbladians are not able to reproduce the KMS conditions and the fluctuation-dissipation relations because of the underlying Markovian approximation, as we discussed in Sec. 7.5.2.

The notion of quantum microreversibility in quantum systems appears to have received even less attention, as well as its connection with some sort of statistical reversibility. The definition proposed in Ref. [64] (also discussed in Ref. [70]) appears to be a natural generalization of the definition in the classical case, as it relates the correlation of operators at two different times with the correlation of the time-reversed ones. However, to our knowledge, the relationship between this condition and thermodynamic equilibrium has never been fully elucidated. Although addressing these issues goes well beyond the scope of the present paper, they represent an interesting subject for future investigations.

7.4 Physical interpretation

In this section we show that if the Keldysh action of a certain system is symmetric (as specified in Sec. 7.3) under the equilibrium transformation \mathcal{T}_β , then the multi-time correlation functions of the relevant fields satisfy the KMS condition [42, 43]. As the latter can be considered the defining property of thermodynamic equilibrium, this shows that the same can be said of the invariance under the equilibrium symmetry.

The KMS condition involves *both* the Hamiltonian generator of dynamics *and* the thermal nature of the density matrix which describes the stationary state of the system: heuristically this condition amounts at requiring that the many-body Hamiltonian which determines the (canonical) population of the various energy levels is the same as the one which rules the dynamics of the system. The equivalence proved here allows us to think of the problem from a different perspective: taking the symmetry as the fundamental property and observing that any time-independent Hamiltonian respects it, we may require it to hold at any scale, beyond the microscopic scale governed by reversible Hamiltonian dynamics alone. In particular, upon coarse graining in a renormalization group picture, only irreversible dissipative terms which comply with the symmetry can be generated in stationary state, and the hierarchy of correlation functions respect thermal fluctuation-dissipation relations. Thus we see how Hamiltonian dynamics favors thermal stationary states (with static correlation functions described by $e^{-\beta H}$) over arbitrary functionals $\rho = \rho(H)$. One explicit technical advantage of the symmetry point of view is that it allows us to utilize the toolbox of quantum field theory straightforwardly and study the implications of its obedience; this is exemplified here by considering the associated Ward-Takahashi identities and by showing the absence of this symmetry in dynamics described by Markovian quantum master equations. We also note that the symmetry can be used as a diagnostic tool for equilibrium states, applied to the dynamic action functional directly instead of testing the whole hierarchy of fluctuation-dissipation relations. It may be present in open system actions with both reversible and dissipative terms.

In the following we consider a quantum system with coherent dynamics generated by the Hamiltonian H , which is in thermal equilibrium at temperature $T = \beta^{-1}$ with density matrix $\rho = e^{-\beta H} / Z$. The KMS condition relies on the observation that for an operator in Heisenberg representation $A(t) = e^{iHt} A e^{-iHt}$, we have the identity

$$A(t)\rho = \rho A(t - i\beta) \quad (7.34)$$

(for simplicity we do not include here a chemical potential but we indicate the necessary modifications at the end of the discussion). This identity effectively corresponds, up to a translation of the time by an imaginary amount, to exchanging the order of the density matrix and of the operator A and therefore, when Eq. (7.34) is applied to a multi-time correlation function, it turns out to invert the time order, which can be subsequently restored by means of the quantum-mechanical time-reversal operation. Accordingly, time reversal naturally appears as an element of the equilibrium symmetry \mathcal{T}_β ; however, invariance under \mathcal{T}_β *does not* necessarily require that H is invariant under the time-reversal operation. A simple example is provided by systems which are subject to an external magnetic field, which, strictly speaking, are not invariant under the quantum-mechanical time reversal, but might still be compatible with the equilibrium symmetry. The application of time reversal yields a representation of the KMS condition that can be readily translated into the Keldysh formalism, as it was first noted in Ref. [46]. In particular, it results in an infinite hierarchy of generalized multi-time quantum FDRs which include the usual FDR for the single-particle correlation and response functions as a special

case (see Ref. [46] and Sec. 7.5.1). One of the main points of this paper is that these FDRs can be also regarded as the Ward-Takahashi identities¹, and that the full hierarchy of FDRs is equivalent to the invariance of the Keldysh action with respect to the equilibrium symmetry transformation.

The argument outlined below, which shows the equivalence between the KMS condition and the thermal symmetry, proceeds in several steps: as preliminaries we review in Secs. 7.4.1 and 7.4.2 how time-ordered and anti-time-ordered multi-time correlation functions can be expressed using the Keldysh technique, and we specify how these correlation functions transform under time reversal. We apply these results to the KMS condition in Sec. 7.4.3: first we discuss its generalization to multi-time correlation functions and then the translation of this generalized version to the Keldysh formalism. This part proceeds mainly along the lines of Ref. [46] with some technical differences. Finally, we establish the equivalence between the resulting hierarchy of FDRs and the thermal symmetry at the end of Sec. 7.4.3.

7.4.1 Multi-time correlation functions in the Keldysh formalism

Two-time correlation functions. Let us first consider a two-time correlation function

$$\langle A(t_A)B(t_B) \rangle \equiv \text{tr} (A(t_A)B(t_B)\rho) \quad (7.35)$$

between two generic operators A and B evaluated at different times t_A and t_B , respectively, in a system described by the density matrix ρ . We assume that the dynamics of the system is coherent and generated by the Hamiltonian H . The two-time correlation function can be represented within the Keldysh formalism as

$$\langle A(t_A)B(t_B) \rangle = \langle A_{-}(t_A)B_{+}(t_B) \rangle, \quad (7.36)$$

irrespective of the relative order of the times t_A and t_B . Hereafter, by $O_{+/-}$ we indicate that a certain operator O has been evaluated in terms of the fields defined on the forward/backward branch of the temporal contour associated with the Keldysh formalism (see, e.g., Refs. [38, 39]). In order to fix the notation and as a preparation for the subsequent discussion of a multi-point correlation function, let us recall here the derivation of Eq. (7.36). The Heisenberg operator A at time t_A is related to the Schrödinger operator at a certain initial time $t_i < t_A$ via

$$A(t_A) = e^{iH(t_A-t_i)} A e^{-iH(t_A-t_i)}, \quad (7.37)$$

with an analogous relation for B . In what follows we are particularly interested in considering the case in which A and B are the field operators $\psi(\mathbf{x})$ or $\psi^\dagger(\mathbf{x})$ evaluated at positions \mathbf{x}_A and \mathbf{x}_B . In order to derive Eq. (7.36) we insert the explicit expressions (7.37) for $A(t_A)$ and $B(t_B)$ in the trace which defines the l.h.s. of Eq. (7.36), see Eq. (7.35). Then, by introducing an additional and arbitrary time t_f such that $t_i < t_{A,B} < t_f$, and by using the property of cyclicity of the trace we may write

$$\langle A(t_A)B(t_B) \rangle = \text{tr} \left(e^{-iH(t_f-t_B)} B e^{-iH(t_B-t_i)} \rho e^{iH(t_A-t_i)} A e^{iH(t_f-t_A)} \right). \quad (7.38)$$

The evolution of the density matrix is adjoint to the evolution of Heisenberg operators, i.e., $\rho(t) = e^{-iHt} \rho e^{iHt}$. Thus, the operator $e^{-iH(t-t')}$ / $e^{iH(t-t')}$ acting from the left/right on the density matrix

¹We use the word ‘‘Ward-Takahashi identity’’ in the sense of Eqs. (7.55,7.57), which is shown to be a consequence of the obedience of the equilibrium symmetry (7.3) in Sec. 7.4.4. Oftentimes, this word is used only if the symmetry transformation is continuous and can thus be presented in a differential form, unlike our case of a discrete transformation.

corresponds to the evolution in time from t' to t . In the correlation function (7.38), the time evolution from t_i to t_f on the left/right of ρ is intercepted by the operator B at time t_B/A at time t_A . In order to convert the r.h.s. of Eq. (7.38) into a path integral, the standard procedure (see, e.g., Refs. [38, 39]) to be followed consists in writing the exponentials of the evolution operators as infinite products of infinitesimal and subsequent temporal evolutions (Trotter decomposition), in between of which one can introduce resolutions of the identity in terms of coherent states carrying an additional label “+” on the left of the density matrix, and a “-” on its right. These coherent states eventually carry a temporal index on the forward (+) and backward (-) branches of the close-time path which characterizes the resulting action; Correspondingly, the operators on the left and on the right of the density matrix turn out to be evaluated on the fields which are defined, respectively, on the forward and backward branches of the closed time path and this yields immediately the equality in Eq. (7.36).

We note, for the sake of completeness, that the expression as a Keldysh functional integral of a simple two-time function is not unique: in fact, it is straightforward to check that rearranging operators in Eq. (7.38) one can equivalently arrive at

$$\langle A(t_A)B(t_B) \rangle = \begin{cases} \langle A_+(t_A)B_+(t_B) \rangle & \text{for } t_A > t_B, \\ \langle A_-(t_A)B_-(t_B) \rangle & \text{for } t_A < t_B. \end{cases} \quad (7.39)$$

However, as we discuss in the following, the choice of Eq. (7.36) naturally lends itself to a generalization to multi-time correlation functions.

Multi-time correlation functions. We define multi-time correlation functions in terms of time-ordered and anti-time-ordered products of operators

$$\begin{aligned} A(t_{A,1}, \dots, t_{A,N}) &= a_1(t_{A,1})a_2(t_{A,2}) \cdots a_N(t_{A,N}) & t_i < t_{A,1} < \cdots < t_{A,N} < t_f, \\ B(t_{B,1}, \dots, t_{B,M}) &= b_M(t_{B,M})b_{M-1}(t_{B,M-1}) \cdots b_1(t_{B,1}) & t_i < t_{B,1} < \cdots < t_{B,M} < t_f, \end{aligned} \quad (7.40)$$

where again the operators a_n and b_m are bosonic field operators. The specific sequence of time arguments in A and B (increasing and decreasing from left to right, respectively) leads to a time-ordering on the Keldysh contour: indeed, the multi-time correlation function can be expressed as a Keldysh functional integral in the form

$$\langle A(t_{A,1}, \dots, t_{A,N})B(t_{B,1}, \dots, t_{B,M}) \rangle = \langle B_+(t_{B,1}, \dots, t_{B,M})A_-(t_{A,1}, \dots, t_{A,N}) \rangle. \quad (7.41)$$

The functional integral on the r.h.s. of this relation can be constructed from a straightforward generalization of Eq. (7.38): after a reshuffling of the operators such that A and B appear respectively on the left and right of the density matrix — as we did above — the temporal evolution can be artificially extended from t_i to t_f and is intercepted on the l.h.s. of the density matrix by operators b_1, \dots, b_M at times $t_{B,1}, \dots, t_{B,M}$ and on the r.h.s. by operators a_1, \dots, a_N at times $t_{A,1}, \dots, t_{A,N}$. Again, the resulting expression for the correlation function can be converted directly into a path integral by inserting resolutions of the identity in terms of coherent states carrying the label “+” corresponding to the forward contour on the l.h.s. of the density matrix and the label “-” for the backward contour on the r.h.s. which leads us to Eq. (7.41).

Anti-time-ordered correlation functions. Not only time-ordered correlation functions such as Eq. (7.41) can be expressed in terms of functional integrals, but also correlation functions which are

anti-time-ordered and which, e.g., are obtained by exchanging the positions of $A(t_{A,1}, \dots, t_{A,N})$ and $B(t_{B,1}, \dots, t_{B,M})$ on the l.h.s. of Eq. (7.41). The construction of the corresponding functional integral can be accomplished with a few straightforward modifications to the procedure summarized above (and presented, e.g., in Refs. [38, 39]). In a stationary state $[\rho, H] = 0$ we can relate all Heisenberg operators on the l.h.s. of Eq. (7.41) to the Schrödinger operators at a later time t_f . Then one finds

$$\langle B(t_{B,1}, \dots, t_{B,M})A(t_{A,1}, \dots, t_{A,N}) \rangle = \langle A_+(t_{A,1}, \dots, t_{A,N})B_-(t_{B,1}, \dots, t_{B,M}) \rangle_{S_b}, \quad (7.42)$$

where the action S_b that describes the backward evolution is related to the action S which enters the forward evolution in Eq. (7.41) simply by a global change of sign.

7.4.2 Time reversal

In this section we first recall some properties of the time-reversal operation T [41] and then discuss its implementation within the Keldysh formalism. T is an antiunitary operator, i.e., it is antilinear (such that $T\lambda = \lambda^*T$ for $\lambda \in \mathbb{C}$) and unitary ($T^\dagger = T^{-1}$). Scalar products transform under antiunitary transformations into their complex conjugates, $\langle \psi|A|\phi \rangle = \langle \tilde{\psi}|\tilde{A}|\tilde{\phi} \rangle^*$, where we denote by $|\tilde{\psi} \rangle = T|\psi \rangle$ and $\tilde{A} = TAT^\dagger$ the state and the Schrödinger operator obtained from the state $|\psi \rangle$ and the operator A , respectively, after time reversal. Accordingly, expressing the trace of an operator in a certain basis $\{\psi_n\}_n$, one finds

$$\text{tr } A = \sum_n \langle \psi_n|A|\psi_n \rangle = \sum_n \langle \tilde{\psi}_n|\tilde{A}|\tilde{\psi}_n \rangle^* = (\text{tr } \tilde{A})^*. \quad (7.43)$$

In the last equality we used the fact that, due to the unitarity of T also the time-reversed set $\{\tilde{\psi}_n\}_n$ forms a basis. Below we find it convenient to define the Heisenberg representation of time-reversed operators such that it coincides with the Schrödinger representation at time $-t_f$ (cf. Eq. (7.37)), i.e., we set

$$\tilde{A}(t_A) = e^{i\tilde{H}(t_A+t_f)}\tilde{A}e^{-i\tilde{H}(t_A+t_f)}. \quad (7.44)$$

Note that this is distinct from the Heisenberg representation defined in Eq. (7.37), according to which Heisenberg and Schrödinger representations coincide at t_i . In a slight abuse of notation we do not indicate this difference explicitly which, however, will not cause confusion: for time-reversed operators we always assume $\tilde{A}(-t_f) = \tilde{A}$ etc. whereas for the “original” operators we have $A(t_i) = A$.

Let us now study the effect of time reversal on the multi-time correlation function (7.41). Due to translational invariance in time, all time arguments of the various operators can be shifted by $t_i - t_f$ without affecting the correlation function. Then, by using Eqs. (7.43) and (7.44), we have

$$\begin{aligned} \langle A(t_{A,1}, \dots, t_{A,N})B(t_{B,1}, \dots, t_{B,M}) \rangle &= \langle \tilde{A}(-t_{A,1}, \dots, -t_{A,N})\tilde{B}(-t_{B,1}, \dots, -t_{B,M}) \rangle_{\tilde{\rho}}^* \\ &= \langle \tilde{B}^\dagger(-t_{B,1}, \dots, -t_{B,M})\tilde{A}^\dagger(-t_{A,1}, \dots, -t_{A,N}) \rangle_{\tilde{\rho}}, \end{aligned} \quad (7.45)$$

where the subscript $\langle \dots \rangle_{\tilde{\rho}}$ indicates that the average is taken with respect to the time-reversed density operator $\tilde{\rho} \equiv T\rho T^\dagger$, which is time-independent. The expectation value on the r.h.s. of Eq. (7.45) is anti-time ordered and therefore it can be rewritten as a Keldysh functional integral by using Eq. (7.42). The l.h.s., instead, is time-ordered and therefore it can be expressed as in Eq. (7.41), such that Eq. (7.45) becomes

$$\langle B_+(t_{B,1}, \dots, t_{B,M})A_-(t_{A,1}, \dots, t_{A,N}) \rangle = \langle \tilde{A}_+^*(-t_{A,1}, \dots, -t_{A,N})\tilde{B}_-^*(-t_{B,1}, \dots, -t_{B,M}) \rangle_{\tilde{S}_b}, \quad (7.46)$$

where the subscript b in \tilde{S}_b indicates that the sign of the action which describes the Hamiltonian evolution on the r.h.s. of this relation has to be reversed, as explained below Eq. (7.42). Such a time-reversed action \tilde{S} differs from the action S which enters Eq. (7.41) because, in the former, the time evolution is generated by \tilde{H} , the initial state is the time reversed density matrix $\tilde{\rho}$, and the integration over time extends from $-t_f$ to $-t_i$. However, this latter difference in the integration domains vanishes as $t_i \rightarrow -\infty$ and $t_f \rightarrow \infty$.

Let us now consider the case in which A and B are products of bosonic field operators. There are no further restrictions on A and B and therefore the l.h.s. of Eq. (7.46) can be generically indicated as $\langle O[\Psi] \rangle$, where $O[\Psi]$ is the corresponding product of fields on the Keldysh contour, which according to the notation introduced in Sec. 7.2 are collected in $\Psi = (\psi_+, \psi_+^*, \psi_-, \psi_-^*)^T$. With this shorthand notation, Eq. (7.46) can be cast in the form

$$\langle O[\Psi] \rangle = \langle O[\mathbb{T}\Psi] \rangle_{\tilde{S}_b}, \quad (7.47)$$

where

$$\mathbb{T}\Psi_\sigma(t, \mathbf{x}) = \Psi_{-\sigma}^*(-t, \mathbf{x}), \quad (7.48)$$

which we thus interpret as the implementation of time reversal in the Keldysh formalism. (With a slight abuse of notation, the same symbol \mathbb{T} is used to indicate both the quantum-mechanical time reversal operator introduced above and the transformation of fields on the Keldysh contour in Eqs. (7.47) and (7.48).) Note that this matches the intuition, that the dynamics of a system is time reversal invariant (TRI), if – loosely speaking – the forward and backward branches of the closed time path are equivalent, in the sense that the sole effect of exchanging the contour indices of the fields as in Eq. (7.48) is a global sign change of the action S_b on the r.h.s. of Eq. (7.47) [38]. In Eq. (7.48) we took into account that the bosonic field operators in the Schrödinger picture and in the real space representation are time reversal invariant, i.e., $\tilde{\psi}(\mathbf{x}) = \mathbb{T}\psi(\mathbf{x})\mathbb{T}^\dagger = \psi(\mathbf{x})$, which allows us to drop the tilde on the transformed field on the r.h.s. of Eq. (7.48). However, we note that in the last line of Eq. (7.45) the Hermitean adjoint operators of those on the l.h.s. appear and this is the reason why both the r.h.s. of Eq. (7.46) and the transformation prescription Eq. (7.48) involves complex conjugation of the fields.

While Eq. (7.46) follows from the second line of Eq. (7.45), one could have equivalently taken its first line as the starting point for deriving a Keldysh time-reversal transformation. Then one would have been lead to

$$\mathbb{T}'\Psi_\sigma(t, \mathbf{x}) = \Psi_\sigma(-t, \mathbf{x}), \quad (7.49)$$

with an additional overall complex conjugation of the correlation function. In some sense, the transformation \mathbb{T}' is closer than \mathbb{T} to the common way of representing the quantum mechanical time reversal, which amounts to a mapping $t \mapsto -t$ and $i \mapsto -i$ [41]. For our purposes, however, \mathbb{T} is of main interest, since it is part of the equilibrium transformation as we describe below.

7.4.3 KMS condition

We now move on to formulate the KMS condition for multi-time correlation functions and its representation in terms of Keldysh functional integrals. For the specific case of a four-time correlation function this is illustrated in Fig. 7.1: as anticipated after Eq. (7.34), the KMS condition involves a contour exchange of the multi-time operators A and B . Graphically speaking, this exchange effectively

reverses the arrows in the second equality in Fig. 7.1 (b), since both A and B turn out to be anti-time ordered when moved to the opposite contour. The appropriate time-ordering can be restored by means of the time reversal transformation introduced in Eq. (7.48) of the previous section. This is a crucial step, as only time-ordered correlation functions can be directly translated into the functional integral by means of the usual Trotter decomposition, which makes the time-reversal transformation indispensable in the construction. In Fig. 7.1 (b) this step is performed after the third equality. However, this does not mean that properties related to equilibrium conditions such as fluctuation-dissipation relations are fulfilled only if the Hamiltonian is invariant under the time-reversal transformation. Indeed, it turns out that multi-time (number of field operators involved $n > 2$) FDRs always involve both the Hamiltonian and its time-reversed counterpart [46], while as we show in Sec. 7.5.1 the single-particle FDR can be stated without reference to the time-reversed Hamiltonian, even if the Hamiltonian is not TRI.

The KMS condition for a two-time function reads²

$$\langle A(t_A)B(t_B) \rangle = \langle B(t_B - i\beta/2)A(t_A + i\beta/2) \rangle. \quad (7.50)$$

This relation can be proved by writing down explicitly the expectation value on the l.h.s. with $\rho = e^{-\beta H}/Z$ and by inserting the definition of the Heisenberg operators reported in Eq. (7.37). The generalization of this procedure to the case of multi-time correlation functions is straightforward and yields

$$\begin{aligned} & \langle A(t_{A,1}, \dots, t_{A,N})B(t_{B,1}, \dots, t_{B,M}) \rangle \\ &= \langle B(t_{B,1} - i\beta/2, \dots, t_{B,M} - i\beta/2)A(t_{A,1} + i\beta/2, \dots, t_{A,N} + i\beta/2) \rangle. \end{aligned} \quad (7.51)$$

The real parts of the time variables on the r.h.s. of this equation are such that the corresponding product of operators is anti-time-ordered (see Fig. 7.1). According to their definition (7.40), A and B correspond to products of operators with, respectively, decreasing and increasing time arguments from right to left. Consequently Eq. (7.51) can be expressed as a functional integral by using Eqs. (7.41) and (7.42) on the l.h.s. and r.h.s., respectively (the presence of an imaginary part in the time arguments of Eq. (7.51) does not constitute a problem: in fact, the vertical part of the time path in Fig. 7.1 can be decomposed as usual in the Matsubara formalism):

$$\begin{aligned} & \langle B_+(t_{B,1}, \dots, t_{B,M})A_-(t_{A,1}, \dots, t_{A,N}) \rangle \\ &= \langle A_+(t_{A,1} + i\beta/2, \dots, t_{A,N} + i\beta/2)B_-(t_{B,1} - i\beta/2, \dots, t_{B,M} - i\beta/2) \rangle_{S_b}. \end{aligned} \quad (7.52)$$

As we did in Eq. (7.47) for the case of time reversal, we may rewrite this equation in the form

$$\langle O[\Psi] \rangle = \langle O[\mathcal{K}_\beta \Psi] \rangle_{S_b}, \quad (7.53)$$

where we define

$$\mathcal{K}_\beta \Psi_\sigma(t) = \Psi_{-\sigma}(t - i\sigma\beta/2). \quad (7.54)$$

²We note that this condition is usually expressed in the form

$$\langle A(t_A)B(t_B) \rangle = \langle B(t_B)A(t_A + i\beta) \rangle.$$

However, an equilibrium state is also stationary and therefore both time arguments on the r.h.s. can be translated by $-i\beta/2$ which leads us immediately to Eq. (7.50). Here we are assuming that the analytic continuation of real-time correlation functions into the complex plane is possible and unambiguous.

(a)

$$Z = \text{tr}(\overleftarrow{e^{-iHt}} \rho \overrightarrow{e^{iHt}})$$

(b)

$$\langle a_1(t_{a_1}) a_2(t_{a_2}) b_2(t_{b_2}) b_1(t_{b_1}) \rangle$$

$$= \text{tr}(\overleftarrow{b_2(t_{b_2})} \overleftarrow{b_1(t_{b_1})} \rho \overrightarrow{a_1(t_{a_1})} \overrightarrow{a_2(t_{a_2})})$$

$$= \text{tr}(\overleftarrow{a_1(t_{a_1} + i\beta/2)} \overleftarrow{a_2(t_{a_2} + i\beta/2)} \rho \overrightarrow{b_2(t_{b_2} - i\beta/2)} \overrightarrow{b_1(t_{b_1} - i\beta/2)})$$

$$= \text{tr}(\overleftarrow{b_1^\dagger(-t_{b_1} + i\beta/2)} \overleftarrow{b_2^\dagger(-t_{b_2} + i\beta/2)} \tilde{\rho} \overrightarrow{a_2^\dagger(-t_{a_2} - i\beta/2)} \overrightarrow{a_1^\dagger(-t_{a_1} - i\beta/2)})$$

$$= \langle \tilde{a}_2^\dagger(-t_{a_2} - i\beta/2) \tilde{a}_1^\dagger(-t_{a_1} - i\beta/2) \tilde{b}_1^\dagger(-t_{b_1} + i\beta/2) \tilde{b}_2^\dagger(-t_{b_2} + i\beta/2) \rangle$$

Figure 7.1. (a) Schematic representation of the Keldysh partition function [38, 39]. The time evolution of the density matrix $\rho(t) = e^{-iHt}\rho e^{iHt}$ can be represented by introducing two time lines to the left and right of ρ . These time lines correspond to the + and - parts of the Keldysh contour, respectively. (b) Schematic representation of the KMS condition for a four-time correlation function $\langle a_1(t_{a_1}) a_2(t_{a_2}) b_2(t_{b_2}) b_1(t_{b_1}) \rangle$ with $t_{a,1} < t_{a,2}$ and $t_{b,1} < t_{b,2}$, where $a_{1,2}$ and $b_{1,2}$ are bosonic field operators. As illustrated by the first equality (light blue box), this correlation function is properly time-ordered and therefore it can be directly represented within the Keldysh formalism with the operators $a_{1,2}$ and $b_{1,2}$ evaluated along the - and + contours, respectively. The thermal density matrix $\rho = e^{-\beta H}/Z$ can be first split into the products of $e^{-\beta H/2} \times e^{-\beta H/2}$ and these two factors can then be moved in opposite directions along the two time lines, with the effect of adding $+i\beta/2$ and $-i\beta/2$ to the time arguments of $a_{1,2}$ and $b_{1,2}$, respectively. After these two factors have been moved to the end of the timelines, due to the cyclic property of the trace, they combine as represented by the second equality (orange box), where the time lines now take detours into the complex plane and the overall time order is effectively reversed as indicated by the arrows which converge towards ρ instead of departing from it as in the case of sketch (a) or of the first equality of sketch (b). The original time ordering can be restored by means of the time-reversal operation \mathbb{T} , upon application of which operators are replaced by time reversal transformed ones, $\tilde{\rho} = \mathbb{T}\rho\mathbb{T}^\dagger$ etc., and signs of time variables are reversed. In addition, due to the anti-unitarity of \mathbb{T} one has to take the Hermitian adjoint of the expression inside the trace. As a result, the order of operators is inverted and one obtains the third equality (green box) which is again properly time ordered. This construction can be generalized to arbitrary correlation functions, leading to Eq. (7.55).

This transformation \mathcal{K}_β can be combined with the time reversal T defined in Eq. (7.48) in order to express the equilibrium transformation \mathcal{T}_β as $\mathcal{T}_\beta = T \circ \mathcal{K}_\beta$.³ By using Eq. (7.47) on the r.h.s. of Eq. (7.53), one concludes that the KMS condition implies

$$\langle O[\Psi] \rangle = \langle O[\mathcal{T}_\beta \Psi] \rangle_{\tilde{S}}, \quad (7.55)$$

which indeed provides a generalized FDR for the correlation function $\langle O[\Psi] \rangle$ [46]. For various choices of the observable $O[\Psi]$ we obtain the full hierarchy of multi-time FDRs which contains as a special case the single-particle FDR (see Sec. 7.5.1). Before demonstrating that this hierarchy (which follows from the validity of the KMS conditions) is equivalent to the invariance of the Keldysh action as expressed by Eq. (7.7), several remarks are in order:

1. Although by means of the time reversal transformation T we were able to restore the time ordering in Eq. (7.52), Eq. (7.55) still involves the time-reversed action \tilde{S} and not the original action S . However, in practice it will typically be clear how \tilde{S} can be obtained from S , e.g., by reversing the signs of external magnetic fields. In the absence of such time-reversal invariance breaking fields the tilde in Eq. (7.55) may be dropped.
2. Eq. (7.55) provides a generalized FDR expressed as products $O[\Psi]$ of fields on the forward and backward branches, which we collect in the four-component vector $\Psi = (\psi_+, \psi_+^*, \psi_-, \psi_-^*)^T$. A more familiar formulation is provided in the Keldysh basis of classical and quantum fields, which allows one to more directly discriminate correlations (expectation values involving only classical fields) from responses (expectation values involving both classical and quantum fields). FDRs provide relations between correlation and response functions.

In order to specify FDRs in the Keldysh basis, let us single out the first factor in this product: assuming it is $\psi_+(X)$, we may write $O[\Psi] = \psi_+(X)O'[\Psi]$, where $O'[\Psi]$ denotes the remaining factors in the product. By forming the linear combination of the expectation value of this expression and of $\psi_-(X)O'[\Psi]$,

$$\frac{1}{\sqrt{2}} (\langle \psi_+(X)O'[\Psi] \rangle + \langle \psi_-(X)O'[\Psi] \rangle) = \langle \phi_c(X)O'[\Psi] \rangle, \quad (7.56)$$

and proceeding analogously with the remaining factors in $O'[\Psi]$, we arrive at a generalized FDR for *classical and quantum fields*, which we can again write as (note that the O appearing here is different from the one in Eq. (7.55)),

$$\langle O[\Phi] \rangle = \langle O[\mathcal{T}_\beta \Phi] \rangle_{\tilde{S}}, \quad (7.57)$$

where $\Phi = (\phi_c, \phi_c^*, \phi_q, \phi_q^*)^T$. The transformation of these fields under \mathcal{T}_β is reported in Eq. (7.5).

The best known FDR concerns the single particle sector. For this case, the explicit FDR is derived in Sec. 7.5.1.

3. In a grand canonical ensemble with density matrix $\rho = e^{-\beta(H-\mu N)}/Z$, where $N = \int_{\mathbf{x}} \psi^\dagger(\mathbf{x})\psi(\mathbf{x})$ is the particle number operator, the KMS condition Eq. (7.51) has to be generalized. To derive the

³Note that it is straightforward to verify that the transformation T is not modified in the presence of complex time arguments.

generalization, again the density matrix has to be split into a product $e^{-\beta(H-\mu N)/2} \times e^{-\beta(H-\mu N)/2}$ (cf. the caption of Fig. 7.1). Then, moving one of the two factors through each of the blocks of operators A and B has not only the effect of adding $+i\beta/2$ and $-i\beta/2$ to the time arguments of the field operators in A and B respectively, as would be the case if $\mu = 0$; Instead, the operators should additionally be transformed as

$$\begin{aligned} e^{\pm\beta\mu N/2}\psi(\mathbf{x})e^{\mp\beta\mu N/2} &= e^{\mp\beta\mu/2}\psi(\mathbf{x}), \\ e^{\pm\beta\mu N/2}\psi^\dagger(\mathbf{x})e^{\mp\beta\mu N/2} &= e^{\pm\beta\mu/2}\psi^\dagger(\mathbf{x}), \end{aligned} \quad (7.58)$$

where the upper and lower signs in the exponents apply to operators which are part of the time-ordered and anti-time-ordered blocks A and B , respectively. This transformation of operators leads to the appearance of factors $e^{\pm\sigma\beta\mu/2}$ in Eq. (7.6).

7.4.4 From KMS to a symmetry of the Keldysh action

In the previous section we showed that the KMS condition within the Keldysh functional integral formalism takes the form of Eq. (7.55). Here we argue further that the latter relation is equivalent to requiring the invariance of the Keldysh action under the equilibrium symmetry \mathcal{T}_β . To this end, we express the expectation values on the left and right hand sides of Eq. (7.55) as the functional integrals

$$\langle O[\Psi] \rangle = \int \mathcal{D}[\Psi] O[\Psi] e^{iS[\Psi]} \quad (7.59)$$

and

$$\langle O[\mathcal{T}_\beta\Psi] \rangle_{\bar{s}} = \int \mathcal{D}[\Psi] O[\mathcal{T}_\beta\Psi] e^{i\bar{s}[\Psi]}, \quad (7.60)$$

respectively. Performing a change of integration variables $\Psi \rightarrow \mathcal{T}_\beta\Psi$ in the last expression, the argument of O simplifies as $\mathcal{T}_\beta\Psi \rightarrow \mathcal{T}_\beta^2\Psi = \Psi$ since \mathcal{T}_β is involutive (see Sec. 7.2). In addition, we show below that the absolute value of the determinant of the Jacobian $\mathcal{J} = \mathcal{D}[\mathcal{T}_\beta\Psi]/\mathcal{D}[\Psi]$ associated with the equilibrium transformation is equal to one, i.e., $|\text{Det } \mathcal{J}| = 1$, and therefore the integration measure does not change. Accordingly, one has

$$\langle O[\mathcal{T}_\beta\Psi] \rangle_{\bar{s}} = \int \mathcal{D}[\Psi] O[\Psi] e^{i\bar{s}[\mathcal{T}_\beta\Psi]}, \quad (7.61)$$

and by comparing this expression to Eq. (7.59) a *sufficient* condition for their equality is indeed Eq. (7.7), which expresses the invariance of the Keldysh action under the equilibrium transformation. In addition, since the observable $O[\Psi]$ in Eqs. (7.55), (7.59), and (7.61) is arbitrary, the condition is also *necessary*, which proves that Eqs. (7.7) and (7.55) (and, consequently, the KMS condition) are equivalent.

It remains to be shown that the Jacobian of the equilibrium transformation \mathcal{T}_β has a determinant with unity absolute value. In frequency and momentum space the Jacobian associated with Eq. (7.3) reads

$$\mathcal{J}(\omega, \mathbf{q}, \omega', \mathbf{q}') = (2\pi)^d \delta^{(d)}(\mathbf{q} + \mathbf{q}') J(\omega, \omega'), \quad (7.62)$$

where

$$J(\omega, \omega') = 2\pi\delta(\omega - \omega') \begin{pmatrix} 0 & e^{\beta\omega/2} & 0 & 0 \\ e^{-\beta\omega/2} & 0 & 0 & 0 \\ 0 & 0 & 0 & e^{\beta\omega/2} \\ 0 & 0 & e^{-\beta\omega/2} & 0 \end{pmatrix}. \quad (7.63)$$

The eigenvectors and eigenvalues of the frequency-dependent part, i.e., the solutions to the equation

$$\int \frac{d\omega'}{2\pi} J(\omega, \omega') v_i(\omega') = \lambda_i v_i(\omega), \quad (7.64)$$

are

$$\begin{aligned} v_1(\omega) &= (0, 0, -e^{\beta\omega/2}, 1)^T, & v_2(\omega) &= (-e^{\beta\omega/2}, 1, 0, 0)^T, \\ v_3(\omega) &= (0, 0, e^{\beta\omega/2}, 1)^T, & v_4(\omega) &= (e^{-\beta\omega/2}, 1, 0, 0)^T, \end{aligned} \quad (7.65)$$

with $\lambda_1 = \lambda_2 = -1$, and $\lambda_3 = \lambda_4 = 1$, so that $\text{Det } J = 1$. As for the momentum-dependent part of the Jacobian matrix Eq. (7.62), we note that its eigenvectors can be constructed with any function $f(\mathbf{q})$ by taking the even and odd combinations $f(\mathbf{q}) \pm f(-\mathbf{q})$:

$$\int_{\mathbf{q}'} (2\pi)^d \delta^{(d)}(\mathbf{q} + \mathbf{q}') (f(\mathbf{q}') \pm f(-\mathbf{q}')) = \pm (f(\mathbf{q}) \pm f(-\mathbf{q})). \quad (7.66)$$

Thus the eigenvalues of this part are ± 1 , and hence the absolute value of the Jacobian matrix is $|\text{Det}(\mathcal{J})| = 1$ as anticipated above.

7.5 Examples

In this section we discuss some concrete examples how the invariance of a given Keldysh action under the equilibrium transformation \mathcal{T}_β can be used in practice. First we show that Eq. (7.55) (or, equivalently, Eq. (7.57)) contains as special case the quantum single-particle FDR. This was also noted in Ref. [46], however, the conceptual difference is that here we may regard the FDR as a Ward-Takahashi identity associated with the equilibrium symmetry. In Sec. 7.5.2 we elaborate on the non-equilibrium nature of Markovian quantum master equation dynamics, which is seen to explicitly violate the equilibrium symmetry.

7.5.1 Single-particle fluctuation-dissipation relation

If we regard the symmetry of the Keldysh action with respect to \mathcal{T}_β in Eq. (7.5) as the defining property of thermodynamic equilibrium, we may consider the generalized FDR in Eq. (7.57) which – as the discussion in the previous section shows – is nothing but the Ward-Takahashi identity associated with the symmetry, as a *consequence* of equilibrium conditions. Then, from the generalized FDR the single-particle FDR [38, 39] can indeed be derived as a special case. The latter reads

$$G^K(\omega, \mathbf{q}) = (G^R(\omega, \mathbf{q}) - G^A(\omega, \mathbf{q})) \coth(\beta\omega/2) = i2 \text{Im } G^R(\omega, \mathbf{q}) \coth(\beta\omega/2), \quad (7.67)$$

where the Keldysh, retarded, and advanced Green's functions are related to expectation values of classical and quantum fields via

$$\begin{aligned} iG^K(\omega, \mathbf{q}) (2\pi)^{d+1} \delta(\omega - \omega') \delta^{(d)}(\mathbf{q} - \mathbf{q}') &= \langle \phi_c(\omega, \mathbf{q}) \phi_c^*(\omega', \mathbf{q}') \rangle, \\ iG^R(\omega, \mathbf{q}) (2\pi)^{d+1} \delta(\omega - \omega') \delta^{(d)}(\mathbf{q} - \mathbf{q}') &= \langle \phi_c(\omega, \mathbf{q}) \phi_q^*(\omega', \mathbf{q}') \rangle, \\ iG^A(\omega, \mathbf{q}) (2\pi)^{d+1} \delta(\omega - \omega') \delta^{(d)}(\mathbf{q} - \mathbf{q}') &= \langle \phi_q(\omega, \mathbf{q}) \phi_c^*(\omega', \mathbf{q}') \rangle. \end{aligned} \quad (7.68)$$

Here we are assuming translational invariance in both time and space, which is reflected in the appearance of frequency- and momentum-conserving δ -functions. The FDR valid in classical systems [36, 37] can be recovered from the quantum FDR Eq. (7.67) by taking the classical limit as described in Sec. 7.3.3. Contrary to what one might suspect a first glance from the appearance of the time-reversed action \tilde{S} in the generalized FDR in Eq. (7.57), the derivation of the single-particle FDR we present in the following is valid *irrespective* of whether the action contains external fields that break TRI.

Let us consider the Ward-Takahashi identity Eq. (7.57) for specific choices of the functional $O[\Phi]$. In particular, by taking O to be equal to the product of two quantum fields, the expectation value on the l.h.s. of Eq. (7.57) has to vanish due to causality and therefore

$$0 = \langle \phi_q(\omega, \mathbf{q}) \phi_q^*(\omega', \mathbf{q}') \rangle = \langle \mathcal{T}_\beta \phi_q(\omega, -\mathbf{q}) \mathcal{T}_\beta \phi_q^*(\omega', -\mathbf{q}') \rangle_{\tilde{S}}. \quad (7.69)$$

Upon inserting the expression of the fields transformed according to Eq. (7.5), one readily finds the FDR

$$G_{\tilde{S}}^K(\omega, \mathbf{q}) = \left(G_{\tilde{S}}^R(\omega, \mathbf{q}) - G_{\tilde{S}}^A(\omega, \mathbf{q}) \right) \coth(\beta\omega/2) \quad (7.70)$$

with the time-reversed action \tilde{S} . Repeating the same steps for the expectation value of the product of two classical fields (i.e., considering the Keldysh Green's function G^K in Eq. (7.68)) and by using the FDR in Eq. (7.70) we find the relation

$$G_{\tilde{S}}^K(\omega, \mathbf{q}) = G^K(\omega, -\mathbf{q}), \quad (7.71)$$

which expresses the transformation behavior of the exact single-particle Keldysh Green's function under time reversal of the Hamiltonian. Finally, by replacing $O[\Phi]$ in Eq. (7.57) with the product $\phi_c(\omega, \mathbf{q}) \phi_q^*(\omega', \mathbf{q})$ of one classical and one quantum field, the l.h.s. renders by definition the retarded Green's function G^R while the r.h.s. can be worked out as explained above. Taking into account Eq. (7.70), one can eliminate the Keldysh Green's function G^K appearing on the r.h.s. in favor of the retarded and advanced Green's functions G^R and G^A , respectively, and eventually finds

$$G_{\tilde{S}}^R(\omega, \mathbf{q}) = G^R(\omega, -\mathbf{q}). \quad (7.72)$$

This relation, together with its complex conjugate (which relates the advanced Green's functions calculated from the original and time-reversed Hamiltonians, respectively) and Eqs. (7.71) and (7.70), yields the FDR (7.67).

7.5.2 Non-equilibrium nature of steady states of quantum master equations

In the realm of classical statistical physics, the coupling of a system to a heat bath and the resulting relaxation to thermodynamic equilibrium are commonly modelled in the framework of Markovian stochastic processes, which can be encoded, e.g., in Langevin equations with Gaussian white noise [61]. The Markovian dynamics of a *quantum* system, on the other hand, is described by a master equation in Lindblad form [44, 45] (or an equivalent Keldysh functional integral). Under specific conditions [69, 71], also in this case the stationary state of this dynamics is described by a thermal Gibbs distribution, such that all *static* properties (equal-time correlation functions etc.) are indistinguishable from thermodynamic equilibrium. However, at the same time *dynamical* signatures of thermodynamic equilibrium such as the KMS condition (see Sec. 7.4.3) and the FDR (see Sec. 7.5.1)

are violated [72, 73]. This violation can be traced back to the fact that the Markovian approximation, which is usually done in deriving this master equation leads to an *explicit* breaking of the equilibrium symmetry as we show in this section – i.e., even though the system is coupled to a bath which resides in thermodynamic equilibrium, the system itself does not reach equilibrium. Physically, this can be understood by noting that the microscopic dynamics underlying an approximate Markovian description is indeed driven. A typical example in the context of quantum optics is an atom with two relevant energy levels separated by a level spacing ω_0 and connected by an external driving laser with frequency ν detuned from resonance by an amount $\Delta = \nu - \omega_0 \ll \omega_0$. Only the driving laser makes the excited level accessible, and the large scale controlling the Markov approximation is given by ω_0 . The upper level is unstable and can undergo spontaneous decay by emitting a photon to the radiation field, which acts as a reservoir. This underpins the combined driven and dissipative nature of such quantum optical systems.

Let us now consider a dissipative contribution to the action that arises upon integrating out a bath that couples linearly to the system degrees of freedom both before and after the Markov approximation, and show that the Markov approximation breaks symmetry with respect to the transformation \mathcal{T}_β . We assume that the bath consists of non-interacting harmonic oscillators $b_{\mu,\sigma}(t)$, labelled by an index μ , which are in thermodynamic equilibrium at a temperature $\beta = 1/T$. The action of the bath is given by

$$S_b = \sum_{\mu} \int_{t,t'} (b_{\mu,+}^*(t), b_{\mu,-}^*(t)) \begin{pmatrix} G_{\mu}^{++}(t, t') & G_{\mu}^{+-}(t, t') \\ G_{\mu}^{-+}(t, t') & G_{\mu}^{--}(t, t') \end{pmatrix}^{-1} \begin{pmatrix} b_{\mu,+}(t') \\ b_{\mu,-}(t') \end{pmatrix}, \quad (7.73)$$

where the Green's functions $iG_{\mu}^{\sigma\sigma'}(t, t') = \langle b_{\mu,\sigma}(t)b_{\mu,\sigma'}^*(t') \rangle$ for the oscillators of the bath read [38, 39]

$$\begin{aligned} G_{\mu}^{+-}(t, t') &= -in(\omega_{\mu})e^{-i\omega_{\mu}(t-t')}, \\ G_{\mu}^{-+}(t, t') &= -i(n(\omega_{\mu}) + 1)e^{-i\omega_{\mu}(t-t')}, \\ G_{\mu}^{++}(t, t') &= \theta(t-t')G_{\mu}^{-+}(t, t') + \theta(t'-t)G_{\mu}^{+-}(t, t'), \\ G_{\mu}^{--}(t, t') &= \theta(t'-t)G_{\mu}^{-+}(t, t') + \theta(t-t')G_{\mu}^{+-}(t, t'). \end{aligned} \quad (7.74)$$

Here $n(\omega) = 1/(e^{\beta\omega} - 1)$ is the Bose distribution function. The coupling between the system and the bath is linear in the bath variables and has strength $\sqrt{\gamma_{\mu}}$,

$$S_{sb} = \sum_{\mu} \sqrt{\gamma_{\mu}} \int_t (L_+^*(t)b_{\mu,+}(t) + L_+(t)b_{\mu,+}^*(t) - L_-^*(t)b_{\mu,-}(t) - L_-(t)b_{\mu,-}^*(t)). \quad (7.75)$$

Here $L_{\sigma}(t)$ are the so-called to the quantum jump operators which we assume to be quasilocal polynomials of bosonic fields resulting from normally ordered operators in a second quantized description (the simplest choice would be $L_{\sigma}(t) = \psi_{\sigma}(t, \mathbf{x})$). The Keldysh functional integral including both system and bath degrees of freedom is quadratic in the latter and, therefore, the bath can be integrated out, which yields a contribution to the action

$$S' = - \int_{\omega_0 - \vartheta}^{\omega_0 + \vartheta} d\omega \gamma(\omega) \nu(\omega) \int_{t,t'} (L_+^*(t), -L_-^*(t)) \begin{pmatrix} G_{\omega}^{++}(t, t') & G_{\omega}^{+-}(t, t') \\ G_{\omega}^{-+}(t, t') & G_{\omega}^{--}(t, t') \end{pmatrix} \begin{pmatrix} L_+(t') \\ -L_-(t') \end{pmatrix}. \quad (7.76)$$

To obtain this form of the action we made the additional assumption that the bath modes form a dense continuum, centered around some central frequency ω_0 and with bandwidth ϑ , which allows

us to replace the sum over μ by an integral over frequencies ω , weighted by a (phenomenologically introduced) density of states $\nu(\omega)$ of the bath modes, $\sum_{\mu} \gamma_{\mu} \sim \int_{\omega_0 - \vartheta}^{\omega_0 + \vartheta} d\omega \gamma(\omega) \nu(\omega)$. Inserting the explicit expressions (7.74) for the bath Green's functions we obtain

$$S' = -i \int_{\omega_0 - \vartheta}^{\omega_0 + \vartheta} \frac{d\omega}{2\pi} \gamma(\omega) \nu(\omega) \left(n(\omega) L_+^*(\omega) L_-(\omega) + (n(\omega) + 1) L_-^*(\omega) L_+(\omega) \right. \\ \left. - \int_{-\infty}^{\infty} \frac{d\omega'}{2\pi} \{ [\theta(\omega' - \omega) (n(\omega) + 1) + \theta(-\omega' + \omega) n(\omega)] L_+^*(\omega') L_+(\omega') \right. \\ \left. + [\theta(-\omega' + \omega) (n(\omega) + 1) + \theta(\omega' - \omega) n(\omega)] L_-^*(\omega') L_-(\omega') \} \right), \quad (7.77)$$

$L_{\sigma}(\omega)$ are the quantum jump operators in frequency space, and $\theta(\omega) = i\mathcal{P}_{\omega}^{-1} + \pi\delta(\omega)$, where $\mathcal{P}_{\omega}^{-1}$ denotes the Cauchy principal value, is the Fourier transform of the Heaviside step function. The terms involving the principal value contribute to the Hamiltonian part of the system Keldysh action and thus can be interpreted as an energy shift. Assuming that the jump operators are quasilocal polynomials of bosonic field operators, $L_{\sigma}(\omega)$ transform as the basic fields, i.e.,

$$\mathcal{T}_{\beta'} L_{\sigma}(\omega) = e^{-\sigma\beta'\omega/2} L_{\sigma}^*(\omega), \quad \mathcal{T}_{\beta'} L_{\sigma}^*(\omega) = e^{\sigma\beta'\omega/2} L_{\sigma}(\omega), \quad (7.78)$$

and inserting these expressions in Eq. (7.77) we find that the contour-diagonal terms (i.e., those involving products $L_{\sigma}^*(\omega) L_{\sigma'}(\omega)$ with $\sigma = \sigma'$, which include, in particular, the energy shift) are invariant due to frequency conservation (cf. the discussion in Sec. 7.3.1) *if the value of β' matches the inverse temperature $\beta = 1/T$ of the bath modes*. On the other hand, for the contour-off-diagonal contributions we have

$$S'_{\text{off-diag}}[\mathcal{T}_{\beta'}\Psi] = -i \int_{\omega_0 - \vartheta}^{\omega_0 + \vartheta} \frac{d\omega}{2\pi} \gamma(\omega) \nu(\omega) \left[n(\omega) e^{\beta'\omega} L_+(\omega) L_-^*(\omega) + (n(\omega) + 1) e^{-\beta'\omega} L_-(\omega) L_+^*(\omega) \right]. \quad (7.79)$$

Again, if $\beta' = \beta$, it is easy to see that also the off-diagonal terms are invariant under the thermal transformation by using the relation $n(\omega) e^{\beta\omega} = n(\omega) + 1$. Then indeed we have $S'[\mathcal{T}_{\beta}\Psi] = S'[\Psi]$.

Let us now consider the same expression Eq. (7.77) after the Markov approximation. For this approximation to be valid, we assume that it is possible to choose a rotating frame in which the evolution of the system is slow compared to the scales of the bath ω_0 and ϑ . This is possible if the system is driven by an external classical field such as a laser, so that the drive frequency bridges the gap between the natural system and bath time scales. Then all jump operators in Eq. (7.76) may be evaluated at the same time t . Additionally we assume that the density of bath states and the coupling of the system to bath are well approximated as constant over the relevant reservoir width, i.e., we set $\gamma(\omega) \nu(\omega) \approx \gamma(\omega_0) \nu(\omega_0)$. Finally, we discard the contour-diagonal terms, which are symmetric under \mathcal{T}_{β} also after performing the Markov approximation, and focus on the contour-off-diagonal terms

$$S'_{\text{off-diag}} = -i\gamma(\omega_0) \nu(\omega_0) \int_{-\infty}^{\infty} \frac{d\omega}{2\pi} \left[\bar{n} L_+^*(\omega) L_-(\omega) + (\bar{n} + 1) L_-^*(\omega) L_+(\omega) \right]. \quad (7.80)$$

Here $\bar{n} = n(\omega_0)$ is the occupation number of the bath mode with frequency ω_0 . Applying the transformation \mathcal{T}_{β} we have

$$S'_{\text{off-diag}}[\mathcal{T}_{\beta}\Psi] = -i\gamma(\omega_0) \nu(\omega_0) \int_{-\infty}^{\infty} \frac{d\omega}{2\pi} \left[\bar{n} e^{\beta\omega} L_+(\omega) L_-^*(\omega) + (\bar{n} + 1) e^{-\beta\omega} L_-(\omega) L_+^*(\omega) \right]. \quad (7.81)$$

The contour-off-diagonal terms are invariant under \mathcal{T}_β only for $\bar{n}e^{\beta\omega} = \bar{n} + 1$ which is obviously not possible for all ω and, therefore, the equilibrium symmetry is explicitly broken by the Markov approximation.

7.6 Conclusions

We demonstrated here that the Keldysh action describing the dynamics of a generic quantum many-body system acquires a certain symmetry \mathcal{T}_β if the evolution occurs in thermal equilibrium. The origin of this symmetry is traced back to the Kubo-Martin-Schwinger (KMS) condition which establishes a relationship between multi-time correlation functions in real and imaginary times of a system in canonical equilibrium at a certain temperature. Fluctuation-dissipation relations are then derived as the Ward-Takahashi identities associated with \mathcal{T}_β . Remarkably, in the classical limit, this equilibrium symmetry reduces to the one known in classical stochastic systems, where it was derived from the assumption of detailed balance. By comparing with this classical case, important questions on the nature of equilibrium in quantum systems arise. In particular, while microreversibility and detailed balance of the dynamics are deeply entangled with the notion of equilibrium in classical stochastic systems, an analogous relationship for quantum systems does not clearly emerge and surely deserves to be investigated further.

The equilibrium symmetry \mathcal{T}_β is expected to play a crucial role in the study of thermalization in quantum systems, in particular when combined with a renormalization-group analysis. In fact, on the one hand, it provides a simple but powerful theoretical tool to check whether a certain system is able to reproduce thermal equilibrium. This can indeed be accomplished by a direct inspection of the microscopic Keldysh action (or of the effective one generated after integrating out some degrees of freedom, e.g., along a renormalization-group flow) which describes the dynamics of the system, rather than checking, for instance, the validity of the fluctuation-dissipation relations among various correlation functions. On the other hand, the equilibrium symmetry might be useful also in order to investigate or characterize possible departures from equilibrium and, in this respect, it would be interesting to consider the case in which the system evolves in a generalized Gibbs ensemble [13, 50–57]. Finally, while we focussed here on the case of bosons, the extension of our analysis to different statistics, for instance fermionic and spin systems, represents an interesting issue.

Acknowledgements. – We would like to thank J. Berges, I. Carusotto, L. F. Cugliandolo, T. Gasenzer, J. M. Pawłowski, T. Prosen, H. Spohn and C. Wetterich for useful discussions. L. M. S. and S. D. gratefully acknowledge support by the START Grant No. Y 581-N16.

Bibliography

- [1] A. Polkovnikov, K. Sengupta, A. Silva, and M. Vengalattore, *Rev. Mod. Phys.* **83**, 863 (2011).
- [2] V. Yukalov, *Laser Phys. Lett.* **8**, 485 (2011).
- [3] A. Lamacraft and J. Moore, in *Ultracold Bosonic and Fermionic Gases*, edited by A. Fetter, K. Levin, and D. Stamper-Kurn (Elsevier, Oxford, 2012) Chap. 7.
- [4] I. Bloch, J. Dalibard, and W. Zwerger, *Rev. Mod. Phys.* **80**, 885 (2008).

- [5] R. M. Stevenson, V. N. Astratov, M. S. Skolnick, D. M. Whittaker, M. Emam-Ismail, A. I. Tartakovskii, P. G. Savvidis, J. J. Baumberg, and J. S. Roberts, *Phys. Rev. Lett.* **85**, 3680 (2000).
- [6] J. J. Baumberg, P. G. Savvidis, R. M. Stevenson, A. I. Tartakovskii, M. S. Skolnick, D. M. Whittaker, and J. S. Roberts, *Phys. Rev. B* **62**, R16247 (2000).
- [7] A. Baas, J.-P. Karr, M. Romanelli, A. Bramati, and E. Giacobino, *Phys. Rev. Lett.* **96**, 176401 (2006).
- [8] J. Kasprzak, M. Richard, S. Kundermann, A. Baas, P. Jeambrun, J. Keeling, F. Marchetti, M. Szymanska, R. Andre, J. Staehli, V. Savona, P. Littlewood, B. Deveaud, and L. Dang, *Nature* **443**, 409 (2006).
- [9] B. Deveaud, ed., *The physics of semiconductor microcavities* (John Wiley & Sons, 2007).
- [10] A. A. Houck, H. E. Tureci, and J. Koch, *Nat. Phys.* **8**, 292 (2012).
- [11] E. T. Jaynes, *Phys. Rev.* **106**, 620 (1957).
- [12] T. Kinoshita, T. Wenger, and D. S. Weiss, *Nature (London)* **440**, 900 (2006).
- [13] M. Rigol, V. Dunjko, V. Yurovsky, and M. Olshanii, *Phys. Rev. Lett.* **98**, 050405 (2007).
- [14] M. Kollar, F. Wolf, and M. Eckstein, *Phys. Rev. B* **84**, 054304 (2011).
- [15] J.-S. Caux and R. Konik, *Phys. Rev. Lett.* **109**, 175301 (2012).
- [16] M. Serbyn, Z. Papić, and D. Abanin, *Phys. Rev. Lett.* **111**, 127201 (2013).
- [17] D. A. Huse, R. Nandkishore, and V. Oganesyan, *Phys. Rev. B* **90**, 174202 (2014).
- [18] V. Ros, M. Müller, and A. Scardicchio, *Nuclear Physics B* **891**, 420 (2015).
- [19] J. Z. Imbrie, arXiv1403.7837 (2014).
- [20] D. Rossini, A. Silva, G. Mussardo, and G. Santoro, *Phys. Rev. Lett.* **102**, 127204 (2009).
- [21] A. Mitra and T. Giamarchi, *Phys. Rev. Lett.* **107**, 150602 (2011).
- [22] A. Mitra and T. Giamarchi, *Phys. Rev. B* **85**, 075117 (2012).
- [23] L. Foini, L. F. Cugliandolo, and A. Gambassi, *Phys. Rev. B* **84**, 212404 (2011).
- [24] L. Foini, L. F. Cugliandolo, and A. Gambassi, *J. Stat. Mech.: Theor. Exp.* **2011**, P09011 (2011).
- [25] A. Mitra, S. Takei, Y. B. Kim, and A. J. Millis, *Phys. Rev. Lett.* **97**, 236808 (2006).
- [26] S. Diehl, A. Micheli, A. Kantian, B. Kraus, H. P. Buchler, and P. Zoller, *Nat. Phys.* **4**, 878 (2008).
- [27] E. G. Dalla Torre, E. Demler, T. Giamarchi, and E. Altman, *Phys. Rev. B* **85**, 184302 (2012).
- [28] E. G. D. Torre, S. Diehl, M. D. Lukin, S. Sachdev, and P. Strack, *Phys. Rev. A* **87**, 023831 (2013).

- [29] A. Chiocchetta and I. Carusotto, EPL (Europhysics Letters) **102**, 67007 (2013).
- [30] L. M. Sieberer, S. D. Huber, E. Altman, and S. Diehl, Phys. Rev. Lett. **110**, 195301 (2013).
- [31] L. M. Sieberer, S. D. Huber, E. Altman, and S. Diehl, Phys. Rev. B **89**, 134310 (2014).
- [32] H.-K. Janssen, Zeitschrift für Physik B Condensed Matter **23**, 377 (1976).
- [33] R. Bausch, H. Janssen, and H. Wagner, Zeitschrift für Physik B Condensed Matter **24**, 113 (1976).
- [34] H. Janssen, in *Dynamical Critical Phenomena and Related Topics*, Lecture Notes in Physics, Vol. 104, edited by C. Enz (Springer Berlin Heidelberg, 1979).
- [35] H. Janssen, in *From Phase Transitions to Chaos, Topics in Modern Statistical Physics*, edited by G. Györgyi, I. Kondor, L. Sasvári, and T. Tél (World Scientific Singapore, 1992).
- [36] C. Aron, G. Biroli, and L. F. Cugliandolo, J. Stat. Mech. **2010**, P11018 (2010).
- [37] C. Aron, D. G. Barci, L. F. Cugliandolo, Z. G. Arenas, and G. S. Lozano, arXiv:1412.7564 (2014).
- [38] A. Kamenev, *Field Theory of Non-Equilibrium Systems* (Cambridge University Press, Cambridge, 2011).
- [39] A. Altland and B. Simons, *Condensed Matter Field Theory*, 2nd ed. (Cambridge University Press, Cambridge, 2010).
- [40] H. Stoof, Journal of Low Temperature Physics **114**, 11 (1999).
- [41] A. Messiah, *Quantum Mechanics II*, 3rd ed. (North-Holland Publishing Company, Amsterdam, 1965).
- [42] R. Kubo, Journal of the Physical Society of Japan **12**, 570 (1957).
- [43] P. Martin and J. Schwinger, Phys. Rev. **115**, 1342 (1959).
- [44] A. Kossakowski, Reports on Mathematical Physics **3**, 247 (1972).
- [45] G. Lindblad, Communications in Mathematical Physics **48**, 119 (1976).
- [46] S. G. Jakobs, M. Pletyukhov, and H. Schoeller, Journal of Physics A: Mathematical and Theoretical **43**, 103001 (2010).
- [47] E. M. Lifshitz and L. P. Pitaevskii, *Statistical Physics, Part 2: Theory of the Condensed State*, 2nd ed. (Pergamon Press, New York, 1980).
- [48] P. Hohenberg and B. Halperin, Reviews of Modern Physics **49**, 435 (1977).
- [49] R. Folk and G. Moser, Journal of Physics A: Mathematical and General **39**, R207 (2006).
- [50] A. Iucci and M. A. Cazalilla, Phys. Rev. A **80**, 063619 (2009).
- [51] E. Jaynes, Phys. Rev. **106**, 620 (1957).

- [52] T. Barthel and U. Schollwöck, *Phys. Rev. Lett.* **100**, 100601 (2008).
- [53] G. Goldstein and N. Andrei, arXiv:1405.4224 (2014).
- [54] B. Pozsgay, M. Mestyán, M. Werner, M. Kormos, G. Zaránd, and G. Takács, *Phys. Rev. Lett.* **113**, 117203 (2014).
- [55] M. Mierzejewski, P. Prelovšek, and T. Prosen, *Phys. Rev. Lett.* **113**, 020602 (2014).
- [56] B. Wouters, J. De Nardis, M. Brockmann, D. Fioretto, M. Rigol, and J.-S. Caux, *Phys. Rev. Lett.* **113**, 117202 (2014).
- [57] F. H. L. Essler, G. Mussardo, and M. Panfil, arXiv:1411.5352 (2014).
- [58] P. Martin, E. Siggia, and H. Rose, *Phys. Rev. A* **8**, 423 (1973).
- [59] De Dominicis, C., *J. Phys. Colloques* **37**, C1 (1976).
- [60] C. De Dominicis, *Phys. Rev. B* **18**, 4913 (1978).
- [61] U. C. Täuber, *Critical Dynamics: A Field Theory Approach to Equilibrium and Non-Equilibrium Scaling Behavior* (Cambridge University Press, Cambridge, 2014).
- [62] C. Gardiner, *Handbook of stochastic methods for physics, chemistry and the natural sciences*, 3rd ed., Springer Series in Synergetics (Springer-Verlag, 2004).
- [63] J. Zinn-Justin, *Quantum Field Theory and Critical Phenomena*, 4th ed., International Series of Monographs on Physics No. 113 (Oxford University Press, Oxford, 2002).
- [64] G. S. Agarwal, *Zeitschrift für Physik* **258**, 409 (1973).
- [65] R. Alicki, *Reports on Mathematical Physics* **10**, 249 (1976).
- [66] A. Kossakowski, A. Frigerio, V. Gorini, and M. Verri, *Communications in Mathematical Physics* **57**, 97 (1977).
- [67] A. Frigerio and V. Gorini, *Communications in Mathematical Physics* **93**, 517 (1984).
- [68] W. A. Majewski, *Journal of Mathematical Physics* **25**, 614 (1984).
- [69] R. Alicki and K. Lendi, in *Handbook of stochastic methods for physics, chemistry and the natural sciences*, Lecture Notes in Physics, Vol. 717 (Springer-Verlag Berlin Heidelberg, 2007).
- [70] H. Carmichael and D. Walls, *Z. Physik B* **23**, 299 (1976).
- [71] C. W. Gardiner and P. Zoller, *Quantum Noise*, 2nd ed., Springer series in synergetics, Vol. 56 (Springer, Berlin Heidelberg, 2000).
- [72] P. Talkner, *Annals of Physics* **167**, 390 (1986).
- [73] G. W. Ford and R. F. O'Connell, *Phys. Rev. Lett.* **77**, 798 (1996).

ACKNOWLEDGMENTS

The past few years have been a fascinating trip into the world of non-bananas, and I am deeply grateful to my supervisor Sebastian Diehl for his guidance on this journey. He has supported me in many ways, both scientifically and non-scientifically (i.e., in real life), and has inspired me in countless discussions, by example and through his continuous encouragement to strive not only for excellence in science, but also for keeping up human virtues in scientific practice. Not least this resulted in – I dare say – some very nice physics we did together. This was further promoted by the benefit I was able to take from him giving me the chance to visit several other research groups and to participate in numerous workshops and conferences. For all of this I am deeply indebted to Sebastian.

In the course of my Ph.D. studies, my scientific knowledge was augmented, broadened and deepened significantly through collaborating with a number of people, whom I would like to thank. This includes Ehud Altman, Jamir Marino, Liang He, Sebastian Huber, John Toner, Andrea Gambassi, and Alessio Chiocchetta. In particular, I gladly embrace the opportunity to thank Ehud for numerous enlightening discussions, his hospitality during my stay at the Weizmann Institute of Science, and for giving me the chance to present my work at conferences on several occasions.

When you are working in physics, life is not always easy: as a natural law, the outcome of the first $N \gg 1$ attempts to solve some scientific problem is bound to be failure. During hard times I took comfort in the most enjoyable atmosphere at work that was created by my colleagues and friends in our research group, Liang, Jamir, Sebastian (Huber, but not the one at ETH), and especially Michael, with whom I shared an office—this has been a very special experience, which I will always keep in warm memory. Indeed, sharing increases the joy and reduces the suffering that is inherent in studying physics, and for this I would like to thank my friends at the Institute for Theoretical Physics, especially Carlo, Lars, and Sebastian (Hofer, this time), and the Ion Physics guys Josi, Samuel, and Matze.

Finally, what would I be without the support from so many people outside of science? It took more than a little help from my friends to bring me to where I am today. Most of all, however, I would like to thank my parents, my sister (in particular, for proofreading parts of this thesis), and my wonderful girlfriend.

Lukas Sieberer, Innsbruck, March 2015

CURRICULUM VITAE

Lukas M. Sieberer

(As of March 2015)

Personal details

Date of birth: March 1st, 1985
Place of birth: Wörgl (Austria)
Citizenship: Austrian
Address: Planötzenhofstraße 1, 6020 Innsbruck, Austria
Phone: +43 650 4110148
E-mail: lukas.sieberer@uibk.ac.at

Education

10/2010–Present Ph. D. in Physics, University of Innsbruck
Supervised by Prof. Dr. Sebastian Diehl
10/2004–8/2010 Diploma in Physics with first class honors, University of Innsbruck
Supervised by Dr. Mikhail Baranov
Thesis: *Superfluid Transition in a Quasi-Two-Dimensional Dipolar Fermi Gas*
05/2003 Matura with highest distinction (high school diploma)
09/1995–05/2003 Bundesrealgymnasium Wörgl (high school)
09/1991–05/1995 Elementary school, Hopfgarten

Civilian service

09/2003–09/2004 Home for the elderly, Hopfgarten

Publications and preprints

5. *Scaling properties of one-dimensional driven-dissipative condensates*
L. He, L. M. Sieberer, E. Altman, and S. Diehl
arXiv:1412.5579 (2014)

4. *Two-Dimensional Superfluidity of Exciton-Polaritons Requires Strong Anisotropy*
E. Altman, L. M. Sieberer, L. Chen, S. Diehl, and J. Toner
Phys. Rev. X, **5**, 011017 (2015)
3. *Nonequilibrium functional renormalization for driven-dissipative Bose-Einstein condensation*
L. M. Sieberer, S. D. Huber, E. Altman, and S. Diehl
Phys. Rev. B, **89**, 134310 (2014)
2. *Dynamical Critical Phenomena in Driven-Dissipative Systems*
L. M. Sieberer, S. D. Huber, E. Altman, and S. Diehl
Phys. Rev. Lett., **110**, 195301 (2013)
1. *Collective modes, stability, and superfluid transition of a quasi-two-dimensional dipolar Fermi gas*
L. M. Sieberer and M. Baranov
Phys. Rev. A, **84**, 063633 (2011)

Invited talks

2. *2D Superfluidity of Exciton-Polaritons Requires Strong Anisotropy*, Quantum correlations out of equilibrium, ETH Zürich, Switzerland, 2014
1. *Universality in Driven-Dissipative Bose-Einstein Condensation*, School on Non-linear Dynamics, Dynamical Transitions and Instabilities in Classical and Quantum Systems, ICTP Trieste, Italy, 2014

Conference talks

2. *2D Superfluidity of Exciton-Polaritons Requires Strong Anisotropy*, DPG spring meeting, Berlin, Germany, 2014
1. *Non-Equilibrium Criticality of Driven Open Many-Body Quantum Systems*, DPG spring meeting, Hannover, Germany, 2013

Seminar talks

6. *Universality in Driven-Dissipative Bose-Einstein Condensation*, Weizmann Institute of Science, Rehovot, Israel, 2014
5. *Universality in Driven-Dissipative Bose-Einstein Condensation*, Technion, Haifa, Israel, 2014
4. *Dynamical Critical Phenomena in Driven-Dissipative Systems*, University of Heidelberg, Germany, 2013
3. *Dynamical Critical Phenomena in Driven-Dissipative Systems*, University of Trento, Italy, 2013

2. *Non-Equilibrium Criticality of Driven Open Many-Body Quantum Systems*, University of Heidelberg, Germany, 2012
1. *Dynamical Critical Phenomena in Driven-Dissipative Systems*, University of Innsbruck, Austria, 2012

Posters

9. *2D Superfluidity of Exciton-Polaritons Requires Strong Anisotropy*, International Winter School and Workshop on “Strongly correlated fluids of light and matter,” Trento, Italy, 2015
8. *2D Superfluidity of Exciton-Polaritons Requires Strong Anisotropy*, DPG spring meeting, Berlin, Germany, 2014
7. *2D Superfluidity of Exciton-Polaritons Requires Strong Anisotropy*, International Conference on Quantum Optics, Obergurgl, Austria, 2014
6. *Dynamical Critical Phenomena in Driven-Dissipative Systems*, Summerschool: Quantum Matter - Foundations and Applications, Granada, Spain, 2013
5. *Dynamical Critical Phenomena in Driven-Dissipative Systems*, International Workshop on Quantum Many Body Systems out of Equilibrium, Dresden, Germany, 2013
4. *Dynamical Critical Phenomena in Driven-Dissipative Systems*, 534. WE-Heraeus Seminar on “Quantum Many-Body Dynamics in Open Systems,” Bad Honnef, Germany, 2013
3. *Dynamical Critical Phenomena in Driven-Dissipative Systems*, DPG spring meeting, Hannover, Germany, 2013
2. *Critical behavior in a driven-dissipative quantum many-body system*, International Conference on Quantum Systems and Technology, Monte Verità, Switzerland, 2012
1. *Collective modes and quantum phases of a quasi-two-dimensional dipolar Fermi gas*, International Conference on Quantum Optics, Obergurgl, Austria, 2012

Awards

- 2006, 2007 University of Innsbruck merit grant in acknowledgment of excellent academic studies
 2003 Bronze medal at the “22. Österreichische Physikolympiade”

Teaching

- 10/2009–01/2010 Tutor for Classical Mechanics exercises, University of Innsbruck
 03/2008–06/2009 Tutor for Electrodynamics exercises, University of Innsbruck
 10/2007–01/2008 Tutor for Classical Mechanics exercises, University of Innsbruck
 03/2007–06/2007 Tutor for Electrodynamics, University of Innsbruck

Lukas Sieberer, Innsbruck, March 2015

